Elsevier Editorial System(tm) for Earth Science Reviews
Manuscript Draft

Manuscript Number: EARTH1319R1

Title: A review of the geology and geodynamic evolution of the Palaeoproterozoic Earaheedy Basin, Western Australia

Article Type: Review Article

Keywords: Earaheedy Basin, Capricorn Orogen, passive margin, granular iron-formation

Corresponding Author: Dr Franco Pirajno,

Corresponding Author's Institution: Geological Survey of Western Australai

First Author: Franco Pirajno

Order of Authors: Franco Pirajno; Roger M Hocking; Steven M Reddy, PhD; Amanda Jones, MSc

Abstract: The Palaeoproterozoic Earaheedy Basin is one of a series of basins that extend for about 700 km east-west and are part of the Capricorn Orogen, situated between the Archaean Pilbara and Yilgarn Cratons. The Earaheedy Basin contains sedimentary rocks that were deposited on the northern passive continental margin of the Yilgarn Craton, probably as a result of continental breakup at 1.8 Ga. The sedimentary rocks of the Earaheedy Group are divided into two Subgroups, Toloo and Miningarra, each representing different depositional environments and aggregating about 3000 m in thickeness. The Tooloo Subgroup consist of basal siliciclastic with minor platform carbonates, overlain by a 600-m-thick succession of Fe-rich rocks (granular iron-formation and hematitic shales). The Miningarra Subgroup is predominantly siliciclastic, but includes stromatolite-bearing carbonate sequences and was deposited during a more active depositional regime. Far field tectonic events at 1.76 and 1.65 Ga resulted in the deformation of the sedimentary package with progressive intensity from north to south, forming the Stanley Fold Belt and giving and overall asymmetric structure to the Basin. These events were followed by a large meteorite impact (Shoemaker Impact Structure), probably in the Neoproterozoic. The Earaheedy Basin is well

endowed with Fe resources, represented by the granular iron-formation (Frere Formation, Tooloo Subgroup), particularly in the Stanley Fold Belt, where there was secondary enrichement.

Suggested Reviewers: Peter Haines PhD
Senior Geoscientist, Geological Survey of WA
peter.haines@dmp.wa.gov.au
expert in Proteozoic basins

Yanjing Chen PhD
Professor, Geology, Peking University
yjchen@pku.edu.cn
expert in Proterozoic systems

A review of the geology and geodynamic evolution of the Palaeoproterozoic Earaheedy Basin, Western Australia

Franco Pirajno[1,2], Roger M. Hocking[1], Steven M. Reddy[3] and Amanda J. Jones[1]

(1) Geological Survey of Western Australia, East Perth, Australia
(2) School of Earth and Geographical Sciences, The University of Western Australia, Crawley, Australia
(3) Dept. Applied Geology, Curtin University of Technology, Perth, Australia

Abstract

The Palaeoproterozoic Earaheedy Basin is one of a series of basins that extend for about 700 km east-west and are part of the Capricorn Orogen, situated between the Archaean Pilbara and Yilgarn Cratons. The Earaheedy Basin contains sedimentary rocks that were deposited on the northern passive continental margin of the Yilgarn Craton, probably as a result of continental breakup at 1.8 Ga. The sedimentary rocks of the Earaheedy Group are divided into two Subgroups, Toloo and Miningarra, each representing different depositional environments and aggregating about 3000 m in thickeness. The Tooloo Subgroup consists of basal siliciclastic rocks with minor platform carbonates, overlain by a 600-m-thick succession of Fe-rich rocks (granular iron-formation and hematitic shales). The Miningarra Subgroup is predominantly siliciclastic, but includes stromatolite-bearing carbonate sequences and was deposited during a more active depositional regime. Far-field tectonic events at 1.76 and 1.65 Ga resulted in the deformation of the sedimentary package with progressive intensity from north to south, forming the Stanley Fold Belt and giving and overall asymmetric structure to the Basin. These events were followed by a large meteorite impact (Shoemaker Impact Structure), probably in the Neoproterozoic. The Earaheedy Basin is well endowed with Fe resources, represented by the granular iron-formation (Frere Formation, Tooloo Subgroup), particularly in the Stanley Fold Belt, where there was secondary enrichement.

1. Introduction

The Earaheedy Basin, together with the Yerrida, Bryah and Padbury basins, form a series of Palaeoproterozoic basinal structures that extend for about 700 km east-west along the southeastern margin of the Capricorn Orogen and the northern margin of the Yilgarn Craton and covers a total area of approximately 70 000 km^2 (Cawood and Tyler, 2004; Pirajno et al. 2004) (Fig. 1). The development of these basins began at about 2.2 Ga and continued for at least 400 Myrs, to about 1.8 Ga and possibly as young as 1.65 Ga, recording periods of sedimentation and igneous activity. The

present-day geometry of these basins is the combined result of tectonic movements which occurred during the ca. 2.0-1.96 Ga Glenburgh Orogeny (Occhipinti et al., 2004), the ca. 1.83-1.78 Ga Capricorn Orogeny (Cawood and Tyler, 2004 and references cited therein) and to a lesser extent the 1.79-1.76 Ga Yapungku Orogeny (Bagas, 2004) and the 1.65 Ga Mangaroon Orogeny (Sheppard et al., 2005). A synopsis of the geological events that formed and shaped the Palaeoproterozoic basins in the eastern Capricorn orogen is presented in Table 1.

The Earaheedy Basin (Bunting, 1986; Pirajno et al., 2004) contains the Earaheedy Group and lies at the easternmost end of the Capricorn Orogen (Cawood and Tyler, 2004; Tyler et al., 1998; Myers et al., 1996). The Basin represents a coastal to outer shelfal, dominantly silciclastic, sedimentary accumulation, with a locally preserved basal fluvial sandstone and conglomerate, interpreted by Jones et al. (2000) and Pirajno et al. (2004) to have accumulated at a passive continental margin along the northeastern edge of the Yilgarn Craton. This passive margin may ultimately represent a continental breakup at 1.8 Ga, perhaps linked to the impingement of a mantle plume, as will be elaborated in Section 7.

Basement to the exposed Earaheedy Basin is the Archaean Yilgarn Craton, and to the west the Yerrida Basin. To the north the Earaheedy Basin is overlain by the sedimentary successions of the Bangemall Supergroup (Scorpion and Salvation Groups). A small outlier of 1.9 Ga rhyodacitic rock (Inbim Inlier) on the northern margin is unconformably overlain by rocks of the Earaheedy Group (Yelma Formation, see below). Locally the Earaheedy Group is intruded by dykes and sills of the Glenayle Dolerite and Prenti Downs Dolerite (Morris and Pirajno, 2005), which are part of the 1076 Ma Warakurna Large Igneous Province (WLIP; Wingate et al. 2004), and by scattered lamprophyre dykes and pipes of unknown age. Apart from the WLIP there are no other igneous rocks that are associated with the sedimentary succession of the Earaheedy Basin, except for minor and thin volcaniclastic horizons in the Frere Formation.

The Earaheedy Basin has an exposed area of 35 308 km^2, in south-central Western Australia. Numerous possible outliers are present about 50-60 km south of the westernmost exposures. These outliers, such as the Kaluweerrie Hills (Allchurch and

Bunting, 1975), Mount Laurence Wells and Mount Wilkinson south of Wiluna (Langford et al., 2000) have sedimentary rocks that include stromatolitic carbonates, which could be part of either the Yerrida Basin or Earaheedy Basin successions. To the west is the easterly trending Mount Leake outlier (Mount Leake Formation), which straddles the Goodin Fault that marks the tectonic boundary between the Yerrida and Bryah Basins, clearly demonstrating that the Mount Leake Formation was deposited well after the tectonic juxtaposition of the Bryah and Yerrida Basins. The Mount Leake Formation consists of a basal jasperoidal chert and green chert breccia about 2 m thick, followed upward by a ferruginous sandstone layer and by beds of cross-bedded, locally glauconitic, quartz arenite. Pirajno and Occhipinti (1998) interpreted the jasperoidal and chert breccia material as a palaeoregolith, developed on an unconformity surface of the Bryah Group. On the basis of stromatolite taxa that are present in the formation, Pirajno and Adamides (2000) proposed a correlation with the Yelma Formation. The presence of these outliers suggest that the original extent of the Basin could have been much larger (Fig. 1).

The Geological Survey of Western Australia (GSWA) began a systematic re-mapping program of the Earaheedy Basin in 1997. The outcome of this program was the publication of the second edition 1:250 000 Nabberu, and eleven 1:100 000 series geological maps (Merrie, Cunyu, Fairbairn, Methwin, Nabberu, Granite Peak, Mudan, Glenayle, Earaheedy, Wongawol, Collurabie, Lee Steere and Von Trueur). The layout of these map sheets with the simplified geology of the Earaheedy Basin is shown in Figure 2. The name of these map sheets are used to identify localities discussed in the text. For more accurate details (e.g. coordinates) on localities, the interested reader is encouraged to contact the first author.

In this paper the results of the field geological mapping, integrated with geochemical data, petrographic and sedimentological work and the available geochronology on rocks of the Earaheedy Basin are presented and discussed, with a view to introducing a model that in the present state of knowledge best explains the geodynamic evolution of the Basin.

2. Previous work

In the last quarter of the 19th century a few explorers ventured into the interior of Western Australia, and those that visited areas within the Earaheedy Basin, include Ernest Giles (Giles, 1889), David Carnegie, Lawrence Wells and John Forrest, who named several localities, such as Frere Range, Sweeney Creek and Pierre Spring. The first geological accounts and maps of the area were published by Talbot (1910; 1914, 1919, 1920, 1926).

Modern geology began with the works of Horwitz (1975a and b; 1976), Hall and Goode (1975, 1978) and Hall et al. (1977). The Earaheedy Basin made international news with the publication of two papers on Gunflint-type microbial assemblages from the Frere Formation (Walter et al., 1976; Tobin, 1990).

In the late 1970s, the Geological Survey of Western Australia commenced regional geological mapping of the map sheets that encompass the Earaheedy area, which resulted in the publication of 1:250 000 scale geological maps and accompanying Explanatory Notes (Bunting, 1980a, b; Bunting et al., 1982; Brakel and Leach, 1980; (Leach and Brakel, 1980). These works culminated with the publication of GSWA Bulletin 131 (Bunting, 1986), which comprehensively describes the lithostratigraphic units, derivation of stratigraphic names and type localities of the Earaheedy Basin. These definitions are not repeated in this paper. The latest GSWA mapping of the Basin, carried out between 1997 and 2004, resulted in some modifications of the stratigraphy as discussed in Pirajno et al. (2004) and detailed in later sections.

Mining companies conducted exploration work in the Earaheedy Basin aimed primarily at the assessment of the iron potential of the iron-formation beds of the Frere Formation and at the Mississippi-Valley type (MVT) mineralization hosted in the carbonate rocks of the Yelma Formation. Other exploration activities included the search for diamonds in lamprophyre dykes, gold in the metamorphosed and deformed rocks in the Stanley Fold Belt and uranium in calcrete. Mineral systems of the Earaheedy Basin are not considered in this paper; these are discussed in some detail in Pirajno et al. (in press).

3. Tectonic setting and regional geology

Post-Archaean tectonic events resulted in the reworking and possible fragmentation of the Yilgarn Craton's northern margin and the formation of depositional systems, while to the northwest, collision and accretionary processes were taking place. North of the Craton's present-day boundary are the Goodin, Marymia and Malmac inliers, all of which represent Archaean granite-greenstone terranes and the northern extension of the Yilgarn Craton (Fig. 1). These inliers are located within the 700-km long belt of Palaeoproterozoic volcano-sedimentary and sedimentary basins, which are considered part of the Capricorn Orogen (Fig. 1). These basins (Bryah-Padbury, Yerrida and Earaheedy), record periods of rifting, sedimentation and volcanism, along the northern passive margin of the Yilgarn Craton. The Yerrida Basin, is the oldest (ca. 2.17 Ga), and began its history as an intracontinental sag, within which low-energy siliciclastics and evaporites accumulated.

To the west, the Bryah-Padbury basins formed during accretion and collision processes, related to the ca. 2.0-1.9 Ga Glenburgh and ca. 1.83-1.78 Ga Capricorn orogenies. An uplift and rifting event affected the Yerrida Basin at 1.84 Ga, resulting in coarse and immature clastic sedimentation together with the eruption of flood basalts (Mooloogool Group). This event also caused the uplift of the Goodin Inlier with its cover of basal siliciclastic and evaporites of the Yerrida Basin, resulting in the formation of olistostrome units (Pirajno et al. 2004; Pirajno 2007). This uplift was followed by stress relaxation and extensional tectonics with asthenospheric upwelling and outpouring of the above-mentioned flood basalts.

To the east a passive margin developed, probably later than this uplift but the precise timing is poorly constrained. Sedimentation in this passive margin consisted of shallow-water clastic and chemical sediments (granular iron formation; GIF), which form the basal succession (Tooloo Subgroup) of the Earaheedy Group. Deposition of the upper part of the Group, the Miningarra Subgroup, was in a uniformly northeast-facing coastal to shelfal basin, with relatively low-energy conditions suggestive of a passive margin. No regional unconformity has been recognized between the two subgroups, but a disconformity may be present. A conglomerate at the base of the Miningarra Subgroup on Wongawol (Fig, 2), composed entirely of cobble- to boulder-size clasts of the underlying Windidda Member of the Frere Formation set in

a ironstone matrix, may record an unconformity. Such an unconformity may be a far-field effect of the ca 1.74 Ga Yapungku Orogeny (Bagas, 2004).

The northern margin of the Earaheedy Basin and the western parts of the Yerrida Basin were deformed, to form the Stanley Fold Belt (Fig. 2), before deposition of the Scorpion Group began at ca. 1.63 Ga. The most probable cause of this was the 1.68-1.62 Ga Mangaroon Orogeny (Sheppard et al., 2005). Detrital zircons dated at 1.8 Ga have been recovered from the upper stratigraphic levels of the Miningarra Subgroup (Halilovic et al., 2004), lessening the probability that the ca 1.74 Ga Yapungku Orogeny was responsible for the Stanley Fold Belt.

The basal units of both the Yerrida and Earaheedy basins, although separated by ca. 300 million years, are characterised by extensive aprons of clastic sediments, mostly mature sandstone. These sediments were generated by erosion of peneplained surfaces. Peneplanation and the generation of large volumes of siliciclastic sediments have been related to domal uplift of continental crust (Pirajno et al. 2004). Basins were starved of clastic sediments after stripping of the craton, resulting in shallow-marine to coastal carbonate and evaporite deposition, which in the Earaheedy Basin coincided with increases in dissolved iron and silica, initiating deposition of chert and iron formations. The subgroup divisions of the Earaheedy Basin indicate a change in the depositional settings, imposed by a higher energy tectonic regime, most likely due to orogenic uplifts, as previously mentioned. The Earaheedy Basin is also characterised by an asymmetry in preserved cross-section, with little deformed southern platform margins and northern margins of intensely deformed rocks (Stanley Fold Belt), typical of foreland basin architecture. There is, however, little indication of foreland basin architecture during deposition. Neither subgroup shows the characteristic, sand-rich, coarsening-upwards pattern (‘molasse’) with supply from the north, or of a foreland bulge near the southern limb of the Earaheedy Basin. The basin’s asymmetry is therefore attributed to orogenic activity after the basin became inactive, primarily during the Mangaroon Orogeny.

3.1 Pre- and post-Earaheedy igneous activity

The Earaheedy Basin is exclusively filled with sedimentary rocks with no temporally associated igneous activity. However, the Earaheedy sedimentary succession is

spatially associated with igneous intrusive rocks of Palaeo- and Mesoproterozoic age, which both intrude or juxtapose the Earaheedy Group. These igneous rocks include, the 1.99 Ga rhyodacitic rocks of the Imbin Inlier, the Glenyale and Prenti Dolerite of the 1.07 Ga Warakurna large igneous province and a suite of ultramafic lamprohyres, some of which are diamondiferous, of uncertain age.

3.1.2 Imbin Inlier

Quartz-feldspar porphyry outcrops are present on the northern margin of the Earaheedy Basin, within the Stanley Fold Belt (Fig. 2). The oucrop area of this quartz-feldspar porphyry extends for approximately 7 km in a west-northwest trend, but aeromagnetic data indicate that its full extent may be in the order of 22 km. This quartz-feldspar porphyry, which was dated by SHRIMP U-Pb method yielding an age of 1990±6 Ma (Table 2); Nelson, 2001a, b), is interpreted as a basement fragment to the Earaheedy Group. The Imbin quartz-feldspar porphyry consists of K-feldspar, quartz and plagioclase albite phenocrysts (about 20% by vol.), from 2 to 4 mm long, in a groundmass predominantly composed of a fine-grained K-feldspar-quartz mosaic with patches and flakes of green Fe-rich biotite (3-4 % by vol). This biotite is of later generation as it fills microfractures and locally surrounds phenocrysts. Leucoxene is an accessory phase. Locally, plagioclase phenocrysts exhibit resorption textures.

3.1.3 Glenayle and Prenti dolerites

In the Glenayle and Carnegie areas a series of mafic sills (Glenayle Dolerite and Prenti Dolerite; Fig. 3) are associated with numerous northeasterly and west-northwesterly trending dykes. The mafic sills and dykes intruded a succession of siliciclastic sedimentary rocks of the Collier Basin (Salvation Group), north of the Earaheedy Basin, as well as parts of the northern and eastern Earaheedy Basin. This sill and dyke complex extends for about 150 km east-southeast and about 60 km in a northerly direction and is buried by Permian glaciogene sedimentary rocks to the east. Individual sills are up to 100 m thick. Some sills consists of several thin (ca 1-2m) sheets one above the other, each separated by a thin veneer of sedimentary rocks, indicating intrusion along bedding planes. Gabbroic textures are common in thicker sills. The total thickness of the Glenyale Dolerite sill complex is not known, but geophysical data suggest that it may extend to depths of 3-4 km (Morris et al., 2003). The mineralogy of the Glenayle Dolerite is dominated by plagioclase and

clinopyroxene with or without orthopyroxene. The main feature of the Glenayle Dolerite is the presence of well developed interstitial granophyre, which tends to increase towards the top of the intrusion, where it can reach 20-30 % by volume, locally forming pods and lenses. Accessory minerals include ilmenite, magnetite and titanomagnetite, quartz and apatite. In places, ilmenite and titanomagnetite occur as poikilitic blebs up to 5 mm across. Where altered, the alteration phases include biotite, hornblende, chlorite, sericite and prehnite. Accessory amounts of sulfides (pyrite and lesser chalcopyrite) are also present. Geochemical analyses of the Glenayle Dolerite can be found in Morris and Pirajno (2005).

The Prenti Dolerite is a petrological variant of the Glenayle Dolerite, and consists of aphanitic to very fine-grained dolerite sills and dykes of (Pirajno and Hocking, 2002). The Prenti Dolerite typically contains 50-55% by volume of plagioclase (An_{56-70}) and granular augite (partially replaced by chlorite and biotite), with an intergranular-glomeroporphyritic texture, defined by bunches of fresh plagioclase crystals. In some samples, disseminated Fe-Ti oxides make up to 10% of the rock. The Glenayle and Prenti Dolerite are part of the 1076 Ma Warakurna Large Igneous Province (Wingate et al. 2004), which covers about $1.5x10^6$ km^2, extending from the sill complexes of the Mesoproterozoic Edmund basin (Bangemall Supergroup; Martin and Thorne, 2004), through to the Glenayle-Prenti sill complexes in the Collier and Earaheedy basins in central Western Australia (Martin and Thorne, 2004; Pirajno et al., 2004), to the Giles mafic-ultramafic layered intrusions in the Musgrave complex in southern central Australia; a total west to east distance in excess of 2400 km. The formation of WLIP is postulated to be the result of a mantle plume that impinged onto the base of the lithosphere at about 1100 Ma (Morris and Pirajno, 2005).

3.1.4 Lamprophyres

Western Mining Corporation (WMC, now BHP Billiton) discovered ultramafic lamprophyre intrusions in the Bulljah Pool area of the Basin and south of the Lee Steere Range, in in the eastern and northeastern parts, respectively, of the Earaheedy Basin. These rocks are unusual in that they contain small diamonds, a privilege normally reserved for kimberlites and lamproites. The lamprophyre intrusions in the Earaheedy Basin, together with marginally diamondiferous kimberlites and

lamprophyres that intruded the Archean Marymia Inlier belong to the Nabberu Kimberlite Province (Shee et al. 1999).

Little published or unpublished information is available for the Jewill lamprophyre intrusions in Lee Steere (Fig. 2). The Jewill lamprophyre intrudes rocks of the Wongawol Formation and forms an east-northeast`trending linear body along a distance of 1.3 km, within which four intrusive bodies (J1 to J4) were identified by drilling and another four inferred from drainage sampling (Carnegie Minerals N. L. Annual Reports 1994; 1995).

The Bulljah Pool ultramafic lamprophyres were studied by Hamilton (1992) and Hamilton and Rock (1990). The age of these rocks remains unresolved. Hamilton (1992) cited a Rb-Sr mica age of 849 ±9 Ma and an unpublished U-Pb zircon age of 305±4 Ma. The Bulljah Pool lamprophyres intruded gently dipping units of the Kulele Limestone and Mulgarra Sandstone (described below). The four known intrusions were named BJ1, BJ2, BJ4 and BJ5 (a BJ3 feature was later recognised not to be a lamprophyre). BJ1 is sill-like, northwest trending and was traced fo about 1 km. BJ2 is possibly a pipe or a lens-like intrusive body with an easterly strike and traced for about 400 m. The sedimentary country rocks (sandstone) display fenitic alteration. BJ4 is small weathered outcrop. BJ5 is the most extensively explored Bulljah Pool ultramafic lamprophyre, whose surface expression appears to be a pipe about 50 m in diameter. Drilling beneath the pipe-like body, however, revealed that BJ5 consists of small dykes contained in a pipe-like breccia with a steep northeastely dip (Hamilton, 1992). Samples obtained from drill cuttings show that the Bulljah Pool lamprophyres mainly consist of abundant phlogopite, perovskite, iron spinel, almandine, diopside, olivine, titanomagnetite, chromite, apatite and trace amounts of picroilmenite, barite, zircon, pyrite, pyrrhotite, K-feldspar and rutile. Calcite and quartz veining are present. Alteration and/or weathering products include gibbsite, chlorite, hematite, kaolinite and smectite (Hamilton and Rock, 1990). The abundant phlogopite is a reddish-brown type, showing zoning and locally chloritised. Olivine is pseudomorphed by serpentine, chlorite and lesser carbonate. Chlorite also form pools that may pseudomorph nepheline or melilite (Hamilton and Rock, 1990). Mineral phases recovered from concentrates obtained from loam samples, in addition to small

diamonds, include chrome pyropes, spinels, ilmenites macrocrysts, chrome diopsides, garnets

Mineral chemistry studies carried out by Hamilton and Rock (1990) show that the phlogopites are Ba-bearing titanian tetraferriphlogopites.This type of phlogopite is common in the groundmass of kimberlites and lamproites, as well as ultramafic lamprophyres (Rock, 1990). Indeed, these micas fall within the field of ultramafic lamprophyres as defined by Rock (1990).

4. The Earaheedy Basin

The Earaheedy Group, as preserved, is a 5-km-thick succession of shallow marine clastic and chemical sedimentary rocks that is divided into two subgroups (Fig. 4; Hall et al., 1977). The Tooloo Subgroup consists of the Yelma Formation (base) and the Frere Formation (top). The overlying Miningarra Subgroup consists of the Chiall Formation (base), Wongawol Formation, Kulele Limestone, and Mulgarra Sandstone (top; Fig. 4). A schematic north-to-south section across the Earaheedy Basin is shown in Figure 5. The regional structure is an asymmetric east-plunging syncline, with a vertical to locally overturned northern limb, due to compressive movements from the northeast, which created a zone of intense deformation along the exposed northern margin of the Earaheedy Basin. This zone of deformation, the previously mentioned Stanley Fold Belt, is characterised by reverse faults and shear zones that consistently dip steeply to the north, the development of slaty cleavage and phyllitic rocks and the appearance of metamorphic minerals (e. g. muscovite, sericite, chlorite). The intensity of deformation gradually decreases southward, but abruptly decreases to the north. Isolated small outcrops immediately north of the fold belt dip at low angles and are otherwise undeformed. In the sections ahead we discuss the available geochronology and describe in some detail the lithostratigraphy of the Earaheedy Group.

4.1 Geochronology

The geochronological data for the Earaheedy Basin are summarised in Table 2. A maximum stratigraphic age of 1.84 Ga is provided by the Mooloogool Group of the Yerrida Basin (Rasmussen and Fletcher, 2002), which the base of the Earaheedy Group unconformably overlies. A minimum stratigraphic age is provided by the overlying Scorpion Group (Bangemall Supergroup, maximum age of 1645 Ma;

Martin and Thorne, 2001). In lieu of other data, Pirajno et al. (2000, 2004) and Jones et al. (2000) attributed deformation of the Earaheedy Group in the fold belt to the second phase of the Yapungku Orogeny (1790 to 1760 Ma; Bagas and Smithies, 1998; Bagas et al., 2000), which records the initial collision of the North Australian and West Australian Cratons (Myers et al., 1996). This is now considered a less probable cause than the Mangaroon Orogeny (1680 - 1620 Ma; Sheppard et al., 2005), which is known largely from the northwestern Capricorn Orogen. Supporting this correlation is an unweighted mean Ar-Ar age of 1648±12 Ma from a muscovite in a schist rock in the Stanley Fold Belt and a detrital U-Pb Shrimp age of 1800 Ma from the upper Mulgarra Sandstone (see details below).

Minimum isotopic ages on glauconite grains in sandstone are provided for the Earaheedy Group by K–Ar and Rb–Sr ages of 1670–1710 Ma and 1556–1674 Ma, respectively (Preiss et al., 1975) from the Yelma Formation, and a K-Ar age of 1685 Ma (Horwitz, 1975a, b) from the base of the Chiall Formation. These ages may be related to post-depositional resetting during a deformational event, or by a thermal event possibly related to igneous activity, or a combination of these events. Pb-Pb mineralization ages of 1.65 Ga and 1.77-1.74 Ga are recorded, from outliers of Yelma Formation overlying the Yerrida Basin and the Sweetwaters Well Member (Fig. 2; Richards and Gee, 1985; Teen, 1996) respectively. These may reflect fluids mobilised during the late stages of the Yapungku Orogeny.

Grey (1994) suggested a depositional age of 1900–1800 Ma based on the stromatolite taxa of the Earaheedy Group and their similarity to taxa in the Duck Creek Dolomite of the upper Wyloo Group (Grey and Thorne, 1985). Pb-Pb whole-rock dating of carbonate in the Yelma Formation returned ages of 2010 Ma and 1950 Ma (Russell et al., 1994).

The current age constraints indicate a maximum age for the upper part of the Earaheedy Group of ca 1800 Ma, which could reflect deposition during the Capricorn Orogeny (1830–1780 Ma; Cawood and Tyler, 2004), or the Mangaroon Orogeny (1680-1620 Ma; Sheppard et al., 2007. The lower part of the Earaheedy Group is even less well constrained. It is unclear from current age constraints whether there was a significant time break between the Mooloogool Group and the lower part of the

Earaheedy Group. There is little evidence in the Earaheedy Group to suggest major active tectonism within the exposed depocentre for the Earaheedy Basin, although there is evidence to support continued sporadic tectonism, such as earthquakes, as suggested by the common presence of ball-and-pillow structures that may be seismites in rocks of the Chiall and Wongawol Formations.

4.1.1 Ar-Ar dating

A sample of quartz-muscovite schist, collected from drill cuttings (ca. 50m depth) located approximately 5 km southeast of Well 7 on the Canning Stock Route was collected for $^{40}Ar/^{39}Ar$ analysis. The sample is possibly derived from deformed and metamorphosed siltstone interbeds in granular iron formation rocks of the Frere Formation and contains aligned muscovite and chlorite in a polygonal aggregate of recrystallised quartz grains. The rock was deformed during the formation of the Stanley Fold Belt.

Argon data were collected from two single grains of white mica (Grain 1 = 400 x 200 um; Grain 2 = 500 x 300 um) hand picked from the crushed whole rock sample. These grains were chosen for analysis because they showed no signs of being broken fragments of larger grains and showed no visible signs of alteration. Analytical procedures and instrument details have been described elsewhere (Reddy et al 2004). Argon data were collected by infra-red laser step-heating of single grains at the Western Australian Argon Isotope Facility, Curtin University of Technology. Data were corrected for measured background, mass spectrometer discrimination and nuclear interference reactions. Correction factors are as follows: $(^{36}Ar/^{37}Ar)Ca$ = 0.000255, $(^{39}Ar/^{37}Ar)Ca$ = 0.00065, and $(^{40}Ar/^{39}Ar)K$ = 0.0015. Corrections for $(^{38}Ar/^{39}Ar)K$ and $(^{38}Cl/^{39}Ar)K$ were not undertaken because of the Proterozoic age and low Cl characteristics of the samples and the short amount of time between irradiation and the time of analyses. $^{40}Ar/^{39}Ar$ ages were calculated using the decay constant quoted by Steiger and Jäger (1977). J values and 1σ errors are noted in Appendix 1. Errors shown in step-heating profiles (Appendix 1) represent analytical errors and do not include J value uncertainties.

4.1.1.1 $^{40}Ar/^{39}Ar$ Results

Muscovite age spectra are reported with 1σ errors in Appendix 1 and plotted with respect to cumulative ^{39}Ar% . Each step-heating profile represents the analysis of a

single mica grain and both white mica grains yield similar ages. All mica analyses have negligible ^{36}Ar, indicating that there is no significant atmospheric ^{40}Ar component in the samples and also precluding the use of inverse isochron ($^{39}Ar/^{40}Ar$ vs $^{36}Ar/^{40}Ar$) plots to recognise any excess ^{40}Ar component. White mica data from individual Grain 1 yield relatively flat apparent age profiles with a range from 1628–1662 Ma and an unweighted mean age of 1648.2 ± 11.7 Ma. Individual step ages show some age variability but this variation is not systematic. Three of the steps define a plateau age of 1658.2 ± 1.4 Ma (MSWD = 1.5) that account for 57.6% of ^{39}Ar release from the sample. Grain 2 shows a similar range of ages (1632-1673 Ma) that yield an unweighted mean age of 1653.6 ± 14.4 Ma. In this case the spectra do not define a statistically valid plateau. In both grains there is no systematic relationship between age and either Cl or Ca content. The data from the two white mica grains therefore yield similar ages of ca.1650Ma

4.1.2 Detrital zircon ages and provenance studies

Halilovic et al. (2004) conducted a study of sediment provenance based on the U-Pb SHRIMP age of detrital zircons. The results of this work are summarised below. Zircon ($ZrSiO_4$) is widely used for detrital dating studies because it is common in many rock types, and is chemically and physically resistant, which enables it to survive cycles of burial, metamorphism and erosion. The application of U-Pb dating of detrital zircons in sedimentary successions provides important constraints for the palaeogeography and tectonic settings of sedimentary basins (e. g. Cawood and Nemchin, 2000; Nelson, 2001a, b). Age spectra provide insights into the nature and age of the source region. In addition, they constrain the timing of sedimentation with the youngest detrital zircons, giving a maximum age for the deposition of the sediments, while the oldest U-bearing minerals grown in situ provide both a lower limit of deposition, as well as valuable information on the timing of later tectonothermal events (Halilovic et al., 2004; McNaughton et al., 1999).

U/Pb data were obtained from 285 detrital zircons from six samples. Three from the basal Yelma Formation, one from the Wandiwarra Member and one from the Princess Range Member of the Chiall Formation, one sample from the stratigraphically youngest unit the Mulgarra Sandstone. Additional to this dataset are 27 zircons from a fine-grained arenite (Yelma Formation) analysed by Nelson (1997).

Archaean and Proterozoic zircon populations are present in all samples except for one sample (JHE-42) of Yelma Formation from the northern margin of the basin, which contains only Archaean zircons. Results are shown on the frequency distribution diagram of Fig. 6.

Sample JHE-31b is a coarse-grained quartz arenite from the base of the Yelma Formation, about 0.5 m above the unconformity surface with granitic rocks of the Yilgarn Craton. Of the 74 zircon grains analysed, 18 show a range in age from approximately 3280 to 2000 Ma (Fig. 6). Zircons with Archaean ages fall into three groups with the youngest analyses of these groups showing a concordia age of 2531±66 Ma. Zircons with a Palaeoproterozoic age fall into four groups, in which the youngest gave an age of 1983±51 Ma (91% concordance).

Forty four zircons were extracted from sample JHE-143 (Yelma Formation, also from just above the basement unconformity), of which 37 show greater than 90% concordance. This sample's Archaean population has a range of ages from 2.95 to 2.60 Ga with a peak at 2.65 Ga (Fig. 6). The Palaeoproterozoic zircon populations show two distinct groups at 2.2 and 2.0 Ga, with the youngest discordant analysis yielding an age of 1990±21 Ma.

Sample JHE-42 is from a fine-to-medium-grained arenite collected from the northern margin of the basin. Here the Yelma Formation is deformed in the Stanley Fold Belt. This sample yielded 15 zircons of which 12 were analysed. Ten analyses with more than 95% concordance gave a unimodal age distribution of between 2.7 and 2.6 Ga (Fig. 6).

Sample JHE-149, a sandstone from the Wandiwarra Member of the Chiall Formation, taken from the southern margin of the Basin. Of the 69 analysed zircons, 48 show a 90% concordance. The Archaean population contains two groups that are clustered around 3.0 and 2.8-2.6 Ga (Fig. 6). The oldest grain indicates an age of 3242±15 Ma. The Palaeoproterozoic population of two groups exhibits age peaks at 2.25 and 2.06 Ga.

Sample JHE-40 is from a quartz arenite of the Princess Ranges Member of the Chiall Formation on Wongawol (Fig. 2). Palaeocurrent data from this site suggest a

general northeasterly direction of sediment transport. Of the 40 grains analysed, 25 have concordancy of 90% or above. The oldest grain yielded an age of 3465±13 Ma, but the majority having a range of between 2.9 and 2.6 Ga. The Palaeoproteroic zircon population yielded ages ranging from 2.3 to 1.8 Ga, with the youngest single grain (97% concordance) having an age of 1876±19 Ma.

Finally, a glauconitic quartz sandstone of the Mulgarra Sandstone, sample JHE-160, was taken from the base of the unit. From this sample 46 detrital zircons were analysed of which 25 show 90% or above concordancy. The Archaean population consist of a single analysis dated at 3190±10 Ma and a series of analyses with a broad peak at 2.7-2.6 Ga (Fig. 6). The Palaeoproterozoic population consists of two groups, one with a peak at around 2.3 Ga, the other with a continuum of ages in the range 2.2 to 1.8 Ga. The youngest grain, 90% concordant, gave an age of 1796±58 Ma. Four discordant analyses range from 1.79 and 1.73 Ga, but with large errors. The youngest most concordant age is 1808±36 Ma.

Cathodoluminescence imaging showed that both Archaean and Proteroizoic grains have oscillatory zoning suggesting an igneous origin. The Archaean zircons are well rounded or are broken fragments of larger grains. A number of Palaeoproterozoic zircons show evidence of recrystallisation.

The analyses of the 285 zircons, augmented by the earlier analyses of 27 zircon grains (Nelson, 1997) show multiple age peaks in Fig. 6 that clearly indicate detrital input from source regions of different ages. The Palaeoproterozoic detritus is dominated by peaks in the age range of 2.3-2.2, 2.0 and 1.8 Ga, whereas those of Archaean age are dominantly in the range 2.7-2.6 Ga, with the oldest in the 3.5 Ga bracket. A likely source of detritus with ages of 2.0 and 1.8 Ga is the southern part of the Gascoyne Complex (Sheppard et al., 2004). More specifically, this detritus could have derived from the granitic rocks of the 2005-1970 Ma Dalgaringa Supersuite of the Glenburgh Terrane (Sheppard et al. 1999; Occhipinti and Sheppard, 2001), whereas the 1.8 Ga zircon grains could have derived from the granites of the 1830-1780 Ma Moorarie Supersuite (Occhipinti et al., 1998). A possible source region for the 2.3-2.2 Ga zircons is the Glenburgh terrane (Gascoyne Complex), on the basis of rims on zircons in basement gneiss of this terrane, which yielded ages of about 2.2-2.4 Ga (Kinny et

al., 2004). The youngest, single zircon grain, dated at 1.8 Ga, is from the Mulgarra Sandstone, and provides a maximum age for the upper Miningarra Subgroup. Another maximum age, for the base of the Earaheedy Group, is given by a U-Pb monazite age of 1843±14 Ma (Rasmussen and Fletcher, 2002) from the Maraloou Formation, which is the youngest lithostratigraphic unit in the Yerrida Basin and is unconformable beneath the western Earaheedy Basin. Both ages are much younger than Pb-Pb carbonate ages for the Yelma Formation (see Table 2; and Russell et al. 1994) of 2.01 and 1.95 Ga, and the $\delta\ ^{13}C_{carb}$ positive excursion in the same rocks suggesting an age of 1.9 Ga (Lindsay and Brasier, 2002). If the latter are correct, they could be taken as supporting the concept of a significant hiatus between the Tooloo and Miningarra Subgroups.

In conclusion, detrital zircon populations, Ar-Ar dating of mica, and a monazite age from immediately beneath the basin, indicate that the deposition in the Earaheedy Basin began at most at about 1.84 Ga, concluded after 1.8 Ga but before 1.65 Ga. Palaeocurrent directions gathered during mapping show that the sediments of its depositional system had a significant source to the west and southwest, which may be related to uplift in the southern Gascoyne Province during the Capricorn Orogeny. The basin succession was deformed, and the Stanley Fold Belt developed, during the 1.68-1.62 Ga Mangaroon Orogeny (Sheppard et al., 2005), and possibly the Yapungku Orogeny at 1.79 -1.76 Ga (Bagas, 2004), although the latter is very close in age to the maximum depositional age of the Mulgarra Sandstone. Alternatively, the Yapungku Orogeny may mark, and be the cause of, an unconformity between the Tooloo and Miningarra Subgroups.

4.2 Lithostratigraphy

The Tooloo Subgroup contains the Yelma and Frere Formations (Figs. 2 and 4). The Miningarra Subgroup comprises, from older to younger, the Chiall Formation, Wongawol Formation, Kulele Limestone and Mulgarra Sandstone (Figs. 2 and 4), aggregating approximately 3000 m in thickness. These lithological units are discussed below.

4.2.1 Yelma Formation

The Yelma Formation is the basal unit of the Earaheedy Group and contains sandstone, shale, carbonate and minor siltstone and conglomerate and records a

regional marine transgression. The formation is quite variable laterally and vertically in both thickness and composition. Sandstone beds in the southeast are trough cross-bedded, with local asymmetric ripples and mudcracks. Scattered stellate pseudomorphs may be after evaporitic minerals. A 100m-thick stromatolitic carbonate facies in the southwest of the basin is differentiated as the Sweetwaters Well Member. At and near the surface, this stromatolitic dolomite is generally altered to chert. A sandy dolomite unit near the base of the Sweetwaters Well Member contains thin intercalations of volcaniclastic shard-rich silty beds that were presumably derived from contemporaneous, but distal, explosive volcanic eruptions. A localised conglomeratic unit, the Yadgimurin Member, lies at the base of the Yelma Formation in the western part of the Earaheedy Basin (Merrie; Fig. 2).

The upper contact with the Frere Formation is marked by the first major occurrence of chert or granular iron-formation (Bunting, 1986), although in places stromatolitic forms persist between granular iron beds for up to 5-6 m above the contact. The thickness of the formation ranges from 3 m in the southeast, through 150 m in the type area (Hall et al., 1977), to at least 500 m in a drillhole in the northwestern part of the basin. Bunting (1986) estimated a thickness of 1500 m in the Stanley Fold Belt, but we interpret this as due to structural repetition.

In the westernmost parts of the Earaheedy Basin, the Yelma Formation is a unit of clastic and dolomitic sedimentary rocks at the base of the Earaheedy Group. This unit occupies much of the northeastern portion of Thaduna (Fig. 2) and consists mainly of quartz arenite, stromatolitic dolomite and chert breccia. In this area, the base of the Yelma Formation, includes quartz lithic sandstone and quartz conglomerate, which lie unconformably on quartz arenite of the Finlayson Member of the Juderina Formation (Yerrida Basin), and is exposed on the southern edge of Lake Gregory (Thaduna, Fig. 2). The main constituents of the lithic sandstone, near the base of the formation are quartzose and sericitised lithic grains, and subordinate polycrystalline quartz, chlorite and turbid feldspar.

Two boreholes drilled 3 km south of Little Well in Thaduna (Fig. 2; Meakins and Watsham, 1994), together with field observations, provide a representative 400 m-thick stratigraphic section of the Yelma Formation. This section, schematically

represented in Figure 7, consists of grey to pink, massive, silicified dolomite beds in the lower part. Argillaceous interbeds are locally present between 350 m and about 200 m below surface. This interval is overlain by a 120 m-thick unit of dolomite with solution breccia interbeds, containing some interstitial kerogen material and sulfides. This is in turn, overlain by about 100 m of pink to grey thinly laminated dolomite, dolomite breccia, ferruginous sandstone and arenite, followed by 20 m of dolomite with microbial laminae. The latter is a distinct rock, which may be part of the Sweetwaters Well Member.

Outcrops on the northwest side of Lake Gregory, consist of dolomite breccia, that is commonly chertified, cream-coloured and fine- to medium-grained, bedded and laminated dolomite with minor lenses of ferruginous sandstone and siltstone, associated with stromatolitic dolomite. In the area around Edingunna Spring (Marymia; Fig. 2), outcrops of these units include silcretized chert breccia, underlain by coarse breccia. This material is underlain by pebble beds, about 2 m thick, comprising subrounded to rounded pebbles up to 5 cm in diameter, dominantly of quartz and chert, and a coarse-grained, poorly sorted quartz (and feldspar?) arenite. The latter is probably the base of the Yelma Formation and may correlate with the Yadgimurrin Member (see below).

Most dolomitic rocks consist of a packed aggregate of small (averaging 0.1 mm) dolomite rhombs, with interstitial iron oxides. The dolomite also locally contains disseminated quartz grains and submicroscopic stylolites. Siltstone interbeds contain quartz, kaolinite, illite and sericite.

Sandstone in the Yelma Formation is typically well sorted and composed of well rounded quartz grains and minor detrital tourmaline and zircon. They are grain-supported and with a diagenetic microcrystalline quartz or chalcedonic quartz cement. Quartz sandstone is present in the eastern parts of the central uplift of the Shoemaker impact structure (Section 6). This rock is cross-bedded and consists of a packed aggregate of rounded quartz grains, showing diagenetic quartz overgrowths and minor detrital tourmaline and interstitial recrystallized quartz.

The Yelma Formation was deposited in a fluvial to coastal setting, with carbonates of the Sweetwaters Well Member developing in a saline coastal-lagoonal

environment. Limited palaeocurrent data for the Yelma Formation on Wongawol suggest that sediment transport was towards the north-northwest. The Yelma Formation is interpreted to record a marine transgression over the Yilgarn Craton. Sedimentary structures suggest a shallow water to partly emergent, fluvial to coastal marine depositional environment, which was locally evaporitic at the base of the Yelma Formation. The upper part of the Yelma Formation suggests quiet water conditions and may reflect deposition in a lagoonal environment developed behind a carbonate bank, possibly represented by the Sweetwaters Well Member. As mentioned in Section 4.1.2, the detrital zircon populations are dominantly 2.6-2.7 Ga in age, with a smaller 2.2 Ga population, and minor 2.0 Ga zircons and suggest the Yilgarn Craton and southern Gascoyne Complex were important sediment sources during basin development.

4.2.1.1 Sweetwaters Well Member

The Sweetwaters Well Member is about 100 m thick and consists mainly of stromatolitic dolomite with sandy dolomite and dolomitic feldspathic sandstone beds at top and bottom of the dolomitic succession. The dolomitic feldspathic sandstone unit at the top of the dolomite grades eastward to a micaceous sandstone and is overlain by granular iron formation rocks of the Frere Formation. The lower contact is marked by about 15 metres of transitional interbedded sandstone and dolomite passing upward to a sandy and feldspathic dolomite unit that contains quartz, microcline, albite, chert and micritic dolomite embedded in a coarse-grained dolomite cement. The Sweetwaters Well Member dolomite is light grey to grey in colour, massive to algal laminated, commonly with stromatolite forms. In northwest Nabberu (Fig. 2), the Sweetwaters Well Member was intersected in a number of drillholes sunk through the Frere Formation (Pirajno, 2004, 2002). Samples of stromatolitic dolomite collected from drill core show two phases or domains of dolomite, one is an aggregate of coarse-grained dolomite crystals, the other is microcrystalline (micritic) and is associated with microbial laminae. The coarser-grained dolomite has intergranular microcrystalline quartz and sericite. In some cases micritic dolomite forms peloids that are cemented by chalcedonic quartz. Locally, the carbonate material is replaced by cryptocrystalline quartz (chert) and chalcedonic quartz.

Along the southern shore of Lake Nabberu (Nabberu; Fig.2), scattered outcrops of Sweetwaters Well Member are generally chertified, except for an area along a small tributary, where there are good exposures of subhorizontal stromatolitic dolomite. Here, the dolomite exhibits fine microbial laminae and includes the stromatolites *Murzuna Nabberuensis, Omachtenia teagiana* and *Asperia digitata* (Fig. 8; Grey 1984; 1994). Drillcore sections indicate that stromatolites are generally present in metre-scale upward-shallowing cycles. They include *Asperia digitata* (Grey 1984; 1994), which is believed to have grown in restricted, quiet water environment, possibly supratidal ponds; *Pilbaria deverella* (Grey, 1984) indicative of moderately high-energy, lagoonal conditions; and *Ephyaltes edingunnensis* (Grey, 1994), which formed in deeper quiet water, and *Murgurra nabberuensis* (Grey, 1984) which colonised moderate energy patch reefs. Details of stromatolite taxa of the Earaheedy Basin can be found in Grey (1984, 1994). Grey (1994) suggests that these stromatolite forms are indicative of an upward shallowing, lagoon to supratidal, environment (Fig. 9A,B). It should be pointed out that the use of stromatolite taxa to identify depositional settings and relative ages is still contentious (see Altermann, 2004 for a brief review). However, in this work the identification of stromatolites does provide useful and reasonable constraints for depositional models, which are also supported by sedimentological evidence.

A sedimentological study, aimed at constraining the depositional environment of the Frere Formation, was carried out by Price (2003). In his study, Price (2003) defined 8 facies in the Frere Formation (see below) and 2 in the Yelma Formation. The facies of the Yelma Formation are: 1) Stromatolitic dolostone and 2) Dolostone. The former is a white creamy dolostone, with gentle wavy laminations and with alternating, ~20 m thick, horizons of *Asperia digitata* and *Pilbaria deverella*. The second facies, is a creamy white dolostone, with weakly developed wavy laminations and rare ripple cross-laminations and has crystalline mosaic fabric. This facies contains rare *Pilbaria deverella*, which as mentioned above may have formed in a shallow lagoonal system.

4.2.1.2 Yadgimurrin Member

This is a localised very coarse, poorly sorted conglomeratic unit with sandstone lenses, about 100 m thick (Bunting, 1986) at the base of the Yelma Formation (Fig. 4), about 10 km southeast of the Baumgarten Reward gold deposit in the Marymia

Inlier (Bagas, 1998a, b). The Member contains clasts that range from approximately 50 mm to 1 m in size, are well rounded and include granite, quartzite, chert, and chert breccia enclosed in an arkosic matrix. Pods and veins of jasperoidal chert and quartz are associated with this conglomerate and may be the result of localised hydrothermal fluid flow along the tectonic contact between the Marymia Inlier and the Yelma Formation (Adamides et al., 2000a). Bunting (1986) suggested that some of these clasts are derived from the underlying Mooloogool Group of the Yerrida Basin (Pirajno et al., 2004). The Yadgimurrin conglomerate was assigned to the Yelma Formation by Bunting (1986) on the basis of the nature of the clasts and a distinct easterly dip. The Yadgimurrin Member is interpreted as a local conglomeratic fan, associated with syndepositional fault movements (Adamides et al., 2000a).

4.2.2 Frere Formation

The Frere Formation, formally defined and described by Hall et al. (1977), records the onset of major Fe oxide precipitation within the Earaheedy Basin and consists of up to four major granular iron-formation intervals, separated by at least three major shale and siltstone bands, and minor carbonate (Fig. 10). The Frere granular iron formation (GIF), an important iron resource, is similar to the Superior iron formations and is one of few of these types of iron formations recorded outside of North America (Goode et al., 1983; Trendall, 2002). The Frere Formation is exposed along the southern and northern margins of the Earaheedy Basin. On the southern margin the Formation is unmetamorphosed, undeformed or only mildly deformed, forming layers that are shallow-dipping to the north. On the northern margin of the Basin, the Frere Formation is deformed and folded into a south-verging synclinal structure with a steep to overturned limb (Stanley Fold Belt, see below). The total thickness of the Frere Formation was estimated by Bunting (1986) at about 1200-1300 m, but field evidence, suggests this thickness may be exaggerated due to structural repetition and we estimate the actual thickness of the Formation to be about 600 m.

The Frere Formation consists of alternating beds of hematitic shale, green chloritic siltstone and granular iron-formation. Granular iron-formation horizons consist of granular iron- beds, typically between 0.5 cm to 20 cm thick, interbedded with jasper, chert, shale and siltstone. Drillcore and outcrop show that chert intraclasts are common and range in size from 1.5 cm to 35 cm. Contact between granular iron

beds and siltstone units are commonly irregular and typically marked by soft-sediment structures, such as rip-up clasts, load and flame structures. The scale of the granular iron beds and siltstone banding ranges from millimetre to metre and up to 100s of metres (micro-, meso- and macroscale) and is similar to that recorded for banded iron-formations (Trendall, 2002; Fig. 11). The intercalated shale bands appear to increase in thickness at the expense of the granular iron-formation, towards the southeast. The upper contact with the Karri Karri Member of the Chiall Formation is transitional and defined as the last major chert, jasper or iron-formation (Hall et al., 1977).

Granular iron formation in the Frere Formation has a strong magnetic signature even through significant overburden, and is negatively magnetised in the south and positively magnetised in the north (Stanley Fold Belt). Overall the Frere Formation forms an almost continuous zone of high total magnetic intensity on aeromagnetic images, delineating the present-day geometry of the basin (Fig. 2B). Along the sourthern margin of the basin, northwest-trending structures are negatively magnetized, whereas east- and north-trending structures, as well as the circular structures that define the Shoemaker impact structure, are positively magnetized. In the Stanley Fold Belt strong positive magnetic signatures define deformation structures such as folds, reverse faults and shear zones.

The granular iron-shale/siltstone couplets of the Frere Formation are indicative of cyclic changes in primary sediment composition that probably relate to sea level changes and supply of iron and silica. Cross-bedding is locally visible in GIF beds, and in general sedimentary structures indicate traction-current deposition.

Granular iron formation in the Frere Formation is texturally and mineralogically similar to those in the Lake Superior region, North America. Walter et al. (1976) and Tobin (1990) described and compared microfossils within the iron-formation with those in the Gunflint Formation in the Superior Province. The Gunflint Iron Formation from that region contains microfossils (Gunflint-type microbial communities) that are similar to those found in the Frere Formation and in the Windidda Formation (Walter et al., 1976; Hall and Goode, 1978; Goode et al., 1983; Tobin, 1990). Gunflint-type microbiota are considered to be characteristic of marine

694 subtidal environments (Tobin, 1990). These microfossils consists of contorted and/or
695 randomly oriented filaments and include Gunflintia *minuta*, Animikiea *septata*,
696 Eoastrion *simplex*, Eoastrion *bifurcatum*, Huraniospora *psilate*, Kakabekia *umbellata*
697 and Archaeorestis *schreiberensis* (Walter et al., 1976; Tobin, 1990).

698 In the Stanley Fold Belt, the Frere Formation is intensely deformed, with tight
699 folds, sheared limbs, and reverse faults. On Rhodes and parts of Mudan (Fig. 2), the
700 Frere Formation is intensely tectonised, forming mylonitic zones that resemble
701 banded iron-formation (Pirajno et al. 2000; Pirajno and Hocking, 2001). Similarly, in
702 the northeast corner of Granite Peak (Fig. 2), exposures of the Frere Formation lie
703 within the Stanley Fold Belt, where the GIF is tightly folded, tectonised and well-
704 laminated, and is termed laminar iron-formation. It resembles banded iron-formation,
705 but contains a pervasive fabric that is interpreted to be a tectonic overprint of the
706 original bedding. Lamellae vary from reasonably continuous to discontinuous lenses
707 and are generally between 10 and 50 mm thick. The limbs of folds in northeast Granit
708 Peak are commonly brecciated and cut by quartz vein stockworks. On Nabberu, the
709 Frere Formation is well-exposed in the Frere Range, along the northern side of Lake
710 Nabberu, and in the Shoemaker impact structure, where it forms the inner collar
711 (Pirajno, 2002).

712 Shale and siltstone intervals which separate GIF beds are similar to those of the
713 Yelma Formation and the Karri Karri Member of the Chiall Formation. They
714 commonly have a bedding fissility, accentuated by weathering. Siltstone is parallel-
715 laminated, and trough and planar cross-laminated. Ripples are typically linguoidal or
716 sinuous and interference patterns are common. Individual laminae are 1 mm to 10mm
717 in thickness. Massive greenish chert is locally present and exhibits remnant peloidal
718 textures and quartz filled fractures, and lies parallel to a northwest trending,
719 negatively magnetized structure. It is interpreted to be GIF that has been strongly
720 silicified and fractured due to fluid flow along this structure.

721 An interesting aspect of the GIF rocks in the Earaheedy Basin is their common
722 association with a small shrub. This shrub, *Micromyrtus ciliata*, is characterised by
723 tiny, crowded bright leaves, pink buds and small white flowers. Where present,

Micromyrtus ciliate is the exclusive vegetation covering areas underlain by granular iron-formation rocks.

4.2.2.1 Textural features, petrography and mineralogy

The textural and petrological features of granular iron-formation were described in detail by Hall and Goode (1978) and Goode et al. (1983). A typical thin section, sketched in Figure 11, provides a good example of microscale banding. A granular iron horizon contains a 1-cm-thick band of closely packed hematite peloids and intraclasts, cemented by orthochemical cryptocrystalline silica (chert) and/or allochemical chalcedony. This band is overlain and underlain by 1-4 mm thick laminae of pale green silt composed of green iron-rich chlorite (Fig. 12b), anhedral hematite, abundant disseminated euhedral magnetite crystals and angular quartz, overprinted by carbonate, and lenticles of chlorite-quartz.

Individual granular iron-formation beds consist of chert (cryptocrystalline silica), iron oxides (hematite and/or magnetite; Fig. 12c, d, e), microplaty hematite (Fig. 12f), and jasper (cryptocrystalline silica with finely disseminated hematite) peloids in a cherty, chalcedonic (allochemical) or jasperoidal (orthochemical) cement (Figs 12a, b, c). Peloids commonly exhibit concentric laminae, especially where the peloids are partially replaced by microcrystalline quartz (Fig. 13 a, b, c, d). Hematite is replaced by microplaty hematite and/or magnetite in GIF beds deformed in the Stanley Fold Belt. In fractures and zones of deformation the granular iron formation beds are pervasively silicified, with the peloids and the interbedded iron-chlorite-rich shale replaced by stilpnomelane. Maghemite and martite replace the hematite and magnetite in zones of supergene alteration. Shale and siltstone units are parallel-laminated, and contain quartz, iron-rich chlorite and disseminated euhedral magnetite. The sphericity of peloids is highly variable and generally depends on the degree of early diagenetic compaction and lithification. The average spherical dimensions of over one hundred peloids indicate the long axes of the ellipse average 0.52 mm, whereas the short axes average 0.26 mm, with a length to width ratio of 2.0. Peloids commonly contain syneresis cracks infilled with quartz or chalcedony.

Examination of drill core reveals that thin bands (few cm) of peloidal carbonate are locally intercalated with the granular iron-formation. Typically, carbonate peloids

exhibit close packing, are plastically deformed and commonly replaced by stilpnomelane and/or euhedral magnetite (Fig. 13d, e, f).

Reflected-light petrographic studies of the granular iron beds reveal that the main iron minerals are hematite (microplaty, blades and irregularly-shaped blebs), magnetite, maghemite, martite and goethite (Figs. 12e, f). Maghemite and martite are products of the oxidation of magnetite, whereas goethite is related to recent weathering. Magnetite crystals are especially common along faults and in deformed Frere Formation.

A possible paragenesis of the iron minerals is:

Hematite → magnetite → martite-hematite→ maghemite → goethite.

This sequence may have resulted from the deposition of primary hematite, followed by hydrothermal magnetite along fault zones, subsequent to oxidation to produce martite and maghemite, and late supergene redistribution of iron to precipitate the goethite.

4.2.2.2 Alteration of granular iron-formation

Alteration of the Frere Formation is common, especially along faults and in fractures around the Shoemaker impact structure and close to the Lockeridge Fault (Fig. 2). This alteration is manifested by cryptocrystalline (chert), microcrystalline and chalcedonic quartz, and carbonate that replace the Fe oxide peloids and the orthochemical ferruginous or jasperoidal matrix. Stilpnomelane and minnesotaite are also present and may be locally abundant. In places, stilpnomelane forms pervasive replacements. Some of the more typical alteration features are illustrated in Figures 14 and 15.

West-northwest of the Shoemaker structure, diamond drillholes intersected Frere Formation rocks that exhibit varying degrees of stratabound alteration. This alteration consists of more than one phase of silicification and replacement by stilpnomelane and carbonate (probably dolomite). The paragenesis of this alteration is difficult to gauge because the same alteration minerals appear in more than one event. However,

783 in general, the following paragenetic sequence can be reconstructed, on the basis of
784 petrographic studies:

785 Hematite peloids → stilpnomelane → chert → carbonate → chlorite + carbonate
786 + magnetite.

787 In places, only one event can be seen, e. g. carbonatisation (Fig. 15a, b), or total
788 replacement of the chloritic siltstone by stilpnomelane (Fig. 15a, b). In other instances
789 two or more alteration events are observed, such as partial silicification overprinting
790 peloids that had been earlier replaced by stilpnomelane (Fig. 15e), and by late
791 magnetite (Fig. 15d, f). Similarly, all stages of carbonatisation are present, from
792 localised development of carbonate rhombs (Fig. 15b, c) to more pervasive carbonate
793 alteration. Late alteration phases include magnetite, which overprints dolomite (Fig.
794 15f) or magnetite + stilpnomelane + chlorite in late fractures that cut across all phases.
795 Peloidal carbonate also exhibits alteration, which consists of microcrystalline silica,
796 chlorite and stilpnomelane, with a late overprint by euhedral magnetite (Fig. 15e, f).

797 Carbonate porphyroblasts and dolomitisation are also associated with the sulfide
798 mineralization in the Sweetwaters Well Member stromatolitic dolomite (Pirajno,
799 2002).

800 Stilpnomelane, a complex K, Ca, Na, Fe, Mg, Al hydrous silicate, is common in
801 iron-formation world-wide and is generally found in Fe and Mn-rich low-grade
802 regionally metamorphosed sedimentary rocks (Deer et al., 1965). Stilpnomelane-rich
803 beds have been reported from the banded iron-formation of the Transvaal Supergroup
804 in South Africa (LaBerge, 1966; Beukes and Klein, 1990) and the Hamersley
805 province in Western Australia (LaBerge, 1966; Trendall, 2002). Here, the
806 stilpnomelane beds have been interpreted as products of low-grade metamorphism of
807 volcanic ash (LaBerge, 1966; Beukes and Klein, 1990). The stilpnomelane, silica and
808 carbonate replacement of beds of granular iron-formation rocks in the Earaheedy
809 Basin is interpreted to be related to K-Si-Ca-CO_2-rich basinal fluids (Pirajno et al., in
810 press). Stilpnomelane preferentially replaces Fe-chlorite-rich siltstone interbeds and a
811 possible reaction to explain the change from Fe-rich chlorite-dominated siltstone beds
812 to stilpnomelane-dominated beds is (Deer et al., 1965):

Fe-rich chlorite (GIF) + SiO_2 + K_2O → stilpnomelane +MgO + Al_2O_3

4.2.2.3 Facies analysis

Price (2003) recognised 8 facies in the Frere Formation, determined on the basis of sedimentary structures, grain size, composition, matrix/cementing material. Details are given in Table 3.

4.2.2.4 Rare earth elements (REE) geochemistry

Price (2003) also conducted a comparative study of the abundance of REE in the granular iron formation with those of two other Precambrian iron formations, Gunflint in Canada and Griquatown in South Africa. The following is summarised from Price's work.

The Gunflint iron formation in Ontario is also a granular iron formation, composed of peloids and ooides in a predominantly quartz cement. Whole rock Sm-Nd isochron dating indicates that the Gunflint iron formation was deposited at around 1900 Ma (Jacobsen and Pimentel-Klose, 1988). The geochemical dataset used by Price (2003) was taken from Derry and Jacobsen (1990). The Griquatown iron formation of the Transvaal basin in South Africa is a granular iron formation that ovelies the Kuruman microbanded iron formation (Beukes and Klein, 1990). The Griquatown iron formation consists of chert-rich peloids and intraclasts in a chert cement (Beukes and Klein, 1990). Radiometric ages indicate that the Kuruman and Griquatown iron formations were deposited between 2357±53 and 2239±90 Ma (Walraven et al., 1990). The geochemical dataset of the Griquatown iron formation was taken from Beukes and Klein (1990). REE patterns for the Gunflint and Griquatown iron formation are shown in Figure 16.

The distribution of samples of peloidal granular iron formation collected during field mapping is shown in Figure 17A.. In addition to REE , these samples were also analysed for major and trace elements by Genalysis Laboratory Services (Perth) using ICP-MS and results are presented in Table 1 in Appendix 2. Eleven samples were selected for the study of REE abundances, all containing in excess of 15 wt % Fe_2O_3. The data were normalised to NASC (North American Shale Composite; Gromet et al., 1984) and the relevant diagram shown in Figure 17B. The REE patterns show a slight HREE depletion relative to LREE, with the exception of 3 samples. Some samples

844 show a marked negative Ce anomaly, and all samples exhibit a weak positive Eu
845 anomaly. By comparison with the Gunflint and Griquatown iron formation, the Frere
846 Formation contains higher REE concentrations. The positive Eu and negative Ce
847 anomalies in the Gunflint and Griquatown possibly represent high temperature
848 hydrothermal input in a seawater dominated system (Beukes and Klein, 1990; Bau
849 and Moller, 1993; Klein and Ladeira, 2000). The similar REE patterns for the
850 Gunflint and Griquatown iron formation suggests a similar depositional mechanism.
851 The differences of the Frere Formation REE patterns may be due to one or more of
852 the following: 1) contamination in the Frere rocks by clastics; this is supported by the
853 high abundances of TiO_2 and Al_2O_3 (see Appendix). 2) The Frere rocks were probably
854 deposited in shallower water than the Gunflint or the Griquatown iron formations; this
855 is shown by differences in HREE patterns and the Ce anomalies.

856 **4.2.2.5 Windidda Member**

857 Bunting (1986) considered the Windidda Formation as a separate unit that
858 overlaid the Frere Formation, but subsequent to mapping showed that the former
859 Windidda Formation is stratigraphically equivalent to the upper part of the Frere and
860 for this reason it is now considered a Member of the Frere Formation. The Windidda
861 Member is typically characterized by poorly defined low relief outcrops and consists
862 of stromatolitic carbonate, shale and siltstone, minor jasperoidal beds and minor
863 granular iron-formation. The shale and siltstone are very similar to shale and siltstone
864 of the Frere Formation. Locally, peloidal jasper is interstitial to stromatolites and thin
865 granular iron beds are interbedded with stromatolitic carbonate. The Karri Karri
866 Member was first mapped as part of the Windidda Formation, but during later work
867 was re-interpreted as part of the Chiall Formation (Fig. 4). The contact of the
868 Windidda Mamber with the overlying Chiall Formation is defined as the top of the
869 uppermost carbonate horizon (Hall et al., 1977). The lower contact with the Frere
870 Formation is placed at the first occurrence of carbonate or the last occurrence of iron
871 formation, chert or jasper. The thickness of the Windidda Member varies laterally.
872 Bunting (1986) estimated the thickness in the type area to be about 800 m, but more
873 reasonable estimates are in general between 60 m and 150 m, and perhaps up to 500
874 m. In places, the proportion of granular jasper is high, forming GIF beds. The cores of
875 concentrically zoned larger granules locally consist of a yellow-green iron silicate

mineral, possibly glauconite or chamosite, which is partially replaced by hematite, suggesting iron-oxides in this sample may be secondary.

Stromatolite forms in the Windidda Member range up to 30 cm in diameter and include *Carnegia wongawolensis, Nabberubia toolooensis, Windidda granulosa and Kulparia* (Grey, 1984). *Carnegia wongawolensis,* is the dominant form recognized on Wongawol (Fig. 2) and forms colonies of branching forms. Locally, peloidal jasper is interstitial to stromatolites and is incorporated within stromatolite laminae. *Windidda granulosa* and the associated abundant ooids in the Windidda Member, are suggestive of sandy shoals and a more agitated environment. The palaeoecological significance of the Sweetwaters Well stromatolites is treated in detail by Grey (1994).

Shale and siltstone dominated units contain laminated to massive carbonate beds of variable thickness that are generally < 1 cm. Jasper beds, which are up to 10 cm in thickness, are interbedded with carbonate in carbonate dominated units. In addition, granular or peloidal jasper locally forms a matrix to stromatolites. Intraclastic carbonate breccias are common in the Windidda Member, becoming more abundant towards the upper part of the formation. Locally, carbonate conglomerate is exposed at the top of the Windidda Member and is commonly transitional to a siliciclastic conglomerate at the base of the Chiall Formation. Clasts are generally well-rounded, up to 15 cm in length, occasionally imbricate and are dominantly carbonate or siltstone. Rare small stromatolites are contained in this horizon. Clasts are cemented by carbonate and contain a glauconite and quartz sandstone matrix.

The Windidda Member is interpreted to reflect a carbonate bank and lagoonal environment that developed synchronous with deposition of granular iron-formation. Minor jasper granules washed into the carbonate bank and lagoonal environment and intraclastic breccias probably reflect storm events.

4.2.3 Depositional environment of the Tooloo Subgroup and the origin of the iron formations

The Earaheedy Basin has a special importance in the tectonostratigraphic record of Palaeoproterozoic terranes because of the presence in the basin stratigraphy of the GIF units of the Frere Formation. The presence of the Frere Formation GIF could be related to a period of mantle plume(s) breakout, which resulted in global magmatism

907 at ca 1.8 Ga, supercontinent breakup, trailing margins and deposition of iron-
908 formations (cf. Barley et al., 2005). In addition, oxygenic photosynthesis associated
909 with the GIF may have contributed to the rise of oxygen levels in the Earth's
910 atmosphere. Granular iron-formation formed in shallow marine continental shelf to
911 coastal conditions. Ferruginous peloids were deposited after some reworking by
912 mechanical processes, with variable terrigenous contamination. The deposition of GIF
913 in the Earaheedy Basin coincides with a decrease in the supply of sand-sized
914 siliciclastic detritus into the basin. According to Beukes and Klein (1992), ferruginous
915 peloids form by accretion in wave- and current-agitated iron-rich waters and
916 following reworking are deposited with variable amounts of terrigenous
917 contamination. In modern clastic-starved marine shelves, amorphous Fe oxide and/or
918 oxyhydroxide peloids (or ooids) appear to form as concretions a few centimetres
919 below the sea floor, as a result of Fe and silica exhalative fluids that rise from the
920 substrate (Heikoop et al., 1996; Donaldson et al., 1999). An alternative view is that
921 the ooids grow from the precipitation of Fe-rich clays that become oxidised to
922 goethite at the sediment-water interface (Donaldson et al., 1999). In either case the Fe
923 oxide/oxyhydroxides alternate with silica to form the concentric laminae. The reason
924 for the Fe oxide-silica alternations is not understood, but it may relate to pulses of
925 fluid emission based on episodic temperature variations (high T, Fe precipitation;
926 lower T silica precipitation). Dehydration and diagenesis would produce hematite and
927 at higher temperatures magnetite and the formation of these ooidal or peloidal
928 structures would occur in a geologically short time. Mechanical reworking by wave
929 action and/or strong currents would account for the classic shape of the ooids
930 (Heikoop et al., 1996).

931 Cross-bedding, locally recognized in GIF beds, indicates dominantly moderate-
932 energy conditions. Local, peloidal carbonate beds that are intercalated with beds of
933 iron-formation do not show evidence of current transport and may represent a
934 particulate sediment that accumulated *in-situ* (Blatt et al., 1980, p. 469). However, the
935 intercalated shale and siltstone horizons show structures best explained by traction-
936 current depositon, from Granite Peak southwards (Fig. 2).

937 The GIF beds, shale, and siltstone all have different iron and silica content both
938 within and between units. This points to a complex, varying interrelationship between

clastic influx, dissolved silica and dissolved iron. The supply of dissolved silica appears to have been variable at all scales, and can be interpreted as a result of fluctuating concentrations. The supply of iron is also interpreted as the result of fluctuating concentrations but with a high proportion of iron remaining in suspension throughout deposition of the Frere Formation. The shale interbedded with granular iron-formation and in major shale horizons may indicate periods where the rates of silica and iron precipitation were low.

Both iron-rich and silica-rich fluids are interpreted to have a distal source. The supply of iron and silica is ultimately related to distal hydrothermal effluents such as a mid-ocean ridge and/or other subaqueous hot springs (e. g. Isley, 1995; Trendall, 2002). Upwelling currents would transport Fe^{2+} and Mn^{2+} away from the discharge vents and precipitation would occur just above the oxic-anoxic interface, where Fe^{2+} and Mn^{2+} are oxidised to Fe^{3+} and Mn^{4+}, respectively (Pirajno and Adamides, 2000). A depositional and tectonic model for the Yelma and Frere Formations (Tooloo Subgroup), based on the stratigraphic, sedimentological and genetic attributes of the granular iron-formation (Trendall, 2002; Isley, 1995; Beukes and Klein, 1992) is shown in Figure 18.

Detailed studies on field and textural features of granular iron-formation in the Earaheedy Group (Hall and Goode, 1978; Goode et al., 1983; Bunting, 1986) clearly show similarities with the iron-formations of the Superior Province of North America (e.g. Kimberley, 1989). Peloidal and oncolytic textures, orthochemical and allochemical cements, iron-rich chlorite, the presence of mineral phases, such as minnesotaite and stilpnomelane, are common in both. These characteristic features have been interpreted as the result of chemical deposition, followed by mechanical reworking of the sediment, whilst still plastic (gel state) (Beukes and Klein, 1990, 1992). The model for the origin of the iron-formation proposed by Beukes and Klein (1990; 1992) and Isley (1995) accounts for the large volumes of iron, but it does not explain the association of iron and silica in grains of possible biogenic origin. Some of the grains classified as peloids (Fig. 12d), may have been originally oncolites (Fig. 13a-f; and Brown et al., 1995). If this is correct, then it is possible that biogenic activity may have played a major role in the development of the granular iron-formation, through a mechanism of bacterial iron oxidation (Nealson, 1982; Brown et

al., 1995). Other models of BIF deposition (Kappler et al., 2005; Konhauser et al., 2002) propose a mechanism for the oxidation of hydrothermal Fe(II) to Fe(III) by anoxygenic photosynthetic bacteria. A possible bacteria-mediated reaction is:

$$4Fe_2 + CO_2 + 11H_2O + \text{light energy} \rightarrow CH_2O + 4Fe(OH)_3\ 8H^+$$

The depositional setting of the Tooloo Subgroup is illustrated in Figure 19.

4.2.4 Chiall Formation

The Chiall Formation combines, as members, the former Wandiwarra Formation and Princess Ranges Quartzite, as well as the Karri Karri Member (see Fig. 4). SHRIMP U-Pb dating of detrital zircons from the Chiall Formation reveal a maximum depositional age of ca 1.8 Ga (Halilovic et al., 2004). The Chiall Formation consists of shale, siltstone and mudstone intercalated with thick sandstone beds and intraclastic breccia. The formation represents a change from combined chemical and fine-grained clastic sedimentation, to coarser-grained clastic deposition. The base of the formation in the south is a breccia of poorly sorted, angular carbonate clasts in a ferruginized and glauconitic sandstone matrix, which led Bunting (1986) to interpret the boundary as a disconformity. Alternatively, the brecciated features of this horizon could have formed through a process of liquefaction and therefore may be a seismite or a tsunamite, as defined by Einsele (2000) and described by Pratt (2002). To the north, the lower part of the Chiall Formation consists of a thick succession of shale, siltstone and mudstone, which has been assigned to the Karri Karri Member. Sandstone overlying the Karri Karri Member was probably deposited below fair-weather wave base, based on graded bedding, mass flow deposits and the lack of cross-bedding attributable to widespread current or wave action.

The thickness of the Chiall Formation was considered by Bunting (1986) to be up to 1500m. Again, we suggest that there has been more structural repetition than was estimated by Bunting (1986), and that the maximum thickness of the formation may only be 1000m. The contact between the Chiall Formation and the underlying Frere Formation is transitional and taken as the top of the last major chert bed or iron-formation. Where the Chiall Formation overlies the Windidda Formation, the contact is taken as the top of the last carbonate bed. The Chiall Formation (Hocking and Jones, 1999; Hocking et al., 2000a,b) consists predominantly of very fine-grained

sandstone, siltstone, shale and mudstone punctuated by fine- to medium-grained sandstone beds and minor conglomerate. The Wandiwarra and Princess Ranges Members which, as mentioned above, were previously considered formations (Hall et al., 1977; Bunting, 1986) were relegated to member status within a single formation after the recognition that they are part of a single depositional package**.**

The base of the Chiall Formation is transitional and laterally variable. In the central part of Wongawol, the base of the Chiall Formation consists of very fine to fine-grained sandstone, siltstone, shale, and mudstone. Further east, conglomerate is interbedded with this facies at the base of the Chiall Formation, with the proportion of conglomerate increasing eastward.

Conglomerate at the base of the Chiall Formation is texturally variable, consisting of poorly-sorted boulder conglomerate and pebble conglomerate. Clasts are locally imbricate and clast type is variable and commonly reflects the underlying lithologies, suggesting a strong local source control. Fine-grained sandstone, siltstone, and carbonate are the dominant clast types with the proportion varying both vertically and along strike. Poorly sorted boulder conglomerate is generally laterally restricted and is weakly bedded. Clasts vary from subrounded to angular, but are typically angular. On Wongawol a poorly sorted, boulder conglomerate is up to 4 m thick and consists of angular clasts of dominantly carbonate and minor sandstone, in a coarse-grained sandstone matrix containing glauconite peloids and cemented by a ferruginous clay. Pebble conglomerate beds, which are interbedded with siltstone, mudstone and glauconitic very fine- and fine-grained sandstone at the base of the Chiall Formation, are typically less than 50 cm thick.

Bunting (1986) suggested that conglomerate at the base of the Chiall Formation may represent a disconformity between the Tooloo and Miningarra Subgroups. However, there is little evidence to support a significant break in sedimentation between the two subgroups. The contact between conglomerate of the Chiall Formation and the Windidda Formation is transitional, except for localized exposures of cobble conglomerate, and reflects a change from carbonate-cemented conglomerate to conglomerate with a sandstone matrix. It is also important to recognize that basal

conglomerate in the Chiall Formation is relatively restricted both laterally and vertically, and mostly overlies carbonate of the Windidda Formation.

Interbedded siltstone, mudstone, shale and fine- to very fine-grained sandstone, which is locally calcareous typifies the lower part of the Chiall Formation below the Princess Ranges Member and is similar to the lower part of the Wongawol Formation. Sandstone contains green iron silicate minerals, especially near the base of the Chiall Formation. These green iron silicate grains are mostly glauconite, but other iron-bearing species such as berthierine and chamosite are probably also present. In addition, jasper peloids are also common at the base of the Chiall Formation in fine and very fine-grained sandstone. Green iron silicate grains are commonly peloidal and oolitic. Locally, the green iron silicate grains are are flattened and deformed in particular beds, indicating they must have been soft and plastic during compaction. The proportion of green iron silicate minerals in these beds is generally high.

Sedimentary structures at the base of the Chiall Formation include parallel lamination, load casts, and minor cross-lamination. These are overlain by symmetrical and asymmetrical ripples, wrinkle marks, and contorted bedding, which are overall more common sedimentary structures in the lower Chiall Formation.

Fine- to medium-grained sandstone-dominated units in the Chiall Formation form prominent topographic ridges in the central areas of the Basin. Textural and compositional maturity increases stratigraphically in fine- to medium-grained sandstone. Sandstone beds predominantly comprise subrounded to rounded quartz, minor chert, feldspar and glauconite, and accessory zircon and tourmaline. Glauconite is generally concentrated at the base of fine- to medium-grained sandstone-dominated units, suggesting it was reworked from underlying shale, siltstone and very fine-grained sandstone facies where glauconite abundances are high. In units mapped as fine- to medium-grained glauconitic sandstone, the proportion of glauconite is generally much higher than in other fine to medium-grained sandstone units in the Chiall Formation.

4.2.4.1 Karri Karri Member

The lower Karri Karri Member consists dominantly of shale and siltstone, with thin interbedded sandstone beds in the upper part of the member. The member is

interpreted as having a maximum thickness of 600m in the north of the Basin (e. g. on Methwin). The lower contact is defined as the top of the last major chert or iron-formation. The upper contact with the Wandiwarra Member is transitional with thin interbedded sandstone beds becoming more common in the upper part of the Karri Karri Member. The contact is taken at the first occurrence of a thick sandstone. In the Stanley Fold Belt, exposures of the member are generally folded, cleaved and cut by small quartz veins.

Lithologically, shale and siltstone resemble similar lithologies to the underlying Frere and Yelma Formations, but generally contain a high proportion of coarse-grained siltstone. Without other stratigraphic control, the shales may be indistinguishable. They are typically delicately parallel laminated with individual lamellae between 1 to 10 mm. Individual sandstone beds in the upper part of the member are typically 5 to 20 cm thick, and fine- to medium-grained.

The delicate, continuous lamination in the Karri Karri Member is indicative of quiet-water deposition probably below fair-weather wavebase, subsequent to a transgression at the top of the Frere Formation. Sandstone beds are interpreted as mass-flow deposits rather than turbidite deposits because of the intraclastic mudstone clasts and traction structures. The iron-rich nature of the rocks indicates that iron remained in suspension even after deposition of the last GIF and the silica and iron supply to the basin had ceased.

4.2.4.2 Wandiwarra Member

The Wandiwarra Member consists dominantly of siltstone and shale, with scattered intercalations of sandstone. Siltstone and shale intervals are generally well exposed on breakaways. Sandstone intervals form resistant cappings on hills. Shale intervals are generally parallel laminated with minor cross lamination. Laminations are typically 0.5 to 5 cm thick. Interbedded sandstone beds range from 5 cm to, less commonly, about 1 m thick. Sandstone dominated intervals consist of sandstone beds with subordinate interbedded siltstone, generally as thin beds. Sandstone beds generally consist dominantly of rounded to subrounded quartz, with minor chert, feldspar, mica, glauconite and tourmaline, and become more mature in the upper part of the member. Bed thickness varies from about 5 cm up to 1.5 m but is typically 10 to 20 cm in thickness. Bedsets generally range from 20 cm to 1 m in thickness. Sedimentary

structures include cross-bedding, asymmetric ripples and hummocky cross-stratification in the lower part of the member. Current lineations, cross bedding, and ripples indicate a dominant palaeocurrent flow direction towards the north.

Sandstone intervals are fine- to medium-grained, poorly to moderately sorted sandstone, and dominantly consist of rounded to subrounded quartz grains and minor chert fragments. It is locally conglomeratic, and interbedded with siltstone, mudstone and shale. Sandstone is poorly to moderately sorted and consists dominantly of rounded to subrounded quartz grains and minor chert fragments. Mudchip intraclasts are common, especially at the base of individual beds. Sedimentary structures in the sandstone include tabular and trough cross-bedding, flute clasts and current lineation. Quartz grains are occasionally coated by hematite granules (Fig. 20a); in other instances Fe oxides tend to replace both quartz and interstitial matrix and can be an important component at some stratigraphic levels (Fig. 20b). Glauconite peloids vary from spherical to elliptical, with an average size of 0.22 mm. Locally, glauconite is oxidised to brown-coloured Fe oxides. It varies from colourless to light-green or brown when weathered, or blue-green when fresh and is locally replaced by a mosaic of quartz grains, which are not in crystallographic continuity with the surrounding authigenic silica. Locally, glauconite is oxidised to brown-coloured iron oxides.

Sedimentary structures in the sandstone include tabular and trough cross-bedding, flute clasts and current lineation. Sandstone pillows within siltstone are found at several locailities, generally as a discontinuous horizon, suggesting sporadic earthquakes as a trigger mechanism. Spectacular megaripples in sandstone beds can be seen on outcrops of the outer collar of the Shoemaker impact structure (Fig. 21; Section 6). The sedimentary structures, in both the shale and sandstone intervals, suggest that the Wandiwarra Member was mostly deposited below wavebase in the wake of a basal transgression, and that shallowing occurred up the stratigraphic sequence.

Brecciated beds of limestone and glauconitic sandstone in a ferruginized sandy matrix are exposed at the base of the Wandiwarra Member 3 km southwest of Kennedy Bore on Wongawol (Fig. 22). The limestone clasts are platey to elongate, and are the same lithology as Windidda Member exposed below the breccia. Scattered quartzite clasts

are also present. The breccia only extends for a few hundred metres laterally, and has not been recognized elsewhere at the base of the Cjiall Formation. It may be ancient tsunami or seismic shock deposits (Fig. 22a, b), but is more likely a rip-up lag at the base of a transgression. If the latter, they provide a strong indication of a significant break between the Tooloo and Miningarra Subgroups, with transgression over a uneven surface after a period of exposure and local weathering.

North of the Shoemaker impact structure (see Section 6), rocks of the Wandiwarra Member outcrop in a series of breakaways along the northern edge of the Lake Nabberu system (Fig. 23). Here, the rocks are gently dipping and deformed into mesoscale folds with east-trending doubly-plunging fold axes and with local reverse faults (Figs. 23, 24).

4.2.4.3 Princess Range Member

The Princess Ranges Member generally comprises shale, siltstone, mudstone units interbedded with very fine-grained sandstone, and siltstone-dominated units and mature quartz arenite. It is characterized by silicified quartz arenite, although quartz arenite is commonly a subordinate lithology to siltstone. On Granite Peak (Fig. 2), mature quartz-arenite-dominated horizons are mostly interpreted to be stratigraphically equivalent to the Princess Ranges Member. The sandstone is generally fine- to medium-grained and typically texturally mature, consisting of well-rounded and well-sorted quartz grains and accessory tourmaline and zircon. Mudchip intraclasts and glauconite peloids are commonly concentrated at the base of fine to medium-grained sandstone dominated units, suggesting high-energy erosional bases. Coarse-grained siltstone and very fine-grained sandstone is comprised dominantly of angular to subrounded quartz, and subordinate glauconite and detrital mica. Locally, the base of the Princess Ranges Member contains coarse-grained sandstone containing pebble-sized subangular to subrounded clasts of vein quartz and sandstone.

Sedimentary structures within the sandstone include symmetrical sharp-crested low amplitude ripples, current lineation, megaripples, shrinkage moulds, trough and planar cross-bedding and cross-lamination. Symmetrical ripples are mostly straight-crested, while asymmetric ripples vary from straight-crested to linguoid (Fig. 25). The sedimentary structures, in combination indicate that the Princess Ranges Member and the stratigraphically equivalent mature quartz arenite in the upper part of the Chiall

Formation were deposited largely in an upper shoreface environment. In places ripple forms suggest shallow to tidal sandflat conditions, based on interference patterns and possible ripple washouts. Sandstone beds are probably tempestites (storm related) and/or seismites (related to earthquakes; Rodriguez-Pascua et al., 2000). Conglomeratic beds may be related to tsunamis.

Fine- to medium-grained sandstone is typically texturally mature, consisting of well-rounded and well-sorted quartz grains and accessory tourmaline and zircon. Mudchip intraclasts and glauconite peloids are commonly concentrated at the base of fine- to medium-grained sandstone dominated units, suggesting high-energy erosional bases. Coarse-grained siltstone and very fine-grained sandstone is comprised dominantly of angular to subrounded quartz, and subordinate glauconite and detrital mica. Locally, the base of the Princess Ranges Member contains coarse-grained sandstone containing pebble-sized subangular to subrounded clasts of vein quartz and sandstone.

4.2.5 Wongawol Formation

The Wongawol Formation (Hall et al., 1977; Bunting, 1986) is a monotonous succession of shale, mudstone, siltstone, very fine-grained feldspathic sandstone, and minor intraclast conglomerate. The lower contact with the Chiall Formation is placed at the top of the uppermost compositionally mature sandstone. The upper contact with the Kulele Limestone, where exposed, is transitional and placed where limestone becomes the dominant lithology (Bunting, 1986). Sandstone in the Wongawol Formation is dominantly very fine-grained, in places silicified, and locally glauconitic. In places, sandstone contains mudchip and well-rounded siltstone intraclasts, with in-situ brecciation of thin siltstone beds. Stromatolites are present at several horizons and include domal features 50 cm wide , 1 m long, and 40 to 60 cm high. Smaller parasitic domal forms encrust larger domes, and the stromatolits are sassociated with mudchip intraclast breccias and oolitic limestones. Compound domal forms up to about 3 m high and 4 m across are present on Lee Steere.

Discontinuous conglomerate bodies are present on Wongawol and southern Lee Steere (Fig.2). Clasts are typically well-rounded, matrix-supported, pebble-sized, and mostly composed of mudstone and carbonate fragments. Both mudstone and

carbonate clasts are interpreted as intraclastic. Intraclast mud-chip conglomerates are well-exposed on Lee Steere. In this area, they are associated with small-to medium-scale pillow structures, possibly developed by sediment loading. On Wongawol, volcaniclastic clasts with vitriclastic textures were recorded by Jones (2004). The clasts contain well-preserved relic glass shards that are uncompacted and show bubble-wall, triple point textures. The matrix consists of poorly sorted, angular to subangular clasts of quartz, feldspar, and biotite, which are dominantly silt to very fine-grained sand sized, in a micritic cement. The provenance of the clasts is unclear as there is no evidence of contemporaneous volcanism in the Earaheedy Basin. They may be from reworking of thin volcaniclastic beds, which have not been preserved, or they may be allochthonous.

Sedimentary structures in the Wongawol Formation include swash marks, ripple washouts, wrinkle marks, ball-and-pillow structures (mostly but not always at sandstone–siltstone interfaces), primary current lineation, and symmetrical and interference ripples. Symmetrical ripples typically have peaked crests and are straight-crested, with wavelengths of 8–10 cm and amplitudes around 2-3 cm. Weakly developed ladder ripples are locally present in the troughs of some symmetrical ripples. These are indicative of deposition in shallow water with intermittent emergence and reworking by swash and possibly wind. Ball-and-pillow structures formed either by loading or as a result of earthquake shock. At one locality, an extensive horizon of contorted bedding, primarily with pillow structures, with thinly bedded rippled siltstone to very fine-grained sandstone lies above an uncontorted interference-rippled siltstone. The ripple morphology indicates very shallow conditions, whereas the contortion shows no consistent orientation, suggestive of earthquake disturbance rather than slope collapse.

On Lee Steere, the Wongawol Formation is folded into multiple east-trending anticlines and synclines, and cut by an network of anastomosing east-trending faults, indicative of mild north-south compression. The intensity of the folding increases northwards, into a pattern (low in the Wongawol Formation and in the Princes Ranges Member) of sheared-out anticlinal and synclinal axes between relatively straight, moderately to steeply dipping fold limbs.

Kulele Limestone

The Kulele Limestone is a cyclic platform succession up to 300 m thick, of interbedded calcarenite, stromatolitic limestone, intraclastic carbonate breccia, oolitic and pisolitic limestone, siltstone, and sandstone. Near Thurraguddy Bore, spectacular large individual stromatolite domes are up to 3.5 m high and 4 m wide. Domes are composed of smaller colonial columnar stromatolites. Compared to the Wongawol Formation, the Kulele Limestone records a slight deepening of the basin and decrease in terrigenous influx. Metre-scale shallowing-upward cycles are present through most of the unit, and record regular minor fluctuations in sea-level in a shallow subtidal setting.

The Kulele Limestone is preserved only in the central-eastern part of the basin, except for a small outlier, near Thurraguddy Bore on Wongawol (Fig. 2). The carbonate (mostly limestone, lesser dolomite) rocks represent the main rock type and they form cyclic sequences separated by clastic units. Cycles are typically about 10 m thick, but locally only a metre thick, and cyclic intervals are separated in places by clastic layers up to 50 m thick. The limestone units are mostly thickly bedded, and internally laminated, with the laminae on scales of 1 to 5 mm. Stromatolites range from small domes a few cm across to large domes, 2 m high and 3 m across, which coalesce to bioherms up to 30 m long (Bunting, 1986). These stromatolite domes are commonly asymmetric and elongated, presumably at right angles to the direction of wave translation – the elongation is approximately perpendicular to the shoreline. This can be seen in the Thurraguddy Bore outlier on Lee Steere and terraces on Carnegie. Bunting (1986) studied the Thurraguddy Bore outlier in detail. There, the basal 25 m of Kulele Limestone is exposed and can be divided into seven cyclic pairs of limestone-shale, each from 2.5 to 7.5 m thick. Each cycle represents a transgressive (limestone)-regressive (shale) couplet. Stromatolites in the outlier form two bands. Band 1 has low domes, up to 100 mm, circular to elongate with length:breadth ratios of about 3:1. Band 2 contains domes up to 2 m high with individual domes reaching 3 m across, forming bioherms 30 m long and 10 m wide. Stromatolite forms in the Kulele Limestone include *Haraheedia kuleliensis* Grey 1984. The large bulbous stromatolites remain unnamed.

Oolitic and pisolitic limestone shows two types of allochems (Bunting, 1986). In one, large pisoliths are elongate with an intraclastic core, surrounded by concentric laminae up to several mm thick. The second type is smaller with both radial and concentric laminae. These features may indicate a two-stage origin, whereby ooliths initially formed in quiet water, then were transported into a more agitated environment. Locally there are breccia layers, characterised by tabular intraclasts up to 200 mm long, forming beds at the base of the limestone cycles. Calcarenites are fine-to medium-grained rocks composed of granular calcite with minor detrital quartz. Shales are typically purple, maroon or grey-greenish in colour and contain white mica and chlorite. Sandstone interbedded with the shaly rocks, contains feldspar, quartz with a calcareous cement and with muscovite and chlorite imparting this rock a degree of fissility. In the upper part of the Formation, sandstone is coarser grained and contains glauconite at the expense of the feldspar, which becomes a minor component (Bunting, 1986).

The stromatolitic limestones and cyclic nature of the Kulele Limestone indicate deposition in shallow-marine nearshore to coastal conditions, with regular short-term sea-level change on a scale of a few metres to perhaps 20 m (based on the thickness of the cycles), possibly driven by orbital forcing. Metre-scale cyclicity has long been viewed as a fundamental component of Phanerozoic platform carbonates (Goldhammer et al., 1987, 1990, 1993; Anderson & Goodwin, 1990, Elrick and Read, 1991), and is commonly, but not always attributed to orbital forcing (Milankovich cyclicity) (Fischer and Bottjer, 1991, Franseen et al., 1991, House and Gale, 1995).

4.2.6 Mulgarra Sandstone

The Mulgarra Sandstone, the youngest component of the Earaheedy Group, consists of fine- to medium-grained, commonly glauconitic sandstone, shale and minor carbonate. Locally, there are intercalations of thin limestone beds, forming a mixed unit up to 40 m thick, and quartzose calcarenite horizons are widespread. Siltstone is widespread, and a significant component of the formation, but rarely outcrops. Some sand units are discrete megaripples totally enclosed by siltstone, and clearly formed as isolated sand-starved megripples on mudflats or an inner shelf. The Mulgarra Sandstone is quite similar to the Wongawol Formation, but for the presence of fine- to medium-grained glauconitic sandstone.

The deposited top is not preserved, and Bunting (1986) estimated the Mulgarra Sandstone was about 100 m thick, but we consider that at least 200 m stratigraphic thickness is exposed in the syncline northwest of Mulgarra Pool. The youngest zircons in a sample from near the base of the Mulgarra Sandstone yielded U-Pb SHRIMP ages of ca 1.8 Ga (Halilovic et al., 2004).

The main scarp of the Timperley Range, northeast of Mt Hoskin, exposes the basal 20 m of the Formation, where it consists of interbedded fine-grained and coarse-grained felspathic quartz arenite, locally ferruginous, and bedded on a 100-200 mm scale. Coarser grained intervals are glauconitic. Both cross bedding and parallel bedding with primary current lineation are present, together with ripples indicative of very shallow water. Flute and load casts, and ball-and-pillow structures are present near the base. The basal contact with the underlying Kulele Limestone is sharp and marked by 1-2 m of shale. Elsewhere, the contact appears to be gradational, with limestone beds gradually decreasing upwards while siltstone and fine-grained sandstone increases

Sedimentary structures and bedforms indicate the Mulgarra Sandstone was deposited in a coastal setting, with environments ranging from a muddy inner shelf with isolated sandy megaripples, through foreshore, beach and possibly tidal sandflat environments, to a washover lagoonal setting. Adhesion surfaces, blowouts and wrinkled surfaces suggest intermittent emergence and exposure, and widespread sediment loading structures indicate continued sporadic earthquakes.

4.2.7 Depositional environment of the Miningarra Subgroup

The Earaheedy Basin deepened northwards during deposition of the Miningarra and Tooloo Subgroups. In the south symmetric and asymmetric ripples, interference ripples, megaripples and trough cross-beds indicate a shallow-water, upper shoreface to foreshore, intermittently emergent, setting. To the north, fine-grained rocks, parallel bedding, and hummocky cross-bedding suggest a dominantly storm-swept sub-wave base marine shelf. Limited palaeocurrent data support this model. The Chiall Formation records a change from iron oxide and chert to iron silicate grains. The presence of iron silicate minerals, such as glauconite, berthierine and chamosite, indicate dominantly low sedimentation rates for the finer grained facies of the lower Chiall Formation. Sedimentary structures suggest that the lower Chiall Formation was

deposited in a shallow marine environment with deposition from below fairweather wave-base grading up into a shallow water, possibly nearshore bathymetry. The conglomerate at the base of the Chiall Formation represents reworking of the underlying lithologies and localized channel fill, and may be a transgressive rip-up deposit formed after a significant break. Sandstone beds are probably tempestites (storm related) and seismites (related to earthquakes; Rodriguez-Pascua et al., 2000). Sedimentary structures in the Princess Ranges Member suggest that it was deposited in a shallow marine to locally emergent environment, which was affected by both wave and current action. These features together with the compositional and textural maturity of coarser sandstone, which indicates a higher energy depositional environment in the Princess Ranges Member, suggest deposition in a tidal sand flat environment for much of the unit.

The Wongawol Formation is similar to the shale, mudstone, siltstone, and very fine-grained sandstone facies in the Chiall Formation. However, sedimentary structures suggest deposition was in a very shallow water to locally emergent environment, similar to but lower energy than that proposed for the Princess Ranges Member. Decreased terrigenous influx and a slight deepening of the basin led to carbonate dominated deposition, forming the Kulele Limestone. This was followed by a return to shallower conditions, greater terrigenous influx, and deposition of the Mulgarra Sandstone in an environment very similar to that for the Wongawol Formation, but slightly higher energy.

5. Stanley Fold Belt

The exposed Earaheedy Basin is deformed into a regional east to east-southeasterly trending, south-verging, asymmetric syncline, which plunges gently towards the southeast. The northern limb is steeply dipping to locally overturned, and forms the Stanley Fold Belt, a 110°- trending structural domain, about 200 km long and up to 35 km wide, and which is characterized by strike-slip faulting, foliation fabrics, tight folding, and reverse faulting. Folding varies in scale, with fold limbs commonly truncated by faults. Faults trend easterly, and include both dip-slip (dipping north), and sinistral strike-slip components. Major structures within the Stanley Fold Belt generally trend east or northwest and are positively magnetized. Sedimentary rocks of the Earaheedy Group are generally weakly metamorphosed, only locally attaining

lower greenschist facies. Typical metamorphic minerals in fine-grained rocks are sericite, and chlorite.

Deformed rocks of the fold belt are exposed in the northeast corner of Granite Peak (Fig. 2). The degree of deformation in the Stanley Fold Belt decreases southward resulting in open, generally gentle folds, locally with an associated axial-plane cleavage. These features are expressed on aeromagnetic images as a series of broad, low-amplitude, east-trending ridges and swales. Doubly-plunging mesoscale folds with wavelengths of 10-20 m (Fig. 24) are well displayed along escarpments (locally referred to as breakaways). Breccias and quartz vein stockworks are commonly associated with the folded rocks. In the transition zone between the Stanley Fold Belt and folded southern margin of the Earaheedy Basin, small-scale disharmonic folding and normal faulting is common.

5.1 Folds, faults and linear (E-W, N-S and NW-SE) structures

North trending structures are probably reactivated basement structures and their orientation is similar to D_3 structures of the Yilgarn Craton, which formed during sinistral transpression (e.g. Wyche and Farrell, 2000; Swager, 1997). A north-south trending structure on Wongawol may be a continuation of a major north to north-northeast trending structure on the eastern margin of the Duketon greenstone belt. The age of initiation of east trending structures is not well constrained (Groenewald et al., 2001). They postdate D_3 structures in the Yilgarn Craton and are thought to be Palaeoproterozoic in age, because an age of 2420 Ma was obtained from some east trending dykes (Nemchin and Pidgeon, 1998). In the northeastern Yilgarn Craton, where they cut the Earaheedy Group they could be either reactivated basement structures, or later features developed during deformation after deposition of the Earaheedy Group. On aeromagnetic imagery, both north- and east-trending structures can be seen to displace northwest-trending, ?bedding-parallel structures in the lower Earaheedy Group (see below), so the last movement on both is at most late Paleoproterozoic. Movement on the east-trending structures is interpreted to have been dominated by vertical displacement. Manganese oxides mineralisation is commonly associated with north-trending structures and quartz fracturing and silicification is present along east-trending structures. The relative timing

relationships between the east-west and north-south structures show ambiguous overprinting relationships.

Northwest trending negatively magnetized structures are interpreted to postdate deposition of the Earaheedy Group. The aeromagnetic signature is consistent with shallow-level, low-angle structures dipping to the northeast and there are no other parallel structures in the northeast Yilgarn Craton. These structures appear to be mostly bedding parallel with the Earaheedy Group, but are not the magnetic response of layering in the Frere Formation and they do not correspond to individual GIF horizons or to any iron-rich layer. Given the intense but continuous nature of these northwest trending features it seems likely they are the product of bedding parallel fluid flow. On Granite Peak (Pirajno et al., 2003) and Merrie (Adamides, 2000) they coincide with silicification of GIF in the Frere Formation and the presence of stilpnomelane in shale and siltstone beds. Aeromagnetic images indicate that movement along east and north structures offset, and therefore postdate, northwest structures. The relative timing relationships between the east-west and north-south structures show ambiguous overprinting relationships. In addition, magnetization along north structures is discontinuous and may reflect localized movement during more than one event.

Folds generally vary from open, upright, gently plunging to localized recumbent folding with the degree and style of folding typically strongly dependant on lithology. Mesoscale folds in fine- to coarse-grained sandstone intervals, typically form doubly plunging, elongate anticlinal features. In siltstone to very fine-grained sandstone dominated intervals, mesoscale folds vary from doubly plunging folds to localized disharmonic folding. Sporadic, northeast trending anticlines, which vary in scale from tens of metres up to approximately 1 km scale, are common in fine to coarse-grained sandstone dominated intervals such as the Princess Ranges Member. Deformation associated with these features is more intense than surrounding areas suggesting they may represent localized space accommodation zones.

The structural history suggests that at least two major deformation events are recorded in the Earaheedy Group. The first major deformation event resulted in low-angle mostly bedding-parallel movement, which produced northwest trending

structures at various scales. A later, predominantly north-south compression resulted in vertical displacement along east-west trending structures. The orientation of the northwest trending structures and the lack of evidence for major displacement or strike-slip movement suggests that the deformation event associated with these structures was due to southwest directed compression. The timing of both of these events is not well constrained. Pb-Pb ages on Pb-Zn mineralization in the Sweetwaters Well Member (Richards and Gee, 1985) and Rb-Sr and K-Ar ages on glauconite (Horwitz, 1975a, b; Preiss et al., 1975), which have probably been reset, suggest a thermal event about c. 1650 Ma. This age coincides with some of the granitoid ages in the Gascoyne Complex and the 1680-1620 Ma Mangaroon Orogeny (Nelson, 2002; Sheppard et al., 2007). This event could be reflected in the north-trending, the east-trending , or the northwest-trending structures that cut the Earaheedy Group.

5.2 Quartz veins

Quartz stockwork veining is developed in granular chert in the Frere Formation (Jones and Pirajno, 2003), where it is cut by major east trending structures. Intense quartz stockwork veining is developed at the intersection of east trending structures with other major structures, such as the Proterozoic northwest oriented structures and the reactivated north-south oriented structures.

Centimetre-thick veins of syntaxial fibrous quartz are common in the sandstone units of the Chiall Formation. The orientation of the veins and the syntaxial quartz fibres enables the gauging of the stress field at the time that the veins were emplaced. On Nabberu and Granite Peak, two sets of quartz veins are present, in which the fibres are oriented 355° (σ_3; least compressive stress), in the older vein set (strike 270°) and 150° (σ_3) in the younger set (vein strike 060°). This implies that the veins may have formed as a result of northeast-southwest directed compression. This compression event is interpreted to reflect tectonic movements associated with the Yapungku Orogeny (Bagas and Smithies, 1998; Smithies and Bagas, 1997; Bagas, 2004), which may have contrbuted to the formation of the Stanley Fold Belt. Ar-Ar dating of micas in the Stanley Fold Belt (Section 4.1) yielded ages of ca. 1650 Ma, suggesting that further deformation may relate to the Mangaroon Orogeny (Sheppard et al., 2005).

6. Shoemaker meteorite impact structure

The Shoemaker impact structure has an outer diameter of about 30 km (Fig. 2) and consists of two well-defined concentric ring synclinal and anticlinal structures, formed in rocks of the Chiall and Frere formations, surrounding Archaean basement rocks (Teague granite and greenstone rocks; Pirajno and Glikson, 1998). The concentric rings form low hills that interrupt the continuity of the west-northwest-trending Frere Range The structure is discussed in detail by Pirajno (2002) and Pirajno et al. (2003) and only a brief review is given here.

Evidence for an impact origin of the Shoemaker impact structure includes:

1. a well-defined circular structure with surrounding rings of synclinal and anticlinal structures, which enclose a core of Archaean basement interpreted as a central uplift (Teague Granite and greenstone rocks).

2. shatter cones in sedimentary rocks in both inner and outer rings.

3. Planar deformation features (PDFs) in quartz crystals of Teague Granite.

The target rocks encompass undeformed and unmetamorphosed sedimentary rocks of the Earaheedy Group, dipping to the northeast about 10-15º and the underlying Archaean granite-greenstone basement of the Yilgarn Craton (Fig. 2; Pirajno et al., 2004). The central basement uplift, with a diameter of 12 km, consists of fractured Archaean granitoids of syenitic composition (Teague Granite). The syenitic composition of the Teague Granite suggests that it could either belong to a late Archaean suite of alkaline plutons that intrude the Yilgarn Craton (Johnson, 1991; Smithies and Champion, 1999), or is the product of alteration of a precursor granitoid by alkali metasomatism related to an impact-generated heat source. Locally, the Teague Granite exhibits partial to pervasive silicification, is fractured and contains hydrothermal minerals, such as fibrous amphibole, garnet, sericite and prehnite, consistent with metasomatism.

The central and the western parts of the inner structure are entirely covered by Quaternary lake sediments and sand dunes. However, aeromagnetic data indicate that granitic (possibly monzogranite) and greenstone rocks are present beneath these

surficial deposits, representing the northern continuation of the Yilgarn Craton beneath the sedimentary cover of the Earaheedy Basin (Pirajno, 2002). The presence of diagnostic impact indicators, suggest that granitic and greenstone rocks form an impact-induced central structural uplift and possibly the basement core of the original crater. The eastern side of the structural uplift is characterized by high total magnetic intensity (TMI), hydrothermal alteration (see below) and the only exposures of the granitoid rocks (Teague Granite). The TMI pattern suggests not only that the upper parts of the original impact structure were eroded away, but also that the entire structure is probably tilted towards the east (Pirajno, 2002).

The age of the Shoemaker impact is not resolved, because of thermal and tectonic resetting of the isotopic systems of the target rocks at 1670-1620 Ma (Mangaroon Orogeny; Sheppard et al., 2007), 1070 Ma (age of the Warakurna large igneous province in the region; Wingate et al., 2004) and ca 550 Ma (age of the Petermann Orogeny; Scrimgeour et al., 1999). The magmatic age of the Teague Granite is Archaean (2648 ± 8 Ma; Nelson, 1999), which is within the range of other granitic rocks in the Yilgarn Craton (e. g. Smithies and Champion, 1999). Bunting et al. (1980a, b) obtained two whole-rock Rb-Sr isochron ages of 1630 and 1260 Ma from samples of Teague Granite. Pirajno (2002) and Pirajno et al. (2003) reported K-Ar and $^{39}Ar/^{40}Ar$ determinations on K-feldspar and illite-smectite separates also from the Teague Granite. The $^{39}Ar/^{40}Ar$ system yielded unreliable results, only providing broad constraints as to a maximum age (<1300 Ma; see Pirajno 2002. p. 36 for details). The K-Ar system gave two ages: 694±25 Ma and 568±20 Ma for K-feldspar and illite-smectite separates, respectively. Pirajno et al. (2003) concluded that the 568±20 Ma K-Ar age determined on illite could represent either resetting due to the Petermann Orogeny, or the formation of illite as a result of post-impact hydrothermal activity.

About 5 km from the eastern shore of Lake Teague, scattered, cm to m-sized round and angular boulders of sandstone are present . This could be a lag deposit of Permian age (Paterson Formation; Bunting et al., 1982; Commander et al., 1982) . Alternatively, because of their position close to the outermost ring and absence of any such lithology elsewhere in the Earaheedy Group in the region, it is also possible that they are either remnants of reworked lithic breccia ejecta, or crater-fill allochthonous breccia (Pirajno, 2002).

6.1 Hydrothermal alteration

In the Shoemaker impact structure the effects of impact energy-induced hydrothermal circulation within the impact aureole are evident in the Teague Granite (Pirajno, 2002) and in rocks of the Yelma and Frere formations (Earaheedy Group) exposed in the eastern inner ring. Outcrops of Teague Granite in the east and southeast are fractured, hydrothermally altered and partially to pervasively silicified. The rocks of the Teague Granite were studied as part of a regional investigation of felsic alkaline rocks of the Yilgarn Craton by Johnson (1991), who concluded that the granitoids that outcrop in the Shoemaker structure were modified by alkali metasomatism resulting in a granitoid of syenitic composition. Johnson's conclusion was confirmed in subsequent studies (Pirajno and Glikson, 1998; Pirajno, 2002; Pirajno et al., 2003).

Pervasive silicification affected rocks of the Yelma Formation (Sweetwaters Well Member), whilst the GIF rocks of the Frere Formation exhibit cross-cutting quartz veining and are partially silicified. In the same area, pods of chert and jasperoidal quartz are present along the eastern margin of the central uplift. The chert material consists mainly of brecciated microcrystalline quartz cemented by chalcedonic quartz. Open spaces are filled with euhedral quartz crystals. These chert pods are interpreted to have formed by precipitation from hydrothermal fluids that circulated along faults and fractures in the eastern sector of Shoemaker impact structure.

It is likely that the meteorite impact that created the Shoemaker impact structure formed a melt sheet which, together with impact-released heat in the central uplift, gave rise to a hydrothermal convection system, within and around the central uplift zone. The melt sheet would have acted as a magma-like heat source within the crater structure and would have formed several hot springs in the crater and surrounding areas. Fluid channels and degassing pipes have been reported from the Ries impact crater in Germany (Newsom et al., 1986). Hydrothermal pods are present in the annular structures associated with the Haughton impact structure in Canada that have been interpreted as hydrothermal pipe structures (Osinski et al., 2001). Similarly, the pods of quartz-jasperoidal material that are present along structural breaks in the eastern rim of the Shoemaker impact structure may be the eroded remnants of fluid channels that fed thermal springs.

7. Depositional setting and geodynamic evolution of the Earaheedy Basin

This section presents a model for the geodynamic evolution of the Earaheedy Basin (Fig. 26), based on an integration of systematic field mapping, sedimentological and petrographic studies, geophysical data (aeromagnetic and gravity) and the available geochronology. The Earaheedy Group consists of both chemical and clastic sediments indicative of a shallow marine to coastal environment, which deepened to the north and northeast (Jones et al, 2000; Pirajno et al., 2004). The exposed rocks represent only the coastal to inner or middle-shelf portion of the continental shelf that was developed on the northern margin of the Yilgarn Craton. Sedimentary deposits of the outer shelf, continental slope and rise are not exposed, suggesting that much of the original depositional system is buried or not preserved. The grain size (dominantly medium-fine sand to silt) indicates dominantly quiet, low-energy conditions, although this could be because coarser material was simply not available due to a low-gradient, weathered, basin hinterland. Deposition was strongly influenced by water chemistry, sediment supply and sea-level fluctuations. Sea-level fluctuations are envisaged to be tectonically-driven, but with short-term eustatic changes in a greenhouse climate (Read et al., 1995) producing metre-scale cyclicity in carbonates and from tens of metres to metre scale cyclicity in the iron formation (iron formation-siltstone bands), and longer term tectonism responsible for increases in sand deposition by either hinterland uplift or basin subsidence. North to northeastward deepening is consistent with the distribution of facies within the basin architecture. The Tooloo Subgroup, which is characterized by GIF, reflects initial transgression (Yelma Formation), followed by intermittent influx of iron and silica into the basin (Frere Formation), whereas the overlying Miningarra Subgroup is characterized by low-energy, sand-poor clastic settings (lower Chiall Formation and Wongawol Formation), marginally sandier clastic settings (upper Chiall Formation and Mulgarra Sandstone), and slightly deeper clastic-starved conditions (Kulele Limestone).

The lithofacies and facies trends of the Earaheedy Group suggest that it was part of a trailing passive margin (Pirajno, 2007; Pirajno et al., 2000, 2004; Jones et al., 2000), characterised by low-magnitude marine transgressions and regressions in response to fluctuating sea-level changes (Fig. 26B), due to a combination of sediment supply, subsidence and eustasy (Eriksson et al., 2001). Typically, trailing passive margins

result from continental breakups (Braun and Beaumont, 1989; Bradley, 2008). Present-day exposed rocks represent only the coastal to shelfal portion of the continental shelf; sedimentary deposits of the continental slope and rise are not exposed, suggesting that much of the original depositional system is buried. The 1.99 Ga rhyodacitic subvolcanic rocks of the Imbin Inlier could be either an exotic fragment from a northern continent, or a fragment of the Dalgaringa Supersuite of the southern Gascoyne Complex that moved eastward by transcurrent movements (Occhipinti et al., 2001). Yet another possibility is that the Imbin rhyodacite is part of a bimodal (felsic-mafic) igneous suite related to continental breakup.

The GIF beds, and primary sedimentary structures preserved within them such as cross-bedding, provide a reasonable indicator of depositional setting, because in order to have large scale deposition of granular facies iron oxides, a widespread shallow-water environment would have been required (e.g. Trendall, 2002; Simonson and Hassler, 1996). The source of iron and silica for the GIF in the Frere Formation is a key element in the understanding of the basin, together with the lack of evidence of contemporaneous volcanism and major deformation. Beukes and Klein (1992) and Isley (1995) considered GIF to be a shallow-water, higher energy equivalent of deeper water banded iron-formation. However, it should be noted that the model for the origin of the iron-formations proposed by Beukes and Klein (1992) and Isley (1995) accounts for the large volumes of iron, but it does not explain the association of iron and silica in grains of possible biogenic origin. Some of the grains classified as peloids, may have been originally oncolites (Brown et al., 1995). If this is correct, then it is possible that biogenic activity may have played a major role in the development of the Earaheedy GIF, through a mechanism of bacterial iron oxidation (e.g. Nealson, 1982; Brown et al., 1995). Models of iron formation genesis suggest that the supply of the soluble Fe^{2+} is provided by hydrothermal effluents in oceanic settings (e.g. spreading centers or mantle-plume related oceanic plateaux; Isley, 1995). During deposition of the Tooloo Subgroup, no oceanic environment is known to have been present in the west. Lithofacies are progressively more distal to the north and northeast, oceans must have been to the north, east and/or northeast (present-day reference frame; Fig. 26B), beneath the presently exposed northwestern Officer Basin or Paterson Orogen.

The boundary between the Tooloo and Miningarra subgroups, at the base of Chiall Formation, reflects a change in depositional setting from a chemically significant, clastic-starved regime to one of greater, though still largely fine-grained, clastic supply. On Wongawol and Windidda (Fig. 2), the contact between the Chiall Formation and the underlying Windidda Formation is defined by a pebble- to cobble-sized conglomerate. Ball-and-pillow deformation is common higher in the succession in the Wandiwarra Member, Wongawol Formation, and Mulgarra Sandstone (especially the Wongawol Formation) indicating regular far-field seismicity or tectonic jiggling of the basin, but not major tectonism such as would result in high energy sandy or conglomeratic deposition. Continued high levels of dissolved iron are indicated by the widespread deposition of glauconitic sandstones. The Kulele Limestone, deposited in a subtidal stromatolitic carbonate environment, reflects a decrease in terrigenous supply, caused either by climatic or tectonic changes. The Mulgarra Sandstone shows a return to shelfal depositional setting of the Wongawol and Chiall Formations. A carbonate interval at the topmost Mulgarra Sandstone may have heralded a return to carbonate deposition, now only barely preserved because of later erosion. Bunting (1986) suggested that the Mulgarra Sandstone is disconformable on the Kulele Limestone, but this has not been confirmed by our work.

Five main sedimentary regimes, driven by sea level balanced against varying clastic influx, can be delineated (Figure 27): An initial transgressive coarser clastic cycle (Yelma Formation) led, through continued transgression and diminished siliciclastic influx, to the deposition of platform carbonates (Sweetwaters Well Member) and culminated with the fine-grained clastic-starved succession of the Frere Formation, albeit with some rhythmicity. Comparatively strong subsidence led to another cycle of clastic sedimentation, manifested by the deposition of the Chiall Formation and then the Wongawol Formation, in a long-term shallowing-upward succession. Lessening of clastic influx, possibly at the end of the Capricorn Orogeny or possibly climate driven, resulted in deposition of the carbonate-dominated Kulele Limestone. This was followed by renewed clastic influx, in continued shallow marine conditions, depositing the Mulgarra Sandstone.

SHRIMP U-Pb dating of detrital zircons suggests that sandstone in the Earaheedy Group was probably sourced predominantly from the Yilgarn Craton and the Gascoyne Complex to the west (Halilovic et al., 2004). Archaean ages are consistent with the Yilgarn Craton as a source. The youngest age of detrital zircons in the lower Tooloo Subgroup imply a 2.0-1.8 Ga source; the only possible source of these Palaeoproterozoic zircons in the immediate region (barring unknown continental fragments elsewhere) is to the west in the southern Gascoyne Complex. The SHRIMP data also suggest that the siliciclastic detritus was sourced from progressively younger sources during the evolution of the basin. The current age constraints for deposition of the Miningarra Subgroup are consistent with deposition beginning during the waning stages of the Capricorn Orogeny, but equally deposition could have been as late as the early stages of the Mangaroon Orogeny, immediately before deformation and development of the Stanley Fold Belt. In the former case, the subgroup may reflect rapid uplift to the west associated with granite intrusion in the western Capricorn Orogen, causing influx of siliciclastic material that overwhelmed the proportion of iron and silica in solution and consequently terminated the deposition of GIF, while favouring the deposition of glauconite peloids. Glauconite peloids, associated with clastic grains, are particularly common in shale, siltstone and very fine-grained sandstone horizons and at the base of medium to coarse-grained sandstone horizons in the Chiall Formation, and in the Mulgarra Sandstone. There is an association between glauconite and ferruginous sandstone, with alternations of glauconite-rich and ferruginous layers. In the latter case, later granite intrusions to the west may have triggered uplift and siliclastic influx to the basin, after a hiatus of sufficient duration to allow lithification of the underlying Tooloo Subgroup.

From the above and given the age constraints, the deposition of the Tooloo Subgroup may have been synchronous with the Capricorn Orogeny, with deposition of the Miningarra Subgroup taking place in the waning stages of the Capricorn Orogeny or at a later time, prior to 1650 Ma. The present-day structure of the Earaheedy Basin along a north-south cross-section is asymmetric, with a broad shallow platform along a southern depositional margin and a strongly deformed northern tectonic margin, with reverse faulting, shearing, tight and recumbent folding, in the Stanley Fold Belt. Rare exposures and drill intersections of undeformed, gently dipping Tooloo Subgroup, including GIF showing syndepositional pinch and swell structures, are

present to the north of the fold belt. The only direct geochronological constraint on the timing of the deformation that formed the Stanley Fold Belt is the ^{39}Ar-^{40}Ar date on metamorphic micas of ca. 1650 Ma; see Table 2 and Section 4.1). Other geochronological hints are provided by SHRIMP U-Pb dating of zircons and monazite from the Malmac Inlier (Fig. 1), which indicate a disturbance event at about 1.72 Ga (Nelson, 2002); SHRIMP U-Pb dating of zircons by McMillan and McNaughton (1995) and Vielreicher and McNaughton (2002), who also detected a disturbance, associated with hydrothermal activity, in the Marymia Inlier at about 1.72 Ga; and the age of epigenetic Mississippi Valley Type (MVT) mineralisation in the Yelma Formation, for which a Pb-Pb model age of 1.74-1.77 Ga was determined (Teen, 199; Pirajno et al., in press).

Based on field data and the geochronological constraints above, we suggest that deposition of the Tooloo Subgroup ceased at about 1800 Ma, followed by a hiatus before deposition of the Miningarra Subgroup commenced in a major transgression at 1770 to perhaps 1750 Ma. The renewed deposition may have triggered fluid expulsion from basinal Tooloo Subgroup, largely by loading of the newly deposited Miningarra Subgroup, with fluids moving south up the basin flanks to form MVT sulfide deposits in carbonate platforms on the southern margin of the basin. Alternatively and following a more conventional model (Garven and Raffensperger, 1997), the MVT mineralisation in the Yelma Formation may reflect tectonic uplift along the Stanley Fold Belt to provide the necessary gravity gradients to drive basinal fluids updip, to form sulfide deposits in carbonate platforms on the southern margin of the basin (Pirajno, 2004). Deposition may have been terminated by the 1720 Ma event affecting the Marymia Inlier. A hiatus then followed prior to far-field deformation in the Mangaroon Orogeny forming the Stanley Fold Belt at about 1650 Ma. This model fits available geochronological data better than our previous model (Pirajno et al., 2004), which attributed formation of the fold belt to the D_2 phase of the Yapungku Orogeny (1.79 -1.76 Ga; Smithies and Bagas, 1997; Bagas and Smithies, 1998; Bagas, 2004), which had a major effect in the Rudall Complex, north of the Earaheedy Basin. The deformation of the Earaheedy Group resulted in its folding into an asymmetrical syncline, conferring the apparent foreland basin-type north-south asymmetry of the Earaheedy Basin as illustrated in Figures 2 and 5, although the depositional

environments and sediment stacking pattern reflect a trailing passive margin rather than a foreland setting.

8. Discussion and conclusions

Many Archean granite-greenstone cratonic blocks are overlain by Archean or Proterozoic stable shelf sedimentary successions or platform covers, following early cratonisation, as for example in the Pilbara and Kaalpvaal Cratons, North China and the Siberian Cratons (e. g. Zhao et al. 2005). The Earaheedy Basin may be a remnant of a post-Archaean platform-style sedimentary cover of the Yilgarn Craton. Cratonic basins and passive margins contain volcano-sedimentary and sedimentary successions, with banded and/or granular iron formations in the period between 2.4 and 1.8 Ga (Beukes and Gutzmer, 2008). The sedimentary rocks typically are represented by clastic sediments (arenite and shales) and shallow marine carbonates, characterised by transgression and regression sequences, reflecting the rise and fall of sea levels. The nature of the depositional systems in the post-Arhaean cratonic environements depends on the relative role of fluvial, aeolian, deltaic and tidal processes, wave and storm activity (Condie 2005). Furthermore, the distribution of the sediments is controlled by regional uplifts, the extent of the shallow seas and climate. Thus, where tectonic uplift is important, continental shelves tend to be narrow and sedimentation is dominated by wave and storm systems. In contrast, if uplift is confined to cratonic margins, fluvial and deltaic systems dominate (Condie, 2005). The reasons for the subsidence of cratonic blocks is not clear. A popular model is lithospheric stretching and thermal doming, followed by collapse. Doming of the lithosphere is a mechanism linked to upwelling asthenosphere or a mantle plume event, causing active erosion of the uplifted crust. Doming is followed by thermal contraction, resulting in the formation of cratonic platform basins and/or marginal basins around an opening ocean, which fill with sediments. A well documented example is the Neoproterozoic Centralian Superbasin, also in Australia, where crustal uplift due to a mantle plume at 825 Ma and subsequent sagging resulted in the deposition of thick successions of marine and fluvial sands (Walter et al. 1994; 1995). Post-Archaean depositional environments developed on the northern margin of the Yilgarn Craton, span some 450 million years, and were conducive to the genesis of a range of mineral systems, including seafloor hydrothermal deposits, extensive beds of

granular iron formation, MVT, the world-class Magellan non-sulphide Pb deposit (Pirajno, 2008), and orogenic Au lode deposits (Pirajno et al., in press).

North of the Yilgarn Craton's present-day boundary are the Goodin, Marymia and Malmac inliers, all of which represent Archaean granite-greenstone terranes and the northern extension of the Yilgarn Craton. These inliers are located within a 700-km long belt of Palaeoproterozoic volcano-sedimentary and sedimentary basins, which are considered part of the Capricorn Orogen (Fig. 1). These basins include the Bryah-Padbury, Yerrida and Earaheedy basins, developed between ca 2.2 and 1.8 Ga, recording periods of rifting, sedimentation and volcanism, along the northern passive margin of the Yilgarn Craton. The Yerrida Basin, is the oldest (ca. 2.17 Ga), and began its history as an intracontinental sag, within which low-energy siliciclastics and evaporites accumulated. To the west, the Bryah-Padbury basins formed during accretion and collision processes, related to the ca. 2.0-1.9 Ga Glenburgh and ca. 1.83-1.78 Ga Capricorn orogenies. An uplift and rifting event affected the Yerrida Basin at 1.84 Ga, resulting in coarse and immature clastic sedimentation together with the eruption of flood basalts (Mooloogool Group). To the east a passive margin developed, probably later than this uplift but the precise timing is poorly constrained. Sedimentation in this passive margin consisted of shallow-water clastic and chemical sediments (granular iron formation), which form the basal succession (Tooloo Subgroup) of the Earaheedy Basin. These events, deposition of the Mooloogool Group (uplift, rifting and volcanism) and the development of Earaheedy passive margin are difficult to explain within the framework of the Capricorn Orogeny. One possibility is that the Earaheedy passive margin formed as a result of continental breakup involving the Yilgarn Craton, perhaps as part of an Archaean supercontinent. During the ca 1.74 Ga Yapungku Orogeny and the 1.65 Ga, Mangaroon Orogeny (Sheppard et al., 2005), the northern margin of the Earaheedy Basin and the western parts of the Yerrida Basin were deformed (Stanley Fold Belt).

The Yerrida and Earaheedy basins are also characterised by an asymmetry in preserved cross-section, with undeformed southern depositional margins and northern (Earaheedy), and northern-northwestern (Yerrida) tectonic margins of intensely deformed rocks, similar to foreland basin architecture (Stanley Fold Belt), but entirely post-depositional in origin; the basins were trailing margin basins and active

depocentres. This may reflect the impingement of continental plates from the north and northeast.

The granular iron formation beds of the Frere Formation in the Earaheedy Basin constitute a significant Fe resource, extending along strike for at least 280 km. In the western parts of the Basin, zones of enrichment due to supergene and tectonic deformation processes, contain between 21 and 66% Fe. Locally, stratiform Fe-Mn oxides with anomalous abundances of Cu, Ba and Pb are hosted in clastic beds of the Wongawol Formation. The origin of the vast amounts of iron and manganese required to form the observed iron and manganese formations in Proterozoic sedimentary basins is controversial, but the popular view is that submarine hydrothermal effluents are the major source of these metals as well as others, such as Cu, Co, Zn, Pb, Au and Ag. Upwelling currents transport iron and manganese in reduced form (Fe^{+2} and Mn^{+2}) from the discharge vents, with precipitation occurring just above the oxic-anoxic interface , where Fe^{2+} and Mn^{2+} are oxidised to Fe^{3+} and Mn^{4+}, with separation being constrained by the Eh-pH conditions (Trendall, 2002). Uplift of fold belts provide the topographic relief that is necessary to cause basinal brines to migrate across the basin, with rates that are measured in several m/year, but that decline over a few million years as erosion progresses. Tectonically- and/or gravity-driven flow in foreland basins is considered as one of the main causes for the origin of the second group of mineral systems, which includes Mississippi Valley type (MVT) deposits, exemplified by the carbonate-hosted Zn-Pb deposits in the Yelma Formation (Earaheedy Basin) and the Magellan non-sulphide Pb deposit (Pirajno, 2008).

The Earaheedy Basin has special importance in the tectono-stratigraphic record of Palaeoproterozoic terranes, not only because of the presence of GIF beds, but also because it provides evidence of an ancient passive margin, which developed o the northern and northeastern margins of the Archaean Yilgarn Craton, hinting at a possible breakup from a larger Archaean continent at ca. 1.8 Ga.

Appendix. Supplementary data

Supplementary data associated with this paper can be found in the online version. At DOI:xxxxxxxxxx

Acknowledgements

This paper is published with the permission of the Director of the Geological Survey of Western Australia. The authors are grateful to Prof P. G. Eriksson for his constructive comments.

References

Adamides, N., 2000., Geology of the Merrie 1:100000 sheet. Geological Survey of Western Australia, 1:100 000 Geological Series Explanatory Notes, 37.

Adamides, N.G., Pirajno, F., and Farrell, T.R., 1999. Geology of the Cunyu 1:100 000 sheet. Geological Survey of Western Australia, 1:100000 Geological Series Explanatory Notes, 21.

Adamides, N.G., Pirajno, F., and Hocking, R.M., 2000. Geology of the Fairbairn 1:100 000 sheet. Geological Survey of Western Australia, 1:100 000 Geological Series Explanatory Notes, 26.

Allchurch, D., and Bunting, J.A., 1975. The Kaluweerie Conglomerate: A Proterozoic fluviatile sediment from the northeast Yilgarn Block, Western Australia. Geological Survey of Western Australia Annual Report 1975, 83-87.

Altermann, W., 2004. Precambrian stromatolites: problems and definitions, classification, morphology and stratigraphy. In: Eriksson, P. G., Altermann, W., Nelson, D. R., Mueller, W. U., Catuneanu, O. (eds), The Precambrian earth: Tempos and events, Precambrian Geology 12: 564-574, Elsevier, Amsterdam

Anderson, E.J., Goodwin, P. W. 1990. The significance of metre-scale allocycles in the quest for a fundamental stratigraphic unit: Journal of the Geological Society London 147, 507–518.

Bagas, L., 1998a. The Archaean Marymia Inlier — a review of its tectonic history and relationships to the Yilgarn Craton. Geological Survey of Western Australia, Annual Review 1997–1998, 85–90.

Bagas, L., 1998b. Geology of the Marymia 1:100000 sheet. Geological Survey of Western Australia, 1:100 000 Geological Series Explanatory Notes, 23.

1820 Bagas, L., 2004. Proterozoic evolution and tectonic setting of the northwest Paterson
1821 Orogen, Western Australia. Precambrian Research, 128, 475-496.

1822 Bagas, L., Smithies, R. H., 1998. Geology of the Connaughton 1:100 000 sheet,
1823 Western Australia. Western Australia Geological Survey, 1:100 000 Geological
1824 Series, Explanatory Notes, 38.

1825 Bagas, L., Williams, I. R., and Hickman, A. H., 2000. Rudall, Western Australia (2nd
1826 Edition): Western Australia Geological Survey, 1:250 000 Geological Series
1827 Explanatory Notes, 50.

1828 Barley, ME, Bekker, A, and Krapež, 2005, Late Archean to Early Paleoproterozoic
1829 global tectonics, environmental change and the rise of atmospheric oxygen: Earth
1830 and Planetary Science Letters 238, 156-171.

1831 Bau, M. and Moller, P., 1993. Rare earth element systematics of the chenmically
1832 precipitated component in Early Precambrian iron formations and the evolution
1833 of the terestial atmosphere-lithopshere system. Geochimica et Cosmochimica
1834 Acta 57, 2239-2249.

1835 Beukes, N.J., and Klein, C., 1990. Geochemistry and sedimentology of a facies
1836 transition — from microbanded to granular iron-formation — in the early
1837 Proterozoic Transvaal Supergroup, South Africa. Precambrian Research 47, 99–
1838 139.

1839 Beukes, N.J., and Klein, C., 1992. Models of iron-formation deposition, *in* The
1840 Proterozoic biosphere: a multidisciplinary study, *edited by* W. Schope and C.
1841 Klein. Cambridge University Press, New York, 147–151.

1842 Beukes, N. J., Gutzmer, J., 2008. Origin and paleoenvironmental siginifcance of
1843 major iron formations at the Archean-Paleoproterozoic boundary. SEG Reviews
1844 15, 5-47.

1845 Blackburn, G., 2003. Troy Creek Pt-Pd-Au prospect, Nabberu District, Western
1846 Australia. CRC LEME Report, 1-2.

1847 Blatt, H., Middleton, G., Murray, R., 1980. Origin of sedimentary rocks, 2nd edition,
1848 Prentice Hall Inc. Englewood Cliffs, NJ, 782 pp.

1849 Bradley, D. C., 2008. Passive margins through earth history. Earth-Science Reviews
1850 91, 1-26.

1851 Brakel, A.T., and Leech, R.E.J., 1980. Trainor, W. A.. Geological Survey of Western
1852 Australia, 1:250 000 Geological Series Explanatory Notes 13.

1853 Braun, J., Beaumont, C., 1989. A physical explanation of the relation between flank
1854 uplifts and the breakup unconformity at rifted continental margins. Geology 17,
1855 760–764.

1856 Brown, D.A., Gross, G.A., and Sawicki, J.A., 1995. A review of the microbial
1857 geochemistry of banded iron-formations. Canadian Mineralogist 33, 1321-1333.

1858 Bunting, J.A., 1980a. Kingston, W.A.. Geological Survey of Western Australia,
1859 1:250 000 Geological Series Explanatory Notes 18.

1860 Bunting, J.A., 1980b. Kingston, Western Australia, Sheet SG 51-10. Australia Bureau
1861 of Mineral Resources and Geological Survey of Western Australia 1:250 000
1862 Geological Series.

1863 Bunting, J.A., 1986. Geology of the eastern part of the Nabberu Basin. Geological
1864 Survey of Western Australia, Bulletin 131, 130.

1865 Bunting, J.A., Brakel, A.T., and Commander, DP, 1982, Nabberu, Western Australia.
1866 Geological Survey of Western Australia, 1:250 000 Geological Series
1867 Explanatory Notes 27.

1868 Cawood, P.A. and Nemchin, A.A., 2000. Provenance record of a rift basin: U/Pb ages
1869 of detrital zircons from the Perth Basin, Western Australia. Sedimentary Geology
1870 134, 209-234.

1871 Cawood, P.A., Tyler, I.M., 2004. Assembling and reactivating the Proterozoic
1872 Capricorn Orogen: lithotectonic elements, orogenies and significance.
1873 Precambrian Research 128, 201-218.

1874 Commander, D.P., Muhling, P.C., and Bunting, J.A., 1982. Stanley, W.A.. Geological
1875 Survey of Western Australia, 1:250 000 Geological Series Explanatory Notes 19.

1876 Condie K.C., 2005. Earth as an evolving planetary system: Elsevier, Amsterdam, pp.
1877 447.

1878 Deer W.A., Howie R.A., Zussman J., 1965. Rock forming minerals, vol 3, Sheet
1879 Silicates. Longmans, London, 270 pp.

1880 Derry, L.A., and Jacobsen, S.B., 1990. The chemical evolution of Precambrian
1881 seawater: evidence from REEs in banded iron formations. Geochimica et
1882 Cosmochimica Acta 54, 2965-2977.

1883 Donaldson, W.S., Plint, A.G., Longstaffe, F.J., 1999. Tectonic and eustatic control on
1884 deposition and preservation of Upper Cretaceous ooidal ironstone and associated
1885 facies: Peace River Arch area, NW Alberta, Canada. Sedimentology 46, 1159-
1886 1182.

1887 Eisenlohr, M., 1989. Final Report, E52/377, E52/378, Clover Tabletop, for the period
1888 13 July 1989 to 27 October 1989, Newmont Australia Ltd. Geological Survey of
1889 Western Australia, Statutory mineral exploration report, Item 4138, A29115.

1890 Elias, M., Bunting, J.A., 1982. Wiluna, W.A.: Geological Survey of Western
1891 Australia, 1:250 000 Geological Series Explanatory Notes 20.

1892 Einsele, G., 2000. Sedimentary basins: evolution, facies and sedimentary budget, 2nd
1893 Ed. Springer-Verlag, Heidelberg, 792 pp.

1894 Elrick, M., Read, J.F., 1991. Cyclic ramp-to-basin carbonate deposits, Lower
1895 Mississippian, Wyoming and Montana, a combined field and computer modelling
1896 study, Journal of Sedimentary Petrology 61, 1194-1224.

1897 Eriksson, P.G., Martins-Neto, M.A., Nelson, D.R., Aspoler, L.B., Chiarenzelli, J.R.,
1898 Catuneau, O., Sarkar, S., Altermann, W., Rautenbach, C.J.D.E.W., 2001. An
1899 introduction to Precambrian basins: their characteristics and genesis. Sedimentray
1900 Geology 141-142, 1-35.

1901 Fischer, A.G., Bottjer, D. J., 1991. Orbital forcing and sedimentary sequences: Journal
1902 of Sedimentary Petrology 61, 1063 - 1069.

1903 Franseen, E.K., Watney, W.L., Kendall, C.G. StC, Ross, W. (eds), 1991, *Sedimentary*
1904 *modelling: Computer simulations and methods for improved parameter*
1905 *definition*: Kansas Geological Survey Bulletin 233, 524 p.

1906 Garven, G., Raffensperger, J.P., 1997. Hydrogeology and geochemistry of ore genesis
1907 in sedimentary basins, in Barnes HL (ed), Geochemistry of ore deposits, 3rd edn,
1908 John Wiley & Sons, 125-189.

1909 Giles, E., 1889. Australia twice traversed; the romance of exploration, being a
1910 narrative compiled from the journals of five exploring expeditions into and
1911 through central South Australia and Western Australia, from 1872 to 1876.
1912 London, Low, Marston, Searle and Rivington.

1913 Goode, A.D.T., Hall, W.D.M., and Bunting, J.A., 1983. The Nabberu Basin of
1914 Western Australia, *in* Iron formation: Facts and problems edited by A. F. Trendall
1915 and R. C. Morris: Developments in Precambrian Geology. Elsevier Monograph 6,
1916 295–323.

1917 Goldhammer, R.K., Dunn, P.A., Hardie, L. A. 1987. High-frequency, glacioeustatic
1918 sealevel oscillations with Milankovich characteristics recorded in Middle Triassic
1919 platform carbonates in northern Italy: American Journal of Science,287, 853-892.

1920 Goldhammer, R.K., Dunn, P.A., Hardie, L. A. 1990. Depositional cycles, composite
1921 sealevel changes, cycle stacking patterns, and the heirarchy of stratigraphic
1922 forcing—examples from platform carbonates of the Alpine Triassic: Geological
1923 Society of America Bulletin 102, 535-562.

1924 Goldhammer, R.K., Lehmann, P.J., Dunn, P.A. 1993. The origin of high-frequency
1925 platform carbonate cycles and third order sequences (Lower Ordovician El Paso

Group, West Texas): constraints from outcrop data and stratigraphic modelling: Journal Sedimentary Petrology 63, 318-359.

Grey, K., 1984. Biostratigraphic studies of stromatolites from the Proterozoic Earaheedy Group, Nabberu Basin, Western Australia. Geological Survey of Western Australia Bulletin 130, 123.

Grey, K., 1994. Stromatolites from the Palaeoproterozoic Earaheedy Group, Earaheedy Basin, Western Australia: Alcheringa 18, 187–218.

Grey, K., Thorne, A.M., 1985. Biostratigraphic significance of stromatolites in upward shallowing sequences of the early Proterozoic Duck Creek Dolomite, Western Australia. Precambrian Research 29, 183-206.

Groenewald, P.B., Painter, M.G.M., and Mccabe, M., 2001. East Yilgarn geoscience database: north Eastern Goldfields, Cunyu to Cosmo Newbery 1:100 000 digital geological data package. Western Australia Geological Survey, Report 83, 39.

Gromet, L.P., Dymek, R.F., Haskin, L.A., and Korotev, R.L., 1984. The "North American Shale Composite": its compilation, major and trace element characteristics. Geochimica et Cosmochinica Acta 48, 2469-2482.

Hall, W.D.M., Goode, A.D.T., 1975. The Nabberu Basin; a newly discovered Lower Proterozoic basin in Western Australia. Geological Society of Australia, First Australian Geological Convention, Abs., 88–89.

Hall, W.D.M., Goode, A.D.T., 1978. The early Proterozoic Nabberu Basin and associated iron formations of Western Australia. Precambrian Research 7, 129–184.

Hall, W.D.M., Goode, A.D.T., Bunting, J.A., Commander, D.P., 1977. Stratigraphic terminology of the Earaheedy Group, Nabberu Basin. Geological Survey of Western Australia, Annual Report 1976, 40–43.

1951 Halilovic, J., Cawood, P.A., Jonaes, J.A., Pirajno, F., Nemchin, A.A., 2004.
1952 Provenance of the Earaheedy Basin, Western Australia: palaeogeographic and
1953 tectonic implications. Precambrian Research 128, 343-366.

1954 Hallberg, J.A., 1987. Postcratonization mafic and ultramafic dykes of the Yilgarn
1955 Block. Australian Journal of Earth Sciences 34, 135–149.

1956 Hamilton, R., 1992. Geology and structural setting of ultramafic lamprophyres from
1957 Bulljah Pool, central Western Australia. Journal of the Royal Society of Western
1958 Australia 75, 51-56.

1959 Hamilton, R., and Rock, N.M.S., 1990. Geochemistry, mineralogy and petrology of a
1960 new find of ultramafic lamprophyres from Bulljah Pool, Nabberu Basin, Yilgarn
1961 Craton, Western Australia. Lithos 24, 275-290.

1962 Heikoop J.M., Tsujita C.J., Risk M.J., Tomascil T., Mah A.J., 1996. Modern iron
1963 ooids from a shallow-marine volcanic setting: Mahegetang, Indonesia. Geology
1964 24, 759-762.

1965 Hocking, R.M., Jones, J.A., 1999. Methwin, W.A. Sheet 3047. Geological Survey of
1966 Western Australia, 1:100 000 Geological Series.

1967 Hocking, R.M., Jones, J.A., Pirajno, F., Grey, K., 2000a. Revised lithostratigraphy for
1968 Proterozoic rocks in the Earaheedy Basin and nearby areas. Geological Survey of
1969 Western Australia, Record 2000/16, 22.

1970 Hocking, R.M., Grey, K., Bagas, L., Stevens, M.K., 2000b. Mesoproterozoic
1971 stratigraphy in the Oldham Inlier, Little Sandy Desert, central Western Australia.
1972 Geological Survey of Western Australia, Annual Review 1999–2000, 49–56.

1973 Horwitz, R.C., 1975a. The southern boundaries of the Hamersley and Bangemall
1974 Basins of sedimentation. Geological Society of Australia, First Australian
1975 Geological Convention, Abs., 88–89.

1976 Horwitz, R.C., 1975b. Provisional geological map at 1:2 500 000 of the north-east
1977 margin of the Yilgarn Block, Western Australia. Australia Commonwealth
1978 Scientific Industrial Research Organization, Mineral Research Lab. Report F10.

1979 Horwitz, R.C., 1976. Two unrecorded basal sections in older Proterozoic rocks of
1980 Western Australia. Australia CSIRO Mineral Research Lab. Report FP 10.

1981 House, M.R., Gale, A.S. (eds), 1995. *Orbital forcing timescales and*
1982 *cyclostratigraphy*: Geological Society Special Publication 85.

1983 Isley, A.E., 1995. Hydrothermal plumes and the delivery of iron to banded iron
1984 formation. The Journal of Geology 103, 169-185.

1985 Jacobsen, S.B., Pimentel-Klose, M.R., 1988. Nd isotopic variations in Precambrian
1986 banded ison formations. Geophysical Research Letters 15, 393-396.

1987 Jackson, J.A., 1997, Glossary of geology (4th edition). Virginia, U.S.A., American
1988 Geological Institute, 769.

1989 Johnson, G.I., 1991. The petrology, geochemistry and geochronology of the felsic
1990 alkaline suite of the eastern Yilgarn block, Western Australia. South Australia,
1991 University of Adelaide, PhD thesis (unpublished).

1992 Jones JA, 2004, Geology of the Wongawol 1:100 000 sheet. Geological Survey of
1993 Western Australia Explnatory Notes 1:100 000 Geological Series, 28p.

1994 Jones, J.A., Pirajno, F., Hocking, RM.., Grey, K., 2000. Revised stratigraphy for the
1995 Earaheedy Group: Implications for the tectonic evolution and mineral potential of
1996 the Earaheedy Basin. Geological Survey of Western Australia, Annual Review
1997 1999–2000, 57–63.

1998 Kappler, A., Pasquero, C., Konhauser, K.O., Newman, D.K., 2005. Deposition of
1999 banded iron formations by anoxygenic phototrophic Fe(II)-oxidizing bacteria.
2000 Geology 33, 865-868.

Kimberley, M.M., 1989. Nomenclature for iron formations: Ore Geology Reviews 5, 1–12.

Kinny, P.D., Nutman, A.P., Occhipinti, S.A., 2004. Recoinnasance dating of events recorded in the southern part of the Capricorn Orogen. Precambrian Research 128, 279-294.

Klein, C., Ladeira, E.A., 2000. Geochemistry and petrology of some Proterzoic banded iron formations of the Quadriletero Ferrifero, Minas Gerais, Brazil. Economic Geology 95, 405-428.

Konhauser, K.O., Hamade, T., Morris, R.C., Ferris, F.G., Southam, G., Raiswell, R., Canfield, D., 2002. Could bacteria have formed the Precambrian banded iron formations? Geology 30, 1079-1082.

LaBerge G.L., 1966. Altered pyroclastic rocks in iron formations in the Hamersley Range, Western Australia. Economic Geology 61, 147-161.

Langford, R.L., Wyche, S., Liu, S.F., 2000. Geology of the Wiluna 1: 100 000 sheet. Geological Survey of Western Australia, 1:100 000 Geological Series Explanatory Notes 26.

Leech, R.E.J., and Brakel, A.T., 1980. Bullen, Western Australia. Geological Survey of Western Australia, 1:250 000 Geological Series Explanatory Notes 11.

Lindsay, J., and Brasier, M., 2002. Did global tectonics drive early biosphere evolution? Carbon isotope record from 2.6 to 1.9 Ga carbonates of Western Australia. Precambrian Research 114, 1-34.

Martin, D.McB., Thorne, A.M., 2004. Tectonic and basin evolution of the Bangemall Supergroup in the northwestern Capricorn Orogen. Precambrian Research, 128, 385-410.

Martin, D.McB., Thorne, A.M., Copp, I.A., 1999. A provisional revised stratigraphy for the Bangemall Group on the Edmund 1:250 000 sheet. Geological Survey of Western Australia, Annual Review 1998–1999, 51–55.

2028 McMillan, N.M., McNaughton, N.J., 1995. The post-magmatic history of felsic rocks
2029 from the Archaean Marymia Dome — a SHRIMP study of the relationship
2030 between zircon morphology, Th/U and geological history. Third Australian
2031 Conference on Geochronology and Isotope Geoscience, Abstracts, 18.

2032 McNaughton, N.J., Rasmussen, B., and Fletcher, I.R., 1999. SHRIMP uranium-lead
2033 dating of diagenetic xenotime in siliciclastic sedimentary rocks. Science 285, 78-
2034 80.

2035 Meakins, AL, and Watsham, S, 1994, Annual Report for the period ended September
2036 30/1993—E52/220, 222, 224, 226, 554, 555, 557, 587, 668, 670, 712, 732, and
2037 E51/321, 357, 367, 391, Ruby Bore–Good Pool Project, Peak Hill SG50-08,
2038 Western Australia (vol. 1 and 2): Western Australia, Geological Survey M-series
2039 Item 8477 (unpublished).

2040 Morris, P.A., Pirajno, F., 2005. Mesoproterozoic sill complexes in the Bangemall
2041 Supergroup, Western Australia. Geology, geochemistry and mineraliazation
2042 potential. Geological Survey of Western Australia Report 99, 75p.

2043 Morris, P.A., Pirajno, F., and Shevchenko, S., 2003. Proterozoic mineralization
2044 identified by integrated regional regolith geochemistry, geophysics and bedrock
2045 mapping in Western Australia. Geochemistry, Exploration, Environment,
2046 Analysis 3, 2003, 13–28.

2047 Myers, J.S., Shaw, R., Tyler, I.M., 1996. Tectonic evolution of Proterozoic Australia.
2048 Tectonics 15-6, 1431-1446.

2049 Nealson, K.H., 1982. Microbiological oxidation and reduction of iron, in Mineral
2050 Deposits and the Evolution of the Biosphere, H. D. Holland and M. Schidlowski
2051 (eds), Springer-Verlag, 51-66.

2052 Nelson, D.R., 1995. Compilation of SHRIMP U–Pb zircon geochronology data, 1994.
2053 Geological Survey of Western Australia, Record 1995/3, 244.

2054 Nelson, D.R., 1997. Compilation of SHRIMP U–Pb zircon geochronology data, 1996.
2055 Geological Survey of Western Australia, Record 1997/2, 189.

Nelson, D.R., 1999. Compilation of SHRIMP U–Pb zircon geochronology data, 1998. Geological Survey of Western Australia, Record 1999/2, 222.

Nelson, D.R., 2001a. An assessment of the determination of depositional ages for Precambrian clastic sedimentary rocks by U-Pb dating of detrital zircons. Sedimentary Geology 141-142, 37-60.

Nelson, D.R., 2001b. Compilation of geochronology data, 2000, Geological Survey of Western Australia Record, 2001/2, 205.

Nelson, D.R., 2002. Compilation of geochronology data, 2001, Geological Survey of Western Australia Record, 2002/2, 282.

Nemchin, A.A., Pidgeon, R.T., 1998. Precise conventional and SHRIMP baddelyite U-Pb age for the Binneringie Dyke, near Narrogin, Western Australia. Australian Journal of Earth Sciences 45, 673-675.

Newsom, H.E., Graup, G., Sewards, T., Keil, K., 1986. Fluidization and hydrothermal alteration of the suevite deposit at the Ries Crater, West Germany, and implications for Mars. Journal of Geophysical Research 91, E239-E251.

Occhipinti, S.A., Sheppard, S., 2001. Stuck between two cratons – latest Archaean crust in the Gascoyne Complex, Western Australia. In: The Fourth International Archaean Symposium, Extended Abstracts, 72-74.

Occhipinti, S.A., Sheppard, S., Nelson, D.R., Myers, J.S., Tyler, I.M., 1998. Syntectonic granite in the southern margin of the Palaeoproterozoic Capricorn Orogen, Western Australia. Australian Journal of Earth Sciences 45, 509–512.

Occhipinti, S.A., Sheppard, S., Myers, J.S., Tyler, I.M., Nelson, D.R., 2001. Archaean and Palaeoproterozoic geology of the Narryer terrane (Yilgarn Craton) and the southern Gascoyne Complex (Capricorn Orogen), Western Australia – A field guide. Geological Survey of Western Australia Record 2001/8, 70.

2081 Osinski, G.R., Spray, G., Lee, P., 2001. Impact-induced hydrothermal activity within
2082 the Haughton impact structure, arctic Canada: generation of a transient, warm,
2083 wet oasis. Meteoritic and Planetary Science 36, 731-745.

2084 Pirajno, F., 1999. Nabberu, W. A. Sheet 3046. Geological Survey of Western
2085 Australia, 1:100 000 Geological Series (1st Edition).

2086 Pirajno, F., 2002. Geology of the Shoemaker Impact Structure, Western Australia.
2087 Geological Survey of Western Australia, Report 82, 52.

2088 Pirajno, F., 2004. Metallogeny in the Capricorn Orogen, Western Australia, the result
2089 of multiple ore-forming processes. Precambrian Research, 128, 411-440.

2090 Pirajno, F., 2007. Metallogeny of Palaeoproterozoic depositional environments on the
2091 northern margin of the Yilgarn Craton. Proceedings of Kalgoorlie '07
2092 Conference, Kalgoorlie, Bierlein F., Knoz-Robinson C. M. (editors), pp 77-79.

2093 Pirajno, F., 2008. Hydrothermal processes and mineral systems. Springer, Berlin,
2094 1250pp

2095 Pirajno, F., Bagas, L., Swager, C.P., Occhipinti, S.A., Adamides, N.G., 1996. A
2096 reappraisal of the stratigraphy of the Glengarry Basin, Western Australia.
2097 Geological Survey of Western Australia, Annual Review 1995–1996, 81–87.

2098 Pirajno, F., Adamides, N.G., 1998. Geology of the Thaduna 1:100 000 sheet.
2099 Geological Survey of Western Australia, 1:100 000 Geological Series
2100 Explanatory Notes 24.

2101 Pirajno, F., Glikson, A. 1998. Shoemaker impact structure, Western Australia.
2102 Celestial Mechanics and Dynamical Astronomy 69, 25–30.

2103 Pirajno F, Occhipinti, SA, 1998, Geology of the Bryah 1:100 000 sheet. Geological
2104 Survey of Western Australia, 1:100 000 Series Explanatory Notes, 41p.

2105 Pirajno, F, Occhipinti, S. A., and Swager, C. P., 1998. Geology and tectonic evolution
2106 of the Palaeoproterozoic Bryah, Padbury and Yerrida Basins (formerly Glengarry

Basin), Western Australia: implications for the history of the south-central Capricorn Orogen. Precambrian Research 90, 119-140.

Pirajno, F., Hocking, R. M., Jones, J.A., 1999. Geology, mineralization and geodynamic evolution of the Palaeoproterozoic Yerrida and Earaheedy Basins, W.A., *in* Two billion years of tectonics and mineralisation *edited by* Watt, GR, and Evans, DAD,: Curtin University of Technology, Tectonics Special Research Centre Conference, Perth, W.A., 1999, Proceedings. Geological Society of Australia, Abstracts Series, no. 56, 30–33.

Pirajno, F., Occhipinti, S.A., Swager, C.P., 1998. Geology and tectonic evolution of the Palaeoproterozoic Bryah, Padbury and Yerrida Basins (formerly Glengarry Basin), Western Australia: implications for the history of the south-central Capricorn Orogen. Precambrian Research 90, 119-140.

Pirajno, F., Adamides, N.G., 2000. Iron–manganese oxides and glauconite-bearing rocks of the Earaheedy Group: implications for the base metal potential of the Earaheedy Basin. Geological Survey of Western Australia, Annual Review 1999–2000, 65–71.

Pirajno, F., Hocking, R.M., Jones, J.A., 2000. Rhodes, W.A. Sheet 3147. Geological Survey of Western Australia, 1:100 000 Geological Series.

Pirajno, F., Hocking, R.M., 2002. Glenayle, W.A. Sheet 3347. Geological Survey of Western Australia, 1:100 000 Geological Series.

Pirajno, F., Hawke, P., Glikson, A.Y., Haines, P.W., Uysal, T., 2003. Shoemaker impact structure, Western Australia: Australian Journal of Earth Sciences 34, No. 5, 775–796.

Pirajno, F., Jones, J.A., Hocking, R.M., Halilovic, J., 2004. Geology and tectonic evolution of Palaeoproterozoic basins of the eastern Capricorn Orogen, Western Australia. Precambrian Research 128, 315-342.

Pirajno, F., Hocking, R. M., Jones, J. A., Reddy, S. J. (in press). Geology and mineral systems of the Palaeoproterozoic Earaheedy Basin, Western Australia. Geological Survey of Western Australia Report

Pratt, B.R., 2002. Storms versus tsunamis: dynamic interplay of sedimentary, diageneitc and tectonic processes in the Cambrian of Montana. Geology 30, 423-426.

Preiss, W.V., Jackson, M.J., Page, R.W., Compston, W., 1975. Regional geology, stromatolite biostratigraphy and isotopic data bearing on the age of a Precambrian sequence near Lake Carnegie, Western Australia. Geological Society of Australia, 1st Australian Geological Convention, Abstracts, 92–93.

Price, J., 2003. Depositional setting of granular iron formation in the Palaeoproterozoic Frere Formation, Earaheedy Basin, Western Australia. BSc (Hon) thesis, unpublished, The University of Western Australia, 80p.

Rasmussen, B., Fletcher, I.R., 2002. Indirect dating of mafic intrusions by SHRIMP U-Pb analysis of monazite in contact metamorphosed shale: an example from the Palaeoproterozoic Capricorn Orogen, Western Australia. Earth and Planetary Science Letters 197, 287-299.

Read, J.F., Kerans, C., Webber, L.J., Sarg, J.F., Wright, F.M., (eds), 1995. Milankovich sea-level changes, cycles, and reservoirs on carbonate platforms in greenhouse and icehouse worlds. SEPM Short Course Notes 35, 212.

Reddy, S.M., Collins, A.S., Buchan, A.C. & Mruma, A. 2004. Heterogeneous excess argon and Neoproterozoic heating in the Usagaran Orogen, Tanzania, revealed by single grain $^{40}Ar/^{39}Ar$ thermochronology. Journal of African Earth Sciences, 39, 165-176.

Richards, J.R., Gee, R.D., 1985. Galena lead isotopes from the eastern part of the Nabberu Basin, Western Australia. Australian Journal of Earth Sciences 32, 47–54.

Rock, N.M.S., 1990. Lamprophyres: the global occurrence, petrology, origin and economic significance of some rocks of deep origin. Blackie, Glasgow, 250 p.

Rodriguez-Pascua, M.A., Clavo, J.P., De Vicente, G., Gomez-Gras, D., 2000. Soft-sediment deformation structures interpreted as seismites in lacustrine sediments of the Prebetic Zone, SE Spain, and their potential use as indicators of earthquake magnitudes during the Late Miocene. Sedimentary Geology 135, 117–135.

Russell, J., Grey, K., Whitehouse, M., Moorbath, S., 1994. Direct Pb/Pb age determination of Proterozoic stromatolites from the Ashburton Nabberu basins, Western Australia, in 8th International Conference on Geochronology, Cosmochronology and Isotope Geology, Berkeley, California, U.S.A., Abstracts. U.S. Geological Survey Circular 1107, 275.

Scrimgeour, I.R., Close, D.F., Edgoose, C.J., 1999. Petermann Ranges SG- 52-7. 1:250000 Geological map series, Explanatory Notes, Northern Territory Geological Survey.

Shee, S.R., Vercoe, S.C., Wyatt, B.A., Hwang, P.H., Campbell, A.N., Colgan, E.A., 1999. Discovery and geology of the Nabberu Kimberlite Province, Western Australia. In: Gurney J. J. (ed) Proceedings of the VIIth International kimberlite conference, Cape Town, 764-772.

Sheppard, S., Occhipinti, S., Nelson, D.R., Tyler, I.M., 1999. Granites of the southern Capricorn Orogen, Western Australia, two billion years of Tectonics and Mineralisation. In: Tectonics Special Research Centre Conference Proceedings, 44-46.

Sheppard, S., Occhpinti, S., Nelson, D.R., 2005. Intracontinental reworking in the Capricorn Orogen, Western Australia: the 1680-1620 Mangaroon Orogeny. Australian Journal of Earth Sciences 52, 443-460.

Sheppard, S., Occhipinti, S., Tyler, I.M., 2004. A 2005-1970 Ma Andean-type batholith in the southern Gascoyne Complex, Western Australia. Precambrian Research 128, 257-277.

2188 Sheppard, S., Rasmussen, B., Muhling, J.R., Farrell, T.R., Fletcher, I.R., 2007.
2189 Grenvillian-aged orogenesis in the Palaeoproterozoic Gascoyne Complex,
2190 Western Australia: 1030-950 Ma reworking of the Proterozoic Capricorn orogen:
2191 Journal of Metamorphic Geology 25, 477-494.

2192 Shoemaker, E.M., Shoemaker, C.S., 1996. The Proterozoic impact record of
2193 Australia: Australian Geological Survey Organisation, Journal of Australian
2194 Geology and Geophysics 16, 379–398.

2195 Simonson, B.M., Hassler, S.W., 1996. Was the deposition of large Precambrian iron
2196 formations linked to major marine transgressions? Journal of Geology 104, 665-
2197 676.

2198 Smithies, R.H., Bagas, L., 1997. High pressure amphibolite-granulite facies
2199 metamorphism in the Palaeoproterozoic Rudall Complex, central Western
2200 Australia. Precambrian Research, 83, 243-265.

2201 Smithies, R.H., Champion, D.C., 1999. Late Archaean felsic alkaline igneous rocks in
2202 the Eastern Goldfields, Yilgarn Craton, Western Australia: a result of lower
2203 crustal delamination?. London Geological Society, Journal 156, 561–576.

2204 Steiger, R. H., Jager, E. 1977. Subcommision on Geochronology: Convention on the
2205 use of decay constants in geo- and cosmochronology. Earth and Planetary
2206 Science Letters**,** 36, 359-362.

2207 Swager, C.P., 1997. Tectono-stratigraphy of the late Archaean greenstone terranes in
2208 the southern Eastern Goldfields, Western Australia. Precambrian Research, 83,
2209 11-42.

2210 Talbot, H.W.B., 1910. Geological observations in the country between Wiluna, Hall's
2211 Creek, and Tanami. Geological Survey of Western Australia, Bulletin 39, 88.

2212 Talbot, H.W.B., 1914. The country between lat. 23˚ and 26˚S, and long. 119˚and
2213 121˚E. Geological Survey of Western Australia, Annual Report 1913, 24–25.

Talbot, H.W.B., 1919. Notes on the geology and mineral resources of parts of the North-West, Central and Eastern Divisions. Geological Survey of Western Australia, Annual Report 1918, 83–93.

Talbot, H.W.B., 1920. Geology and mineral resources of the North-west, Central, and Eastern Divisions. Between Long. 119˚ and 122˚ E., and Lat. 22˚ and 28˚ S.. Geological Survey of Western Australia, Bulletin 83, 226.

Talbot, H.W.B., 1926. A geological reconnaissance in the Central and Eastern Divisions between 122˚ 30'E and 123˚ 30'E Longitude, and Lat. 25˚ 30'S and 28˚ 15'S Latitude. Geological Survey of Western Australia, Bulletin 87, 30.

Teen, M.T., 1996. Silicification and base metal mineralization within the Earaheedy Basin, Western Australia. BSc (Hon) thesis (unpublished), Centre for Ore Deposit and Exploration Studies, University of Tasmania, 128 p.

Tobin, K.J., 1990. The paleoecology and significance of the Gunflint-type microbial assemblages from the Frere Formation (Early Proterozoic), Nabberu Basin, Western Australia. Precambrian Research, 47, 71–81.

Trendall, A.F., 2002. The significance of iron-formation in the Precambrian stratigraphic record. In: Altermann, W. and Corcoran, L. (eds), Precambrian sedimentary environments: A modern approach to ancient depositional systems, 33-66, Blackwell Science, Oxford.

Tyler, I. M., Pirajno, F., Bagas, L., Myers, J.S., 1998. Geology and mineral deposits of the Proterozoic of Western Australia. AGSO Journal of Geology and Geophysics 17, 223–244.

Vielreicher, N.M., McNaughton, N.J., 2002. SHRIMP U-Pb geochronology of magmatism and thermal event in the Archaean Marymia Inlier, central Western Australia. International Journal of Earth Sciences (Geol Rundsch) 91, 406-432.

Walraven, F., Armstrong, R.A., Kruger, F.J., 1990. A chronostratigraphic framework for the north-central Kaapvaal Craton, the Bushveld Complex and the Vredefort structure. Tectonophysics 171 23-48.

2242 Walter, MR, Goode, ADT, and Hall, JA, 1976, Microfossils from the a newly
2243 discovered Precambrian stromatolitic iron formation in Western Australia:
2244 Nature, 261, 221-223.

2245 Walter, M.R., Veevers, J.J., Calver, C.R., Grey, K., 1995. Late Proterozoic
2246 stratigraphy of the Centralian Superbasin, Australia. Precambrian Research, 73,
2247 173–175.

2248 Wingate, M.T.D., Pirajno, F., Morris, P.A., 2004. The Warakurna large igneous
2249 province: a new Mesoproterozoic large igneous province in west-central
2250 Australia. Geology 32, 105-108.

2251 Wyche, S., Farrell, T.R., 2000. Regional geological setting of the Yandal greenstone
2252 belt, northeast Yilgarn Craton. Yandal Greenstone Belt, Australian Institute of
2253 Geoscientists, Bulletin 32, 41-50.

2254 Zhao G.C., Min, S., Wilde S.A., Li S.Z., 2005. Late Archean to Paleoproterozoic
2255 evolution of the North China Craton: key issues revisited. Precambrian Research
2256 136, 177-202.

2257

FIGURE CAPTIONS

Figure 1 Tectonic units of the Capricorn Orogen and postion of the Earaheedy Basin; E gerton Inlier, M Marymia Inlier, S Sylvania Inlier. Modified from Pirajno et al. (2004)

Figure 2 A) Simplified geology of the Earahedy Basin and covering 1:100 000 scale map sheets; B) Aeromagnetic image of the northern margin of the Yilgarn Craton and eastern Capricorn Orogen basin systems (outlined); note scale difference with (A)

Figure 3 Field photographs of Prenti Dolerite on Von Treuer; a) aerial view of a Prenti Dolerite sill (outlined); b) view of the same sill from the ground; c) outcrop of Prenti Dolerite in contact with sandstone of the Chiall Formation. After Morris and Pirajno (2005).

Figure 4 Stratigraphic column of the Earaheedy Group

Figure 5 Schematic north-south cross-section of the Earahedy Basin and stratigraphy

Figure 6 Frequency distribution diagram of SHRIMP zircon ages of six samples from the Yelma Formation; also includes a summary plot from Nelson (2001). The dashed line is the Archean-Proterozoic boundary taken at 2500 Ma. Numbers (e.g. 12/10) refer to total number of zircon analyses (shaded area) against the number of analyses more than 90% concordant (line on graph). After Halilovic et al. (2004)

Figure 7 Stratigraphy of the Yelma Formation on THADUNA, derived from drillhole CTW002 and outcrops near Lake Gregory. After Pirajno and Adamides (1998)

Figure 8 Outcrops of Sweetwaters Well Member stromatolitic; a) microbial laminites; b) *Omachtenia teagiana* (Grey 1984); c) unidentified stromatolite forms; d) drill core with *Asperia digitata* and *Pilbaria deverella* (Grey 1984). After Pirajno et al. (2004)

Figure 9 Models of depositional environment for the Yelma Formation and associated stromatolite colonies

Figure 10 Simplified stratigraphic column of the Tooloo Subgroup, compiled from drill core and field observations. The granular iron-formation has at least four bands (F1 Gif to F4 GIF) with three intercalated shale-siltstone bands; the topmost siltsone band could belong to the Windidda Member

Figure 11 Macro- (a), meso- (b), and microscale (c) banding of granular iron-formation of the Frere Formation; hematite peloids are cemented by quartz or quartz-carbonate. After Pirajno (2008)

Figure 12 Photomicrographs of granular iron-formation in the Frere Formation: a) intraclast and jasperoidalpeloids in a siliceous matrix; b)chloritic shale intercalated

with peloidal iron-formation. The pale green chlorite is a ferroan clinochlore (X-ray diffraction analysis) associated with quartz, kaolinite, and opaque;c) peloidal ironstone; d) detail of (c); e) disseminated euhedral magnetite crystals in chloritic siltstoneband; f) detail of peloid composed of microplaty hematite minerals. a) to d) plane-polarized light; e) and f) reflected light. After Pirajno et al. (2004)

Figure 13 Photomicrographs showing aspects of alteration of granular iron-formation in the Frere Formation: peloids partly replaced by cryptocrystalline quartz (chert) and cemented by allochemical dolomite; b) with cross-cutting quartz–chlorite–carbonate veinlet; dark concentric laminae in the peloids are composed ofhematite; c) detail of replacement of peloid by cryptocrystalline quartz; d) peloidal carbonate intercalated with granular iron-formation; here the peloid in centre of photomicrograph is replaced by chlorite (core) and microplaty hematite along the margins, surrounding material is dolomite, chlorite, and microcrystalline quartz; e) and f) carbonate peloids partly replaced by hematite and cemented by chlorite,?orthochemical dolomite and locally stilpnomelane (not visible in this section). All in plane-polarized light, except for a) which is with crossed polars. After Pirajno et al. (2004)

Figure 14 Stilpnomelane alteration of granular iron-formation in the Frere Formation: a) photomicrograph showing sheafs of acicular stilpnomelane (crossed polars; b) photomicrograph showing green-pleochroic stilpnomelane crystals cutting through chalcedonic quartz (brown; plane polarized light; c) drillcore showing typical granular iron-formation beds (red bands with chert intraclasts), intercalated with dark-coloured shale; d) drillcore of silicified and stilpnomelane-altered granular iron-formation and shale interbeds; e) close-up of core showing massive stilpnomelane (dark material) and partially silicified and stilpnomelane-altered peloidal ironformation. After Pirajno et al. (2004)

Figure 15 Photomicrographs showing aspects of alteration of granular iron-formation in the Frere Formation: a) transitional boundary between hematite peloids (lower right) and carbonate replacement (left); b) chloritic shale intercalated with granular iron-formation, showing disseminated carbonate blebs (up to 2 mm across) overprinting the chlorite minerals; c) peloid entirely replaced by stilpnomelane and cut by a veinlet of iron oxides (?magnetite); the matrix is crypto- and microcrystalline quartz; d) pervasively silicified (crypto- and microcrystalline quartz) granular iron-formation overprinted by euhedral dolomite, which is in turn cut by a veinlet of iron oxides and stilpnomelane; e) granular iron-formation pervasively replaced by crypto- and microcrystalline quartz (light-coloured areas), overprinted by euhedral dolomite. Note ghost of peloid on left of image; f) complex alteration patterns are represented in this section; iron oxide peloids are replaced by stilpnomelane and perhaps minnesotaite, the matrix is entirely silicified (chalcedonic quartz is brown and microcrystalline quartz is white), and both are overprinted by euhedral magnetite. a), b), and f) plane-polarized light; c–e) crossed polars. After Pirajno et al. (2004)

Figure 16 Rare earth elements (REE) patterns for the Gunflint (Derry and Jacobsen 1990) and Griquatown (Beukes and Klein, 1990) granular iron formations, normalised to North American Shale Composite (Gromet et al. 1984). Note positive Eu anomalies and negative Ce anomalies. From Price (2003)

Figure 17 a) Distribution of the Frere Formation in the Earaheedy Basin and locations of samples analysed for rare earth elements; b) REE patterns of the Frere granular iron-formation, normalised to North American Shale Composiet (Gromet et al., 1984). Note weak positive Eu anomalies, Ce exhibits both positive and negative anomalies. After Price (2003) and Pirajno, unpublished data

Figure 18 Depositional and tectonic model for the Tooloo Subgroup of the Earaheedy Basin: at about 1800 Ma iron oxides were deposited on a continental shelf, with granular iron-formation at shallower depths and banded iron-formation deposited further down the continental slope. Lateral equivalents deposited in deeper settings consist of carbonate and sulfide facies. Iron was possibly sourced from hydrothermal effluents in an oceanic basin either from a spreading centre or from an oceanic plateau. After Pirajno et al. (2004) and Morris et al (2003)

Figure 19 Depositional system of granular iron-formation, ooids and peloids are shore facies and form as a result of wave action, siltstone and shale deposition occurs as offshore facies. After Price (2003)

Figure 20 Photomicrographs in plane-polarized light of rocks from the Princess Ranges Member, Chiall Formation: a) sandstone with rounded quartz grains coated by hematite granules, a feature that is typical of red beds; b) glauconitic sandstone; glauconite grains are about 0.6 mm across and are partially oxidized (brown); c) grain-supported sandstone. Quartz grains with interstitial clay, quartz, muscovite, and iron oxides; d) glauconitic sandstone of the Wandiwarra Member from the outer ring of the Shoemaker impact structure, composed of quartz grains and glauconite (pale green). Dark vein is probably pseudotachylite; e) and f) chloritic mudstone composed of quartz and iron-rich chlorite (green). The chlorite has replaced ?detrital muscovite. After Pirajno et al. (2004)

Figure 21 Mega-ripple marks in Chiall Formation (Princess Ranges Member) sandstone, along the northestern part of the outer collar of the Shoemaker impact structure. After Pirajno et al. (2004)

Figure 22 Mass flow deposits at the base of the Wandiwarra Member: a) sedimentary mass-flow deposit and b) fluidized arenite, representing possible tsunamite or seismite. After Pirajno et al. (2004)

Figure 23 Escarpmemts (breakaways) in Wandiwarra Member quartz sandstone and siltstone at the northern margin of Nabberu, showing mesoscale folding and thrusting. The beds are capped by iron-rich weathered residual quartz sandstone and siltstone in situ. After Pirajno et al. (2004)

Figure 24 Doubly plunging mesoscale fold in Wandiwarra Member quartz sandstone. Sketch below shows the overall style of folding in this area. After Pirajno et al. (2004)

Figure 25 Linguoidal ripple marks in very fine grained sandstone of the Princess Range Member, 3 km northeast of Wadjinyanda Pool

Figure 26 Geodynamic evolution of the Earaheedy Basin. See text for details

Figure 27 Time-space diagram of deposition of Earahedy Group lithologies, in response with sea level fluctuations. Details in text

Figure 1
Click here to download high resolution image

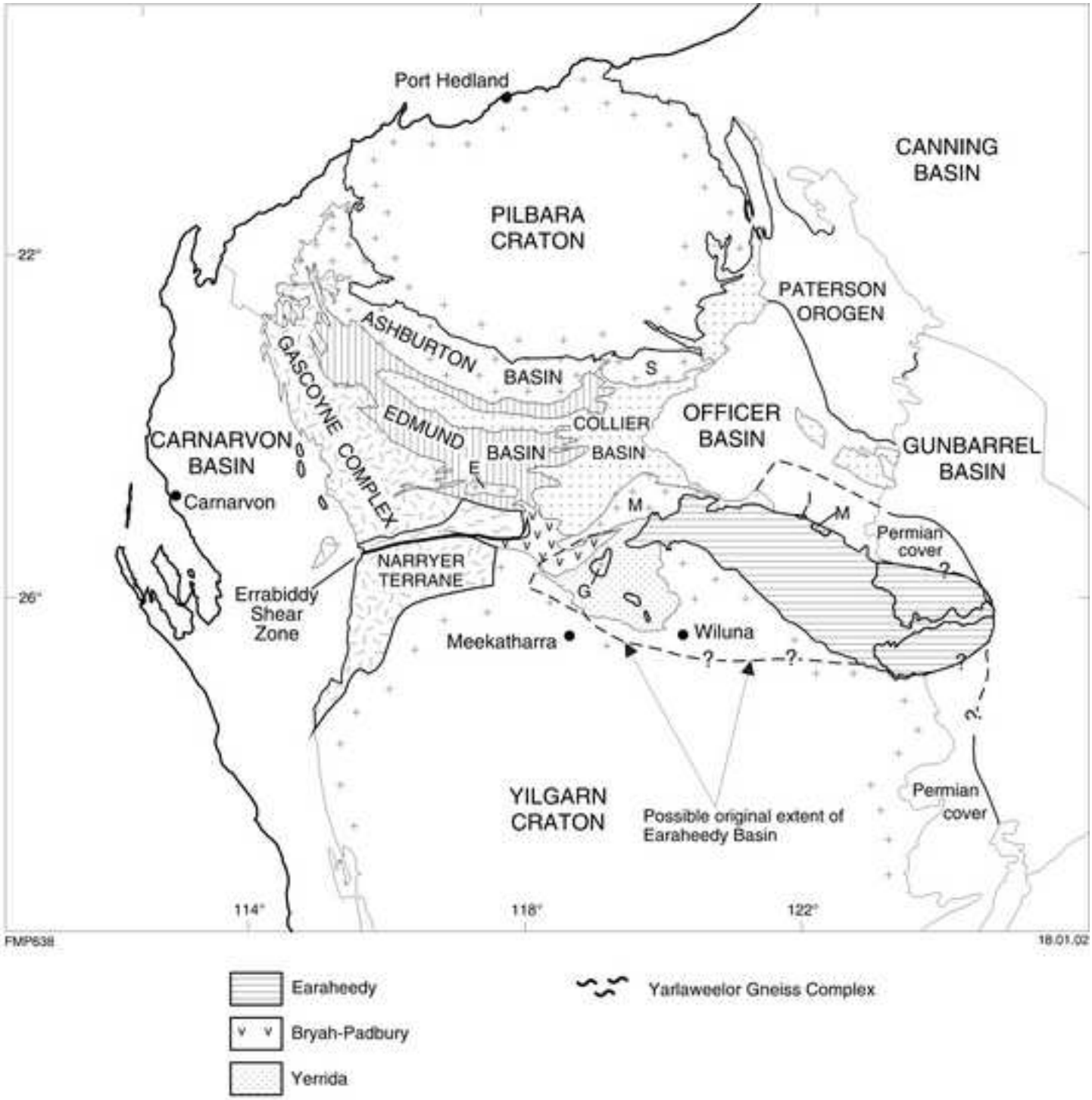

Figure 1

Figure 2

Click here to download high resolution image

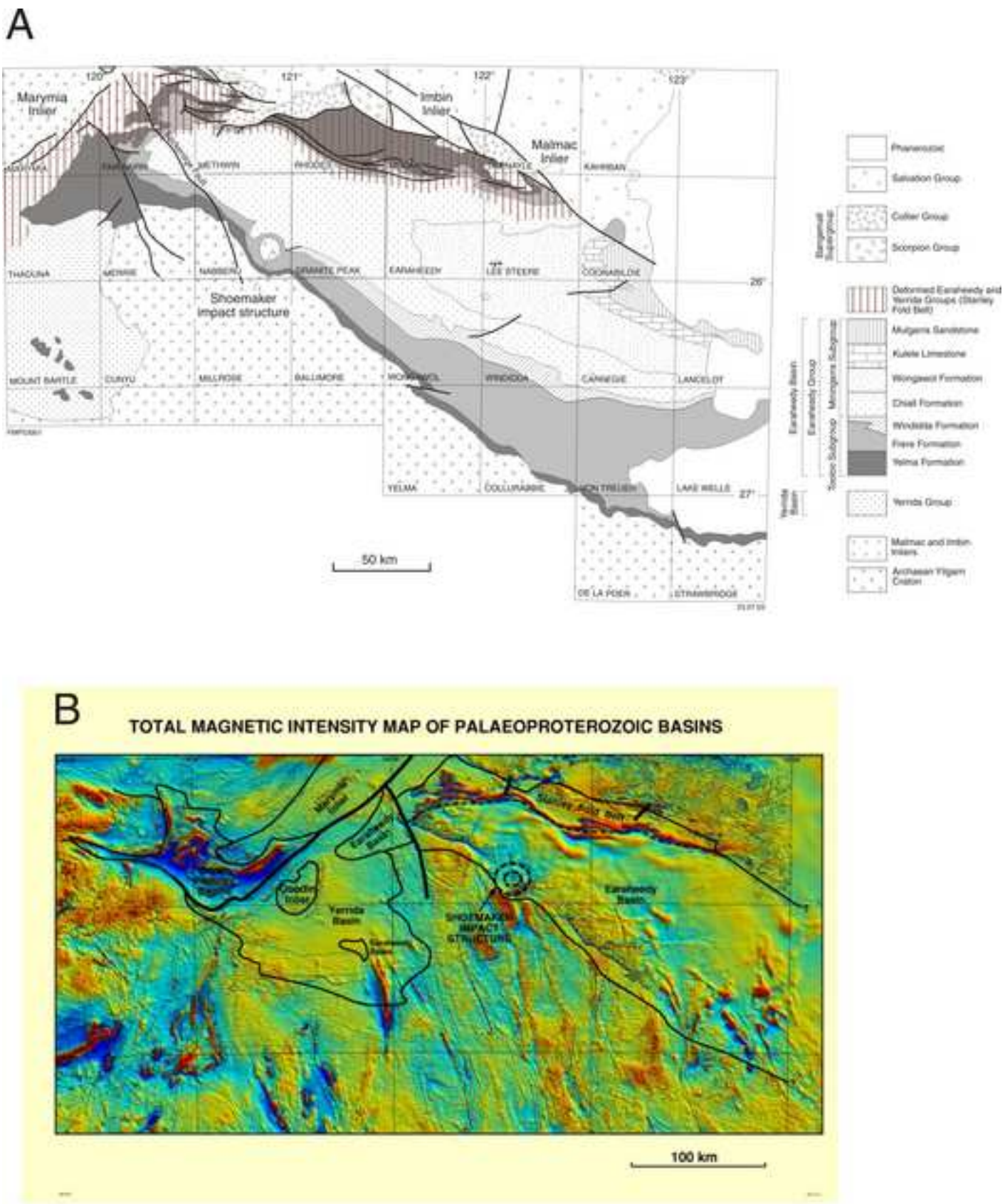

Figure 2

Figure 3

Click here to download high resolution image

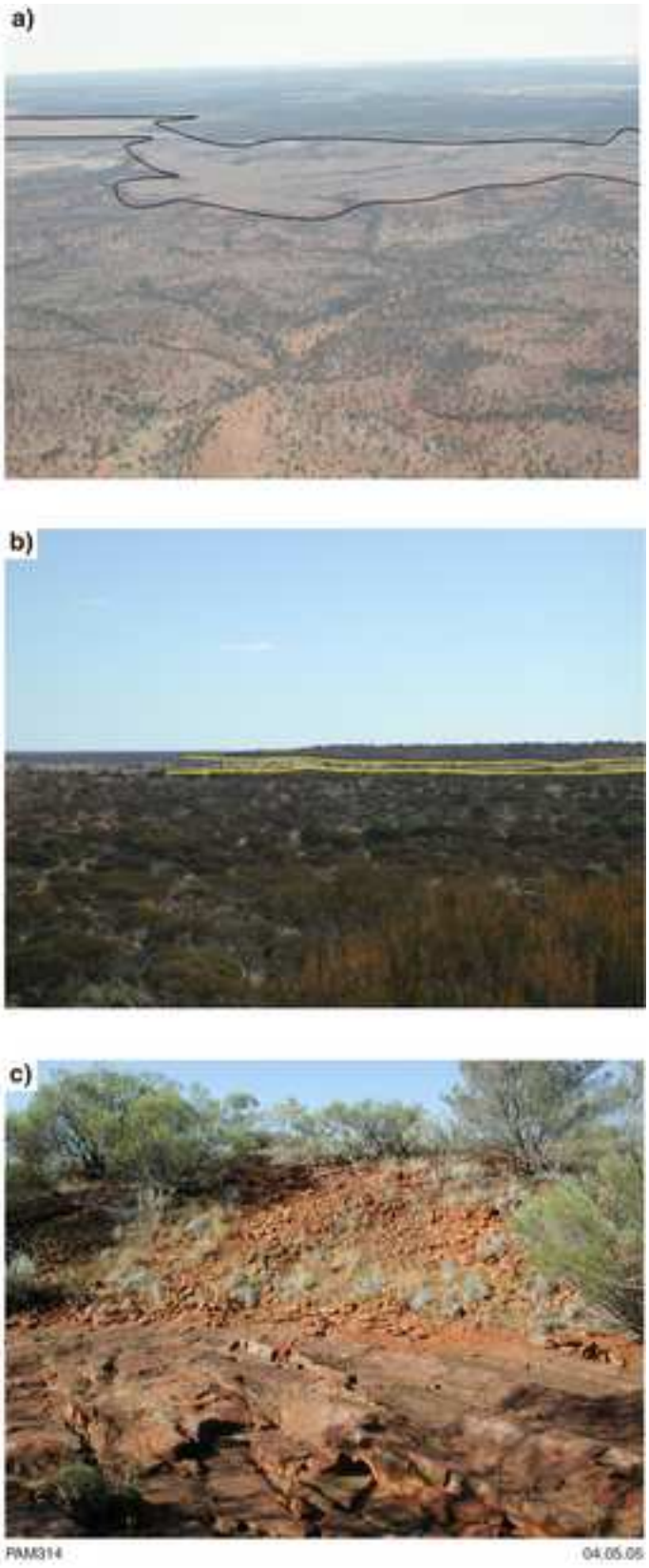

Figure 3

Figure 4

Click here to download high resolution image

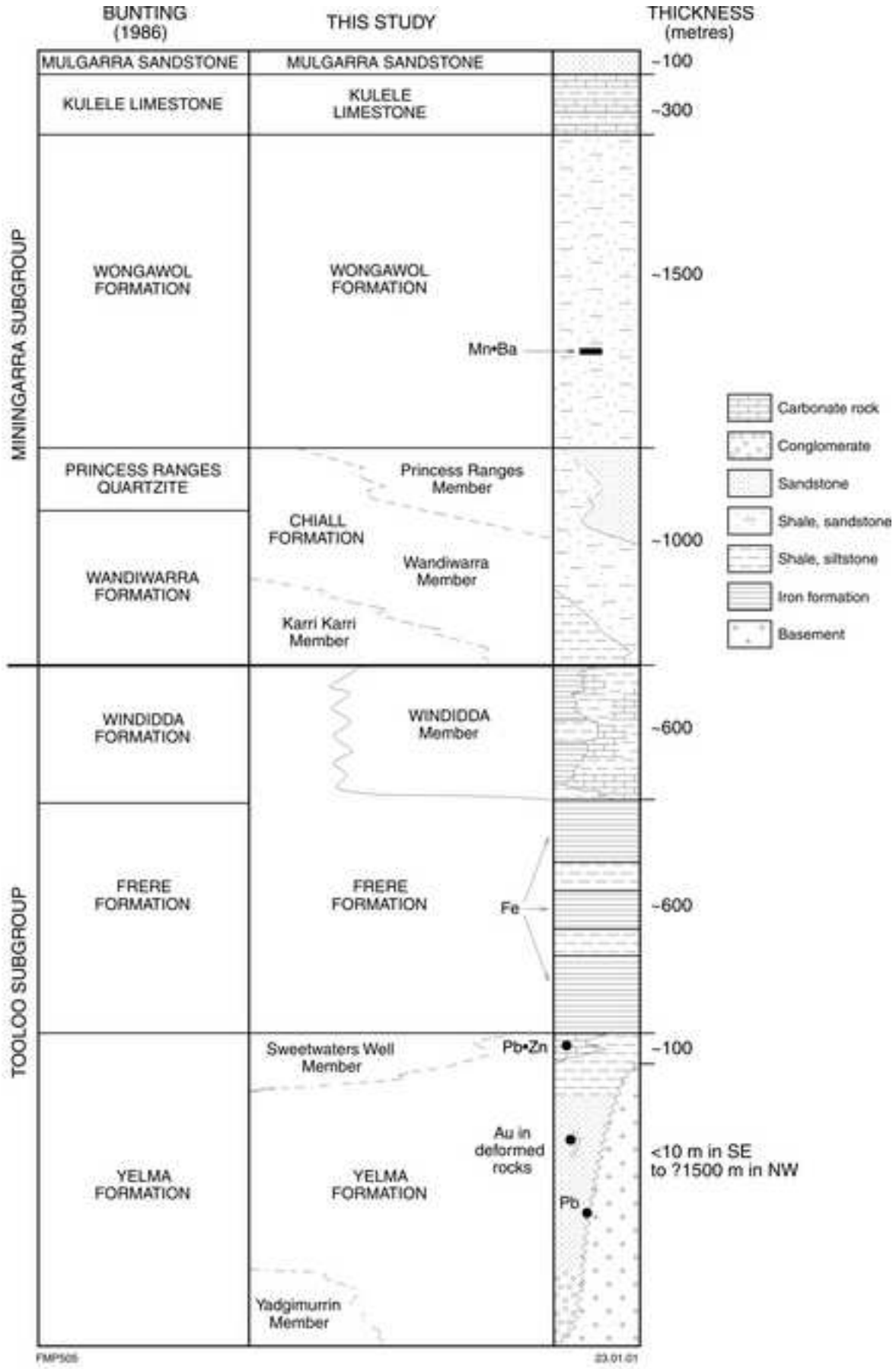

Figure 4

Figure 5

Click here to download high resolution image

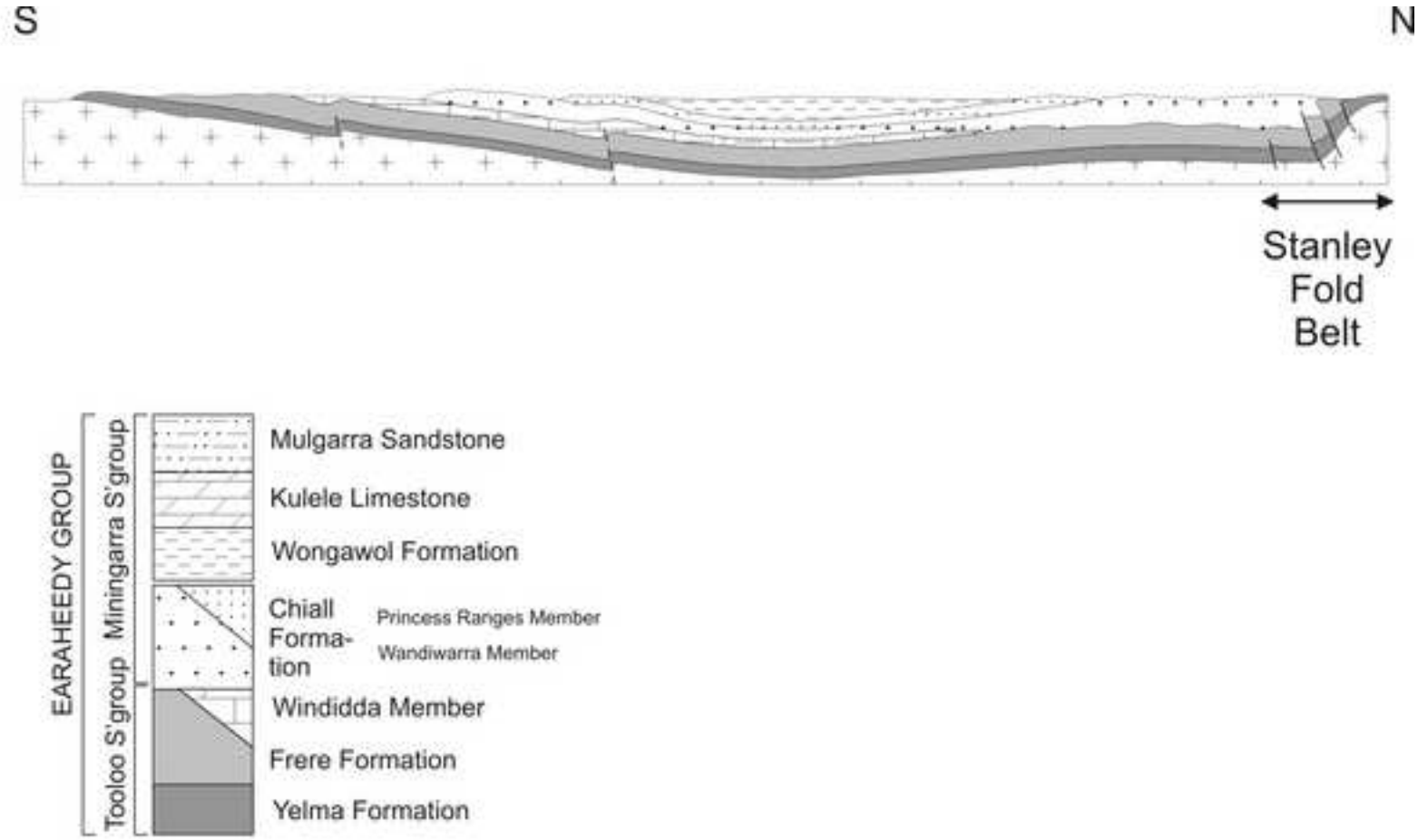

Figure 5

Figure 6

Click here to download high resolution image

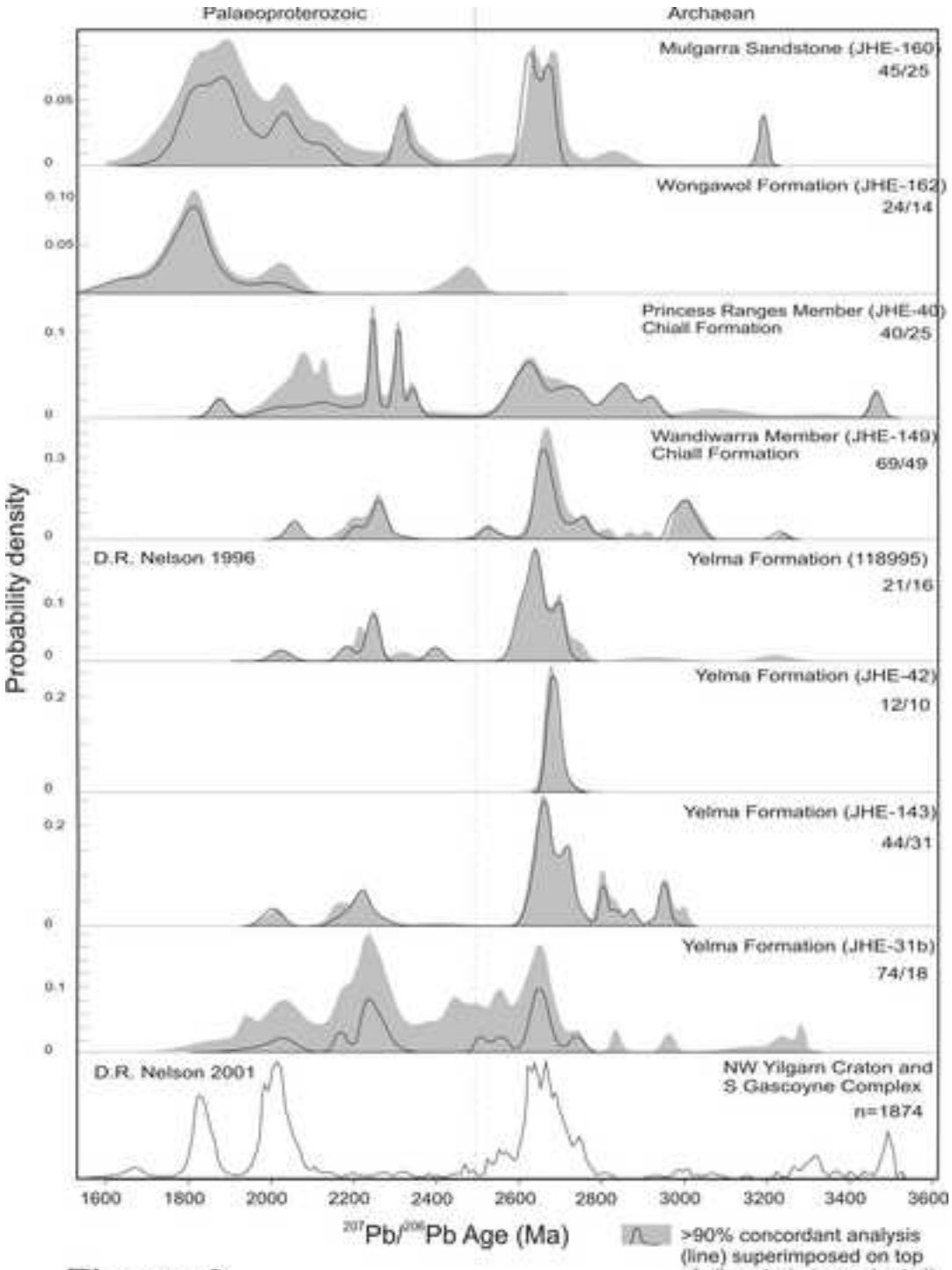

Figure 6

Figure 7

Click here to download high resolution image

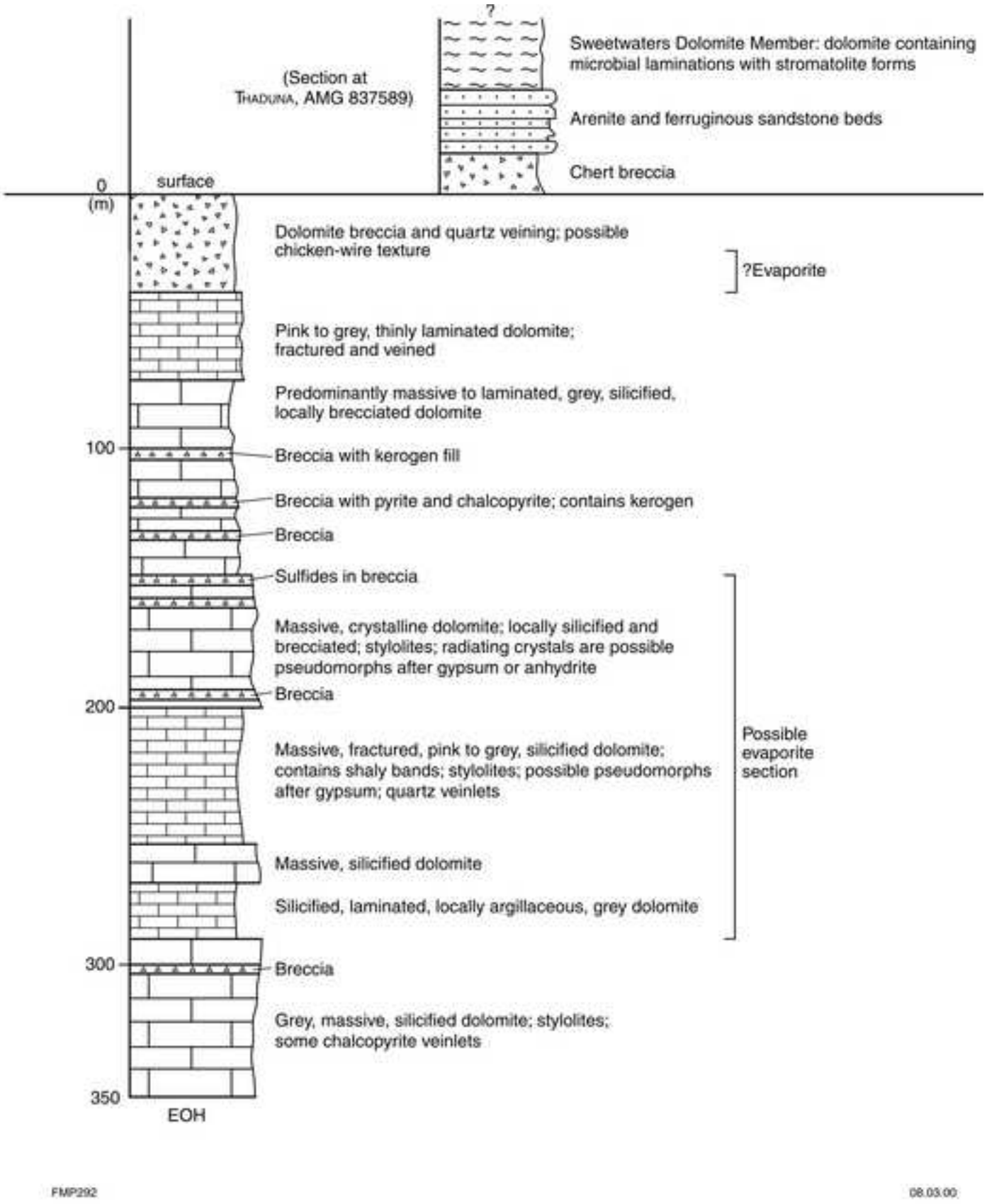

Figure 7

Figure 8

Click here to download high resolution image

Figure 8

Figure 9

Click here to download high resolution image

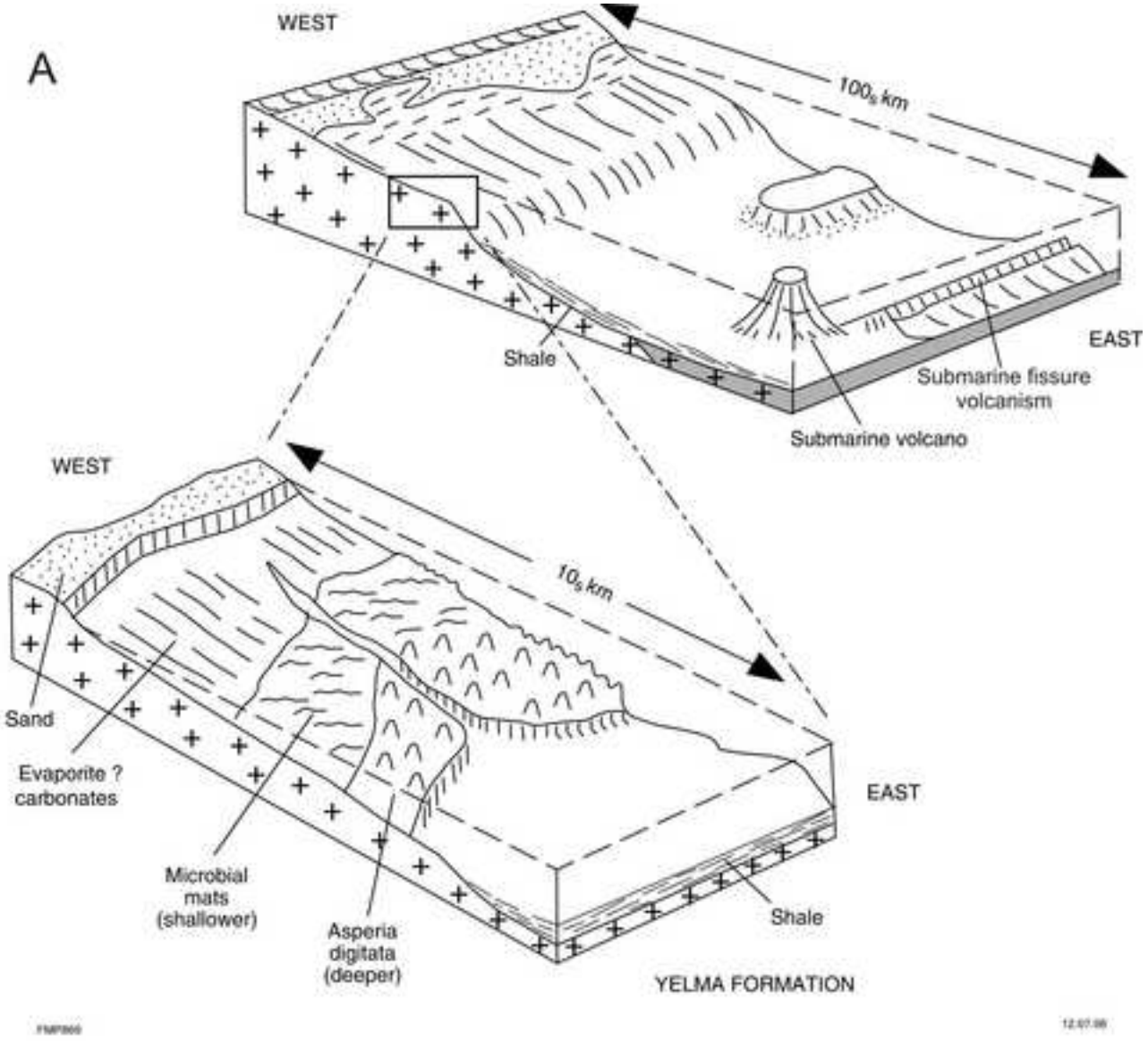

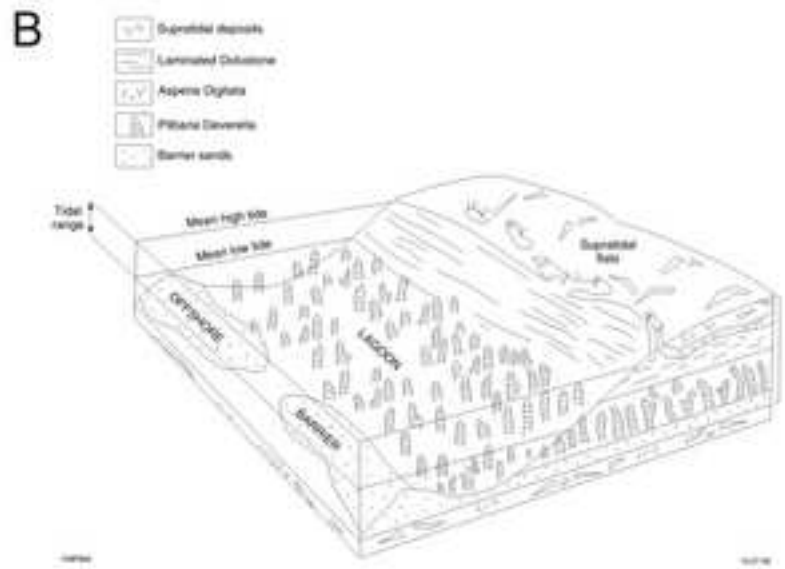

Figure 9

Figure 10

Click here to download high resolution image

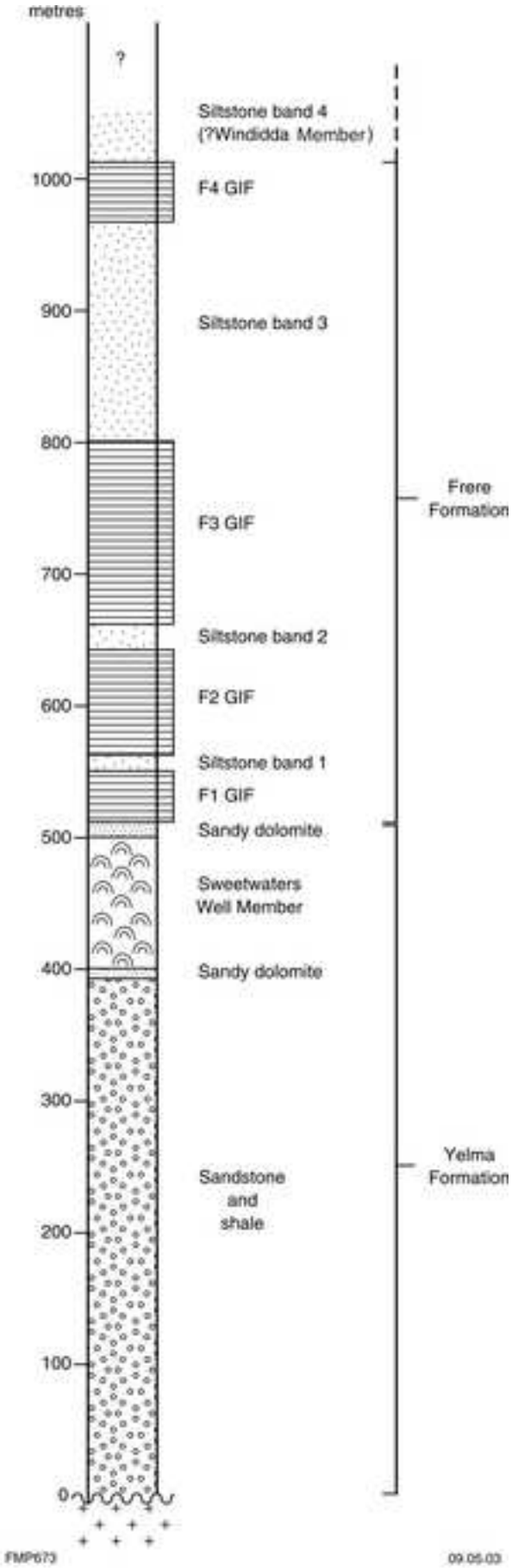

Figure 10

Figure 11

Click here to download high resolution image

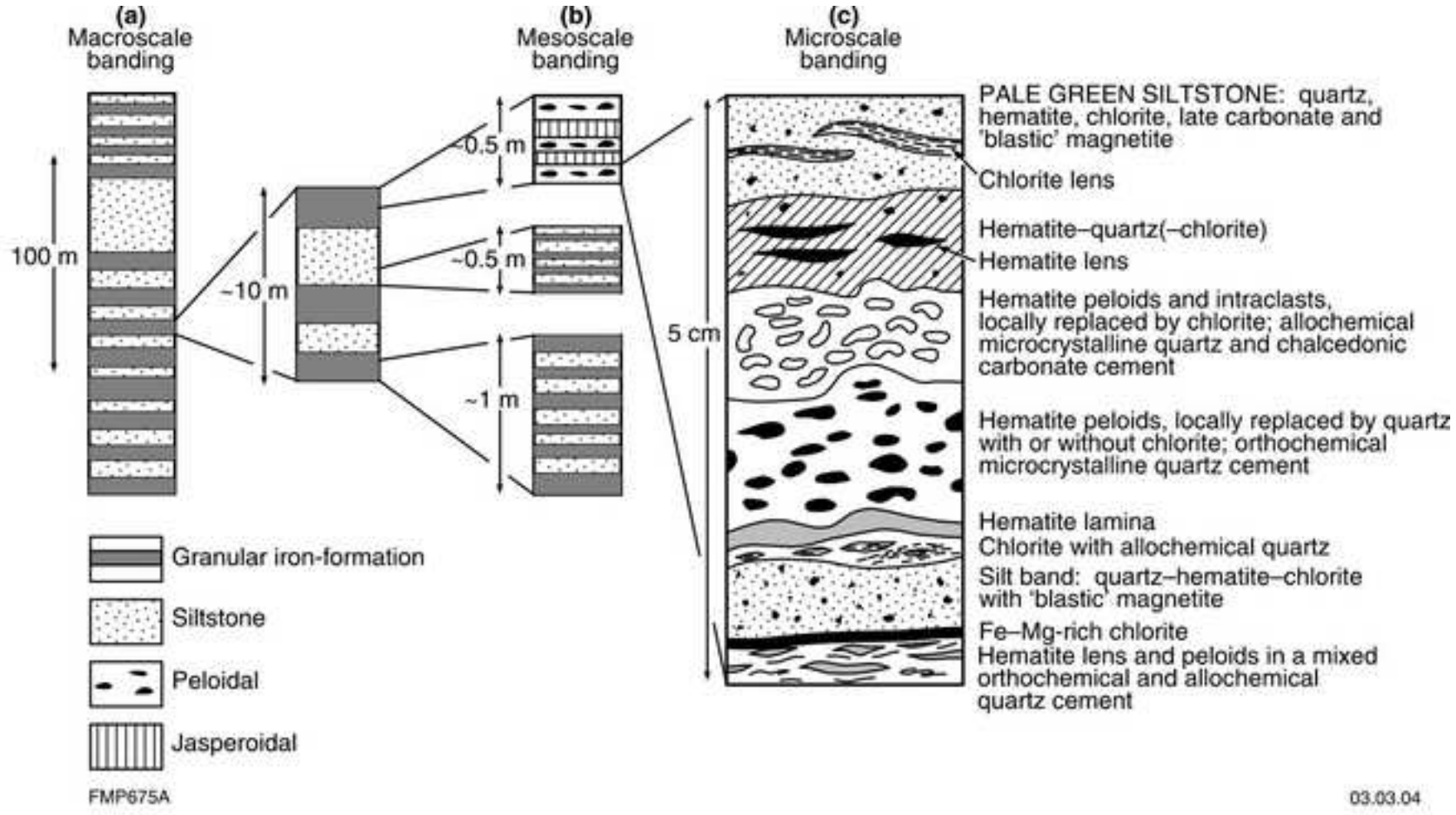

Figure 11

Figure 12

Click here to download high resolution image

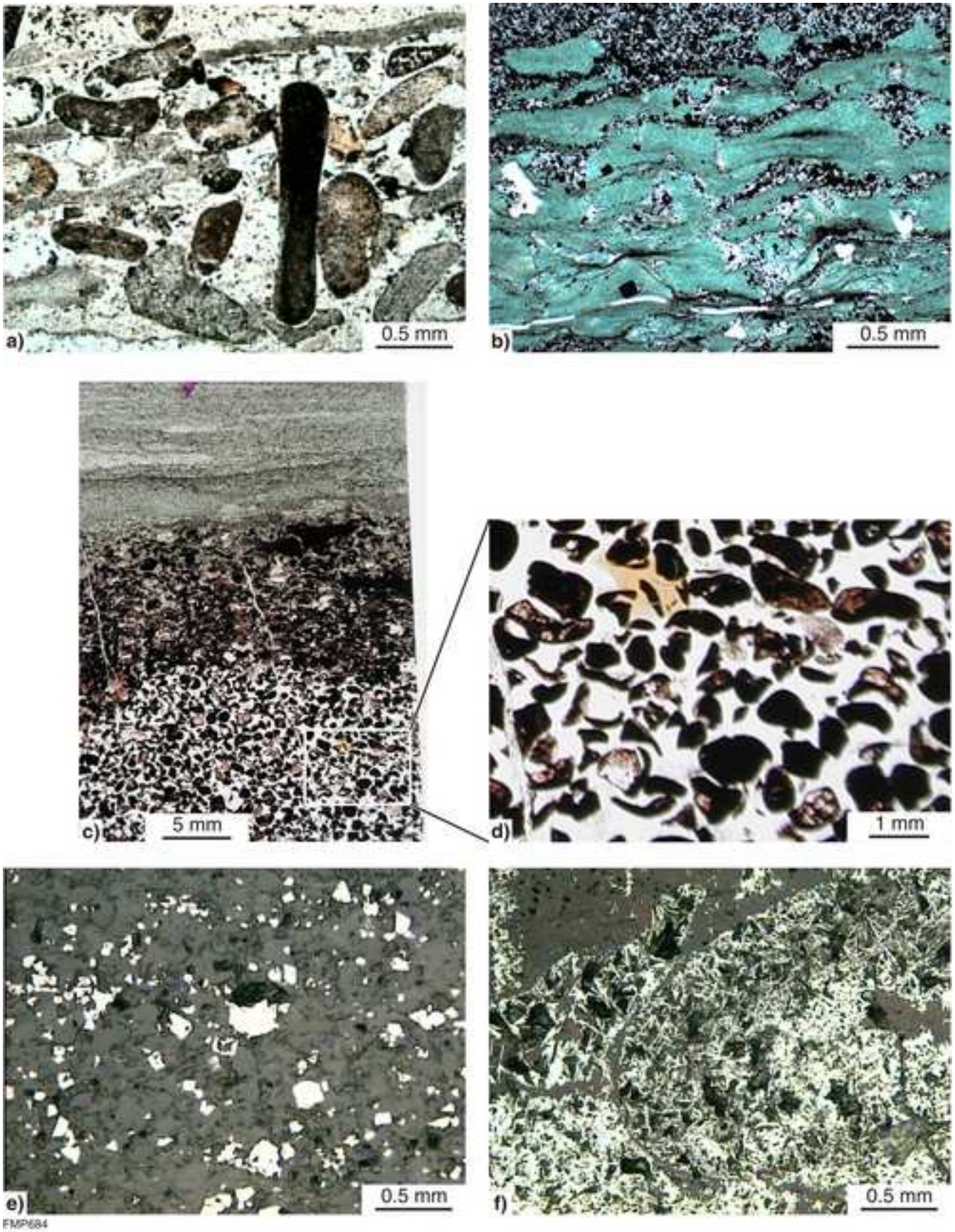

Figure 12

Figure 13

Click here to download high resolution image

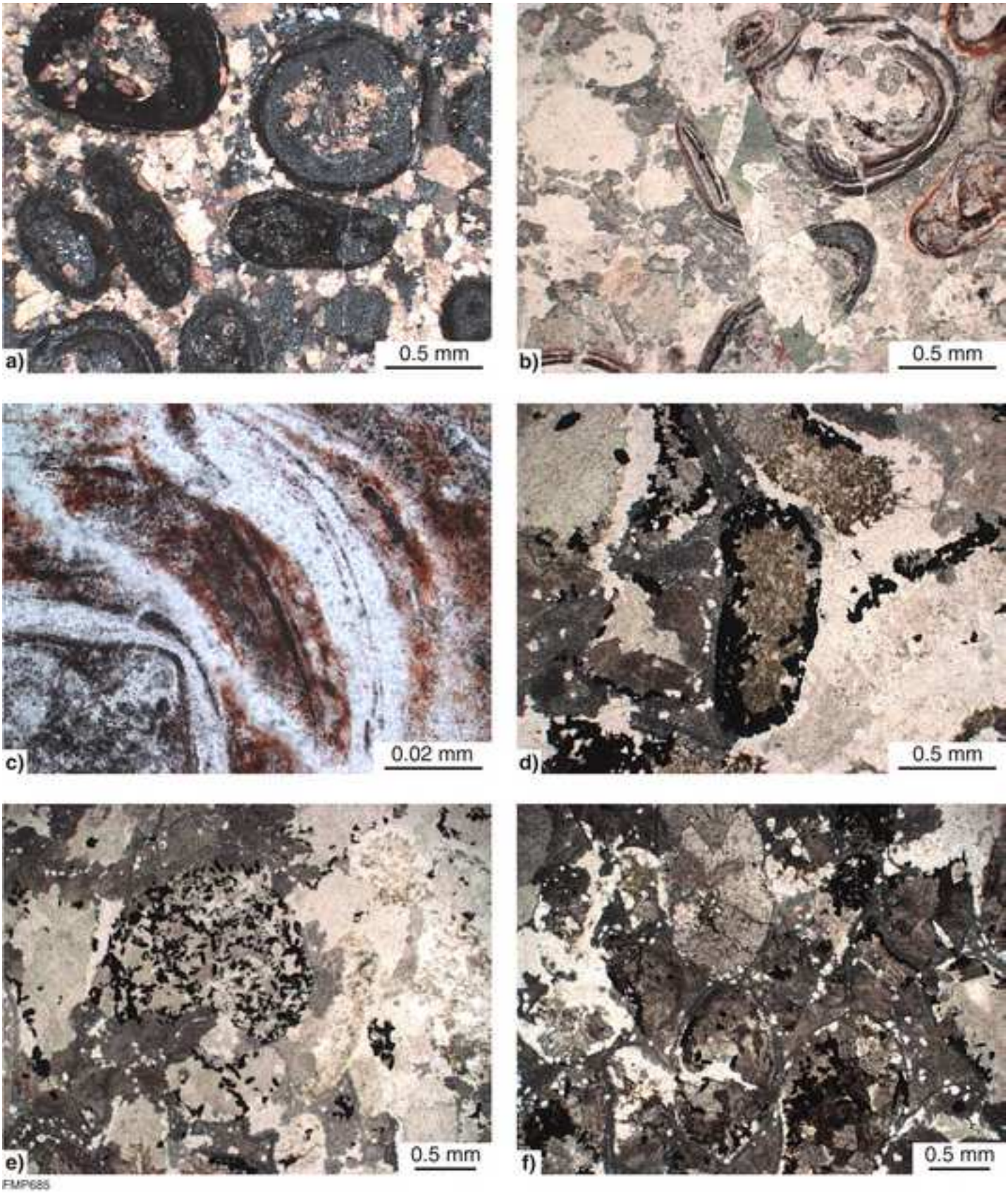

Figure 13

Figure 14

Click here to download high resolution image

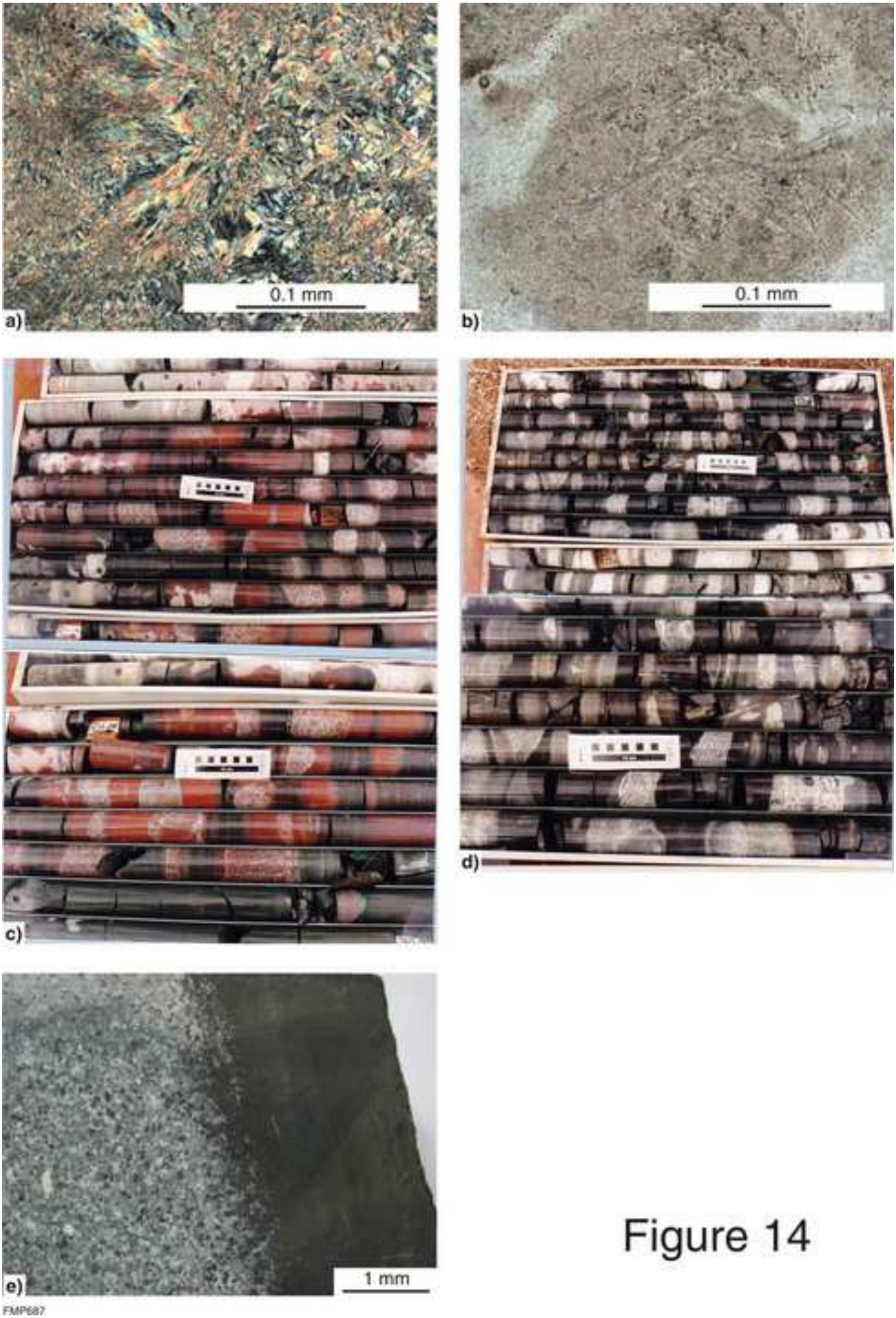

Figure 14

Figure 15
Click here to download high resolution image

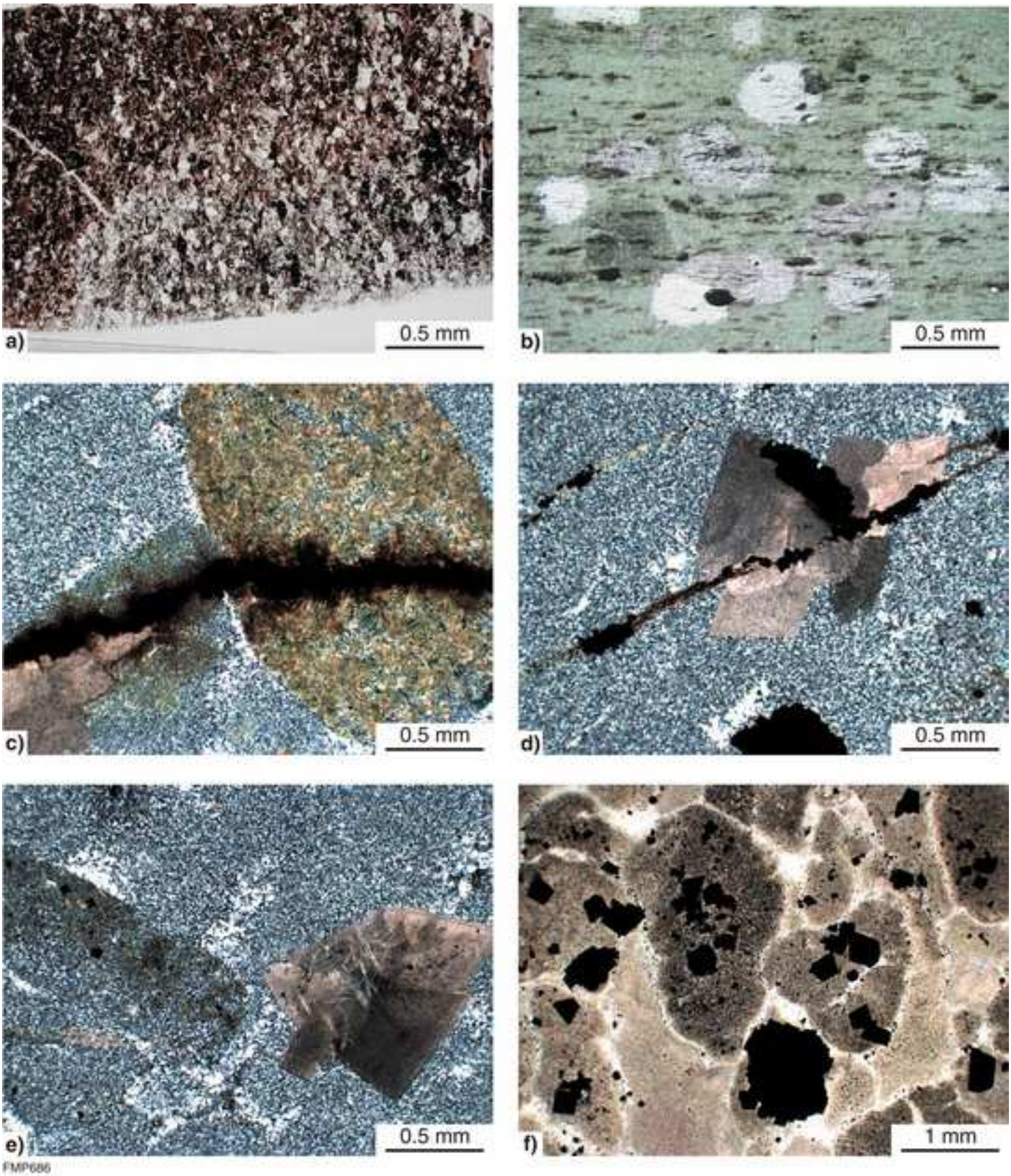

Figure 15

Figure 16

Click here to download high resolution image

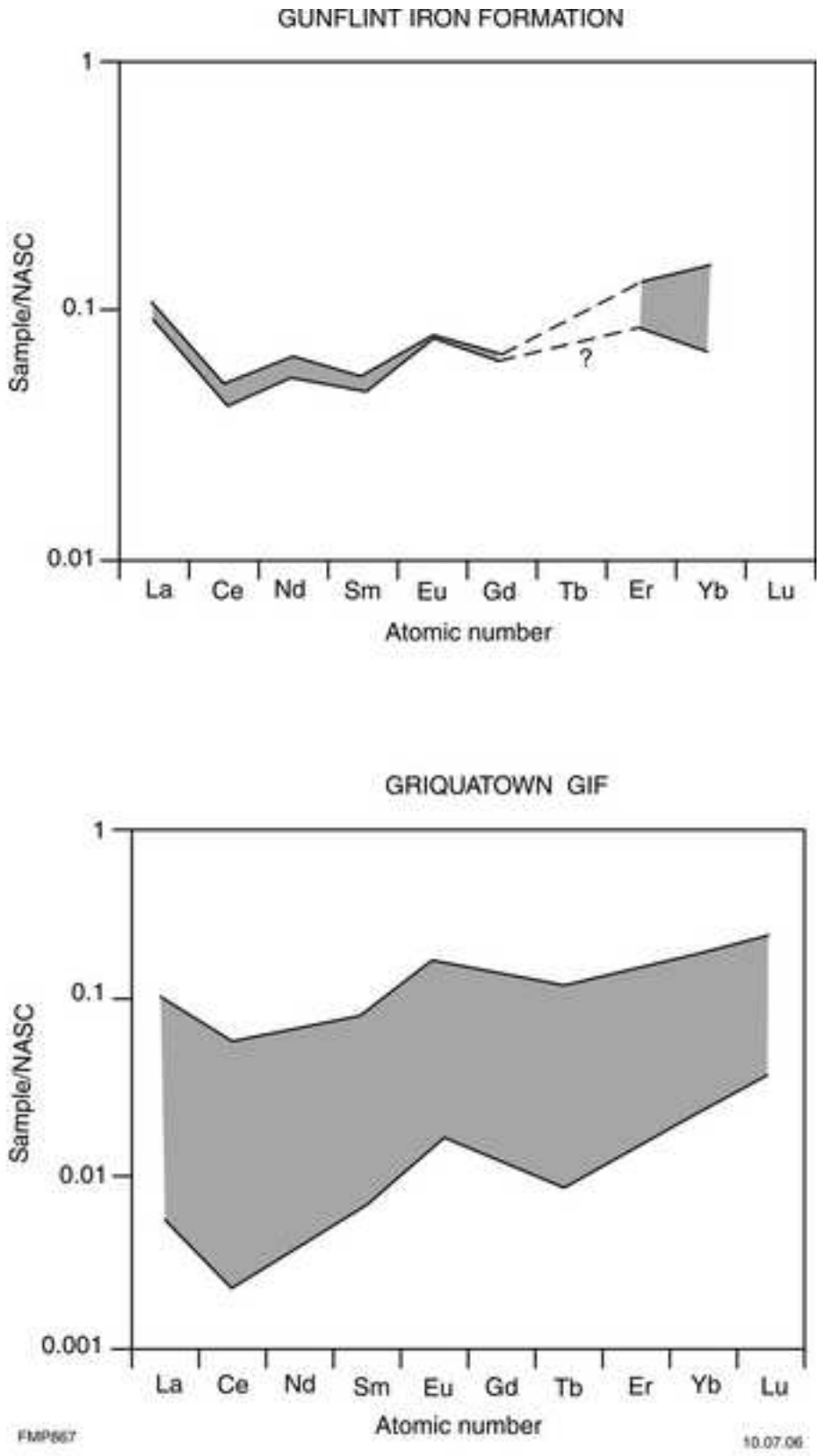

Figure 16

Figure 17

Click here to download high resolution image

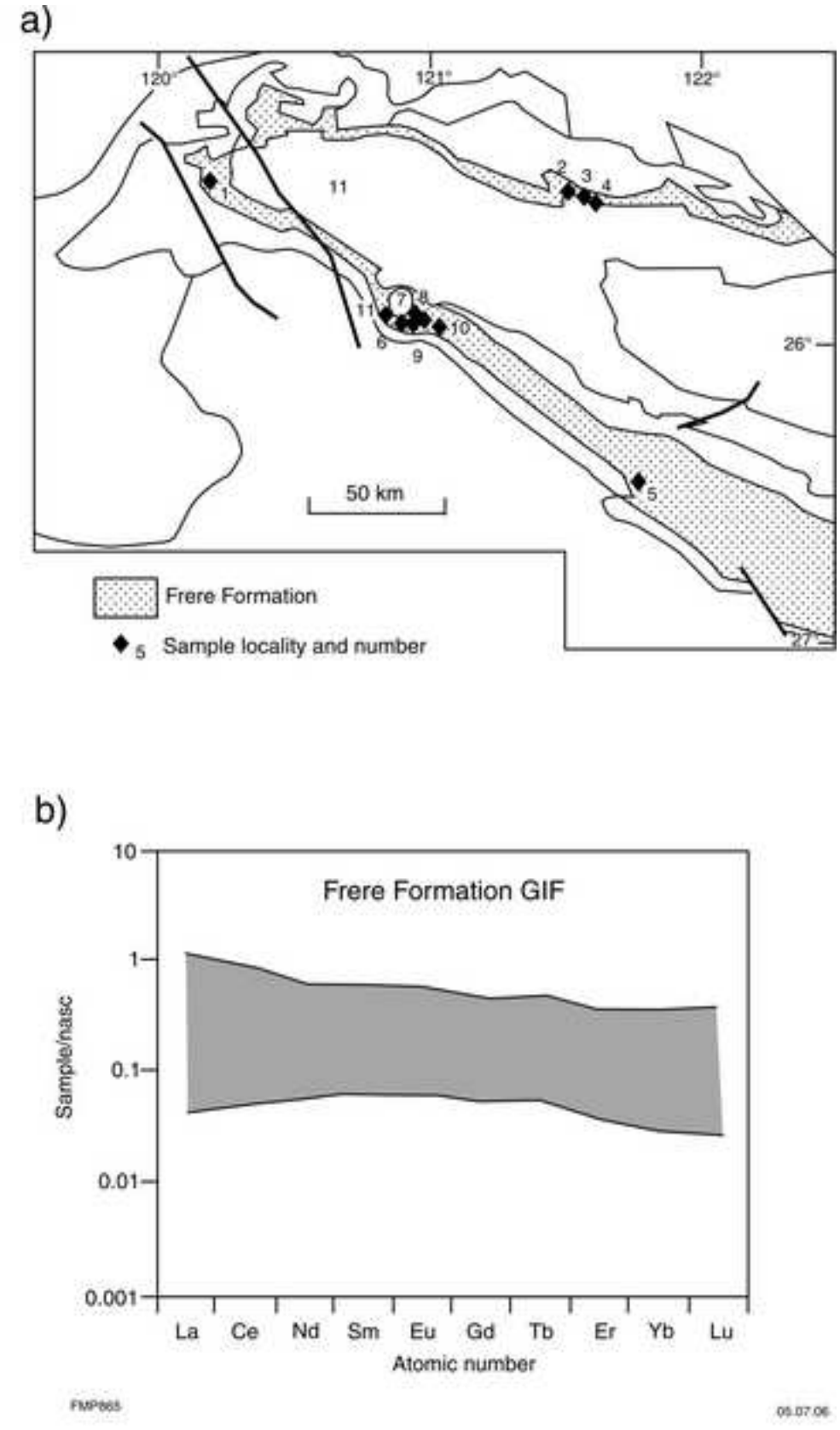

Figure 17

Figure 18
Click here to download high resolution image

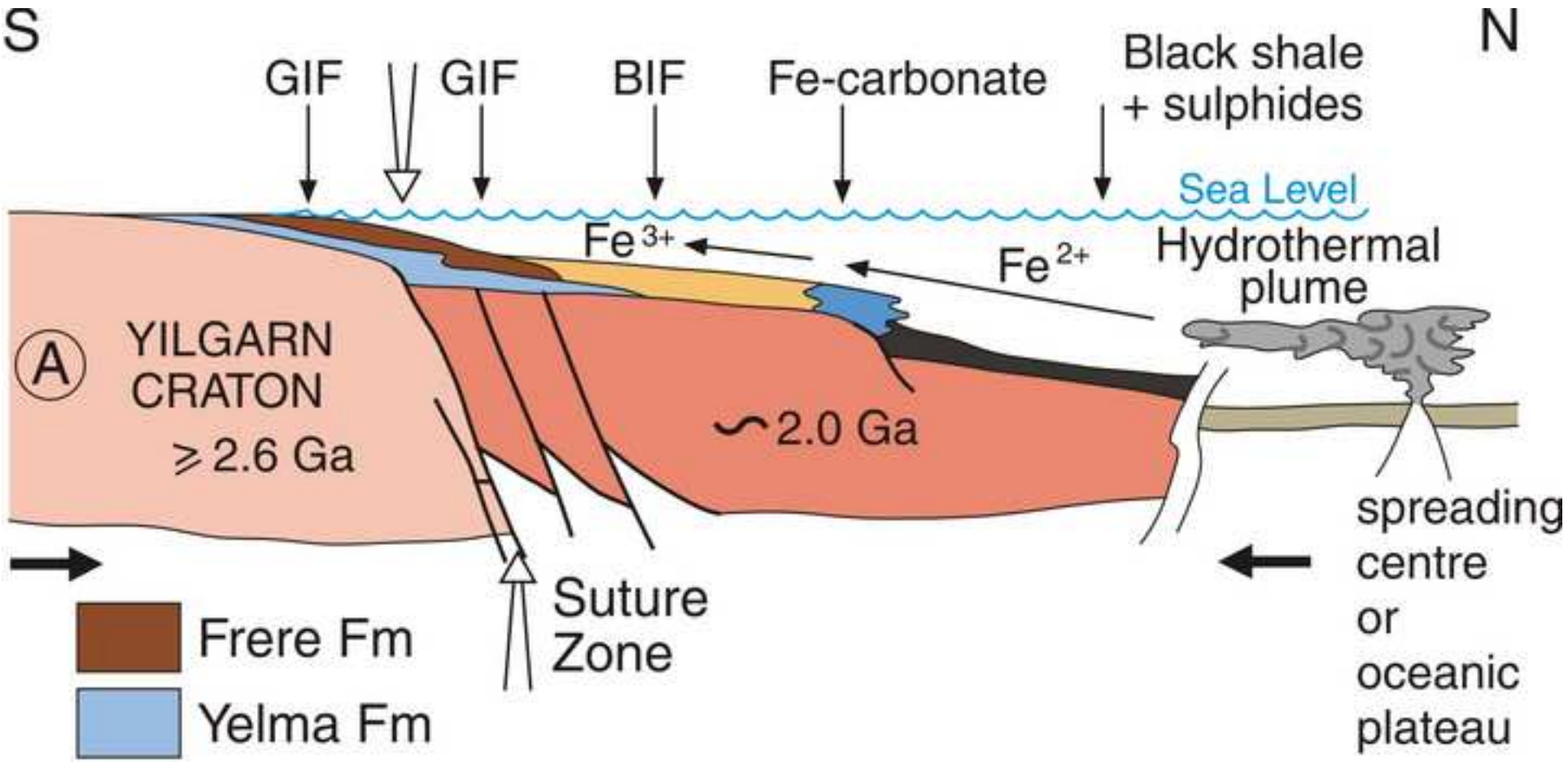

Figure 18

Figure 19

Click here to download high resolution image

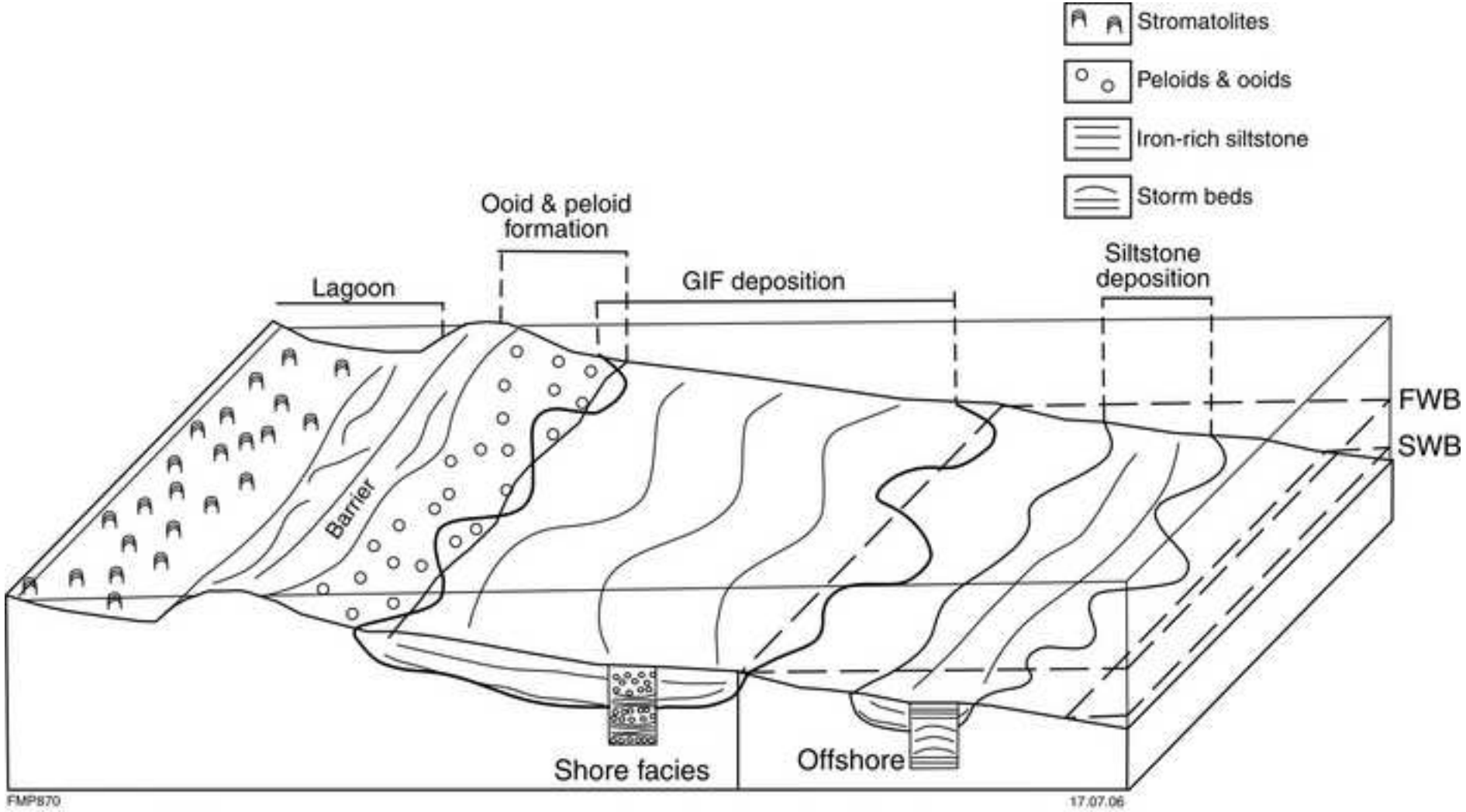

Figure 19

Figure 20
Click here to download high resolution image

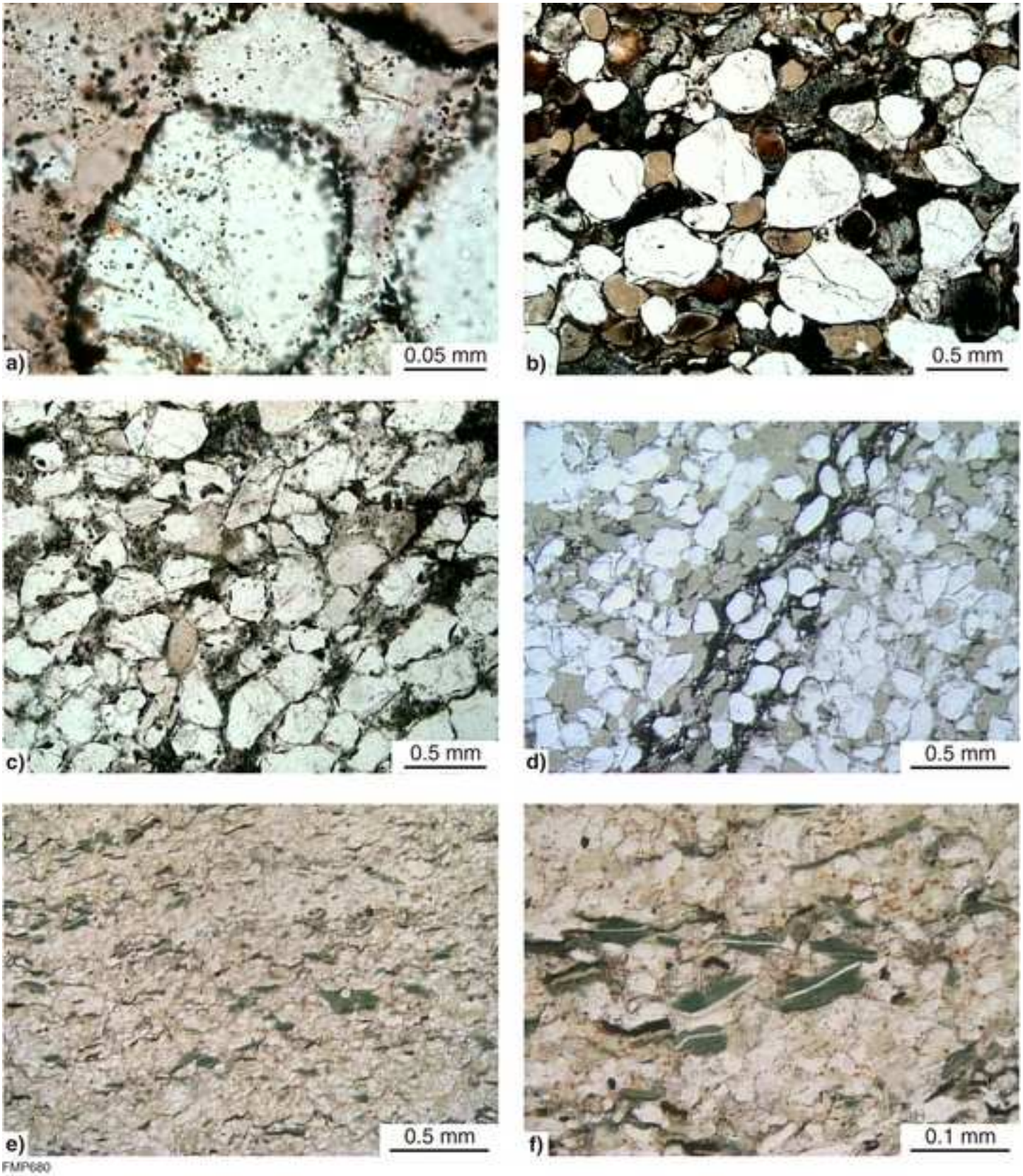

Figure 20

Figure 21
Click here to download high resolution image

FMP695

Figure 21

Figure 22
Click here to download high resolution image

FMP697

Figure 22

Figure 23
Click here to download high resolution image

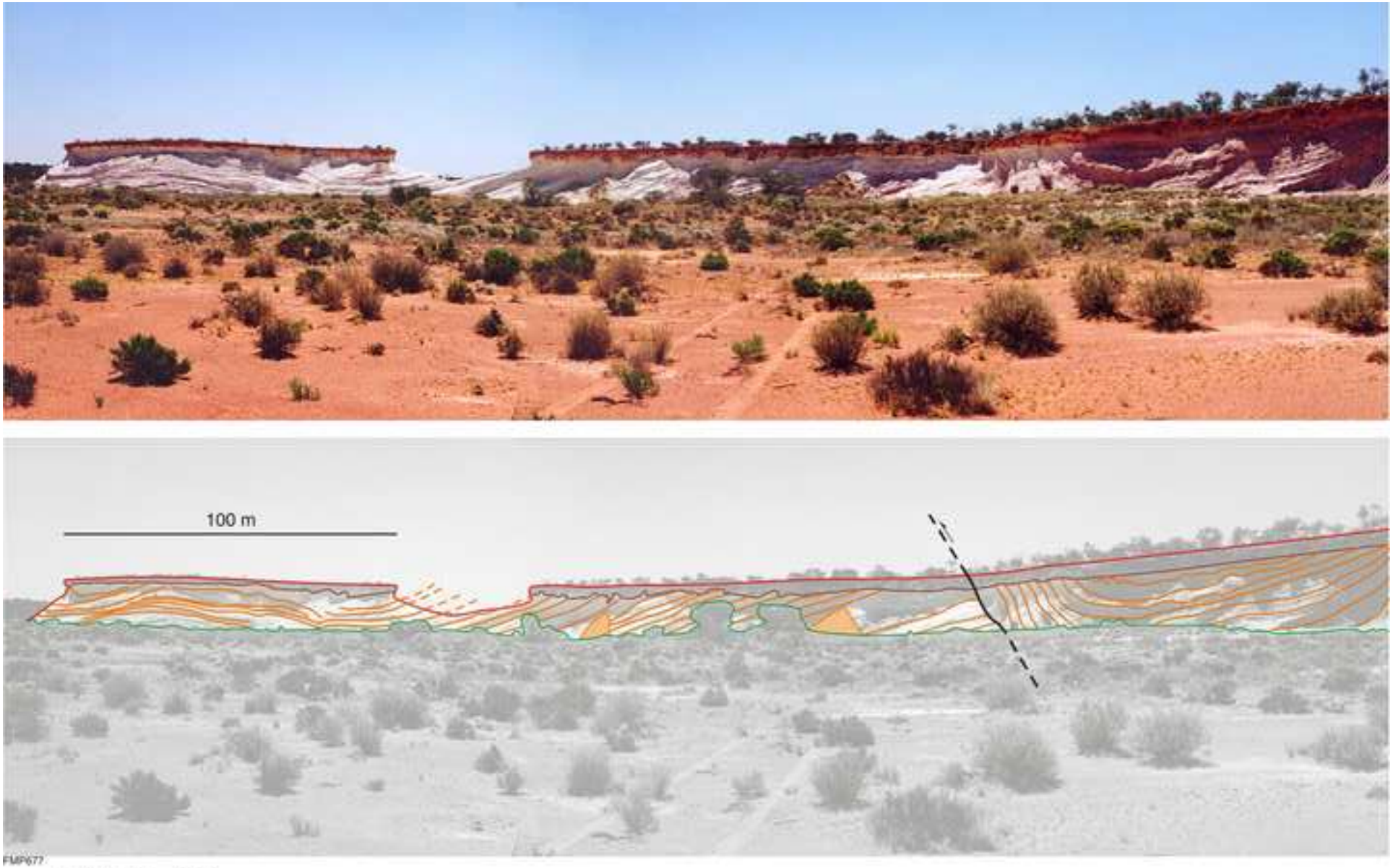

Figure 23

Figure 24
Click here to download high resolution image

Figure 24

Figure 25
Click here to download high resolution image

Figure 25

Figure 26

Click here to download high resolution image

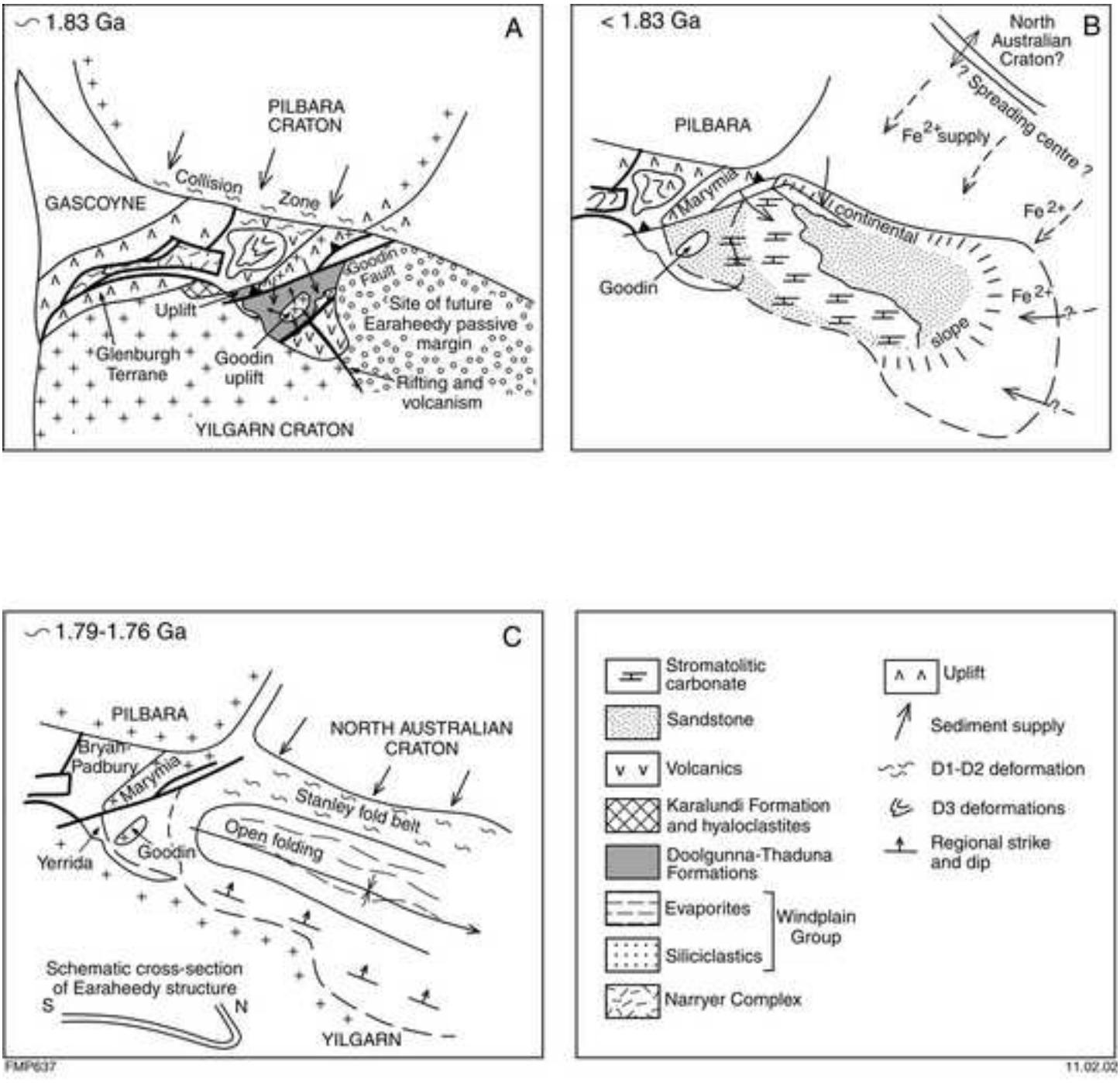

Figure 26

Figure 27
Click here to download high resolution image

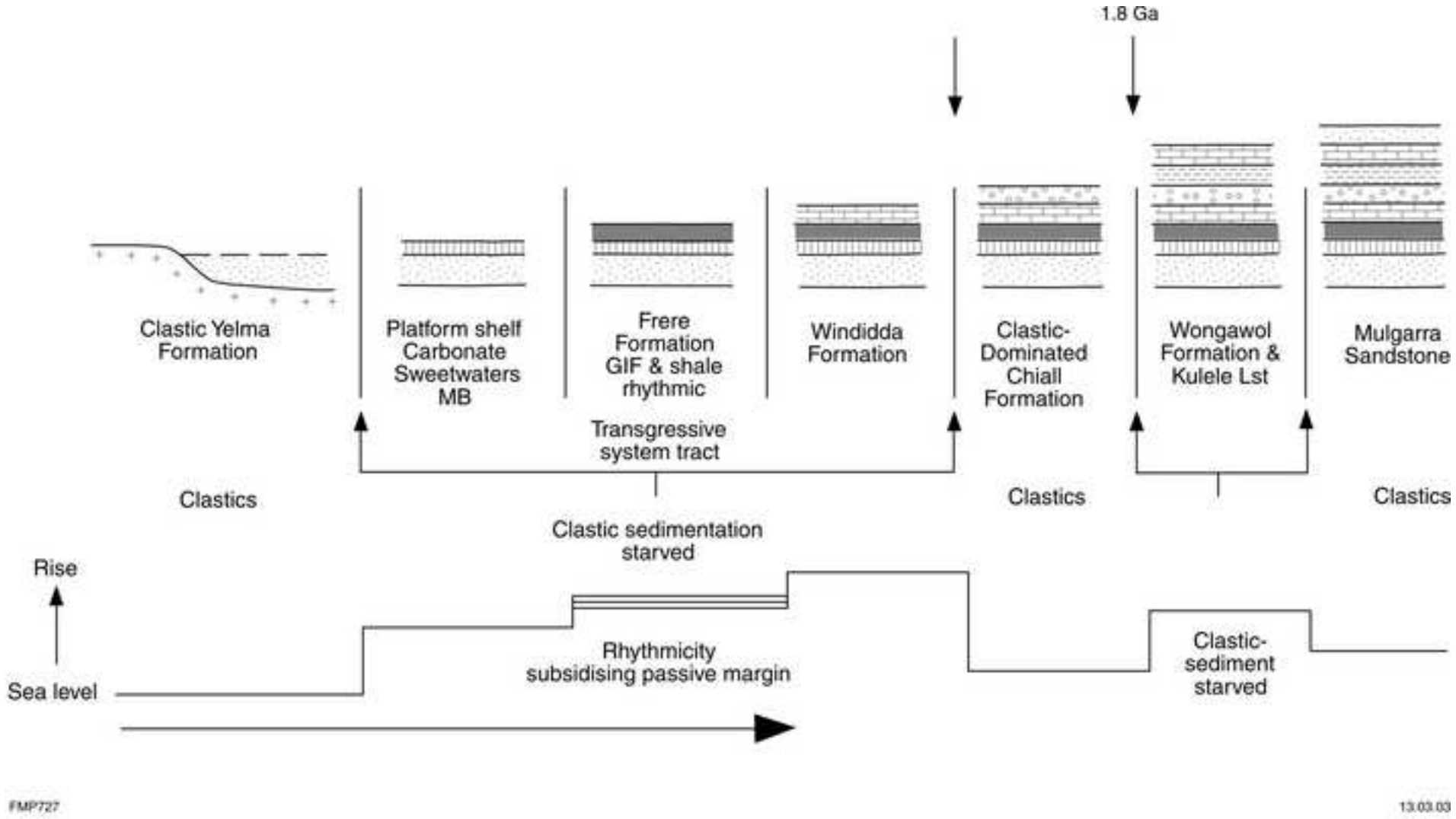

Figure 27

Tables 1, 2, 3

Click here to download Table: Tables 1_3.doc

TABLE 1 Summary of major tectono-thermal events in the Capricorn Orogen that are relevant to the geodynamic evolution of the Earaheedy Basin

Approx. age (Ga)	West: Bryah, Yerrida, Padbury	East: west-central: Earaheedy	Other related events
> 2.6	Northern Yilgarn Craton; Goodin and Marymia Inliers	Northern Yilgarn Craton; Malmac Inlier	
<2.2-2.1	Deposition of lower Yerrida Group (Windplain Subgroup, evaporite and siliciclastics), in intracratonic sag basin		
2.0	Sea-floor spreading in ocean separating Glenburgh terrane from northwest margin of Yilgarn Craton; birth of Narracoota ocean floor.		West-or northwest facing subduction on Glenburgh terrane (Southern Gascoyne Cx)
2.0-1.99 Glenburgh Orogeny	• Convergence of Yilgarn Craton and Glenburgh terrane (southern Gascoyne complex); • Emplacement of oceanic crust (Narracoota Formation) and rifting of Marymia Inlier from northern margin of Yilgarn; eruption of basaltic hyaloclastites • Closing of oceanic arm between NW Yilgarn and Glenburgh terrane and accretion of juvenile crust to NW Yilgarn margin and Yerrida sag structure. Deposition of Bryah Group (Narracoota, Ravelstone Fms).	Emplacement (?tectonic?intrusive) of rhyodacite (Imbin Inlier); possible correlative of Dalgaranga Supersuite (Southern Gascoyne terrane).	Emplacement of 2.0-1.98 Ga granites of Dalgaranga Supersuite Emplacement of 1.97 Ga Nardoo granite (Glenburgh terrane;
1.96	Deposition of Padbury Gp, in small foreland basin on top of Bryah Group;		
~ 1.83 Capricorn Orogeny	• Convergence and oblique collision of Pilbara and Yilgarn cratons; compression with uplift and deformation around Goodin and Marymia inliers;Bryah and Padbury Basins become a fold-and-thrust belt; associated orogenic gold lodes. • Yerrida Basin evolves from a sag to a foreland basin, with deposition of immature sediments (Thaduna-Doolgunna Fms) from orogenic highlands; • Rejuvenation and deepening of Yerrida Basin ahead of compression front, leads to reactivation of ancient fractures		1.82 Ga Moorarie Supersuite; granite intrusions in Narryer terrane (Yarlaweelor Cx); emplacement of 1.81-1.79 Ga granites of Moorarie Supersuite in Glenburgh terrane (Sheppard et al. and Occhipinti et al., this volume)

	with euption of continental tholeiites (Killara Fm); sedimentation of immature sediments continues; • Continental volcanism ceases, deposition of lake sediments (Maraloou Fm) in Yerrida Basin		
Post-Capricorn Orogeny		Initiation of passive margin along northeast and east margins of Yilgarn Craton; deposition of Tooloo Subgp (Earaheedy Basin) • Yelma shelf carbonates and sandstone; sediments provenance from orogenic uplifts in west and Yilgarn in the south); • deposition of granular iron formation on shelf, black shales in deeper waters (continental rise). Fe and Mn oxide mineralisation	Continental breakup and sea floor spreading to the ?east and/or northeast; mid-ocean ridge volcanism supplies dissolved Fe and Mn to the Earaheedy passive margin
1.79-1.74 Yapungku Orogeny	Convergence of North Australian and West Australian cratons; south-directed compression	Mild uplift and erosion of Tooloo Subgroup	
		Second phase of Earaheedy Basin evolution, post-breakup sediments; shedding of detritus from uplifted areas in the west into northwards-deepening passive margin basin, deposition of glauconitic Miningarra Subgp (1.8 Ga detrital zircons in topmost formation)	Cessation of sea floor spreading north and east of Yilgarn Craton
1.68-1.62 Mangaroon Orogeny		Deformation of Earaheedy Group to the north: Stanley Fold Belt; this fold belt does not affect the westernmost or southeastern parts of the Earaheedy Gp, where it unconformably overlies the Yerrida Gp (W) or onlaps NE Yilgarn Craton (SE). MVT style deposits in carbonate rocks and structurally controlled Au and Mn mineralisation in Stanley Fold Belt	
1.64	Deposition of Edmund Group (Edmund Basin)	Deposition of Scorpion Group	
1.46	Intrusion of dolerite sills into Edmund Group		
<1.46-1.22	Deformation of Edmund Group	Deformation of Scorpion Group, ?evaporite expulsion from Scorpion Diapir, foreland basin development northeast of Earaheedy Basin (Ward and Oldham Inliers)	
1.20->1.07	Deposition of Collier Group (Collier Basin)	Deposition of Salvation Group and Manganese Group, upper Collier Group	
1.13-0.8		Miles Orogeny, SW-directed compression and deformation	
1.07	Intrusion of mafic sills and dykes into Collier and Edmund Groups	Intrusion of mafic sills and dykes (Glenayle Dolerite) into Salvation Group and in ?eastern Earaheedy Basin, extrusion of tholeeitic lavas in the east (Empress 1); mafic magmatism in Musgrave Complex (1.06 Ga)	Warakurna LIP
<1.07- >0.85	Edmundian Orogeny and deformation of Edmund and Collier Basins	Mild deformation of Scorpion and Salvation Groups	
0.83		Initial depositon in NW Officer Basin, of basal sand overlain by evaporitic mixed sequence (Buldya Group)	

Table 2 Summary of geochronological data for the Earaheedy Basin

Formation		Locality	Coordinates	Rock/Mineral (detrital zircon age from youngest)	Age (Ma)	Method	Reference
Earaheedy Basin							
Mulgarra Sandstone		LEE STEER	Not available	sandstone/detrital zircon	1808±36	U-Pb SHRIMP	Halilovic et al. (2004)
Chiall Formation	Princess Ranges Member	WONGAWOL	Not available	sandstone/detrital zircon	1876±19	U-Pb SHRIMP	Halilovic et al. (2004)
	Wandiwarra Member	VON TUREUR	Not available	sandstone/detrital zircon	2050-2500	U-Pb SHRIMP	Halilovic et al. (2004)
	Wandiwarra Member	KINGSTON 1:250 000, WONGAWOL	121° 57' E, 26° 14' S	sandstone/glauconite	1685± 35	K-Ar	Horwitz, 1975
Yelma Formation		NE DUKETON 1:250 000, DE LA POER		sandstone/glauconite	1590-1710	Rb-Sr	Preiss et al., 1975
					1670-1710	K-Ar	Preiss et al., 1975
		MUDAN	Not available	sandstone/detrital zircon	2700-2600	U-Pb SHRIMP	Halilovic et al. (2004)
		NABBERU	120° 56' 33"E, 25° 53' 11"S	sandstone/detrital zircon	2027± 23	U-Pb SHRIMP	Nelson (1997)
				carbonate (*Yandilla meekatharrensis)*	2008± 68	Pb-Pb	Russell et al., 1994
	Stanley Fold belt	RHODES	120° 33' E, 25° 20' S	muscovite	1653.6 ± 14.4	Ar-Ar	this work

		MERRIE	Not available	carbonate (*Pilbaria deverella*)	1946± 71	Pb-Pb	Russell et al., 1994
Mineralisation							
Yelma Formation	Sweetwaters Well Member	NABBERU 1:250 000, MERRIE	Not available	dolomite/galena	~1700	Pb-Pb	Richards and Gee, 1985
		NABBERU MEREWHETHER	Not available	galena	1770-1740	Pb-Pb	Teen (1996)
		NABBERU 1:250 000, MERRIE	120.66356E/25.67088N	dolomite/galena	~1650	Pb-Pb	this work
		NABBERU 1:250 000		galena	~1700	Pb-Pb	Johnston and Hall, 1980
		MEREWETHER	119.94547E/26.53371S	carbonate	~1650	Pb-Pb	Le Blanc Smith et al., 1995
Shoemaker Impact Structure		NABBERU	Not available	quartz-albite whole rock	~1630	Rb-Sr	Bunting et al., (1980a, b)
		NABBERU	120.92714E/25.83184S	quartz-albite whole rock	2648	U-Pb SHRIMP	Nelson
Basement							
Malmac Inlier		LEE STEERE	122.14028E/25.49902S	Granite	1724	U-Pb SHRIMP	Nelson (in prep)XXXX
Imbin Inlier		MUDAN	121.75981E/25.36113E	rhyodacite/zircon	1990	U-Pb SHRIMP	Nelson (2000)
Possible? Outlier Earaheedy Basin							
Mt Leake Formation		BRYAH	118.70438E/25.91409S	quartz arenite/detrital zircon	1832± 37	U-Pb SHRIMP	Nelson (1997)
		BRYAH	118.66766E/25.79373S	sandstone/detrital zircon	1785± 11	U-Pb SHRIMP	Nelson (1997)
		SW PEAK HILL 1:250 000	Not available	sandstone/glauconite	1573	K-Ar	Butt et al., 1977

TABLE 3 Frere Formation GIF Facies (after Price, 2003)

Name	*Description*	*Depositional processes*
Planar-Laminated Siltstone	Dark to light grey siltstone. Planar laminations. Light laminae are composed of quartz, dark laminae are clay rich. Angular quartz and mica are the dominant grains, with an average grain- size of 0.05 mm (<0.1 mm). Chlorite replacement is common.	Very low energy. Suspension settling (very flat planar laminae) or weak traction current activity (gentle wavy laminations)
Peloidal GIF	Red, white or grey GIF. Lack of internal laminations (no platey minerals), allochems elongated horizontally from load deformation. Allochems are 0.5 to 3 mm, can be peloids (ferruginous chert, rounded to angular), pisoids or ooids (round, concentric laminations). Peloids are the dominant allochem. Can be broken and angular and have cracks. Allochems set in a jasper or chert cement and/or matrix.	Agitated, oxic environment to form peloids High energy to rework the peloids, and redeposit.
Iron-rich Siltstone	Green to black siltstone. Planar laminations**.** Dominated by iron-rich iron-oxides and chlorite with quartz and clay.	Very low energy. Suspension settling (planar laminae) or weak traction current activity (gentle wavy laminations
Stromatolitic GIF	Red to grey colour. Laminations are wavy. In thin section, angular iron oxide grains define laminations of *Windidda granulosa & cf. ?Kulparia*. Pisoids and ooids are the dominant allochems, ~2 mm diameter. These are round, have concentric laminations and are locally concentrated. Relatively undamaged. The fabric is a mosaic of 0.01 to 1 mm carbonated crystals with irregular crystal boundaries (xenotopic).	Traction currents to produce wavy sediment laminations Abundant life suggests warm and oxygenated environment, above photic zone. *Windidda granulosa* indicates agitated environment (Grey, pers. comm.). Ooids formed in agitated shallow environment proximal to depositional environment
Quartzose GIF	Quartz rich 20-200 mm thick GIF units interbedded with 20-200 mm siltstone units. Weakly developed wavy laminations. Peloids 1;5 mm in diameter are carbonate or made up of 0.2 mm quartz grains. Chert matrix or recrystallised chalcedony cement	High energy to deposit the coarse grains.

Heterolithic Claystone and Siltstone	Black and white heterolithic siltstone/very fine sandstone and claystone. 5 mm-thick white and black layers. Wavy laminations. **White:** ~1.5 mm grains made up of chert and very fine quartz. Compressed, flat and round. **Black:** Claystone sized grains. Elongate, thin, white clay is present. There are 0.5 mm opaque iron oxides throughout facies, mainly in the chert.	Low to moderate energy. Weak traction currents to produce wavy laminations. Alternating energy conditions to produce Grain-size variations. Heterolithic bedding suggestive of storm fluvial or tidal setting
HCS Siltstone	Light grey siltstone. Laminations at low angles, and slightly wavy. Swaley cross-laminations and ripple cross-lamination are abundant. Scattered angular opaque grains and clay concentrate in thin layers. ~0.5 mm angular quartz grains dominant. Elongate brown-clay aligned with laminations, wavy and intergranular to quartz.	Combined directional flow to produce the ripple cross-laminations HCS suggestive of above storm wave-base and below fairweather wave-base.
Heterolithic Cross-Laminated Siltstone	Light-grey siltstone and yellow fine-sandstone (heterolithic). Alternating coarser (0.15–0.2 mm) and finer layers (0.05 mm) shows the wavy, low-angle laminations. Ripple cross-laminations are common. Angular quartz grains are the dominant mineral, with some elongate brown clay.	Combined directional flow to produce ripple cross-laminations Alternating higher and lower energy to produce the grainsize variation. Heterolithic bedding suggestive of storm (below fairweather Wave base), fluvial or tidal setting

*** Revision Notes**

Click here to download Revision Notes: Reply_to_Editor and Reviewer.doc

REPLY TO EDITOR AND REVIEWER

Dear Editor,

We acknowledge the constructive comments made by Prof Erikkson in his review of our paper and have, as a result, effectively complied with his suggestions. This necessitated a change of the title, which now is: A review of the geology and geodynamic evolution of the Earaheedy Basin, Western Australia

Details provided below in RED

Looking forward to hearing from you

Regards

Franco Pirajno and co-authors

COMMENTS FROM EDITORS AND REVIEWERS

Editor (Miall):
On the basis of the review report and my own reading, I recommend your paper for acceptance with major revisions (especially shortening, as indicated by reviewer #1). Please accept our apologies for this long delay but it proved to be very difficult to obtain a second review.

Reviewer #1: The paper has much potential, but gives the impression to the reader of a very lengthy geological survey-type report which has been minimally recast to make a paper. The writing style is also rather that of a survey report, with many unit descriptions giving the relevant geology from different parts of the exposed basin for that specific unit - instead, one would much rather see a focused summary of regional lithological and depositional facies variation across the basin for a specific formation, followed by details of lithofacies, palaeocurrents etc etc and then a brief interpretation - quite often, interpretation is mixed with description of facts. The writing style also assumes a certain local knowledge, with what I presume to be farm names sometimes capitalised, sometimes not, and various areas, geological features, orogenies etc etc which might be quite clear to Australian geologists are not necessarily so obvious to a general international reader. The paper needs to be aimed at the international reader lacking detailed knowledge. What the text really needs is a thorough edit, for a number of typos and spelling mistakes, but mostly to provide focus and shortening and a really scientific style of writing rather than that of a report.

This has been amended and the MS is now clearly more focussed on an international readership. Also, we have rearranged the text, with regional lithological and depositional facies treated as appropriate in the light of the available data.

Radical shortening is necessary - sections 8, 9 and 10 should be left out altogether, and this will entail removing "mineral systems" from the title - rather restrict the paper to a review of the evolution of the Earaheedy basin, and leave the mineral systems for a separate paper. Many of the figures can also be left out to achieve even more shortening (e.g., combine Figs. 2 and 12 into one). Examples of shortening needed: page 14, line 311 - having said that methodology is described elsewhere (ref.), then follows a desciption of it all anyway; or, page 15, entire first paragraph can be left out; repetition on page 36 - see lines 847 and 852-3 etc.etc.

Sections 8, 9 and 10 of original MS have been deleted

Technical points:
(a)stromatolites - in several places recourse is had to using different morphologies to identify specific environments or even relative ages - this is fairly dangerous and many carbonate workers no longer support this kind of interpretation for such stromatolite details - see a paper by W. Altermann (2004, pp.564-574 in "The Precambrian Earth: tempos and events" ed. by PG Eriksson et al., Elsevier, Amsterdam) for a recent summary of the many problems inherent in trying to read too much from stromatolites.

Yes, a paragraph to this effect has been added and Altermann cited

(b)page 25, line 591 - state that rip-up clasts are soft-sediment structures - granted, they are soft when eroded, but they are essentially erosive features.

Agreed, they are erosive features

(c) line 920-1 (and several places later on in the paper) - refer to "shale, siltstone and mudstone" - what is the difference here? - siltstone and mudstone are subdivisions of the general term "mudrock", but shale is essentially a field mapping term meaning "laminated mudrock" to most people - this use of shale with the other two terms which are really analogous is confusing.

There should be no confusion; we use the term shale to indicate a mudstone or siltstone that shows fissility

(d) line 927 - breccia formed through liquefaction? - breccias have been broken up in a lithified state.

We believe that the term liquefaction is appropriate, a liquefied bed appears as a breccia once that it is lithified; in our case both are compatible

(e) lines 981-2 - refer to silicate grains which are oolitic - how do these form?

By accretion and reference is provided in text

(f) line 1019 - discriminate between "mass-flow" and "turbidite" deposits - the latter are also sediment-gravity flow deposits.

Yes and we have stated that the deposits are mass-flow rather than turbidite

(g) line 1073 - deposition below wave-base - but these deposits contain rills (line 1068) - rills reflect exposure and falling water levels.

We prefer to take out the term rills

(h) line 1143 - "wave currents" - waves form through wind and currents largely through density/temperature differences and rotational forces.

Wave and currents is used by Beukes and Klein, 1992 (cited in the text)

(i) line 1459 - "tectonically-driven eustatic sea level changes" - eustatic sea level changes are those of global scale, due to changes in either water volume or total ocean basin volume, which are differentiated from those of more local scale due to tectonic movement of a craton, basin or part thereof. See also line 1521.

Quite right; we believe that these sea level changes are tectonically driven; the term eustatic has been deleted

(j) lines 1488-9 - carbonate deposition during lowstand? - not that likely.

Lowstand deleted

(k) lines 1504-1505 - this statement is over-obvious - "transgressions and regressions in response to fluctuating sea-level changes".

Yes, the statement has been modified

Minor typos:
(1)line 62 - replace "unconformable" by "unconformably";
(2) line 72 - insert "possible" before "outliers";
(3) line 81 - insert second bracket at end of reference in parantheses;
(4) line 206 - add "s" to end of "intrude";
(5) line 357 - separate "fortyfour" into two words;
(6) line 620 - remove full stop before bracket;
(7) line 772 - fix language here;

(8) line 863 - replace "are" by "is";
(9) line 898 - by "alchemical" is "allochemical" meant?

All of the above has been fixed

(10) lines 917-918 - a fence diagram of some sort would make these relationships much clearer.

Not necessary; figure 4 is more than adequate

(11) in many places in the paper, inconsistent use of hyphens with grain size terms - fine-grained and fine grained;
(12) line 1033 - replace "are" with "is";
(13) line 1151 - replace "f" with "of";
(14) line 1243 - insert "to" before "postdate";
(15) lines 1283-4 - insert commas into references;
(16) line 1312 - add "s" to "include";
(17) line 1351 - insert "of" before "Teague";
(18) line 1411 - insert "be" before "the";
(19) line 1472 and elsewhere "Erikson et al., 2002" - spelling - Eriksson; also in the reference, the name of co-author "Aspler" should be spelled correctly;
(20) line 1474 - replace "to" by "on";
(21) line 1588 - add brackets to "1995" and a comma thereafter;
(22) line 1598 - remove "G" after "6".

All of the above has been fixed

Pat Eriksson 06.05.2008

Appendix 1

Click here to download Background dataset for online publication only: Appendix1_Ar_Ar_Data Summary.xls

Appendix 2

Click here to download Background dataset for online publication only: Appendix2_geochem_tables.doc

Geology and mineral systems of the Palaeoproterozoic Earaheedy Basin, Western Australia

by

Franco Pirajno[(1)], Roger M. Hocking[(1)], Steven M. Reddy[(2)] and J. A. Jones[(3)]

(1) Geological Survey of Western Australia, Perth, Australia
(2) Dept. Applied Geology, Curtin University, Perth, Australia
(3) not yet available

Abstract

The Palaeoproterozoic Earaheedy Basin is one of a series of basins that extend for about 700 km east-west and are part of the Capricorn Orogen, situated between the Archaean Pilbara and Yilgarn Cratons. The Earaheedy Basin contains sedimentary rocks that were deposited on the northern passive continental margin of the Yilgarn Craton, probably as a result of continental breakup at 1.8 Ga. The sedimentary rocks of the Earaheedy Group are divided into two Subgroups, Toloo and Miningarra, each representing different depositional environments and aggregating about 3000 m in thickeness. The Tooloo Subgroup consist of basal siliciclastic with minor platform carbonates, overlain by a 600-m-thick succession of Fe-rich rocks (granular iron-formation and hematitic shales). The Miningarra Subgroup is predominantly siliciclastic, but includes stromatolite-bearing carbonate sequences and was deposited during a more active depositional regime. Far field tectonic events at 1.76 and 1.65 Ga resulted in the deformation of the sedimentary package with progressive intensity from north to south, forming the Stanley Fold Belt and giving and overall asymmetric structure to the Basin. These events were followed by a large meteorite impact (Shoemaker Impact Structure), probably in the Neoproterozoic. The Earaheedy Basin is well endowed with Fe resources, represented by the granular iron-formation (Frere Formation, Tooloo Subgroup), particularly in the Stanly Fold Belt, where there was secondary enrichement. Other mineral systems in the Basin include MVT deposits, the giant nonsulfide Magellan Pb deposit and localised structurally controlled Fe, Mn and precious metal occurrences. In addition, diamondiferous lamprophyres, U and V are also present.

1. Introduction

The Earaheedy Basin, together with the Yerrida, Bryah and Padbury basins, form a series of Palaeoproterozoic basinal structures that extend for about 700 km east-west along the southeastern margin of the Capricorn Orogen and the northern margin of the

Yilgarn Craton and covering a total area of approximately 70 000 km^2 (Cawood and Tyler, 2004; Pirajno et al. 2004) (Fig. 1). The development of these basins began at about 2.2 Ga and continued for almost 400 Myrs, to about 1.8 Ga, recording periods of sedimentation and igneous activity. The present-day geometry of these basins is the combined result of tectonic movements which occurred during the ca. 2.0-1.96 Ga Glenburgh Orogeny (Occhipinti et al., 2004), the ca. 1.83-1.78 Ga Capricorn Orogeny (Cawood and Tyler, 2004 and references cited therein) and to a lesser extent the 1.79-1.76 Ga Yapungku Orogeny (Bagas et al., 2004) and the 1.65 Ga Mangaroon Orogeny (Sheppard et al., 2005). A synopsis of the geological events that formed and shaped the Palaeoproterozoic basins in the eastern Capricorn orogen is presented in Table 1.

The Earaheedy Basin (Bunting, 1986; Pirajno et al., 2004), contains the Earaheedy Group and lies at the easternmost end of the Capricorn Orogen (Cawood and Tyler, 2004; Tyler et al., 1998; Myers et al., 1996). The Basin represents a coastal to near-shore sedimentary accumulation, which was interpreted by Jones et al. (2000) and Pirajno et al. (2004) to have accumulated at a passive continental margin along the northeastern edge of the Yilgarn Craton. This passive margin may ultimately represent a continental breakup at 1.8 Ga, perhaps linked to the impingment of a mantle plume, as will be elaborated in the section on *Depositional setting and geodynamic evolution.*

Basement to the exposed Earaheedy Basin is the Archaean Yilgarn Craton, and to the west the Yerrida Basin. To the north the Earaheedy Basin is overlain by the sedimentary successions of the Collier Basin (Bangemall Supergroup). A small outlier of 1.9 Ga rhyodacitic rock (Inbim Inlier) on the norther margin is unconformable overlain by rocks of the Yelma Formation (Earaheedy Group; see below). Locally the Earaheedy Group is intruded by dykes and sills of the Glenayle Dolerite and Prenti Downs Dolerite (Morris and Pirajno, 2005), which are part of the 1076 Ma Warakurna Large Igneous Province (WLIP; Wingate et al. 2004), and by a number of lamprophyre dykes and pipes of unknown age. Apart from the WLIP there are no other igneous rocks that are associated with the sedimentary succession of the Earaheedy Basin.

The Earaheedy Basin has an exposed area of ca. 40000 km^2, in south-central Western Australia. The original extent of the Basin could have been much larger because numerous outliers are present about 50-60 km south of the westernmost exposures. These outliers, such as the Kaluweerrie Hills (Allchurch and Bunting, 1975), Mount Laurence Wells and Mount Wilkinson south of Wiluna (Langford et al., 2000) have sedimentary rocks that include stromatolitic carbonates, which could be part of either the Yerrida Basin or Earaheedy Basin depositional systems.

The Geological Survey of Western Australia (GSWA) began a systematic re-mapping program of the Earaheedy Basin in 1997. The outcome of this program was the publication of the second edition 1:250 000 Nabberu, and eleven 1:100 000 series geological maps (Merrie, Cunyu, Fairbairn, Methwin, Nabberu, Granite Peak, Mudan, Glenayle, Earaheedy, Wongawol, Collurabie, Lee Steere and Von Trueur.The layout of these map sheets with the simplified geology of the Earaheedy Basin is shown in Figure 2. The name of these map sheets are used to identify localities discussed in the text.

In this paper the results of the field geological mapping, integrated with geochemical data, petrographic work and the available geochronology on rocks of the Earaheedy Basin are presented and discussed, with a view to introducing a model that in the present state of knowledge best explains the geodynamic evolution of the Basin and its associated mineral systems.

2. Previous work

In the last quarter of the 19th century a few explorers ventured into the interior of Western Australia, and those that visited areas within the Earaheedy Basin, include Ernest Giles, David Carnegie, Lawrence Wells and John Forrest, who named several localities, such as Frere Range, Sweeney Creek and Pierre Spring. The first geological accounts and maps of the area were published by Talbot (1910; 1914, 1919, 1920, 1926).

Modern geology began with the works of Horwitz (1975a and b; 1976), Hall and Goode (1975, 1978), Hall et al. (1977). The Earaheedy Basin made international news with the publication of two papers on Gunflint-type microbial assemblages from the Frere Formation (Walter et al., 1976; Tobin, 1990).

In the late 1970s, the Geological Survey of Western Australia commenced regional geological mapping of the map sheets that encompass the Earaheedy area, which resulted in the publication of 1:250 000 scale geological maps and Explanatory Notes for Kingston (Bunting, 1980a, b; Bunting et al., 1982; Brakel and Leach, 1980; (Leach and Brakel, 1980). These works culminated with the publication of GSWA Bulletin 131 (Bunting, 1986), which comprehensively describes the lithostratigraphic units, derivation of stratigraphic names and type localities of the Earaheedy Basin. These definitions are not repeated in this paper. The latest GSWA mapping of the Basin, carried out between 1997 and 2004, resulted in some modifications of the stratigraphy as discussed in Pirajno et al. (2004) and detailed in later sections.

Mining companies conducted exploration work in the Earaheedy Basin aimed primarily at the assessment of the iron potential of the iron-formation beds of the Frere Formation and at the Mississippi-Valley type (MVT) mineralization hosted in the carbonate rocks of the Yelma Formation. Other exploration activities included the search for diamonds in lamprophyre dykes, gold in the metamorphosed and deformed rocks in the Stanley Fold Belt and uranium in calcrete. Results and details of this exploration are discussed in *Mineral systems.*

3. Tectonic setting and regional geology

Post-Archaean tectonic events resulted in the reworking and possible fragmentation of the Yilgarn Craton's northern margin and the formation of depositional systems, while to the northwest, collision and accretionary processes were taking place. North of the Craton's present-day boundary are the Goodin, Marymia and Malmac inliers, all of which represent Archaean granite-greenstone terranes and the northern extension of the Yilgarn Craton. These inliers are located within the 700-km long belt of Palaeoproterozoic volcano-sedimentary and sedimentary basins, which are considered part of the Capricorn Orogen (Fig. 1). These basins (Bryah-Padbury, Yerrida and Earaheedy), record periods of rifting, sedimentation and volcanism, along the northern margin of the Yilgarn Craton. The subgroup lithostratigraphic divisions of the Earaheedy Basin indicate a change in the depositional settings, imposed by a high-energy tectonic regime, most likely due to orogenic uplifts, as previously mentioned. During the ca 1.74 Ga Yapungku Orogeny and the 1.68-1.62 Ga, Mangaroon Orogeny (Sheppard et al., 2005), the northern margin of the Earaheedy

Basin and the western parts of the Yerrida Basin were deformed (Stanley Fold Belt). This multi-stage deformation resulted in the characteristic cross-section asymmetry of the Earaheedy Basin, with undeformed southern platform margins and northern margins of intensely deformed rocks, typical of foreland basin architecture.

3.1 Pre- and post-Earaheedy igneous activity

The Earaheedy Basin is exclusively filled with sedimentary rocks with no temporally associated igneous activity. However, the Earaheedy sedimentary succession is spatially associated with igneous intrusive rocks of Palaeo- and Mesoproterozoic age, which both intrude or juxtapose the Earaheedy Group. These igneous rocks include, the 1.99 Ga rhyodacitic rocks of the Imbin Inlier, the Glenyale and Prenti Dolerite of the 1.07 Ga Warakurna large igneous province and a suite of ultramafic lamprohyres, some of which are diamondiferous, of uncertain age.

3.1.2 Imbin Inlier

Quartz-feldspar porphyry outcrops are present on the northern margin of the Earaheedy Basin, within the Stanley Fold Belt. The oucrop area of this quartz-feldspar porphyry extends for approximately 7 km in a west-northwest trend, but aeromagnetic data indicate that its full extent may be in the order of 22 km. This quartz-feldspar porphyry, which was dated by SHRIMP U-Pb method yielding an age of 1990±6 Ma (Table 2); Nelson, 2001a, b), is interpreted as a basement fragment to the Earaheedy Group. The Imbin quartz-feldspar porphyry consists of K-feldspar, quartz and plagioclase albite phenocrysts (about 20% by vol.), from 2 to 4 mm long, in a groundmass predominantly composed of a fine-grained K-feldspar-quartz mosaic with patches and flakes of green Fe-rich biotite (3-4 % by vol). This biotite is of later generation as it fills microfractures and locally surrounds phenocrysts. Leucoxene is an accessory phase. Locally, plagioclase phenocrysts exhibit resorption textures.

3.1.3 Glenayle and Prenti dolerites

In the Glenayle and Carnegie areas a series of mafic sills (Glenayle Dolerite and Prenti Dolerite) are associated with numerous northeasterly and west-northwesterly trending dykes (not shown in Fig. 2). The mafic sills and dykes intruded a succession of siliciclastic sedimentary rocks of the Collier Basin, north of the Earaheedy Basin, as well as parts of the eastern Earaheedy Basin. This sill and dyke complex extends for about 150 km east-southeast and about 60 km in a northerly

direction and becomes buried by Permian glaciogene sedimentary rocks to the east. Individual sills may reach up to 100 m in thickness. Some sills consists of several thin (ca 1-2m) sheets one above the other, separated by a thin veneer of sedimentary rocks. The total thickness of the Glenyale Dolerite sill complex is not known, but geophysical data suggest that it may extend to depths of 3-4 km (Morris et al., 2003). The mineralogy of the Glenayle Dolerite is dominated by plagioclase and clinopyroxene with or without orthopyroxene. The main feature of the Glenayle Dolerite is the presence of well developed interstitial granophyre, which tends to increase towards the top of the intrusion, where it can reach 20-30 % by volume, locally forming pods and lenses. Accessory minerals include ilmenite, magnetite and titanomagnetite, quartz and apatite. In places, ilmenite and titanomagnetite occur as poikilitic blebs up to 5 mm across. Where altered, the alteration phases include biotite, hornblende, chlorite, sericite and prehnite. Accessory amounts of sulfides (pyrite and lesser chalcopyrite) are also present. Geochemical analyses of the Glenayle Dolerite can be found in Morris and Pirajno (2005).

The Prenti Dolerite is a petrological variant of the Glenayle Dolerite, and consists of aphanitic to very fine-grained dolerite sills and dykes of (Pirajno and Hocking, 2002). The Prenti Dolerite typically contains 50-55% by volume of plagioclase (An_{56-70}) and granular augite (partially replaced by chlorite and biotite), with an intergranular-glomeroporphyritic texture, defined by bunches of fresh plagioclase crystals. In some samples, disseminated Fe-Ti oxides make up to 10% of the rock. The Glenayle and Prenti Dolerite are part of the 1076 Ma Warakurna Large Igneous Province (Wingate et al. 2004), which covers about $1.5x10^6$ km^2, extending from the sill complexes of the Mesoproterozoic Edmund basin (Bangemall Supergroup; Martin and Thorne, 2004), through to the Glenayle-Prenti sill complexes in the Collier and Earaheedy basins in central Western Australia (Martin and Thorne, 2004; Pirajno et al., 2004), to the Giles mafic-ultramafic layered intrusions in the Musgrave complex in southern central Australia; a total west to east distance in excess of 2400 km. The formation of WLIP is postulated to be the result of a mantle plume that impinged onto the base of the lithosphere at about 1100 Ma (Morris and Pirajno, 2005).

3.1.4 Lamprophyres

Western Mining Corporation (WMC, now BHP Billiton) discovered ultramafic lamprophyre intrusions in the Bulljah Pool area of the Basin and south of the Lee Steere Range, in in the eastern and northeastern parts, respectively, of the Earaheedy Basin. These rocks are unusual in that they contain small diamonds (see *Mineral systems*), a privilege normally reserved for kimberlites and lamproites. The lamprophyre intrusions in the Earaheedy Basin, together with marginally diamondiferous kimberlites and lamprophyres that intruded the Archean Marymia Inlier belong to the Nabberu Kimberlite Province (Shee et al. 1999).

Little published or unpublished information is available for the lamprophyre Jewill intrusions in Lee Steere (Fig. 2). The Jewill lamprophyre intrude rocks of the Wongawol Formation and forms an east-northeast`trending linear body along a distance of 1.3 km, within which four intrusive bodies (J1 to J4) were identified by drilling and another four inferred from drainage sampling (Carnegie Minerals N. L. Annual Reports 1994; 1995).

The Bulljah Pool ultramafic lamprophyres were studied by Hamilton (1992) and Hamilton and Rock (1990). The age of these rocks remains unresolved. Hamilton (1992) cited a Rb-Sr mica age of 849 ±9 Ma and an unpublished U-Pb zircon age of 305±4 Ma. The Bulljah Pool lamprophyres intruded gently dipping units of the Kulele Limestone and Mulgarra Sandstone. The four known intrusions were named BJ1, BJ2, BJ4 and BJ5 (a BJ3 feature was later recognised not to be a lamprophyre). BJ1 is sill-like, northwest trending and was traced fo about 1 km. BJ2 is possibly a pipe or a lens-like intrusive body with an easterly strike and traced for about 400 m. The sedimentary country rocks (sandstone) display fenitic alteration. BJ4 is small weathered outcrop. BJ5 is the most extensively explored Bulljah Pool ultramafic lamprophyre, whose surface expression appears to be a pipe about 50 m in diameter. Drilling beneath the pipe-like body, however, reveals that BJ5 consists of small dykes contained in a ?tectonic breccia pipe-like breccia with a steep northeastely dip (Hamilton, 1992). Samples obtained from drill cuttings show that the Bulljah Pool lamprophyres mainly consist of abundant phlogopite, perovskite, iron spinel, almandine, diopside, olivine, titanomagnetite, chromite, apatite and trace amounts of picroilmenite, barite, zircon, pyrite, pyrrhotite, K-feldspar and rutile. Calcite and

quartz veining are present. Alteration and/or weathering products include gibbsite, chlorite, hematite, kaolinite and smectite (Hamilton and Rock, 1990). The abundant phlogopite is a reddish-brown type, showing zoning and locally chloritised. Olivine is pseudomorphed by serpentine, chlorite and lesser carbonate. Chlorite also form pools that may pseudomorph nepheline or melilite (Hamilton and Rock, 1990). Mineral phases recovered from concentrates obtained from loam samples, in addition to small diamonds, include chrome pyropes, spinels, ilmenites macrocrysts, chrome diopsides, garnets

Mineral chemistry studies carried out by Hamilton and Rock (1990) show that the phlogopites are Ba-bearing titanian tetraferriphlogopites.This type of phlogopite is common in the groundmass of kimberlites and lamproites, as well as ultramafic lamprophyres (Rock, 1990). Indeed, these micas fall within the field of ultramafic lamprophyres as defined by Rock (1990).

4. The Earaheedy Basin

The Earaheedy Group is a 5-km-thick succession of shallow marine clastic and chemical sedimentary rocks that is divided into two subgroups (Fig. 3; Hall et al., 1977). The Tooloo Subgroup consists of the Yelma Formation (base) and the Frere Formation (top). The overlying Miningarra Subgroup consists of the Chiall Formation (base), Wongawol Formation, Kulele Limestone, and Mulgarra Sandstone (top; Fig. 3). A schematic north-to-south section across the Earaheedy Basin is shown in Figure 5. The regional structure is an asymmetric east-plunging syncline, with a vertical to locally overturned northern limb, due to compressive movements from the northeast, which created a zone of intense deformation along the exposed northern margin of the Earaheedy Basin. This zone of deformation, the previously mentioned Stanley Fold Belt, is characterised by reverse faults and shear zones that consistently dip steeply to the north, the development of slaty cleavage and phyllitic rocks and the appearance of metamorphic minerals (e. g. muscovite, sericite, chlorite). The intensity of deformation gradually decreases southward, but abruptly decreases to the north. Isolated small outcrops immediately north of the fold belt dip at low angles and are otherwise undeformed. In the sections ahead we discuss the available geochronology and describe in some detail the lithostratigraphy of the Earaheedy Group.

4.1 Geochronology

The geochronological data for the Earaheedy Basin are summarised in Table 2 .

A maximum stratigraphic age of 1.84 Ga is provided by the Mooloogool Group of the Yerrida Basin (Rasmussen and Fletcher, 2002), which the base of the Earaheedy Group unconformably overlies. A minimum stratigraphic age is provided by the overlying Bangemall Supergroup (maximum age of 1645 Ma; Martin and Thorne, 2001). Pirajno et al. (2000) and Jones et al. (2000) attributed deformation of the Earaheedy Group in the fold belt to the second phase of the Yapungku Orogeny (1790 to 1760 Ma; Bagas and Smithies, 1998; Bagas et al., 2000), which records the initial collision of the North Australian and West Australian Cratons (Myers et al., 1996). This age constraint is considered uncertain, however, because there is little evidence to constrain the timing of deformation in the Stanley Fold Belt or the rest of the basin. An Ar-Ar age from a muscovite in a schist rock in the Stanley Fold Belt, yielded an unweighted mean age of 1648±11.7 Ma (see details below).

Minimum isotopic ages on glauconite grains in sandstone are provided for the Earaheedy Group by K–Ar and Rb–Sr ages of 1670–1710 Ma and 1556–1674 Ma, respectively (Preiss et al., 1975) from the Yelma Formation on DE LA POER, and a K-Ar age of 1685 Ma (Horwitz, 1975a, b) from the base of the Chiall Formation on WONGAWOL. These ages may be related to post-depositional resetting during a deformational event, or by a thermal event possibly related to igneous activity, or a combination of these events. Pb-Pb mineralization ages of 1.65 Ga and 1.77-1.74 Ga are recorded, from the Magellan deposit in outliers of Yelma Formation overlying the Yerrida Basin and the Sweetwaters Well Member on MERRIE, (Richards and Gee, 1985; Teen, 1996) respectively.

Grey (1994) suggested a depositional age of 1900–1800 Ma based on the stromatolite taxa of the Earaheedy Group and their similarity to taxa in the Duck Creek Dolomite of the upper Wyloo Group (Grey and Thorne, 1985). Pb–Pb whole-rock dating of carbonate in the Yelma Formation returned ages of 2010 Ma and 1950 Ma (Russell et al., 1994).

The current age constraints suggest the upper part of the Earaheedy Basin is ca 1800 Ma in age, which reflects deposition during the Capricorn Orogeny (1830–1780

Ma; Cawood and Tyler, 2004). The lower part of the Earaheedy Group is less well constrained. It is unclear from current age constraints whether there was a significant time break between the Mooloogool Group and the lower part of the Earaheedy Group. There is little evidence in the Earaheedy Group to suggest major active tectonism within the exposed depocentre for the Earaheedy Basin, although there is evidence to support regional tectonism, such as the presence of seismites in rocks of the Chiall Formation.

4.1.1 Ar-Ar dating

A sample (GSWA 171772) collected from drill cuttings (c.50m depth) located approximately 5km southeast of Well 7 on the Canning Stock Route (51J 33103E 7211839N – WGS84) was collected for $^{40}Ar/^{39}Ar$ analysis. The sample is a quartz-muscovite-chlorite schist, possibly derived from deformed and metamorphosed siltstone interbeds in granular iron formation rocks of the Frere Formation. The sample contains aligned muscovite and chlorite in a polygonal aggregate of recrystallised quartz grains. The rock was deformed during the formation of the Stanley Fold Belt.

4.1.1.1 Sample Description and Analytical Procedure

Argon data were collected from two single grains of white mica (Grain 1 = 400 x 200 um; Grain 2 = 500 x 300 um) handpicked from the crushed whole rock sample. These grains were chosen for analysis because they showed no signs of being broken fragments of larger grains and showed no visible signs of alteration. Analytical procedures and instrument details have been described elsewhere (Reddy et al 2004). Prior to irradiation samples were loaded with biotite age standard Tinto B, with a K-Ar age of 409.24 ± 0.71 Ma (Rex and Guise 1995), to monitor the neutron flux gradient. The package was Cd-shielded and irradiated in the H5 position of the McMaster University Nuclear Reactor, Hamilton, Canada, for 90 hours. The Tinto B standards yield a J value for the sample of 0.020528 with a J value error of 0.5%. Argon data were collected by infra-red laser step-heating of single grains at the Western Australian Argon Isotope Facility, Curtin University of Technology; a facility operated by a consortium comprising Curtin University and the University of Western Australia. Data were corrected for measured background, mass spectrometer discrimination and nuclear interference reactions. Correction factors are as follows:

322 ($^{36}Ar/^{37}Ar$)Ca = 0.000255, ($^{39}Ar/^{37}Ar$)Ca = 0.00065, and ($^{40}Ar/^{39}Ar$)K = 0.0015.
323 Corrections for ($^{38}Ar/^{39}Ar$)K and ($^{38}Cl/^{39}Ar$)K were not undertaken because of the
324 Proterozoic age and low Cl characteristics of the samples and the short amount of
325 time between irradiation and the time of analyses. $^{40}Ar/^{39}Ar$ ages were calculated
326 using the decay constant quoted by Steiger and Jäger (1977). J values and 1σ errors
327 are noted in Appendix 1. Errors shown in step-heating profiles (Appendix 1) represent
328 analytical errors and do not include J value uncertainties.

329 ### 4.1.2 Detrital zircon ages and provenance studies

330 Halilovic et al. (2004) conducted a study of sediment provenance based on the U-
331 Pb SHRIMP age of detrital zircons. The results of this work are summarised below.
332 Zircon ($ZrSiO_4$) is widely used for detrital dating studies because it is common in
333 many rock types, and is chemically and physically resistant, which enables it to
334 survive cycles of burial, metamorphism and erosion. The application of U-Pb dating
335 of detrital zircons in sedimentary successions provides important constraints for the
336 palaeogeography and tectonic settings of sedimentary basins (e. g. Cawood and
337 Nemchin, 2000; Nelson, 2001a, b). Age spectra provide insights into the nature and
338 age of the source region. In addition, they constrain the timing of sedimentation with
339 the youngest detrital zircons, giving a maximum age for the deposition of the
340 sediments, while the oldest U-bearing minerals grown in situ provide both a lower
341 limit of deposition, as well as valuable information on the timing of later
342 tectonothermal events (Halilovic et al., 2004; McNaughton et al., 1999).

343 U/Pb data were obtained from 285 detrital zircons from six samples. Three from
344 the basal Yelma Formation, one from the Wandiwarra Member and one from the
345 Princess Range Member of the Chiall Formation, one sample from the
346 stratigraphically youngest unit the Mulgarra Sandstone. Included in this dataset are 27
347 zircons from a fine-grained arenite (Yelma Formation) analysed by Nelson (1997).
348 Archaean and Proterozoic zircon populations are present in all samples except for one
349 sample (JHE-42) of Yelma Formation from the northern margin of the basin, which
350 contains only Archaean detritus. Results are shown on the frequency distribution
351 diagram of Fig. 6. Sample JHE-31b is a coarse quartz arenite from the base of the
352 Yelma Formation, about 0.5 m above the unconformity surface with the underlying
353 Yilgarn Craton granitic rocks. Of the 74 zircon grains analysed, 18 show a range in

age from approximately 3280 to 2000 Ma (Fig. 6). Zircons with Archaean ages fall into three groups with the youngest analyses of these groups showing a concordia age of 2531±66 Ma. Zircons with a Palaeoproteroic age fall into four groups, in which the youngest gave an age of 1983±51 Ma (91% concordance). Fortyfour zircons were extracted from sample JHE-143 (Yelma Formation, also from just above the basement unconformity), of which 37 show greater than 90% concordance. This sample's Archaean population has a range of ages from 2.95 to 2.60 Ga with a peak at 2.65 Ga (Fig. 6). The Palaeoproterozoic zircon populations show two distinct groups at 2.2 and 2.0 Ga, with the youngest discordant analysis yielding an age of 1990±21 Ma. Sample JHE-42 is from a fine-to-medium grained arenite collected from the northern margin of the basin. Here the Yelma Formation is deformed in the Stanley Fold Belt. This sample yielded 15 zircons of which 12 were analysed. Ten analyses with more than 95% concordance gave a unimodal age distribution of between 2.7 and 2.6 Ga (Fig. 6). Sample JHE-149, a sandstone from the Wandiwarra Member of the Chiall Formation, was taken about 20 km westnorthwest from the Prenti Downs homestead. Of the 69 analysed zircons, 48 show a 90% concordance. The Archaean population contains two groups that are clustered around 3.0 and 2.8-2.6 Ga (Fig. 6). The oldest grain indicates an age of 3242±15 Ma. The Palaeoproterozoic population of two groups exhibits age peaks at 2.25 and 2.06 Ga. Sample JHE-40 is from a quartz arenite of the Princess Ranges Member of the Chiall Formation in a well exposed 32 m thick section, 2-3 km southeast of Wondjiyanda Pool on Wongawol (Fig. 2). Palaeocurrent data from this site suggest a general northeasterly direction of sediment transport. Of the 40 grains analysed, 25 have concordancy of 90% or above. The oldest grain yielded an age of 3465±13 Ma, but the majority having a range of between 2.9 and 2.6 Ga. The Palaeoproteroic zircon population yielded ages ranging from 2.3 to 1.8 Ga, with the youngest single grain (97% concordance) having an age of 1876±19 Ma. Finally, a glauconitic quartz sandstone of the Mulgarra Sandstone, sample JHE-160, was taken from the base of the unit. From this sample 46 detrital zircons were analysed of which 25 show 90% or above concordancy. The Archaean population consist of a single analysis dated at 3190±10 Ma and a series of analyses with a broad peak at 2.7-2.6 Ga (Fig. 6). The Palaeoproterozoic population consists of two groups, one with a peak at around 2.3 Ga, the other with a continuum of ages in the range 2.2 to 1.8 Ga. The youngest grain, 90% concordant, gave an age of 1796±58

Ma. Four discordant analyses range from 1.79 and 1.73 Ga, but with large errors. The youngest most concordant age is 1808±36 Ma.

Cathodoluminescence imaging showed that both Archaean and Proteroizoic grains have oscillatory zoning suggesting an igneous origin. The Archaean zircons are well rounded or are broken fragments of larger grains. A number of Palaeoproterozoic zircons show evidence of recrystallisation.

The analyses of the 285 zircons, augmented by earlier analyses of 27 zircon grains (Nelson, 1997) indicate that there was a substantial component of detritus of Palaeoproterozoic age. However, the presence of zircons of Archaean age also points to a mixed provenance. The multiple age peaks in Fig. 6 clearly suggest detrital input from source regions of different ages. The Palaeoproterozoic detritus is dominated by peaks in the age range of 2.3-2.2, 2.0 and 1.8 Ga, whereas those of Archaean age are dominantly in the range 2.7-2.6 Ga, with the oldest in the 3.5 Ga bracket. A likely source of detritus with ages of 2.0 and 1.8 Ga is the southern part of the Gascoyne Complex (Sheppard et al., 2004). More specifically, this detritus could have derived from the granitic rocks of the 2005-1970 Ma Dalgaringa Supersuite of the Glenburgh Terrane (Sheppard et al. 1999; Occhipinti and Sheppard, 2001), whereas the 1.8 Ga zircon grains could have derived from the granites of the 1830-1780 Ma Moorarie Supersuite (Occhipinti et al., 1998). The Imbin Inlier (see *Depositional Setting and Geodynamic Evolution of the Earaheedy Basin*) could represent a fragment of the Dalgaringa Supersuite. A possible source region for the 2.3-2.2 Ga zircons is the Glenburgh terrane (Gascoyne Complex), on the basis of rims on zircons in basement gneiss of this terrane, which yielded ages of about 2.2-2.4 Ga (Kinny et al., 2004). The youngest, single zircon grain, is in the upper part of the Mulgarra Sandstone, dated at 1.8 Ga and considering that units of this formation are in stratigraphic conitinuity with underlying successions, provides the minimum age for the Earaheedy depositional system. This result conflicts with the Pb-Pb carbonate ages for the Yelma Formation (see Table 2; and Russell et al. 1994) of 2.01 and 1.95 Ga and the $\delta\ ^{13}C_{carb}$ positive excursion at 1.9 Ga in the same rocks (Lindsay and Brasier, 2002). However, the 1.8 Ga age of the detrital zircon in the Mulgarra Sandstone corresponds well with the 1843±14 Ma U-Pb monazite age (Rasmussen and Fletcher, 2002) of the youngest

lithostratigraphic unit (Maraloou Formation) that uncorformably underlies the Yelma Formation, oldest unit of the Earaheedy Basin.

In conclusion, detrital zircon populations, together with palaeocurrent directions (unpublished data) indicate that the Earaheedy Basin is approximately 1.8 Ga and that the sediments of its depositional system had a significant source to the west and southwest, which is possibly related to uplift in the southern Gascoyne Province during the Capricorn Orogeny. This was followed by at least two tectonic events, the Yapungku orogeny at 1.79 -1.76 Ga (Bagas, 2004) and the 1.68-1.62 Ga Mangaroon orogeny (Sheppard et al., 2005). The Stanley Fold Belt was formed as a result of these tectonic events.

4.2 Lithostratigraphy

The Tooloo Subgroup contains the Yelma and Frere Formations (Figs. 2 and 3). The Miningarra Subgroup comprises, from older to younger, the Chiall Formation, Wongawol Formation, Kulele Limestone and Mulgarra Sandstone (Figs. 2 and 3), aggregating approximately 3000 m in thickness. These lithological units are discussed below.

4.2.1 Yelma Formation

The Yelma Formation is the basal unit of the Earaheedy Group and contains sandstone, shale, carbonate and minor siltstone and conglomerate and records a regional marine transgression. The formation is quite variable laterally and vertically in thickness and composition. Sandstone beds in the southeast are trough cross-bedded, with local asymmetric ripples and mudcracks. Scattered stellate pseudomorphs may be after evaporitic minerals. A 100m-thick stromatolitic carbonate facies in the southwest of the basin is differentiated as the Sweetwaters Well Member. At and near the surface, this stromatolitic dolomite is generally altered to chert. A sandy dolomite unit near the base of the Sweetwaters Well Member contains thin intercalations of volcaniclastic shard-rich silty beds that were presumably derived from contemporaneous, but distal, explosive eruptions. A localised conglomeratic unit, the Yadgimurin Member, lies at the base of the Yelma Formation in the western part of the Earaheedy Basin (Merrie; Fig. 2).

448 The upper contact with the Frere Formation is marked by the first major occurrence
449 of chert or granular iron-formation (Bunting, 1986), although in places stromatolitic
450 forms persist between granular iron beds for up to 5-6 m above the contact. The
451 thickness of the formation ranges from 3 m in the southeast, through 150 m in the
452 type area (Hall et al., 1977), to at least 500 m in a drillhole in the northwestern part of
453 the basin. Bunting (1986) estimated a thickness of 1500 m in the Stanley Fold Belt,
454 but we interpret this as due, in part, to structural repetition.

455 In the westernmost parts of the Earaheedy Basin, the Yelma Formation is a unit
456 of clastic and dolomitic sedimentary rocks at the base of the Earaheedy Group. This
457 unit occupies much of the northeastern portion of Thaduna (Fig. 2), near and around
458 Lake Gregory and consists mainly of quartz arenite, stromatolitic dolomite and chert
459 breccia. In this area, the base of the Yelma Formation, includes quartz lithic sandstone
460 and quartz conglomerate, which lie unconformably on quartz arenite of the Finlayson
461 Member, and is exposed 1.5 km east of Freshwater Well, on the southern edge of
462 Lake Gregory. The main constituents of the lithic sandstone, near the base of the
463 formation are quartzose and sericitised lithic grains, and subordinate polycrystalline
464 quartz, chlorite and turbid feldspar.

465 Two boreholes drilled 3 km south of Little Well in Thaduna (Fig. 2; Meakins and
466 Watsham, 1994), together with field observations, provide a representative 400 m-
467 thick stratigraphic section of the Yelma Formation. This section, schematically
468 represented in Figure 7, consists of grey to pink, massive, silicified dolomite beds in
469 the lower part. Argillaceous interbeds are locally present between 350 m and about
470 200 m below surface. This interval is overlain by a 120 m-thick unit of dolomite with
471 solution breccia interbeds, containing some interstitial kerogen material and sulfides.
472 This is in turn, overlain by about 100 m of pink to grey thinly laminated dolomite,
473 dolomite breccia, ferruginous sandstone and arenite, followed by 20 m of dolomite
474 with microbial laminae. The latter is a distinct rock, which may be part of the
475 Sweetwaters Well Member.

476 Outcrops on the northwest side of Lake Gregory, consist of dolomite breccia, that
477 is commonly chertified, cream-coloured and fine- to medium-grained, bedded and
478 laminated dolomite with minor lenses of ferruginous sandstone and siltstone,

associated with stromatolitic dolomite. In the area around Edingunna Spring, outcrops of these units include silcretized chert breccia, underlain by coarse breccia. This material is underlain by pebble beds, about 2 m thick, comprising subrounded to rounded pebbles up to 5 cm in diameter, dominantly of quartz and chert, and a coarse-grained, poorly sorted quartz (and feldspar?) arenite. The latter is probably the base of the Yelma Formation and may correlate with the Yadgimurrin Member (see below).

Most dolomitic rocks consist of a packed aggregate of small (averaging 0.1 mm) dolomite rhombs, with interstitial iron oxides. The dolomite also locally contains disseminated quartz grains and submicroscopic stylolites. Siltstone interbeds contain quartz, kaolinite, illite and sericite.

Sandstone in the Yelma Formation is typically well sorted and composed of well rounded quartz grains and minor detrital tourmaline and zircon. They are grain-supported and with a diagenetic microcrystalline quartz or chalcedonic quartz cement. Quartz sandstone is present in the eastern parts of the central uplift of the Shoemaker impact structure. This rock is cross-bedded and consists of a packed aggregate of rounded quartz grains, showing diagenetic quartz overgrowths and minor detrital tourmaline and interstitial recrystallized quartz.

The Yelma Formation was deposited in a fluvial to coastal setting, with carbonates of the Sweetwaters Well Member developing in a saline coastal-lagoonal environment. Limited palaeocurrent data for the Yelma Formation on Wongawol suggest that sediment transport was towards the north-northwest. The Yelma Formation is interpreted to record a marine transgression over the Yilgarn Craton. Sedimentary structures suggest a shallow water to partly emergent, fluvial to coastal marine depositional environment, which was locally evaporitic at the base of the Yelma Formation. The upper part of the Yelma Formation suggests quiet water conditions and may reflect deposition in a lagoonal environment developed behind a carbonate bank, possibly represented by the Sweetwaters Well Member. As mentioned previously, the detrital zircon populations are dominantly 2.6-2.7 Ga in age, with a smaller 2.2 Ga population, and minor 2.0 Ga zircons and suggest the Yilgarn Craton and southern Gascoyne Complex were important sediment sources during basin development.

4.2.1.1 Sweetwaters Well Member

The Sweetwaters Well Member is about 100 m thick and consists mainly of stromatolitic dolomite with sandy dolomite and dolomitic feldspathic sandstone beds at top and bottom of the dolomitic succession. The dolomitic feldspathic sandstone unit at the top of the dolomite grades eastward to a micaceous sandstone and is overlain by granular iron formation rocks of the Frere Formation. The lower contact is marked by about 15 metres of transitional interbedded sandstone and dolomite passing upward to a sandy and feldspathic dolomite unit that contains quartz, microcline, albite, chert and micritic dolomite embedded in a coarse-grained dolomite cement. The Sweetwaters Well Member dolomite is light grey to grey in colour, massive to algal laminated, commonly with stromatolite forms. In northwest Nabberu (Fig. 2), the Sweetwaters Well Member was intersected in a number of drillholes sunk through the Frere Formation (Edgar, 1994; Feldtmann, 1995; 1996; Dörling, 1998a to d (see also section on *Mineralization and mineral systems*). Samples of stromatolitic dolomite collected from drill core show two phases or domains of dolomite, one is an aggregate of coarse-grained dolomite crystals, the other is microcrystalline (micritic) and is associated with microbial laminae. The coarser-grained dolomite has intergranular microcrystalline quartz and sericite. In some cases micritic dolomite forms peloids that are cemented by chalcedonic quartz. Locally, the carbonate material is replaced by cryptocrystalline quartz (chert) and chalcedonic quartz.

Scattered outcrops of Sweetwaters Well Member, which occur along the southern shore of Lake Nabberu, about 9 km east-northeast of Horse Bore, are generally chertified, except for an area along a small tributary, where there are good exposures of subhorizontal stromatolitic dolomite. Here, the dolomite exhibits fine microbial laminae and includes the stromatolites *Murzuna Nabberuensis, Omachtenia teagiana* and *Asperia digitata* (Fig. 8; Grey 1984; 1994). Drillcore sections indicate that stromatolites are generally present in metre-scale upward-shallowing cycles. They include *Asperia digitata* (Grey 1984; 1994), which is believed to have grown in restricted, quiet water environment, possibly supratidal ponds; *Pilbaria deverella* (Grey, 1984) indicative of moderately high-energy, lagoonal conditions; and *Ephyaltes edingunnensis* (Grey, 1994), which formed in deeper quiet water, and *Murgurra nabberuensis* (Grey, 1984) which colonised moderate energy patch reefs.

Details of stromatolite taxa of the Earaheedy Basin can be found in Grey (1984, 1994). Grey (1994) suggests that these stromatolite forms are indicative of an upward shallowing, lagoon to supratidal, environment (Fig. 9A,B).

A sedimentological study, aimed at constraining the depositional environment of the Frere Formation, was carried out by Price (2003). In his study, Price (2003) defined 8 facies in the Frere Formation (see below) and 2 in the Yelma Formation. The facies of the Yelma Formation are: 1) Stromatolitic dolostone and 2) Dolostone. The former is a white creamy dolostone, with gentle wavy laminations and with alternating, ~20 m thick, horizons of *Asperia digitata* and *Pilbaria deverella*. The second facies, is a creamy white dolostone, with weakly developed wavy laminations and rare ripple cross-laminations and has crystalline mosaic fabric. This facies contains rare *Pilbaria deverella*, which as mentioned above may have formed in a shallow lagoonal system.

4.2.1.2 Yadgimurrin Member

This is a localised very coarse, poorly sorted conglomeratic unit with sandstone lenses, about 100 m thick (Bunting, 1986) at the base of the Yelma Formation (Fig. 2), about 10 km southeast of the Baumgarten Reward gold deposit in the Marymia Inlier (Bagas, 1998a, b). The Member contains clasts that range from approximately 50 mm to 1 m in size, are well rounded and include granite, quartzite, chert, and chert breccia enclosed in an arkosic matrix. Pods and veins of jasperoidal chert and quartz are associated with this conglomerate and may be the result of localised hydrothermal fluid flow along the tectonic contact between the Marymia Inlier and the Yelma Formation (Adamides et al., 2000a). Bunting (1986) suggested that some of these clasts are derived from the underlying Mooloogool Group of the Yerrida Basin (Pirajno et al., 2004). The Yadgimurrin conglomerate was assigned to the Yelma Formation by Bunting (1986) on the basis of the nature of the clasts and a distinct easterly dip. The Yadgimurrin Member is interpreted as a local conglomeratic fan, associated with syndepositional fault movements (Adamides et al., 2000a).

4.2.2 Frere Formation

The Frere Formation, formally defined and described by Hall et al. (1977), records the onset of major Fe oxide precipitation within the Earaheedy Basin and consists of up to four major granular iron-formation intervals, separated by at least three major shale and siltstone bands, and minor carbonate (Fig. 10). The Frere

575 granular iron formation, an important iron resource, is similar to the Superior iron
576 formations and is one of few of these types of iron formations recorded outside of
577 North America (Goode et al., 1983; Trendall, 2002). The Frere Formation is exposed
578 along the southern and northern margins of the Earaheedy Basin. On the southern
579 margin the Formation is unmetamorphosed, undeformed or only mildly deformed,
580 forming layers that are shallow-dipping to the north. On the northern margin of the
581 Basin, the Frere Formation is deformed and folded into a south-verging synclinal
582 structure with a steep to overturned limb (Stanley Fold Belt, see below). The total
583 thickness of the Frere Formation was estimated by Bunting (1986) at about 1200-1300
584 m, but field evidence, suggests this thickness may be exaggerated due to structural
585 repetition and we estimate the actual thickness of the Formation to be about 600 m.

586 The Frere Formation consists of alternating beds of hematitic shale, green
587 chloritic siltstone and granular iron-formation. Granular iron-formation horizons
588 consist of granular iron- beds, typically between 0.5 cm to 20 cm thick, interbedded
589 with jasper, chert, shale and siltstone (Fig. 11). Drillcore and outcrop show that chert
590 intraclasts are common and range in size from 1.5 cm to 35 cm. Contact between
591 granular iron beds and siltstone units are commonly irregular and typically marked by
592 soft-sediment structures, such as rip-up clasts, load and flame structures. The scale of
593 the granular iron beds and siltstone banding ranges from millimetre to metre and up to
594 100s of metres (micro-, meso- and macroscale) and is similar to that recorded for
595 banded iron-formations (Trendall, 2002; Fig. 11). The intercalated shale bands appear
596 to increase in thickness at the expense of the granular iron-formation, towards the
597 southeast. The upper contact with the Karri Karri Member of the Chiall Formation is
598 transitional and defined as the last major chert, jasper or iron-formation (Hall et al.,
599 1977).

600 Granular iron formation in the Frere Formation has a strong magnetic signature
601 even through significant overburden, and is negatively magnetised in the south and
602 positively magnetised in the north (Stanley Fold Belt). Overall the Frere Formation
603 forms an almost continuous zone of high total magnetic intensity on aeromagnetic
604 images, delineating the present-day geometry of the basin (Fig. 12). Along the
605 sourthern margin of the basin, northwest-trending structures are negatively
606 magnetized, whereas east- and north-trending structures, as well as the circular

607 structures that define the Shoemaker impact structure, are positively magnetized. In
608 the Stanley Fold Belt strong positive magnetic signatures define deformational
609 structures such as folds, reverse faults and shear zones.

610 The granular iron-shale/siltstone couplets of the Frere Formation are indicative of
611 cyclic changes in primary sediment composition that probably relate to sea level
612 changes and supply of iron and silica. Cross-bedding is locally visible in granular
613 iron-formation beds, and in general sedimentary structures indicate traction-current
614 deposition.

615 Granular iron-formations in the Frere Formation are texturally and
616 mineralogically similar to those in the Lake Superior region, North America. Walter
617 et al. (1976) and Tobin (1990) described and compared microfossils within the iron-
618 formation with those in the Gunflint Formation in the Superior Province. The Gunflint
619 Iron Formation from that region contains microfossils (Gunflint-type microbial
620 communities) that are similar to those found in the Frere Formation, at Camel Well
621 and in the Windidda Formation at Tooloo Bluff, (Walter et al., 1976; Hall and Goode,
622 1978; Goode et al., 1983; Tobin, 1990). Gunflint-type microbiota are considered to be
623 characteristic of marine subtidal environments (Tobin, 1990). These microfossils
624 consists of contorted and/or randomly oriented filaments and include Gunflintia
625 *minuta*, Animikiea *septata*, Eoastrion *simplex*, Eoastrion *bifurcatum*, Huraniospora
626 *psilate*, Kakabekia *umbellata* and Archaeorestis *schreiberensis* (Walter et al., 1976;
627 Tobin, 1990).

628 In the Stanley Fold Belt, the Frere Formation is intensely deformed, with tight
629 folds, sheared limbs, and reverse faults. On Rhodes and parts of Mudan (Fig. 2), the
630 Frere Formation is intensely tectonised, forming mylonitic zones that resemble
631 banded iron-formation (Pirajno et al. 2000; Pirajno and Hocking, 2001). On Nabberu,
632 the Frere Formation is well-exposed in the Frere Range, along the northern side of
633 Lake Nabberu, and in the Shoemaker impact structure, where it forms the inner collar
634 (Pirajno, 2002). In the northeast corner of Granite Peak (Fig. 2), exposures of the
635 Frere Formation lie within the Stanley Fold Belt. Here, the granular iron-formation is
636 tightly folded, tectonised and well-laminated, and is termed laminar iron-formation. It
637 resembles banded iron-formation, but contains a pervasive fabric that is interpreted to

be a tectonic overprint of the original bedding. Lamellae vary from reasonably continuous to discontinuous lenses and are generally between 10 and 50 mm thick. The limbs of folds in northeast Granit Peak are commonly brecciated and cut by quartz vein stockworks.

Shale and siltstone intervals which separate granular iron-formation beds are similar to those of the Yelma Formation and the Karri Karri Member of the Chiall Formation. They commonly have a bedding fissility, accentuated by weathering. Siltstone is parallel-laminated, and trough and planar cross-laminated. Ripples are typically linguoidal or sinuous and interference patterns are common. Individual laminae are 1 mm to 10mm in thickness. Massive greenish chert is locally on present on Granite Peak. The chert exhibits remnant peloidal textures and quartz filled fractures, and lies parallel to a northwest trending, negatively magnetized structure. It is interpreted to be granular iron-formation that has been strongly silicified and fractured due to fluid flow along this structure.

An interesting aspect of the granular iron-formation rocks is their common association with a small shrub. This shrub, *Micromyrtus ciliata*, is characterised by tiny, crowded bright leaves, pink buds and small white flowers. Where present, *Micromyrtus ciliate* is the exclusive vegetation covering areas underlain by granular iron-formation rocks.

4.2.2.1 Textural features, petrography and mineralogy

The textural and petrological features of granular iron-formation were described in detail by Hall and Goode (1978) and Goode et al. (1983). A typical thin section, sketched in Figure 11, provides a good example of microscale banding. A granular iron horizon contains a 1-cm-thick band of closely packed hematite peloids and intraclasts, cemented by orthochemical cryptocrystalline silica (chert) and/or allochemical chalcedony. This band is overlain and underlain by 1-4 mm thick laminae of pale green silt composed of green iron-rich chlorite (Fig. 13b), anhedral hematite, abundant disseminated euhedral magnetite crystals and angular quartz, overprinted by carbonate, and lenticles of chlorite-quartz.

Individual granular iron-formation beds consist of chert (cryptocrystalline silica), iron oxides (hematite and/or magnetite; Fig. 13c, d, e), microplaty hematite (Fig. 13f),

669 and jasper (cryptocrystalline silica with finely disseminated hematite) peloids in a
670 cherty, chalcedonic (allochemical) or jasperoidal (orthochemical) cement (Figs 13 a,
671 b, c). Peloids commonly exhibit concentric laminae, especially where the peloids are
672 partially replaced by microcrystalline quartz (Fig. 14 a, b, c, d). Hematite is replaced
673 by microplaty hematite and/or magnetite in iron formation beds deformed in the
674 Stanley Fold Belt. In fractures and zones of deformation the granular iron formation
675 beds are pervasively silicified, with the peloids and the interbedded iron-chlorite-rich
676 shale replaced by stilpnomelane. Maghemite and martite replace the hematite and
677 magnetite in zones of supergene alteration. Shale and siltstone units are parallel-
678 laminated, and contain quartz, iron-rich chlorite and disseminated euhedral magnetite.
679 The sphericity of peloids is highly variable and generally depends on the degree of
680 early diagenetic compaction and lithification. The average spherical dimensions of
681 over one hundred peloids indicate the long axes of the ellipse average 0.52 mm,
682 whereas the short axes average 0.26 mm, with a length to width ratio of 2.0. Peloids
683 commonly contain syneresis cracks infilled with quartz or chalcedony.

684 Examination of drill core reveals that thin bands (few cm) of peloidal carbonate
685 are locally intercalated with the granular iron-formation. Typically, carbonate peloids
686 exhibit close packing, are plastically deformed and commonly replaced by
687 stilpnomelane and/or euhedral magnetite (Fig. 14d, e, f).

688 Reflected-light petrographic studies of the granular iron beds reveal that the main
689 iron minerals are hematite (microplaty, blades and irregularly-shaped blebs),
690 magnetite, maghemite, martite and goethite (Figs. 13e, f). Maghemite and martite are
691 products of the oxidation of magnetite, whereas goethite is related to recent
692 weathering. Magnetite crystals are especially common along faults and in deformed
693 Frere Formation.

694 A possible paragenesis of the iron minerals is:

695 Hematite → magnetite → martite-hematite→ maghemite → goethite.

696 This sequence may have resulted from the deposition of primary hematite,
697 followed by hydrothermal magnetite along fault zones, subsequent to oxidation to

produce martite and maghemite, and late supergene redistribution of iron to precipitate the goethite.

4.2.2.2 Alteration of granular iron-formation

Alteration of the Frere Formation is common, especially along faults and in fractures around the Shoemaker impact structure and close to the Lockeridge Fault (see *Mineral systems*). This alteration is manifested by cryptocrystalline (chert), microcrystalline and chalcedonic quartz, and carbonate that replace the Fe oxide peloids and the orthochemical ferruginous or jasperoidal matrix. Stilpnomelane and minnesotaite are also present and may be locally abundant. In places, stilpnomelane forms pervasive replacements. Some of the more typical alteration features are illustrated in Figures 15 and 16.

West-northwest of the Shoemaker structure, diamond drillholes intersected Frere Formation rocks that exhibit varying degrees of stratabound alteration. This alteration consists of more than one phase of pervasive silicification and replacement by stilpnomelane and carbonate (probably dolomite). The paragenesis of this alteration is difficult to gauge because the same alteration minerals appear in more than one event. However, in general, the following paragenetic sequence can be reconstructed, on the basis of petrographic studies:

Hematite peloids → stilpnomelane → chert → carbonate → chlorite + carbonate + magnetite.

In places, only one event can be seen, e. g. carbonatisation (Fig. 16a, b), or total replacement of the chloritic siltstone by stilpnomelane (Fig. 16a, b). In other instances two or more alteration events are observed, such as partial silicification overprinting peloids that had been earlier replaced by stilpnomelane (Fig. 16e), and by late magnetite (Fig. 16d, f). Similarly, all stages of carbonatisation are present, from localised development of carbonate rhombs (Fig. 16b, c) to more pervasive carbonate alteration. Late alteration phases include magnetite, which overprints dolomite (Fig. 16f) or magnetite + stilpnomelane + chlorite in late fractures that cut across all phases. Peloidal carbonate also exhibits alteration, which consists of microcrystalline silica, chlorite and stilpnomelane, with a late overprint by euhedral magnetite (Fig. 16e, f).

Carbonate porphyroblasts and dolomitisation are also associated with the sulfide mineralization in the Sweetwaters Well Member stromatolitic dolomite (Yelma Formation), as discussed in more detail in *Mineral systems*.

Stilpnomelane, a complex K, Ca, Na, Fe, Mg, Al hydrous silicate, is common in iron-formation world-wide and is generally found in Fe and Mn-rich low-grade regionally metamorphosed sedimentary rocks (Deer et al., 1965). Stilpnomelane-rich beds have been reported from the banded iron-formation of the Transvaal Supergroup in South Africa (LaBerge, 1966a; Beukes and Klein, 1990) and the Hamersley province in Western Australia (LaBerge, 1966b; Trendall, 2002). Here, the stilpnomelane beds have been interpreted as products of low-grade metamorphism of volcanic ash (LaBerge, 1966a, b; Beukes and Klein, 1990). The stilpnomelane, silica and carbonate replacement of beds of granular iron-formation rocks in the Earaheedy Basin is interpreted to be related to K-Si-Ca-CO_2-rich basinal fluids (see *Mineral systems*). Stilpnomelane preferentially replaces Fe-chlorite-rich siltstone interbeds and a possible reaction to explain the change from Fe-rich chlorite-dominated siltstone beds to stilpnomelane-dominated beds is (Deer et al., 1965) :

Fe-rich chlorite (GIF) + SiO_2 + K_2O → stilpnomelane +MgO + Al_2O_3

4.2.2.3 Facies analysis

Price (2003) recognised 8 facies in the Frere Formation, determined on the basis of sedimentary structures, grain size, composition, matrix/cementing material. Details are given in Table 3.

4.2.2.4 Rare earth elements (REE) geochemistry

As part of his thesis work, Price (2003) also conducted a comparative study of the abundance of REE in the granular iron formation with those of two other Precambrian iron formations, Gunflint in Canada and Griquatown in South Africa. The following is summarised from Price's thesis.

The Gunflint iron formation in Ontario is also a granular iron formation, composed of peloids and ooides in a predominantly quartz cement. Whole rock Sm-Nd isochron dating indicates that the Gunflint iron formation was deposited at around 1900 Ma (Jacobsen and Pimentel-Klose, 1988). The geochemical dataset used in this

work was taken from Derry and Jacobsen (1990). The Griquatown iron formation of the Transvaal basin in South Africa is a granular iron formation that ovelies the Kuruman microbanded iron formation (Beukes and Klein, 1990). The Griquatown iron formation consists of chert-rich peloids and intraclasts in a chert cement (Beukes and Klein, 1990). Radiometric ages indicate that the Kuruman and Griquatown iron formations were deposited between 2357±53 and 2239±90 Ma (Walraven et al., 1990). The geochemical dataset of the Griquatown iron formation was taken from Beukes and Klein (1990). REE patterns for the Gunflint and Griquatown iron formation are shown in Fig. 17.

The distribution of samples of peloidal granular iron formation collected during field mapping by GSWA geologists is shown in Fig. 18A.. In addition to REE , these samples were also analysed for major and trace elements by Genalysis Laboratory Services (Perth) using ICP-MS and results are presented in Table 1 in Appendix 2. Eleven samples were selected for the study of REE abundances, all containing in excess of 15 wt % Fe_2O_3; the data were normalised to NASC (North American Shale Composite; Gromet et al., 1984) and the diagram shown in Fig. 18B. The REE patterns show a slight HREE depletion relative to LREE, with the exception of 3 samples. Some samples show a marked negative Ce anomaly, and all samples exhibit a weak positive Eu anomaly. By comparison with the Gunflint and Griquatown iron formation, the Frere Formation contains higher REE concentrations. The positive Eu and negative Ce anomalies in the Gunflint and Griquatown possibly represent high temperature hydrothermal input in a seawater dominated system (Beukes and Klein, 1990; Bau and Moller, 1993; Klein and Ladeira, 2000). The similar REE patterns for the Gunflint and Griquatown iron formation suggests a similar depositional mechanism. The differences of the Frere Formation REE patterns may be due to one or more of the following: 1) contamination in the Frere rocks by clastics; this is supported by the high abundances of TiO_2 and Al_2O_3 (see Appendix). 2) The Frere rocks were probably deposited in shallower water than the Gunflint or the Griquatown iron formations; this is shown by differences in HREE patterns and the Ce anomalies.

4.2.2.5 Windidda Member

Bunting (1986) considered the Windidda Formation to overlie the Frere Formation, but subsequent to mapping of both Nabberu and Granite Peak showed that

the former Windidda Formation is stratigraphically equivalent to the upper part of the Frere and for this reason it is now considered a Member of the Frere Formation. The Windidda Member is typically characterized by poorly defined low relief outcrops and consists of stromatolitic carbonate, shale and siltstone, minor jasperoidal beds and minor granular iron-formation. The shale and siltstone are very similar to shale and siltstone of the Frere Formation. Locally, peloidal jasper is interstitial to stromatolites and thin granular iron beds are interbedded with stromatolitic carbonate. The Karri Karri Member was mapped on Nabberu as part of the Windidda Formation, but during later work was re-interpreted as part of the Chiall Formation. The contact of the Windidda Mamber with the overlying Chiall Formation is defined as the upper carbonate horizon (Hall et al., 1977). The lower contact with the Frere Formation is defined as the first occurrence of carbonate or the last occurrence of iron formation, chert or jasper. The thickness of the Windidda Formation varies laterally. Bunting (1986) estimated the thickness of the type area to be about 800 m. We revised the thicknesss of the Windidda Member to be between 60 m and 150 m, but could be as much as 500 m on Windidda. In places, the proportion of granular jasper is high, forming granular iron-formation beds. On Wongawol, the cores of concentrically zoned larger granules occasionally consist of a yellow-green iron silicate mineral, possibly glauconite or chamosite, which is partially replaced by hematite, suggesting iron-oxides in this sample may be secondary.

Stromatolite forms in the Windidda Member range up to 30 cm in diameter and include *Carnegia wongawolensis, Nabberubia toolooensis, Windidda granulosa and Kulparia* (Grey, 1984). *Carnegia wongawolensis,* is the dominant form recognized on WONGAWOL and forms colonies of branching forms. Locally, peloidal jasper is interstitial to stromatolites and is incorporated within stromatolite laminae. *Windidda granulosa* and the associated abundant ooids in the Windidda Member, are suggestive of sandy shoals and a more agitated environment. The palaeoecological significance of the Sweetwaters Well stromatolites is treated in detail by Grey (1994).

Shale and siltstone dominated units contain laminated to massive carbonate beds of variable thickness that are generally < 1 cm. Jasper beds, which are up to 10 cm in thickness, are interbedded with carbonate in carbonate dominated units. In addition, granular or peloidal jasper locally forms a matrix to stromatolites. Intraclastic

carbonate breccias are common in the Windidda Member, becoming more abundant towards the upper part of the formation. Locally, carbonate conglomerate is exposed at the top of the Windidda Member and is commonly transitional to a siliciclastic conglomerate at the base of the Chiall Formation. Clasts are generally well-rounded, up to 15 cm in length, occasionally imbricate and are dominantly carbonate or siltstone. Rare small stromatolites are contained in this horizon. Clasts are cemented by carbonate and contain a glauconite and quartz sandstone matrix.

Inliers of stromatolitic carbonate, surrounded by Chiall Formation, about 7.5 km southwest of Wadjinyanda Pool (Wongawol), are considered part of the Windidda Formation because of the similarity in stromatolite forms. The carbonate is interpreted to have been uplifted along a north-south trending reactivated Archaean structure. Stromatolites in this area are typically elongate with their long axis up to 30 cm, suggesting current action.

The Windidda Formation is interpreted to reflect a carbonate bank and lagoonal environment that developed synchronous with deposition of granular iron-formation. Minor jasper granules washed into the carbonate bank and lagoonal environment and intraclastic breccias probably reflect storm events.

4.2.3 Depositional environment of the Tooloo Subgroup and the origin of the iron formations

The Earaheedy Basin has a special importance in the tectonostratigraphic record of Palaeoproterozoic terranes because of the presence in the basin stratigraphy of the GIF units of the Frere Formation. The presence of the Frere Formation GIF could be related to a period of mantle plume(s) breakout, which resulted in global magmatism at ca 1.8 Ga, supercontinent breakup, trailing margins and deposition of iron-formations (cf. Barley et al., 2005). In addition, oxygenic photosynthesis associated with the GIF may have contributed to the rise of oxygen levels in the Earth's atmosphere. Granular iron-formation formed in shallow marine continental shelf to coastal conditions. Ferruginous peloids accreted in wave- and current-agitated iron-rich waters (Beukes and Klein, 1992), and were deposited after some reworking by mechanical processes, with variable terrigenous contamination. The deposition of granular iron-formation in the Earaheedy Basin coincides with a decrease in the supply of sand-sized siliciclastic detritus into the basin. Granular iron-formation beds

probably formed in shallow waters on a continental shelf. According to Beukes and Klein (1992), ferruginous peloids form by accretion in wave- and current-agitated iron-rich waters and following reworking are deposited with variable amounts of terrigenous contamination. In modern clastic-starved marine shelves, amorphous Fe oxide and/or oxyhydroxide peloids (or ooids) appear to form as concretions a few centimetres below the sea floor, as a result of Fe and silica exhalative fluids that rise from the substrate (Heikoop et al., 1996; Donaldson et al., 1999). An alternative view is that the ooids grow from the precipitation of Fe-rich clays that become oxidised to goethite at the sediment-water interface (Donaldson et al., 1999). In either case the Fe oxide/oxyhydroxides alternate with silica to form the concentric laminae. The reason for the Fe oxide-silica alternations are not understood, but it may relate to pulses of fluid emission based on episodic temperature variations (high T, Fe precipitation; lower T silica precipitation). Dehydration and diagenesis would produce hematite and at higher temperatures magnetite and the formation of these ooidal or peloidal structures would occur in a geologically short time. Mechanical reworking by wave action and/or strong currents would account for the classic shape of the ooids (Heikoop et al., 1996).

Cross-bedding, locally recognized in granular iron-formation beds, indicates dominantly moderate-energy conditions. Local, peloidal carbonate beds that are intercalated with beds of iron-formation do not show evidence of current transport and may represent a particulate sediment that accumulated *in-situ* (Blatt et al., 1980, p. 469). However, the intercalated shale and siltstone horizons show tractional structures, from GRANITE PEAK southwards.

The granular iron beds, shale, and siltstone all have different iron and silica content both within and between units. This points to a complex, varying interrelationship between clastic influx, dissolved silica and dissolved iron. The supply of dissolved silica appears to have been variable at all scales, and can be interpreted as a result of fluctuating concentrations. The supply of iron is also interpreted as the result of fluctuating concentrations but with a high proportion of iron remaining in suspension throughout deposition of the Frere Formation. The shale interbedded with granular iron-formation and in major shale horizons may indicate periods where the rates of silica and iron precipitation were low.

Both iron-rich and silica-rich fluids are interpreted to have a distal source. The supply of iron and silica is ultimately related to distal hydrothermal effluents such as a mid-ocean ridge and/or other subaqueous hot springs (e. g. Isley, 1995; Trendall, 2002). Upwelling currents would transport Fe^{2+} and Mn^{2+} away from the discharge vents and precipitation would occur just above the oxic-anoxic interface, where Fe^{2+} and Mn^{2+} are oxidised to Fe^{3+} and Mn^{4+}, respectively (Pirajno and Adamides, 2000). A depositional and tectonic model for the Yelma and Frere Formations (Tooloo Subgroup), based on the stratigraphic, sedimentological and genetic attributes of the granular iron-formation (Trendall, 2002; Isley, 1995; Beukes and Klein, 1992) is shown in Figure 19.

Detailed studies on field and textural features of granular iron-formation in the Earaheedy Group (Hall and Goode, 1978; Goode et al., 1983; Bunting, 1986) clearly show similarities with the iron-formations of the Superior Province of North America (e.g. Kimberley, 1989). Peloidal and oncolytic textures, orthochemical and alchemical cements, iron-rich chlorite, the presence of mineral phases, such as minnesotaite and stilpnomelane, are common in both. These characteristic features have been interpreted as the result of chemical deposition, followed by mechanical reworking of the sediment, whilst still plastic (gel state) (Beukes and Klein, 1990, 1992). The model for the origin of the iron-formation proposed by Beukes and Klein (1990; 1992) and Isley (1995) accounts for the large volumes of iron, but it does not explain the association of iron and silica in grains of possible biogenic origin. Some of the grains classified as peloids (Fig. 13D), may have been originally oncolites (Fig. 14A-F; and Brown et al., 1995). If this is correct, then it is possible that biogenic activity may have played a major role in the development of the granular iron-formation, through a mechanism of bacterial iron oxidation (Nealson, 1982; Brown et al., 1995). Other models of BIF deposition (Kappler et al., 2005; Konhauser et al., 2002) propose a mechanism for the oxidation of hydrothermal Fe(II) to Fe(III) by anoxygenic photosynthetic bacteria. A possible bacteria-mediated reaction is:

$$4Fe_2 + CO_2 + 11H_2O + \text{light energy} \rightarrow CH_2O + 4Fe(OH)_3\ 8H^+$$

The depositional setting of the Tooloo Subgroup is illustrated in Figure 20 (Price, 2003).

4.2.4 Chiall Formation

The Chiall Formation combines, as members, the former Wandiwarra Formation and Princess Ranges Quartzite, as well as the Karri Karri Member. SHRIMP U-Pb dating of detrital zircons from the Chiall Formation reveal a maximum depositional age of ca 1.8 Ga (Halilovic et al., 2004). The Chiall Formation consists of shale, siltstone and mudstone intercalated with thick sandstone beds and intraclastic breccia. The formation represents a change from combined chemical and fine-grained clastic sedimentation, to coarser-grained clastic deposition. The base of the formation in the south is a breccia of poorly sorted, angular carbonate clasts in a ferruginized and glauconitic sandstone matrix, which led Bunting (1986) to interpret the boundary as a disconformity. The brecciated features of this horizon suggest that it may have formed through a process of liquefaction and therefore may be a seismite or a tsunamite, as defined by Einsele (2000) and described by Pratt (2002). To the north, the lower part of the Chiall Formation consists of a thick succession of shale, siltstone and mudstone, which has been assigned to the Karri Karri Member. Sandstone overlying the Karri Karri Member was probably deposited below fair-weather wave base, based on graded bedding, mass flow deposits and the lack of cross-bedding attributable to widespread current or wave action.

The thickness of the Chiall Formation was considered by Bunting (1986) to be up to 1500m. We suggest that there has been more structural repetition than was estimated by Bunting (1986), and that the maximum thickness of the formation may only be 1000m. The contact between the Chiall Formation and the underlying Frere Formation is transitional and taken as the top of the last major chert bed or iron-formation. Where the Chiall Formation overlies the Windidda Formation, the contact is taken as the top of the last carbonate bed. The Chiall Formation (Hocking and Jones, 1999; Hocking et al., 2000a,b) consists predominantly of very fine grained sandstone, siltstone, shale and mudstone punctuated by fine- to medium-grained sandstone beds and minor conglomerate. The Wandiwarra and Princess Ranges Members which, as mentioned above, were previously considered formations (Hall et al., 1977; Bunting, 1986) were relegated to member status within a single formation after the recognition that they are part of a single depositional package**.**

The base of the Chiall Formation is transitional and laterally variable. In the central part of Wongawol, the base of the Chiall Formation consists of very fine to fine-grained sandstone, siltstone, shale, and mudstone. Further east, conglomerate is interbedded with this facies at the base of the Chiall Formation, with the proportion of conglomerate increasing eastward.

Conglomerate at the base of the Chiall Formation is texturally variable, consisting of poorly-sorted boulder conglomerate and pebble conglomerate. Clasts are locally imbricate and clast type is variable and commonly reflects the underlying lithologies, suggesting a strong local source control. Fine-grained sandstone, siltstone, and carbonate are the dominant clast types with the proportion varying both vertically and along strike. Poorly sorted boulder conglomerate is generally laterally restricted and is weakly bedded. Clasts vary from subrounded to angular, but are typically angular. On Wongawol a poorly sorted, boulder conglomerate is up to 4 m thick and consists of angular clasts of dominantly carbonate and minor sandstone, in a coarse-grained sandstone matrix containing glauconite peloids and cemented by a ferruginous clay. Pebble conglomerate beds, which are interbedded with siltstone, mudstone and glauconitic very fine and fine-grained sandstone at the base of the Chiall Formation, are typically less than 50 cm thick.

Bunting (1986) suggested that conglomerate at the base of the Chiall Formation may represent a disconformity between the Tooloo and Miningarra Subgroups. However, there is little evidence to support a significant break in sedimentation between the two subgroups. The contact between conglomerate of the Chiall Formation and the Windidda Formation is transitional, except for localized exposures of cobble conglomerate, and reflects a change from carbonate-cemented conglomerate to conglomerate with a sandstone matrix. It is also important to recognize that basal conglomerate in the Chiall Formation is relatively restricted both laterally and vertically, and mostly overlies carbonate of the Windidda Formation.

Interbedded siltstone, mudstone, shale and fine to very fine-grained sandstone, which is locally calcareous typifies the lower part of the Chiall Formation below the Princess Ranges Member and is similar to the lower part of the Wongawol Formation. Sandstone contains green iron silicate minerals, especially near the base of the Chiall

Formation. These green iron silicate grains are mostly glauconite, but other iron-bearing species such as berthierine and chamosite are probably also present. In addition, jasper peloids are also common at the base of the Chiall Formation in fine and very fine-grained sandstone. Green iron silicate grains are commonly peloidal and oolitic. Locally, the green iron silicate grains are are flattened and deformed in particular beds, indicating they must have been soft and plastic during compaction. The proportion of green iron silicate minerals in these beds is generally high.

Sedimentary structures at the base of the Chiall Formation include parallel lamination, load casts, and minor cross-lamination. These are overlain by symmetrical and asymmetrical ripples, rills, wrinkle marks, and contorted bedding, which are overall more common sedimentary structures in the lower Chiall Formation.

Fine- to medium-grained sandstone-dominated units in the Chiall Formation form prominent topographic ridges in the central areas of the Basin. Textural and compositional maturity increases stratigraphically in fine- to medium-grained sandstone. Sandstone beds predominantly comprise subrounded to rounded quartz, minor chert, feldspar and glauconite, and accessory zircon and tourmaline. Glauconite is generally concentrated at the base of fine- to medium-grained sandstone-dominated units, suggesting it was reworked from underlying shale, siltstone and very fine grained sandstone facies where glauconite abundances are high. In units mapped as fine to medium-grained glauconitic sandstone, the proportion of glauconite is generally much higher than in other fine to medium grained sandstone units in the Chiall Formation.

4.2.4.1 Karri Karri Member

The lower Karri Karri Member consists dominantly of shale and siltstone, with thin interbedded sandstone beds in the upper part of the member. The member is interpreted as having a maximum thickness of 600m in the north of the Basin (e. g. on Methwin). The lower contact is defined as the top of the last major chert or iron-formation. The upper contact with the Wandiwarra Member is transitional with thin interbedded sandstone beds becoming more common in the upper part of the Karri Karri Member. The contact is taken at the first occurrence of a thick sandstone. In the Stanley Fold Belt, exposures of the member are generally folded, cleaved and cut by small quartz veins.

Lithologically, shale and siltstone resemble similar lithologies to the underlying Frere and Yelma Formations, but generally contain a high proportion of coarse grained siltstone. Without other stratigraphic control, the shales may be indistinguishable. They are typically delicately parallel laminated with individual lamellae between 1 to 10 mm. Individual sandstone beds in the upper part of the member are typically 5 to 20 cm thick, and fine to medium grained.

The delicate, continuous lamination in the Karri Karri Member is indicative of quiet-water deposition probably below fair-weather wavebase, subsequent to a transgression at the top of the Frere Formation. Sandstone beds are interpreted as mass-flow deposits rather than turbidite deposits because of the intraclastic mudstone clasts and traction structures. The iron-rich nature of the rocks indicates that iron remained in suspension even after deposition of the last granular iron-formation and the silica and iron supply to the basin had ceased.

4.2.4.2 Wandiwarra Member

The Wandiwarra Member consists dominantly of siltstone and shale, with scattered intercalations of sandstone. Siltstone and shale intervals are generally well exposed on breakaways. Sandstone intervals form resistant cappings on hills. Shale intervals are generally parallel laminated with minor cross lamination. Laminations are typically 0.5 to 5 cm thick. Interbedded sandstone beds range from 5 cm to, less commonly, about 1 m thick. Sandstone dominated intervals consist of sandstone beds with subordinate interbedded siltstone, generally as thin beds. Sandstone beds are generally quartz wackes that consist dominantly of rounded to subrounded quartz, with minor chert, feldspar, mica, glauconite and tourmaline, and become more mature in the upper part of the member. Bed thickness varies from about 5 cm up to 1.5 m but are typically 10 to 20 cm in thickness. Bedsets generally range between 20 cm to 1 m in thickness. Sedimentary structures include cross-bedding, asymmetric ripples and hummocky cross-stratification in the lower part of the member. Current lineations, cross bedding, and ripples indicate a dominant palaeocurrent flow direction towards the north.

Sandstone intervals consist of fine- to medium-grained sandstone, which is locally conglomeratic, and interbedded with siltstone, mudstone and shale. Sandstone is poorly to moderately sorted and consists dominantly of rounded to subrounded

quartz grains and minor chert fragments. Mudchip intraclasts are common, especially at the base of individual beds. Sedimentary structures in the sandstone include tabular and trough cross-bedding, flute clasts and current lineation. Quartz grains are occasionally coated by hematite granules (Fig. 21a); in other instances Fe oxides tend to replace both quartz and interstitial matrix and can be an important component at some stratigraphic levels (Fig. 21b). Glauconite peloids vary from spherical to elliptical, with an average size of 0.22 mm. Locally, glauconite is oxidised to brown-coloured Fe oxides. It varies from colourless to light-green or brown when weathered, or blue-green when fresh and is locally replaced by a mosaic of quartz grains, which are not in crystallographic continuity with the surrounding authigenic silica.

North of the Shoemaker impact structure (see *Structure*), rocks of the Wandiwarra Member outcrop in a series of breakaways along the northern edge of the Lake Nabberu system (Fig. 22). Here, the rocks are gently dipping and deformed into mesoscale folds with east-trending doubly-plunging fold axes and with local reverse faults (Figs. 22, 23). Spectacular megaripples in sandstone beds can be seen 6.5 km southeast of Bitter Pool, on outcrops of the outer collar of the Shoemaker impact structure (Fig. 24). Three km southwest of Kennedy Bore, brecciated beds of glauconitic sandstone are exposed, which may represent ancient tsunami or seismic shock deposits (Fig. 25a, b).

4.2.4.3 Princess Range Member

The Princess Ranges Member generally comprises shale, siltstone, mudstone units interbedded with very fine-grained sandstone and siltstone dominated units and mature quartz arenite. On Granite Peak, mature quartz arenite dominated horizons are mostly interpreted to be stratigraphically equivalent to the Princess Ranges Member. Sedimentary structures within the sandstone include symmetrical sharp crested low amplitude ripples, current lineation, mega ripples, rills, shrinkage moulds, trough and planar cross-bedding and cross-lamination. Symmetrical ripples are mostly straight-crested, while asymmetric ripples vary from straight-crested to linguoid (Fig. 26).

The sedimentary structures mentioned above, in both the shale and sandstone intervals, suggest that the Wandiwarra Member and stratigraphically equivalent lower

Chiall formation were mostly deposited below wavebase and that shallowing occurred up the stratigraphic sequence. The Princess Ranges Member and stratigraphically equivalent mature quartz arenite in the upper part of the Chiall Formation on GRANITE PEAK were deposited in an upper shoreface environment. Sandstone beds are probably tempestites (storm related) and/or seismites (related to earthquakes; Rodriguez-Pascua et al., 2000). Conglomeratic beds may be related to tsunamis.

Fine- to medium-grained sandstone is typically texturally mature, consisting of well-rounded and well-sorted quartz grains and accessory tourmaline and zircon. Mudchip intraclasts and glauconite peloids are commonly concentrated at the base of fine to medium-grained sandstone dominated units, suggesting high-energy erosional bases. Coarse-grained siltstone and very fine-grained sandstone is comprised dominantly of angular to subrounded quartz, and subordinate glauconite and detrital mica. Locally, the base of the Princess Ranges Member contains coarse-grained sandstone containing pebble-sized subangular to subrounded clasts of vein quartz and sandstone.

4.2.5 Wongawol Formation

The Wongawol Formation (Hall et al., 1977; Bunting, 1986) is a monotonous succession of shale, mudstone, siltstone, very fine-grained feldspathic sandstone, and minor conglomerate. The lower contact with the Chiall Formation is placed at the top of the uppermost mature sandstone. The upper contact with the Kulele Limestone is locally not exposed, but is transitional and placed where limestone becomes the dominant lithology (Bunting, 1986). Sandstone in the Wongawol Formation is dominantly very fine grained, commonly silicified, and locally glauconitic. Locally, sandstone contains mudchip and well-rounded siltstone intraclasts, with in-situ brecciation of thin siltstone beds.

Sedimentary structures include swash marks, ripple washouts, wrinkle marks, ball-and-pillow structures at sandstone–siltstone interfaces, primary current lineation, and symmetrical and interference ripples. Symmetrical ripples typically have peaked crests and are straight-crested, with wavelengths of 8–10 cm and amplitudes around 2-3 cm. Weakly developed ladder ripples are locally present in the troughs of some symmetrical ripples.

Exposure of conglomerate is localized and clasts are typically well-rounded, matrix-supported, pebble-sized, and composed of carbonate and volcaniclastic fragments. Carbonate clasts may be intraclastic because carbonate beds increase in abundance higher in the Wongawol Formation. The volcaniclastic clasts contain vitriclastic textures. These clasts may represent reworking of thin volcaniclastic beds, which have not been preserved, or they may be allochthonous. The matrix consists of poorly sorted, angular to subangular clasts of quartz, feldspar, and biotite, which are dominantly silt to very fine-grained sand sized in a micritic cement.

Kulele Limestone

The Kulele Limestone is a cyclic platform succession (up to 300 m thick), consisting of carbonate units, which are separated by shale and sandstone. Carbonate units are stromatolitic, oolitic, and pisolitic. Large individual stromatolite domes are up to 3.5 m high and 4 m wide and may include minor columns. Compared to the Wongawol Formation, the Kulele Limestone records a slight deepening of the basin and decrease in terrigenous influx. Metre-scale shallowing-upward cycles are present through most of the unit, and record regular minor fluctuations in sea-level in a shallow subtidal setting.

The Kulele Limestone comprises a package of calcarenite, stromatolitic limestone, intraclastic carbonate breccia, oolitic and pisolitic limestone, shale and sandstone. The Formation is approximately 300 m thick and is essentially confined to the central-eastern part of the Basin, except for a small outlier, near Thurraguddy Bore, where some spectacular large stromatolite forms are present. The carbonate (mostly limestone, lesser dolomite) rocks represent the main rock type and they form cyclic sequences separated by clastic units. Each cycle is from 1 to 10 m thick, with the intervening clastic layers up to 50 m thick (Bunting, 1986). The limestone units are thickly bedded and laminated, with the laminae on scales of 1 to 5 mm. Stromatolites range from small domes a few cm across to large domes, 2 m high and 3 m across, which coalesce to bioherms up to 30 m long (Bunting, 1986). These stromatolite domes can be asymmetric and elongated, and this is especially evident in the Thurraguddy outlier on Lee Steere, as described in detail by Bunting (1986), from whose work the following is summarised. At Thurraguddy Bore the basal 25 m of Kulele Limestone is exposed and can be divided into seven cyclic pairs of limestone-

shale, each from 2.5 to 7.5 m thick. Each cycle represents a transgressive (limestone)-regressive (shale) event. Stromatolies in the Thurraguddy Bore outlier form two bands. Band 1 has low domes, up to 100 mm, circular to elongate with length:breadth ratios of about 3:1. Band 2 contains domes up to 2 m high with individual domes reaching 3 m across, forming bioherms 30 m long and 10 m wide. Stromatolite forms in the Kulele Limestone include *Haraheedia kuleliensis* Grey 1984. The large bulbous stromatolites remain unnamed. The elongation of the stromatolite domes is attributed to wave currents perpendicular to the shore (e.g. Playford and Cockbain, 1976), as can be seen in modern day stromatolites at Shark Bay, in Western Australia.

Oolitic and pisolitic limestone shows two types of allochems. In one, large pisoliths are elongate with an intraclastic core, surrounded by concentric laminae up to several mm thick. The second type is smaller with both radial and concentric laminae. These features may indicate a two-stage origin, whereby ooliths were formed in quiet water at first, then transported into a more agitated environment (Bunting, 1986). Locally there are breccia layers, characterised by tabular intraclasts up to 200 mm long, forming beds at the base f the limestone cycles. Calcarenites are fine-to medium-grained rocks composed of granular calcite with minor detrital quartz. Locally, some glauconite may be also present. Shales are typically purple, maroon or grey-greenish in colour and contain white mica and chlorite. Sandstone interbedded with the shaly rocks, contains feldspar, quartz with a calcareous cement and with muscovite and chlorite imparting this rock a degree of fissility. In the upper part of the Formation, sandstone is coarser and contains glauconite at the expense of the feldspar, which becomes a minor component.

4.2.6 Mulgarra Sandstone

The Mulgarra Sandstone consists of sandstone, locally glauconitic, shale and minor carbonate, with a maximum thickness of at least 100 m. The deposited top is not preserved. The unit is very similar to the Wongawol Formation. The youngest zircons from the Mulgarra Sandstone (top of Earaheedy Group) yielded U-Pb SHRIMP ages of ca 1.85 Ga (Halilovic et al., 2004). The main scarp of the Timperley Range exposes the basal 20 m of the Formation, and consist of medium-grained quartz arenite, locally ferruginous, and bedded on a 100-200 mm scale. This unit is composed of quartz (ca. 90%) with feldspar and glauconite making up the rest.

Sedimentary structures include flute and load casts, current lineation, current ripples and ball and pillow structures. The basal contact with the underlying Kulele Limestone is sharp and marked by 1-2 m of shale. Locally, the clastic nature of the Formation changes with the intercalations of thin limestone beds, forming a mixed unit up to 40 m thick.

4.2.7 Depositional environment of the Miningarra Subgroup

The Earaheedy Basin deepened northwards during deposition of the Miningarra and Tooloo Subgroups. In the south symmetric and asymmetric ripples, interference ripples, megaripples, rills, and trough cross-beds indicate a shallow-water upper shoreface to foreshore, intermittently emergent, setting. To the north, fine-grained rocks, parallel bedding, and hummocky cross-bedding suggest a dominantly storm-swept sub-wave base marine shelf. Limited palaeocurrent data support this model. The Chiall Formation records a change from iron oxide and chert to iron silicate grains. The presence of iron silicate minerals, such as glauconite, berthierine and chamosite, indicate dominantly low sedimentation rates for the finer grained facies of the lower Chiall Formation. Sedimentary structures suggest that the lower Chiall Formation was deposited in a shallow marine environment with deposition from below fairweather wave-base grading up into a shallow water possibly nearshore deposits. The conglomerate at the base of the Chiall Formation represents reworking of the underlying lithologies and localized channel fill. Sedimentary structures in both the shale and sandstone intervals of the Wandiwarra Member indicate that it was deposited dominantly below fairweather wavebase, but shallowed up in the upper part of the member. Sandstone beds are probably tempestites (storm related) and seismites (related to earthquakes; Rodriguez-Pascua et al., 2000). Sedimentary structures in the Princes Ranges Member suggest that it was deposited in a shallow-water marine to locally emergent environment, which was affected by both wave and current action. These features together with the compositional and textural maturity of coarser sandstone, which indicates a higher energy depositional environment in the Princess Ranges Member, suggest deposition in a tidal sand flat environment.

The Wongawol Formation is similar to the shale, mudstone, siltstone, and very fine-grained sandstone facies in the Chiall Formation. Sedimentary structures suggest deposition was in shallow water to locally emergent environment and is interpreted to

be a similar environment to the tidal sand flat proposed for the Princess Ranges Member. The depositional environment of the Mulgarra Sandstone is shallow marine and is probably a regressive sandstone phase of the Kulele Limestone (Bunting, 1986).

5. Stanley Fold Belt

The exposed Earaheedy Basin is deformed into a regional east to east-southeasterly trending, south-verging, asymmetric syncline, which plunges gently towards the southeast. The northern limb is steeply dipping to locally overturned, and forms the Stanley Fold Belt, a 110°- trending structural domain, which is about 200 km long and up to 35 km wide, and which is characterized by strike-slip faulting, foliation fabrics, tight folding, and reverse faulting. Folding varies in scale, with fold limbs commonly truncated by faults. Faults trend easterly, and include both dip-slip (dipping north), and sinistral strike-slip components. Major structures within the Stanley Fold Belt generally trend east or northwest and are positively magnetized. Sedimentary rocks of the Earaheedy Group are generally weakly metamorphosed, only locally attaining lower greenschist facies. Typical metamorphic minerals in fine-grained rocks are sericite, and chlorite.

Deformed rocks of the fold belt are exposed in the Muir Range (northeast corner of Granite Peak). The degree of deformation in the Stanley Fold Belt decreases southward resulting in open, generally gentle folds, locally with an associated axial-plane cleavage. These features are expressed on aeromagnetic images as a series of broad, low-amplitude, east-trending ridges and swales. Doubly-plunging mesoscale folds with wavelengths of 10-20 m (Fig. 23) are well displayed along the breakaways north of Lake Edith Withnell and Lake Karri Karri. Breccias and quartz vein stockworks are commonly associated with the folded rocks. In the transition zone between the Stanley Fold Belt and folded southern margin of the Earaheedy Basin, small-scale disharmonic folding and normal faulting is common .

5.1 Folds, faults and E-W structures

North trending structures are probably reactivated basement structures and their orientation is similar to D_3 structures of the Yilgarn Craton, which formed during sinistral transpression (e.g. Wyche and Farrell, 2000; Swager, 1997). A major north-

south trending structure on WONGAWOL may be a continuation of a major north to north-northeast trending structure on the eastern margin of the Duketon greenstone belt. The age of east trending structures is not well constrained (Groenewald et al., 2001). They postdate D_3 structures in the Yilgarn Craton and are thought to be Palaeoproterozoic in age, because an age of 2420 Ma was obtained from some east trending dykes (Nemchin and Pidgeon, 1998). In the northeastern Yilgarn Craton the age of east trending structures is poorly constrained, and it is unclear whether they represent reactivated basement structures or developed during a deformation event after deposition of the Earaheedy Group. Movement on the east trending structures is interpreted to have been dominated by vertical displacement. Manganese is commonly associated with north trending structures and quartz fracturing and silicification is present along east trending structures.

Northwest trending negatively magnetized structures are interpreted postdate deposition of the Earaheedy Group. The aeromagnetic signature is consistent with shallow-level, low-angle structures dipping to the northeast. The northwest trending structures are unlikely to represent features of the Yilgarn Craton because they are not parallel to other structures in the northeast Yilgarn Craton. Instead, these structures appear to be mostly bedding parallel with the Earaheedy Group, but are not the magnetic response of layering in the Frere Formation. The features do not correspond to individual granular iron-formation horizons nor do they correspond to any iron-rich layer. Given the intense but continuous nature of these northwest trending features it seems likely they are the product of bedding parallel fluid flow. On GRANITE PEAK (Pirajno et al., 2003) and MERRIE (Adamides, 2000) they coincide with silicification of granular iron-formation in the Frere Formation and the presence of stilpnomelane in shale and siltstone beds. Aeromagnetic images indicate that movement along east and north structures offset, and therefore postdate, northwest structures. The relative timing relationships between the east-west and north-south structures show ambiguous overprinting relationships. In addition, magnetization along north structures is discontinuous and may reflect localized movement during more than one event.

Folds generally vary from open, upright, gently plunging to localized recumbent folding with the degree and style of folding typically strongly dependant on lithology.

Mesoscale folds in fine to coarse-grained sandstone intervals, typically form doubly plunging, elongate anticlinal features. In siltstone to very fine-grained sandstone dominated intervals, mesoscale folds vary from doubly plunging folds to localized disharmonic folding. Sporadic, northeast trending anticlines, which vary in scale from tens of metres up to approximately 1 km scale, are common in fine to coarse-grained sandstone dominated intervals such as the Princess Ranges Member. Deformation associated with these features is more intense than surrounding areas suggesting they may represent localized space accommodation zones.

The structural history suggests that at least two major deformation events are recorded in the Earaheedy Group. The first major deformation event resulted in low-angle mostly bedding-parallel movement, which produced northwest trending structures at various scales. A later, predominantly north-south compression resulted in vertical displacement along east-west trending structures. The orientation of the northwest trending structures and the lack of evidence for major displacement or strike-slip movement suggests that the deformation event associated with these structures was due to southwest directed compression. The timing of both of these events is not well constrained. Pb-Pb ages on Pb-Zn mineralization in the Sweetwaters Well Member (Richards and Gee, 1985) and Rb-Sr and K-Ar ages on glauconite (Horwitz, 1975a, b; Preiss et al., 1975), which have probably been reset, suggest a thermal event about c. 1650 Ma. This age coincides with some of the granitoid ages in the Gascoyne Complex and the 1680-1620 Ma Mangaroon Orogeny (Nelson 2002; Sheppard et al. 2007).

5.2 Quartz veins

Quartz stockwork veining is developed in granular chert in the Frere Formation (Jones and Pirajno, 2003), where it is cut by major east trending structures. Intense quartz stockwork veining is developed at the intersection of east trending structures with other major structures, such as the Proterozoic northwest oriented structures and the reactivated north-south oriented structures.

Centimetre-thick veins of syntaxial fibrous quartz are common in the sandstone units of the Chiall Formation. The orientation of the veins and the syntaxial quartz fibres enables the gauging of the stress field at the time that the veins were emplaced.

On Nabberu and Granite Peak, two sets of quartz veins are present, in which the fibres are oriented 355° (σ_3; least compressive stress), in the older vein set (strike 270°) and 150° (σ_3) in the younger set (vein strike 060°). This implies that the veins may have formed as a result of northeast-southwest directed compression. This compression event is interpreted to reflect tectonic movements associated with the Yapungku Orogeny (Bagas and Smithies, 1998; Smithies and Bagas, 1997; Bagas, 2004), which may have contrbuted to the formation of the Stanley Fold Belt. Ar-Ar dating of micas in the Stanley Fold Belt (see Geochronology) yielded ages of ca. 1650 Ma, suggesting that further deformation may relate to the Mangaroon Orogeny (Sheppard et al., 2005).

6. Shoemaker meteorite impact structure

The Shoemaker impact structure has an outer diameter of about 30 km (Fig. 3B) and consists of two well-defined concentric ring synclinal and anticlinal structures, formed in rocks of the Chiall and Frere formations, surrounding Archaean basement rocks (Teague granite and greenstone rocks; Pirajno and Glikson, 1998). The concentric rings form low hills that interrupt the continuity of the west-northwest-trending Frere Range The structure is discussed in detail by Pirajno (2002) and Pirajno et al. (2003) and only a brief review is given here.

Evidence for an impact origin of the Shoemaker impact structure include:

1. a well-defined circular structure with surrounding rings of synclinal and anticlinal structures, which enclose a core of Archaean basement interpreted as a central uplift (Teague Granite and greenstone rocks).

2. shatter cones in sedimentary rocks in both inner and outer rings.

3. Planar deformation features (PDFs) in quartz crystals of Teague Granite.

The central basement uplift, with a diameter of 12 km, consists of fractured Archaean granitoids of syenitic composition (Teague Granite).. The syenitic composition of the Teague Granite suggests that it could either belong to a late Archaean suite of alkaline plutons that intrude the Yilgarn Craton (Johnson, 1991; Smithies and Champion, 1999), or is the product of alteration of a precursor granitoid

by alkali metasomatism related to an impact-generated heat source. Locally, the Teague Granite exhibits partial to pervasive silicification, is fractured and contains hydrothermal minerals, such as fibrous amphibole, garnet, sericite and prehnite, consistent with metasomatism.

The target rocks consist of strata that are shallowly dipping to the northeast (about 10-15º), including undeformed and unmetamorphosed sedimentary rocks of the Earaheedy Group, overlying Archaean granite-greenstone basement of the Yilgarn Craton (Fig. 2; Pirajno et al., 2004). The central and the western parts of the inner structure are entirely covered by Quaternary lake sediments and sand dunes. However, aeromagnetic data indicate that granitic (possibly monzogranite) and greenstone rocks are present beneath these surficial deposits, representing the northern continuation of the Yilgarn Craton beneath the sedimentary cover of the Earaheedy Basin (Pirajno, 2002). The presence of diagnostic impact indicators, suggest that granitic and greenstone rocks form an impact-induced central structural uplift and possibly the basement core of the original crater. This central uplift has a diameter of about 12 km. The eastern side of the structural uplift is characterized by high total magnetic intensity (TMI), hydrothermal alteration and the only exposures of the granitoid rocks (Teague Granite). The TMI pattern suggests not only that the upper parts of the original impact structure were eroded away, but also that the entire structure is probably tilted towards the east (Pirajno, 2002).

The age of the Shoemaker impact is not resolved, because of thermal and tectonic resetting of the isotopic systems of the target rocks at 1670-1620 Ma (reactivation of the Capricorn Orogen; Tyler, 2005), 1070 Ma (age of the Warakurna large igneous province in the region; Wingate et al., 2004) and ca 550 Ma (age of the Petermann Orogeny; Scrimgeour et al., 1999). The magmatic age of the Teague Granite is Archaean (2648 ± 8 Ma; Nelson, 1999), which is within the range of other granitic rocks in the Yilgarn Craton (e. g. Smithies and Champion, 1999). Bunting et al. (1980a, b) obtained two whole-rock Rb-Sr isochron ages of 1630 and 1260 Ma from samples Teague Granite. Pirajno (2002) and Pirajno et al. (2003) reported K-Ar and $^{39}Ar/^{40}Ar$ determinations on K-feldspar and illite-smectite separates also from the Teague Granite. The $^{39}Ar/^{40}Ar$ system yielded unreliable results, only providing broad constraints as to a maximum age (<1300 Ma; see Pirajno 2002. p. 36 for details). The K-Ar system gave two ages: 694±25 Ma and 568±20 Ma for K-feldspar and illite-

smectite separates, respectively. Pirajno et al. (2003) concluded that the 568±20 Ma K-Ar age determined on illite could represent either resetting due to the Petermann Orogeny, or the formation of illite as a result of post-impact hydrothermal activity.

About 5 km from the eastern shore of Lake Teague, scattered, cm to m-sized round and angular boulders of sandstone are present . This could be a lag deposit of Permian age (Paterson Formation; Bunting et al., 1982; Commander et al., 1982) . Alternatively, because of their position close to the outermost ring and absence of any such lithology elsewhere in the Earaheedy Group in the region, it is also possible that they are either remnants of reworked lithic breccia ejecta, or crater-fill allochthonous breccia (Pirajno, 2002).

6.1 Hydrothermal alteration

In the Shoemaker impact structure the effects of impact energy-induced hydrothermal circulation within the impact aureole are evident in the Teague Granite (Pirajno, 2002) and in rocks of the Yelma and Frere formations (Earaheedy Group) exposed in the eastern inner ring. Outcrops of Teague Granite in the east and southeast are fractured, hydrothermally altered and partially to pervasively silicified. The rocks of the Teague Granite were studied as part of a regional investigation of felsic alkaline rocks of the Yilgarn Craton by Johnson (1991), who concluded that the granitoids that outcrop in the Shoemaker structure were modified by alkali metasomatism resulting in a granitoid of syenitic composition. Johnson's conclusion was confirmed in subsequent studies (Pirajno and Glikson, 1998; Pirajno, 2002; Pirajno et al., 2003), in which the Teague Granite was subdivided into three units: syenite, quartz syenite and a leucocratic alkali feldspar granite.

The leucocratic alkali feldspar granite is probably the result of stages of silicification of the Teague Granite. This silicification was in places pervasive, whereby the entire granitoid is replaced by quartz (silica flooding). In places, fibrous amphibole (actinolite-tremolite) infills microfractures in the rock and in a network of cracks in andradite garnet crystals that are locally present in the Teague Granite. Andradite garnets have also been found in hydrothermally altered rocks in the Manson impact structure. Greenstone enclaves in the Teague Granite are cut by quartz-albite veinlets, associated with selvages of diopside (Pirajno, 2002). All these features are evidence that hydrothermal minerals were precipitated during phases of post-impact hydrothermal activity. The petrography and overall chemistry of the

Teague Granite shows that it is of syenitic affinity and alkaline composition, with the mineral assemblages and textural relationships suggesting that it is derived from alkali metasomatism of a precursor granitoid (Johnson, 1991; Pirajno, 2002).

Pervasive silicification affected rocks of the Yelma Formation (Sweetwaters Well Member), whilst the granular iron formation rocks of the Frere Formation exhibit cross-cutting quartz veining and are partially silicified. In the same area, pods of chert and jasperoidal quartz are present along the eastern margin of the central uplift. The chert material consists mainly of brecciated microcrystalline quartz cemented by chalcedonic quartz. Open spaces are filled with euhedral quartz crystals. These chert pods are interpreted to have formed by precipitation from hydrothermal fluids that circulated along faults and fractures in the eastern sector of Shoemaker impact structure.

It is likely that the meteorite impact that created the Shoemaker impact structure formed a melt sheet which, together with impact-released heat in the central uplift, gave rise to a hydrothermal convection system, within and around the central uplift zone. The melt sheet would have acted as a magma-like heat source within the crater structure and would have formed several hot springs in the crater and surrounding areas. Fluid channels and degassing pipes have been reported from the Ries impact crater in Germany (Newsom et al., 1986). Hydrothermal pods are present in the annular structures associated with the Haughton impact structure in Canada that have been interpreted as hydrothermal pipe structures (Osinski et al., 2001). Similarly, the pods of quartz-jasperoidal material that are present along structural breaks in the eastern rim of the Shoemaker impact structure may the eroded remnants of fluid channels that fed thermal springs.

7. Depositional setting and geodynamic evolution of the Earaheedy Basin

The Earaheedy Group consists of both chemical and clastic sediments indicative of a shallow marine to coastal environment, which deepened to the north and northeast (Jones et al, 2000; Pirajno et al., 2004). The exposed rocks represent only the coastal to upper shelf portion of the continental shelf that was developed on the northern margin of the Yilgarn Craton. Sedimentary deposits of the continental slope and rise are not exposed, suggesting that much of the original depositional system is buried or eroded. The two depositional sequences of the Tooloo and Miningarra

Subgroups provide interesting clues. The Tooloo Subgroup, which is characterized by granular iron-formation, reflects the intermittent influx of iron and silica into the basin, whereas the overlying Miningarra Subgroup is characterized first by clastic sediment-starved conditions (Wongawol Formation and Kulele Limestone) and then by fine to coarse-grained sandstone reflecting an abundant supply of coarser clastic material. The source of iron and silica for the granular iron-formations in the Frere Formation is a key element in the understanding of the basin as is the lack of evidence of contemporaneous volcanism and major deformation. Beukes and Klein (1992) and Isley (1995) considered granular iron-formation to be a shallow-water, higher energy equivalent of deeper water banded iron-formation. The generally north- and northeastwards-deepening, passive-margin model for Earaheedy Basin of Pirajno (2007), Pirajno et al. (2000; 2004) and Jones et al. (2000) is consistent with this interpretation. In the case of the Earaheedy Basin, the iron could have been sourced from a hydrothermal effluent, such as a mid-ocean ridge or vocanism associated with a submarine volcanic plateau, which was located northeast and/or east of the presently exposed margin of the basin (Jones et al., 2000; Pirajno et al., 2004).

Deposition of the Miningarra Subgroup therefore reflects an increased influx of fine to coarse-grained sand sized detritus. SHRIMP U-Pb dating of detrital zircons suggests that sandstone in the Earaheedy Group was probably sourced predominantly from the Yilgarn Craton and the Gascoyne Complex to the west (Halilovic et al., 2004). It also suggests that this siliciclastic detritus was sourced from progressively younger sources during the evolution of the basin. In addition, ball-and-pillow deformation is common higher in the succession in the Wongawol Formation (Bunting, 1986). A tectonically driven model is certainly consistent with current age constraints that suggest deposition of the Earaheedy Group may have been more or less synchronous with the Capricorn Orogeny. Thus, the Miningarra Subgroup is interpreted to reflect rapid uplift in the west, causing influx of siliciclastic material that overwhelmed the proportion of iron and silica in solution and consequently terminated the deposition of granular iron-formation, while favouring the deposition of glauconite peloids. Glauconite peloids, associated with clastic grains, are particularly common in shale, siltstone and very fine-grained sandstone horizons and at the base of medium to coarse-grained sandstone horizons in the Chiall Formation.

There is an association between glauconite and ferruginous sandstone, with alternations of glauconite-rich and ferruginous layers.

Therefore, the depositional dynamics at the boundary between the Tooloo and Miningarra Subgroups may reflect either sedimentary processes, or tectonism, or a combination of the two. This change is interpreted here to have been related to tectonically-driven eustatic sea level changes. The boundary between the Tooloo and Miningarra subgroups (base of Chiall Formation) reflects a change in depositional setting from a chemical, clastic-starved regime to one of abundant clastic supply. In Figure 27, five main sedimentary cycles, controlled by sea level changes, are illustrated, they are: 1) Coarser clastic cycle of the Yelma Formation, leading up to a sea level rise with the deposition of platform carbonates (Sweetwaters Well Member) and culminating with the fine-grained clastic-sedimentation starved succession of the Frere Formation, albeit with some rhythmicity. Comparatively strong subsidence leads to another cycle of coarser clastic sedimentation, manifested by the deposition of the Chiall Formation. A cycle of clastic-sediment starved conditions is shown by the deposition of the Kulele Limestone, followed by a final cycle of slight subsidence with the deposition of the Mulgarra Sandstone.

The evolution of sedimentary basins is largely controlled by magmatism, tectonism, sediment supply and eustasy (Erikson et al., 2001). In the eastern Capricorn, present-day subdued relief and paucity of outcrops, together with limited geochronological constraints, place limitations to our understanding of the geodynamic evolution of the Earaheedy Basin (Pirajno et al., 2004; Pirajno, 2007). However, the use of geophysical data (aeromagnetic and gravity) in conjunction with systematic field geological mapping and geochemical surveys of regolith materials have helped in identifying the extent of covered bedrock and major structures (Morris et al., 1997, 1998; Davy et al., 1999; Morris et al., 2000, 2003). This integrated knowledge permits a reasonable level of insight, which provides the necessary foundation for the construction of geotectonic models. In the following sections a model for the geodynamic evolution of the Earaheedy Basin is discussed and illustrated in Figure 28. The basal units of the Earaheedy Basin, are characterised by extensive aprons of clastic sediments, mostly mature sandstone. These sediments were generated by erosion of peneplained surfaces. Peneplanation and the generation of

large volumes of siliciclastic sediments have been related to domal uplift of continental crust (Pirajno et al. 2004). The basin was starved of clastic sediments after stripping of the craton, resulting in shallow-marine to coastal carbonate deposition, possibly in late highstand and subsequent lowstand phase, which in the Earaheedy Basin coincided with increases in dissolved iron, initiating deposition of chert and iron formations. The magnitude of the eustatic change, as reflected by relative bathymetric change in the basins, was low, with prolonged highstand-type deposition. The subgroup lithostratigraphic divisions of the Earaheedy Basin indicate a change in the depositional settings, imposed by a high-energy tectonic regime, most likely due to orogenic uplifts. As mentioned previously, the Earaheedy Group consists of both chemical and clastic sediments, which are indicative of a shallow marine to coastal environment, which deepened to the north to northeast (Jones et al, 2000; Pirajno et al., 2004). The granular iron-formation beds (Frere Formation) provide a reasonable indicator of depositional setting, because in order to have large scale deposition of granular facies iron oxides, a shallow-water environment, probably a continental shelf (passive margin) would have been required (e. g. Trendall, 2002; Simonson and Hassler, 1996).

The lithofacies of the Earaheedy Group suggest that it was part of a trailing passive margin, characterised by low-magnitude marine transgressions and regressions in response to fluctuating sea-level changes (Fig. 28B), due to a combination of sediment supply, subsidence and eustasy (Erikson et al., 2001). Typically, trailing passive margins result from continental breakups (Braun and Beaumont, 1989). Present-day exposed rocks represent only the coastal to upper shelfal portion of the continental shelf; sedimentary deposits of the continental slope and rise are not exposed, suggesting that much of the original depositional system is buried. The 1.99 Ga rhyodacitic subvolcanic rocks of the Imbin Inlier could be either an exotic fragment from a northern continent, or a fragment of the Dalgaringa Supersuite of the southern Gascoyne terrane that moved eastward by transcurrent movements (Occhipinti et al., 2001). Yet another possibility is that the Imbin rhyodacite is part of a bimodal (felsic-mafic) igneous suite related to continental breakup.

The grain size (dominantly medium-fine sand to silt) indicates dominantly quiet, low-energy conditions, although this could be because coarser material was simply not available due to a low-gradient, weathered, basin hinterland. Deposition was strongly influenced by water chemistry, sediment supply and sea-level fluctuations. Sea-level fluctuations are envisaged to be both eustatic and tectonic, with short-term eustatic changes in a greenhouse climate (Read et al., 1995) producing metre-scale cyclicity in carbonates and from tens of metres to metre scale cyclicity in the iron formation (iron formation-siltstone bands), and longer term tectonism responsible for increases in sand deposition by either hinterland uplift or basin subsidence. North to northeastward deepening is consistent with the distribution of facies within the basin architecture.

The range in detrital zircon ages suggests both Archaean and Palaeoproterozoic sources for the Earaheedy Group. Archaean ages are consistent with the Yilgarn Craton as a source. The youngest age of detrital zircons in the lower Tooloo Subgroup imply a 2.0-1.8 Ga source; the only possible source of these Palaeoproterozoic zircons in the immediate region (barring unknown continental fragments elsewhere) is the southern Gascoyne Complex in the west. As mentioned above, the source of iron for the granular iron-formations in the Frere Formation is a key element in the understanding of the basin as is the lack of evidence of contemporaneous volcanism and major deformation. Beukes and Klein (1992) and Isley (1995) considered that granular iron-formation formed as the shallow water, higher energy equivalent of deeper water banded iron-formations. However, it should be noted that the model for the origin of the iron-formations proposed by Beukes and Klein (1992) and Isley (1995) accounts for the large volumes of iron, but it does not explain the association of iron and silica in grains of possible biogenic origin. Some of the grains classified as peloids, may have been originally oncolites (Brown et al., 1995). If this is correct, then it is possible that biogenic activity may have played a major role in the development of the Earaheedy granular iron-formation, through a mechanism of bacterial iron oxidation (e. g. Nealson, 1982; Brown et al., 1995). Recent models of iron formation genesis suggest that the supply of the soluble Fe^{2+} is provided by hydrothermal effluents in oceanic settings (e. g. spreading centers or mantle-plume related oceanic plateaux; Isley, 1995). During deposition of the Tooloo Subgroup, no

oceanic environment is known to have been present in the west. From known rock distributions, oceans must have been to the north, east and/or northeast (Fig. 28B).

The Miningarra Subgroup heralded a new phase of sedimentation still in a passive margin setting, with a dominant clastic sediment input from areas of orogenic uplift in the west and/ore northwest (i. e. Pilbara-Yilgarn tectonic interaction and Capricorn Orogeny; Fig. 28B). This is supported by the presence of sedimentary breccias, suggestive of in situ liquefaction and interpreted as seismites, and ball-and-pillow (hydroplastic) loading structures throughout the Miningarra Subgroup, which are indicative of far-field seismic and tectonic activity. The rapid influx of coarser siliciclastic rocks into the basin overwhelmed the chemical deposition of Fe oxides (granular iron-formation) and favoured instead the deposition of glauconitic sandstones. The Kulele Limestone, deposited in a subtidal stromatolitic carbonate environment, reflects a decrease in terrigenous supply, caused either by climatic or tectonic changes. The Mulgarra Sandstone shows a return to shelfal depositional setting of the Wongawol and Chiall Formations. A carbonate interval at the topmost Mulgarra Sandstone may have heralded a return to carbonate deposition, now only barely preserved because of later erosion. Bunting (1986) suggested that the Mulgarra Sandstone may disconformably overlie the Kulele Limestone, but this has not been confirmed by our work.

From the above and given the age constraints, the deposition of the Earaheedy Group was essentially synchronous with the Capricorn orogeny. The present-day structure of the Earaheedy Basin along a north-south cross-section is asymmetric, with a broad shallow platform along the southern margin and a strongly deformed northern margin, with reverse faulting, shearing, tight and recumbent folding, in the Stanley Fold Belt. Precise geochronological constraints on the timing of deformation of the Stanley Fold Belt are lacking, although the ^{39}Ar-^{40}Ar dating of metamorphic micas yielded an age of ca. 1650 Ma; see Table 2 and *Geochronology*). Based on field data, we tentatively interpret the Stanley Fold Belt as the result of a transpressive event, possibly linked to the D_2 phase of the Yapungku Orogeny (1.79 -1.76 Ga; Smithies and Bagas, 1997; Bagas and Smithies, 1998; Bagas., 2004), which had a major effect in the Rudall Complex, north of the Earaheedy Basin. The Ar-Ar age of ca. 1650 may represent resetting of the Ar-Ar systems during the 1680-1620 Ma

Mangaroon Orogeny (Sheppard et al., 2005). The Yapungku Orogeny was a major event that records the collision of the West Australian Craton with the North Australian Craton (Myers et al., 1996; Smithies and Bagas, 1997). This is consistent with other results including: a) palaeomagnetic studies by Li (2000), who concluded that the West and North Australian cratons joined together at about 1.7 Ga; b) recent SHRIMP U-Pb dating of zircons and monazite from the Malmac Inlier, which indicate a disturbance event at about 1.72 Ga (Nelson, 2002); and c) SHRIMP U-Pb dating of zircons by McMillan and McNaughton., 1995 and Vielreicher and McNaughton (2002) also detected a disturbance, associated with hydrothermal activity, in the Marymia Inlier at about 1.72 Ga. The timing of this deformation also ties in reasonably well with the epigenetic Mississippi Valley Type mineralisation in the Yelma Formation, for which a Pb-Pb model age of 1.74-1.77 Ga was determined (Teen, 1996), suggesting that tectonic uplift along the Stanley Fold Belt provided the necessary gravity gradients to drive basinal fluids updip, to form sulfide and oxide deposits in carbonate platforms on the southern margin of the basin (Pirajno, 2004). The deformation of the Earaheedy Group at this time resulted in its folding into an asymmetrical syncline, conferring the distinctive foreland basin-type north-south asymmetry of the Earaheedy Basin as illustrated in Fig. 6G, although the depositional environment reflects a trailing passive margin rather than a foreland setting.

8. Lithostratigraphic unit of uncertain age: Sydney Heads Pass Conglomerate

The Sydney Heads Pass Conglomerate is confined to a small area around Sydney Heads Pass (Earaheedy; Fig. 2), where up to 20 metres of conglomerate is exposed in a cliff face. The sequence dips at about 20°SE, and overlies steeply dipping Yelma Formation with marked angular unconformity. The unit comprises alternations of coarse and fine conglomerate with local lenses of highly ferruginous sandstone (Fig. 31). The conglomerate is clast supported, with rounded cobbles up to 15–20 cm in diameter in a sandy matrix. Clasts include ferruginous sandstone probably derived from the Frere Formation, quartz and chert. Scattered imbricated clasts suggest current flow from the south. Directly east of the Pass, coarse conglomerate contains rounded cobbles exceeding 30 cm in diameter. The conglomerate fines upwards, and is increasingly interbedded with poorly sorted, flaggy sandstone and shale. The conglomerate is interpreted as a fluvial deposit, probably in an incised hinterland

valley. At one level, a sandy pisolitic ironstone (Fig. 29) that clearly dips with the remainder of the conglomerate is interpreted as a syndepositional ferricrete.

The stratigraphic position of the Sydney Heads Pass Conglomerate is uncertain. It postdates deformation of the Earaheedy Group, but is itself moderately folded. It is therefore unlikely to be Phanerozoic or even Neoproterozoic (as the Neoproterozoic is virtually unfolded on Mudan to the north), and may be a hinterland correlative of the older or younger parts of the Bangemall Supergroup, or an entirely distinct local deposit. Commander et al. (1982) suggested that it may be a remnant of a more extensive intermontane deposit, an ancient analogue of the Eocene Robe Pisolite of the Hamersley Basin.

9. Mineral systems

The mineral systems of the Earaheedy Basin can be assigned to two groups: syn-depositional and late-post depositional. To the former belong the granular iron formation (Frere Formation) and glauconite-bearing sandstones (Chiall and Wongawol Formations), to the latter belong diagenetic and deformation-related modifications to the layers of granular iron formation, the carbonate-hosted base metal sulfides of the Sweetwaters Well Member (Mississippi Valley type), the structurally controlled ore systems that include Au, Mn, and the nonsulfide Pb of the Magellan world-class deposit, diamondiferous lamprophyres and calcrete U. A review of ore deposit models in the Capricorn Orogen can be found in Pirajno (2004). Genetic models that are proposed to explain the development and distribution are treated for each category in the appropriate section. The distribution of mineral deposits and occurrences in the Earaheedy Basin are shown in Figure 30. comprehensive report on the mineral occurrences and exploration potential of the Earaheedy Basin and surrounding areas is provided in a report by Abeysinghe (2005).

9.1 Iron and manganese

The Frere Formation was considered to be highly prospective for iron ore with exploration occurring between 1973 and 1978 and recently revived due to high demand for iron ore. Details of granular iron formation mineralisation in the Earaheedy Basin can be found in Abeysinghe (2005). During exploration several zones of supergene iron enrichment within granular iron-formation were identified.

The Superior-type granular iron-formation beds of the Frere Formation extend along strike for a total of approximately 500 km (Fig. 3B), thus constituting a significant iron resource. In the western parts of the Basin, zones of supergene-enriched iron oxides contain between 21 and 66 % Fe (Bunting, 1986; Pirajno and Adamides, 2000; Pirajno, unpublished data). In the Stanley Fold Belt, along the northern margin of the Earaheedy Basin, the granular iron-formation beds contain platy hematite and magnetite mineralisation that is spatially associated with strike-slip and/or reverse faults. The extent of this hematite-magnetite enrichment is revealed by aeromagnetic images, which indicate a total strike length of approximately 280 km. In addition, minor stratiform Mn and Fe oxides with anomalous abundances of Cu, Ba and Pb are present within the Wongawol Formation (Pirajno and Adamides, 2000). Least-weathered granular iron-formation within the Frere Formation contains various amounts of iron. Bunting (1986) reported Fe enrichment in some units, ranging from 27 – 47 % Fe, with less than 0.06% P_2O_5. Analyses of grab samples of granular iron-formation rocks (Pirajno, unpublished data, 2001) gave values ranging from 20 to 39% Fe, with P_2O_5 from 0.05 to 0.9%. Enrichment of secondary iron oxides (hematite and goethite) is common in areas close to faults as a result both of hydrothermal fluids and weathering processes. Such enriched zones may have economic potential. To the northwest on Fairbairn, platy hematite is present in a predominantly shaly sequence near the top of the Frere Formation in the Miss Fairbairn Hills and Hawkins Knob areas (Adamides et al., 2000b). Iron enrichment was interpreted as the result of localized chemical weathering (Robinson and Gellatly, 1978) and drilling indicated that the high grade zones encountered during surface sampling were both small and sulfurous. The decrease in Fe content with depth indicates that much of the high Fe resulted from weathering processes. Drilling at Hawkins Knob yielded assays ranging from 10 to 49% Fe, with an average of 29.4 % Fe (Broken Hill Proprietary Ltd, 1978). Surface samples of granular iron formation from Mount Cecil Rhodes, on Rhodes assayed from 61 to ca. 64.5% Fe, with P and S contents of 0.05 and 0.06 %, respectively. Assays of 27 surface samples, collected along the northwestern margin of the Shoemaker impact structure, returned values ranging from 60 to 69.6% Fe, averaging 62.6 % Fe, 0.03% P and 0.18% S. At the western end of the Frere Range, Ivan Well area, surface samples of granular iron formation assayed more than 60% Fe, with 0.16% P and 0.07% S. Drilling intersections in this area gave 10 m at 40% Fe, 4 m at at 41.6% Fe, 57 m at 25.4% Fe and 7 m at 43% Fe (Abeysinghe, 2005).

9.1.1 Glauconite in the Earaheedy Group

Glauconite, is a micaceous mineral with the general formula $(K,Na,Ca)_{1.2–2.0}(Fe^{+3},Al,Fe^{+2},Mg)_4[Si_7AlO_{20})\ (OH)_4.n(H_2O)$. It is generally deposited in shallow marine continental shelves (water depths of 50-500m), and has a spatial association with iron and manganese formations (Kimberley, 1989; Ostwald and Bolton, 1992).

In the Earaheedy Group glauconite is commonly present at several stratigraphic levels and is particularly well developed in sandstones of the Chiall and Wongawol Formations. Glauconite rich sandstone beds locally alternate with ferruginous sandstone beds. The presence of glauconite supports the shallow water depositional regime for these formations (Einsele, 2000). In the sandstone units of these formations, glauconite is in the form of pellets or peloids associated with clastic grains (Fig. 31). Locally, the glauconite pellets are deformed and/or streaked out (Bunting, 1986), perhaps indicating that they pseudomorphed mud clasts. Petrographically, the glauconite, varies from colourless to light-green, or brown when weathered, or blue-green when fresh; it is commonly replaced by a mosaic of quartz grains, which are not in crystallographic continuity with the surrounding authigenic silica.

There is an association between glauconite and ferruginous sandstone, with alternations of glauconite-rich and ferruginous layers. Here, the peloids of the glauconite-rich layers are set in a black, fine-grained, probably manganiferous material.

9.1.2 Structurally-controlled Fe and Mn mineralisation

Iron-manganese mineralization in the Earaheedy Basin is present as: a) structurally-controlled quartz-iron-manganese oxide veins hosted by steeply-dippping shale units of the Karri Karri Member (Windidda Member); and b) stratiform iron and manganese oxide bands interbedded with sandstone and siltstone of the Wongawol Formation. The distribution of these occurrences are shown in Figure 30

The quartz-iron-manganese oxide veins have easterly trends, thicknesses of 2 to 8 m and a maximum strike length of about 100 m. The stratiform iron-manganese oxides are spatially associated with layers of banded siliceous ironstone (jasper) and grey-green chert containing minor pyrite, chalcopyrite and sphalerite (Bunting, 1986).

The presence of sulfides suggests the establishement of temporary anoxic conditions in a generally oxic environment. The nature and composition of the iron and manganese oxides are not known, but it is possible that the main components are hematite and pyrolusite. The host sandstone typically contains detrital white mica, glauconite and accessory amounts of tourmaline and zircon. The host sandstones have adhesion surfaces, symmetrical ripple marks and small-scale cross-laminations, suggesting deposition in very shallow water, and intermittently emergent, conditions.

Chemical analyses of samples from the quartz-iron-manganese oxide veins and the stratiform iron-manganese oxides are in Table 2 in Appendix 2. These analyses show that, apart from manganese, the oxides have anomalous abundances in copper (up to 1400 ppm), cobalt (up to 620 ppm), barium (up to 7800 ppm) and lead (up to 580 ppm). High barium values suggest the presence of barite, whereas the high metal abundances (Cu, Co, Pb) may be due to the fixing of these elements by the manganese oxides.

9.1.3 Discussion

The presence of a thick succession of Lake Superior-type granular iron-formations in the Earaheedy Basin (Goode et al., 1983), stratiform iron-manganese oxides and glauconite-bearing sandstones suggests that deposition of these sediments took place in a continental shelf environment, as previously discussed.

Iron and manganese are geochemically similar and in many instances they are precipitated together, but separation can and does occur during precipitation from hydrothermal fluids, depending on Eh-pH environmental conditions. Almost complete separation of these two elements is known from the iron and manganese formation of the Transvaal Basin in South Africa (e.g. Klein and Beukes, 1992). Force and Cannon (1988) suggested that at low Eh, iron solubility is low, due to the uptake of iron by sulfur ligands, precipitating sulfides. On the other hand and under the same conditions, manganese solubility is high, because there is no comparable manganese sulfide (alabandite, MnS, is uncommon in sedimentary rocks; Force and Maynard, 1991). In oxic environments, iron and manganese also tend to precipitate separately, again in response to Eh and pH conditions, with iron oxides predominantly precipitating in deeper water (continental slope, at lower Eh for a given pH) and

manganese oxides in shallower waters (on the shelf, at higher Eh for a given pH) (Schissel and Aro, 1992).

The association of glauconite-bearing sandstone and iron-manganese oxides has been investigated by Ostwald and Bolton (1992). These authors found that there is a genetic relationship between them. Glauconite tends to form in deeper offshore water, whereas manganese oxide precipitation occurs along palaeoshore lines. In addition, glauconite enhances the manganese content of the water because it removes iron from the system (Ostwald and Bolton, 1992). In other words, glauconite fixes iron in the clastic sediments, rather similar to pyrite fixing iron in black shales. In this way, waters moving along the shelf are enriched in manganese, which is then precipitated as oxide (Mn^{2+}). Anoxic conditions prevail basinward from the iron-formation, iron-manganese oxides and glauconite zones, resulting in deposition of black shales (e. g. Windidda Member).

The origin of the vast amounts of iron and manganese required to form the observed iron and manganese formations in Proterozoic sedimentary basins is controversial, but a popular view is that subaqueous hot springs are the major source of these metals as well as others, such as Cu, Co, Zn, Pb, Au and Ag (e. g. Isley, 1995). Upwelling currents transport iron and manganese in reduced form (Fe^{+2} and Mn^{+2}) from the discharge vents, with precipitation occurring just above the oxic-anoxic interface (Fig. 19), where Fe^{2+} and Mn^{2+} are oxidised to Fe^{3+} and Mn^{4+}, with separation being constrained by the Eh-pH conditions mentioned above. An important facet of this model (Fig. 19) is that carbonate and sulfide facies (sulfidic shale) are the lateral and deeper water equivalents of iron and manganese oxide zones. Black shale-hosted sulfide deposits have been reported from China and Canada, where they formed along a transitional shelf zone, between a platform and a deeper water setting (Coveney et al., 1992). In addition, copper, lead and zinc may exist in deltaic or lagoonal-facies sandstone, vertically or laterally to glauconite-bearing units. A situation of this kind is recorded from the eastern Atlantic passive continental margin of Africa, where copper, lead and zinc deposits are present at several localities in Lower Cretaceous sandstones, between Angola and Gabon, and in Morocco (Caia, 1976).

Apart from the iron-manganese mineralization in restricted parts of the Earaheedy Basin, fringing areas of black-shale deposition, the structurally controlled quartz-iron-manganese oxides are hosted by rocks of the Karri Karri Member (Windidda Formation), where they are deformed in the Stanley Fold Belt. This suggests that tectonism led to the dewatering of the sedimentary succession and the localization of fluids along fractures and faults. If this is correct then base metal sulfides and gold, could be present in areas of the Stanley Fold Belt. This model is supported by the presence of auriferous quartz veins in mylonite zones in the Troy Creek area, to the west (RHODES map sheet; Pirajno and Hocking, 2000).

On the basis of the sedimentological character, tectonic setting, presence of iron-manganese oxides and glauconite, we suggest that the Earaheedy Basin is very prospective for stratabound sedimentary rock-hosted base metal sulfides deposits.

9.2 Precious and base metals

In the Stanley Fold Belt precious and base metal mineralisation is hosted in the deformed rocks of the Yelma Formation along Troy Creek on Rhodes where two mineralised zones were identified during a drilling program, namely: Gossan and North Chert (Kellow, 1991; Blackburn, 2003). The Gossan zone extends for about 400 m, and as the name implies it consists of gossanous material (mainly goethite) with grab samples assaying 185 ppb Au, 360 ppm Cu, 400 ppm Zn, 540 ppm As, and 6 ppm Ag (Blackburn, 2003). Kellow (1991) reported drill intersections of 0.34% Cu over 9.6 m and 0.44 ppm Au over 6m and 3.2 ppm over 1 m. Subsequent drilling intersected 16 m of massive to semimassive sulfides at a depth of 107 m (Blackburn, 2003). Best results in this particular intersection yielded 2.98% Cu and 0.12 ppm Au over 2 m. About 700 m eastsoutheast of the sulfide body is a nearly vertical shear zone-controlled zone of Pt-Pd-Au mineralisation, in which drilling results gave 4 m at 1 ppm Pt+Pd+Au and a 1 m interval at 0.54 ppm Pt, 0.48 ppm Pd and 0,25 pp Au (Blackburn, 2003). This is the North Chert zone, with a strike length of about 600 m (Kellow, 1991), in which drilling intersected 1 m at 0.62% Zn and 3.7 m at 0.63 ppm Au (Blackburn, 2003).

The rock types in the Troy Creek area include quartz-muscovite schist, phyllite, shale, pelitic schist, recrystallised limestone, minor iron formation, all metamorphosed to greenschist facies. Mylonitic bands are also present and are

subparallel to the main deformation fabric (S_1) in the area. Sedimentary bedding is still recognisable and is nearly vertical and striking northeast. An S_1 foliation strikes 300º and an S_2 crenulation cleavage strikes 270º. The northwest-trending Troy Creek Fault is a 2 km wide thrust, dipping 70º to the northeast and marked by quartz veins and mylonite zones. Quartz lenticles and small veins are common in these rocks and are parallel to the main foliation trends. Larger quartz veins in the area of two types: post-tectonic massive clear quartz and syntectonic Fe-oxides rich quartz cut by the S_1 fabrics. Chert bands or lenses are also present and consist of grey-green coloured siliceous material, which in thin section consists of recrystallised quartz locally with relic colloform banding barite crystals.

The Troy Creek mineralisation (sulfide lenses, quartz veins and chert) is contained within the thrust zone and in the immediate hanging wall rocks. The mineralisation appears to be a mix of stratabound (sulfide zones) and structurally-controlled orogenic lode veins. The presence of relic barite in chert and carbonate units suggests that Troy Creek initially may have been a stratabound Mississipi Valley Type (see below) sulfide deposit that was deformed and metamorphosed during deformation. This deformation resulted in the partial redistribution of ore metals in quartz veins during S_1, and later affected by S_2 which resulted in more quartz veining and secondary microcrystalline silica, forming the chert bands.

9.3 Mississippi Valley Type (MVT) Zn-Pb-Cu-Ba

Zinc-Pb-Cu-Ba mineralisation is hosted in stromatolitic carbonate rocks of the Sweetwaters Well Member of the basal Yelma Formation, west of the Shoemaker impact structure (Pirajno, 2002). Sphalerite, galena, pyrite, and chalcopyrite are present as fracture and vug fills, or replacement of stromatolitic carbonate. This mineralization is known from a number of localities, distributed discontinuously along 50 km of strike length (Fig. 32). On Merrie (Adamides, 2000), Zn-Pb sulfide mineralization is found in the interstices of stromatolite columns in the Sweetwaters Well area. Elsewhere, except for the Iroquois prospect close to the Shoemaker structure, the mineralization does not outcrop, but was intersected in drillholes (see cross-section in Fig. 33) at depths ranging from 100 to 350 metres, beneath the Frere Formation (Fig. 34). These base metal prospects, 6 km west-northwest of Mount Teague (Fig. 32) were investigated in detail by Renison Goldfields Consolidated,

following a systematic diamond and reverse-circulation drilling program (Edgar, 1994; Feldtmann, 1995; Dörling, 1998a, b, c. d). Best assay results of reported drillcore intersections gave 11m @1.3 % Zn and 0.2 % Pb, 3m @ 2.3 % Zn and 0.2 % Pb, 6m @ 1.86 % Zn and 0.23 % Pb, 20m @ 0.88 %zn and 0.1 % Pb. Best assay results reported from reverse circulation (RC) drilling gave 13m @ 2.36 % Zn and 0.72 % Pb. Barium values from mineralised rock chip samples range from 1000 to 4000 ppm (Dörling, 1997a, b, c, d; 1996a, b; 1998a, b, c, d; Feldtmann, 1995).

The Sweetwaters Well Member base metal mineralization has many features that are consistent with carbonate-hosted Mississippi Valley-type ore deposits (MVT), namely: colloform textures, shelf carbonate host at the margins of a sedimentary basin (Garven and Raffensperger, 1997), and low-temperature and moderate salinity fluids (Teen, 1996). McQuitty and Pascoe (1998) suggested that the Magellan nonsulfide Pb deposit (see below) and the Sweetwaters Well Member Zn-Pb occurrences are part of the same MVT mineralising event. The timing of deformation phases along the northern margin of the Earaheedy Basin (Stanley fold Belt), ties in reasonably well with the MVT mineralisation in the Yelma Formation, for which a Pb-Pb model age of 1.74-1.77 Ga was determined (Teen, 1996). This implies that tectonic uplift along the Stanley fold Belt provided the necessary gravity gradients to cause bring migration, to form sulfide and oxide deposits in carbonate platforms in the southern margin of the basin. On Thaduna, disseminations of chalcopyrite and pyrite are associated with kerogen in dolomite breccia of the Yelma Formation in drillcore from Cork Tree Well (Meakins and Watsham, 1994; Pirajno and Adamides, 1998). In one drillhole, sulfide mineralization (mainly pyrite and chalcopyrite), is associated with specks of kerogen in dolomite breccia. Breccia clasts are rimmed by fine pyrite and kerogen, and open spaces are filled with euhedral quartz and chalcedony. This occurrence was also investigated by Rasmussen and Krapez (2000), who found small quantities of sulphoarsenides, arsenides, uraninite and cassiterite. This occurrence, revealed by a diamond drillhole, is hosted in fractured dolomitised limestone of the Yelma Formation in the western part of the Earaheedy Basin, near the unconformity with the underlying Windplain Group (Yerrida Basin; Pirajno and Adamides, 1998). On the basis of textural relationships, Rasmussen and Krapez (2000) concluded that hydrocarbon migration and sulfide mineralization were synchronous, but they also recognised multiple phases of hydrothermal fluid circulation.

Ore minerals include pyrite and sphalerite, with minor amounts of galena, chalcopyrite, bornite and tetrahedrite (Fig. 35a, b). These sulfides are associated with jig-saw breccias, open spaces, microfracture infills and microbial laminae. Cross-cutting barite veins are locally present, usually in silicified dolomite. Minor amounts of pyrobitumen, associated with sulfides, have also been identified (Teen, 1996).

Textural relationships indicate three stages of mineralization paragenesis. They are: I) pyrite-dolomite; II) microcrystalline quartz-chalcedony-quartz-pyrite-sphalerite-galena-chalcopyrite-bornite-tetrahedrite; III) dolomite-quartz-pyrite-sphalerite-galena. Sphalerite is typically zoned (Fig. 35d), banded and/or colloform, dark in colour and therefore Fe-poor, and commonly contains inclusions of galena. Typically, sphalerite either replaces microbial laminae, columnar stromatolites (*Asperia digitata*) or is found as open-space fillings (Fig. 35c, d). The mineralization in open space cavities indicates that sphalerite is the oldest ore mineral, and was followed by dolomite and late pyrite. The euhedral calcite shows growth zones rich in fluid inclusions, for which homogenization temperature measurements indicate relatively high temperatures (Teen, 1996). This worker examined 126 fluid inclusions in 14 samples from 5 prospects, westnorthwest of the Shoemaker Impact Structure at distances ranging from 20 to 70 km from the centre of the structure. The fluid inclusions examined range in size from < 5 to 100 µm. Primary fluid inclusions are two-phase with liquid-vapour ratios of between 10 and 20 vol. %, whereas secondary inclusions are much smaller (about 9 µm) but are also two-phase, with liquid-vapour ratios also of 10-20 %. Homogenization temperatures of primary inclusions range from 97 to 258^{0}C, with a mean of 178^{0}C; calculated salinities range from 2 to 24 NaCl wt% equivalent (Fig. 36). Based on T_h and salinity data, Teen (1996) recognised four types of fluids in secondary inclusions: 1) T_h 97-189^{0}C, average 130^{0}C, salinity 22-24 NaCl wt% eq.; 2) T_h 108-246^{0}C, average 160^{0}C, salinity 3-16.5 NaCl wt% eq.; 3) T_h 105-203^{0}C, average 153^{0}C, salinity 1.3-3.3 NaCl wt% eq.; 4) T_h 85-99^{0}C, average 89^{0}C, salinity not known. Teen (1996) suggested that the second fluid type, which is found in late stage quartz veins, is a fluid that could have remobilized earlier mineralization.

The fluid inclusions (primary and secondary) data briefly described above suggest that hydrothermal activity in the region was multiphase. The range of T_h and

salinities are consistent with those that are usually found in MVT ore deposits (90-120^{0}C; around 20 % NaCl equivalent; Garven and Raffensperger, 1997; Wilkinson, 2001). However, evidence of temperatures in excess of 250^{0}C near the Shoemaker Impact Structure suggests a heat source, other than the basinal geothermal gradients considered responsible for fluid flow and hydrothermal systems in sedimentary basins (e. g. Garven and Raffensperger, 1997; Tóth and Almási, 2001).

In one sample of dolomitic feldspathic sandstone, from the base of the succession in the Navajo prospect, sericite, iron sulfides and sphalerite infill microfractures. Pyrite is always of late generation and occurs both as euhedral crystals that replace sphalerite and as fine disseminations. In other cases, pyrite infills dissolution seams. Hydrothermal dolomite is associated with the mineralization and is typically characterized by large anhedral to euhedral crystals, up to 2 mm long, that infill open spaces.

9.3.1 Nonsulfide Pb

The large stratabound Magellan Pb deposit (Fig. 30), near the town of Wiluna, is hosted in Earaheedy Group outliers in the southeast of the Yerrida Basin. The mineralisation is accompanied by silicification and sericitic alteration of the host sandstone and silicified stromatolitic dolomite of the Yelma Formation close to, or at the unconformity with the underlying Windplain Group (Yerrida Basin; Pirajno et al., 1998; 2004; Pirajno, 2004). Magellan is an unusual mineral deposit, described by McQuitty and Pascoe (1998), and containing cerrusite ($PbCO_3$), plattnerite (PbO_2), coronadite ($PbMn_8O_{16}$), pyromorphite ($Pb_5(PO_4)_3Cl$) and plumbogummite ($PbAl_3(PO_4)_2$ $(OH)5H_2O$) as ore minerals. Its discovery was announced by Renison Goldfields Consolidated in 1993, with resources estimated at approximately 220 Mt at 2.2% lead. A feasibility study of the Magellan prospects was completed in 2001 by Ivernia West Inc., with proven and probable ore reserves totalling 8.5 x 10^6 tonnes at 7.12% Pb (www.ivernia.com). Later estimates give measured and indicated resources of 21.4 Mt grading 5.8% Pb, and inferred resources of 7.2 Mt grading 4.6% Pb (SEG Newsletter, 2006). A cross-section of the deposit is shown in Fig.ure 37.
Immature wacke is one of the host rocks, and is characterised by selectively pervasive sericitic and kaolinitic alteration. The lead minerals are paragenetically late and form replacement mineral of the matrix of the host rock. Trace element analyses of ore

materials indicate anomalous abundances of Ba (1000–1828 ppm), Mn (1900–3672 ppm), and Cu (257–400 ppm). No sulfides or other metals are present. Homogenisation temperatures of primary fluid inclusions in mineralised quartz range from 180 to 220ºC, with salinities of 9-15 wt% NaCl equivalent (McQuitty and Pascoe, 1998).

Similar mineralization exists in smaller prospects to the south of Magellan, mainly along the unconformity surface between the Juderina Formation (Windplain Group) and small outliers of the Earaheedy Group. These include the Canon, Cortez, Drake, Pizarro prospects, distributed west and southwest from the Magellan deposit.

It is possible, that this unusual type of mineralisation is associated with the migration of low-temperature late basinal fluids along permeable lithotypes (e.g. sandstone). However, the lack of sulfides and the unique presence of oxide minerals would suggest that the deposit may be somehow related to palaeoweathering processes, under physico-chemical conditions which were conducive to the oxidation and subsequence mobilisation of Pb. The Pb carbonate mineralisation could have resulted from the intense weathering of a precursor MVT deposit in the carbonate rocks of the Yelma Formation, in which the sulfides were completely weathered out with removal of the more mobile elements, such as S, Fe and Zn. The Pb was re-precipitated as a carbonate due to the presence of abundant Ca in the degrading carbonate rocks. If this is the case, the Magellan nonsulfide Pb deposit may be a variant of the nonsulfide Zn deposits (see Hitzman et al., 2003 for a comprehensive review). Alternatively, The Pb metal could have been sourced from the breakdown of K-feldspar during weathering, which is then mobilised as a soluble complex in groundwater (Biørlikke and Sangster, 1981).

The origin of the Magellan nonsulfide Pb deposit, and nearby similar prospects (Canon, Cortez, Drake, Pizarro) is likely to be associated with the oxidation of MVT-related Zn and Pb sulfides. The oxidation of these sulfide minerals lead to a progressive replacement by carbonates and oxides. The resulting supergene deposits can be of three types (Hitzman et al., 2003): 1) direct-replacement; 2) wall-rock replacement and 3) karst fill. Direct-replacement nonsulfide are derived from MVT sulfides are essentially Zn-rich gossans and tend to be mineralogically simple, with mineral species such as smithsonite, hemimorphite and hydrozincite. During supergene oxidation of sulfides abundant acid is formed to completely leach the Zn

metal in the near-surface. This leaching results in the formation of jasperodal gossans with Fe oxides and cerussite and lesser other metal carbonates (Hitzman et al. 2003). It is in this regime that residual Pb-rich deposits, such as Magellan, can form by the complete removal of Zn. Carbonate-rich (limestone, dolomite, calcareous sandstone) rocks are needed for this type of mineralisation to form due to their high reactivity. The acidic groundwaters flow downward from the original sulfide body near or exposed at the surface, permeates into and reacting with the calcareous wallrocks, and forming a replacement nonsulfide deposit that tends to be vertically zoned from Pb at and near the surface to Zn oxides at depth. If this model of ore genesis is correct it may imply that at Magellan Zn oxides may still exist at depth. The progressive replacement of a MVT sulfide body produces as end-products mainly chalcedonic silica-hematite and cerussite, as observed at Magellan. The oxidation-destruction of primary sulfides provides a low pH environment and sulfate-bearing solutions that can leach and carry metals. Pyrite, marcasite and Fe-rich sphalerite are needed to form large quantities of acid solutions. In some cases, it is probable that oxidation is mediated by thermophilic bacteria.

In conclusion, the genesis of supergene Zn, Zn-Pb, Pb nonsulfide deposits is lilnked to the presence of primary sulfides, generally MVT, but can also be other styles, such as volcanogenic massive sulfides (VMS) as documented for the Skorpion nonsulfide deposit in Namibia (Hitzman et al. 2003 and references therein); permeable and reactive wall rocks; climatic and hydrogeological conditions that can promote extensive oxidation.

9.4 Uranium and vanadium

On Nabberu, about 6 km north of Lake Teague (Fig. 30), non-pedogenic calcrete, 12 to 15 m thick, hosts carnotite mineralization, with values of between 10 and 700 ppm U (average 45 ppm) (Bunting, 1986; Morris et al, 1997). A trench exposed three lenses of carnotite encrusted calcrete, each about 1 m thick. Drilling intersections yielded values from 50 to 850 ppm U_3O_8 (Lindeman, 1972). At another locality, Bridle Face Outcamp, about 10 km south of Mount Teague, Uranerz Australia Ltd obtained drill intersecations of 192 ppm U_3O_8 over 4 m and 220 U_3O_8 over 1 m. The source of the U is not known, but it is possible that Archaean basement rocks provided this metal.

Uranium and vanadium enrichement associated with surficial duricrust and playa sediments is not uncommon in Western Australia, where they tend to occur in valley calcrete (non-pedogenic; Butt et al., 1984). The hydrochemistry of the groundwaters that are largely responsible for this type of mineralisation is generally neutral to alkaline and producing Si-, Ca-, Mg- and CO_2-metasomatic alteration of the host rocks leading to the formation of calcrete duricrusts by replacement of the overlying clay and sand in the upper 10 metres of the host sediment. The principal U-V mineral is carnotite (general formula is $K_2(UO_2)2V_2O_8{\cdot}3H_2O$), which usually occurs disseminated in the calcrete and/or fills voids and small fissures. In hot and arid climates with occasional rainfall and with evaporation exceeding precipitation, U^{+4} (insoluble) is oxidised to U^{+6} (soluble) and able to form minerals such as carnotite.

Rare earth elements (REE)

The Teague Granite, because of its alkaline nature, was investigated for REE mineralization by Metals Exploration NL (Metals Exploration, Annual Report, 1983). Results of this work indicated Ce and La values of up to 1550 and 570 ppm, respectively, in the more syenitic components of the Teague Granite. However, these results could not be substantiated during subsequent studies (Metals Exploration Annual Report, 1984). Average Ce and La abundances in Teague Granite are 150 and 100 ppm, respectively (Pirajno, 2002).

9.5 Diamonds

Diamondiferous ultramafic lamprophyre (and perhaps lamproite) intrusions are present on Fairbairn, Methwin, Lee Steere and Carnegi (Fig. 30). At Miss Fairbairn Hills, following a drilling program by Stockdale Prospecting on a magnetic anomaly, bulk samples from two costeans produced 52 macrodiamonds and microdiamonds, for a total of 0.83 carats (Mitchell, 1993). Drilling on two magnetic anomalies in the same area intersected kimberlitic material containing microdiamonds (Mitchell, 1993, 1995a). On Methwin gem quality macrodiamonds were recovered from bulk gravel sampling.

Diamonds have been recovered from Jewill and Bulljah Pool ultramafic lamprophyres The largest diamond, a 1.73 carat stone, was recovered from the Jewill lamprophyre.

Lesser sized macrodiamonds were also recovered. Bulk sampling of up to 150 t of material from Bulljah Pool did not returned diamonds, although indicator minerals, such as chrome spinel and pyrope garnet were found (Clifford, 1993).

Exploration efforts aimed at locating diamondiferous kimberlite or ultramafic lamprophyre pipes have successfully outlined target areas thought to be prospective. Indicator minerals such as chromites, phlogopites, chrome-diopside have been recovered during regional sampling programs and their chemical signatures are reported to be consistent with a kimberlitic origin (Livingstone Resources, 1998).

10. Discussion and conclusions

Many Archean granite-greenstone cratonic blocks are overlain by Archean or Proterozoic stable shelf sedimentary successions or platform covers, following early cratonisation, as for example in the Pilbara and Kaalpvaal Cratons, North China and the Siberian Cratons (REF; Zhao et al. 2005). The Earaheedy Basin may be a remnant of a post-Archaean platform-style sedimentary cover of the Yilgarn Craton. Cratonic basins and passive margins contain volcano-sedimentary and sedimentary successions, with banded and/or granular iron formations in the period between 2.4 and 1.8 Ga. The sedimentary rocks typically are represented by clastic sediments (arenite and shales) and shallow marine carbonates, characterised by transgression and regression sequences, reflecting the rise and fall of sea levels. The nature of the depositional systems in the post-Arhaean cratonic environements depends on the relative role of fluvial, aeolian, deltaic and tidal processes, wave and storm activity (Condie 2005). Furthermore, the distribution of the sediments is controlled by regional uplifts, the extent of the shallow seas and climate. Thus, where tectonic uplift is important, continental shelves tend to be narrow and sedimentation is dominated by wave and storm systems. In contrast, if uplift is confined to cratonic margins, fluvial and deltain systems dominate (Condie, 2005). The reasons fro the subsidence of cratonic blocks is not clear. A popular model is lithospheric stretching and thermal doming, followed by collapse. Doming of the lithosphere is a mechanism linked to upwelling asthenosphere or a mantle plume event, causing active erosion of the uplifted crust. Doming is flowed by thermal contraction, resulting in the formation of cratonic platform basins and/or marginal basins around an opening ocean, which fill with sediments. A well documented example is the Neoproterozoic Centralian

Superbasin, also in Australia, where crustal uplift due to amnatole plume at 825 Ma and subsequent sagging resulted in the deposition of thick successions of marine and fluvial sands (Walter et al. 1994; 1995).

Post-Archaean depositional environments developed on the northern margin of the Yilgarn Craton, span some 450 million years, and were conducive to the genesis of a range of mineral systems, including seafloor hydrothermal deposits, extensive beds of granular iron formation, MVT, the world-class Magellan non-sulphide Pb deposit, and orogenic Au lode deposits.

North of the Yilgarn Craton's present-day boundary are the Goodin, Marymia and Malmac inliers, all of which represent Archaean granite-greenstone terranes and the northern extension of the Yilgarn Craton. These inliers are located within a 700-km long belt of Palaeoproterozoic volcano-sedimentary and sedimentary basins, which are considered part of the Capricorn Orogen (Fig. 1). These basins include the Bryah-Padbury, Yerrida and Earaheedy basins, developed between ca 2.2 and 1.8 Ga, recording periods of rifting, sedimentation and volcanism, along the northern passive margin of the Yilgarn Craton. The Yerrida Basin, is the oldest (ca. 2.17 Ga), and began its history as an intracontinental sag, within which low-energy siliciclastics and evaporites accumulated. To the west, the Bryah-Padbury basins formed during accretion and collision processes, related to the ca. 2.0-1.9 Ga Glenburgh and ca. 1.83-1.78 Ga Capricorn orogenies. An uplift and rifting event affected the Yerrida Basin at 1.84 Ga, resulting in coarse and immature clastic sedimentation together with the eruption of flood basalts (Mooloogool Group). This event also caused the uplift of the Goodin Inlier with its cover of basal siliciclastic and evaporites of the Yerrida Basin (Windplain Group). This uplift was followed by stress relaxation and extensional tectonics with asthenospheric upwelling and outpouring of flood basalts. These basal sedimentary rocks were shed, forming spectacular olistostrome units, into surrounding sub-basins. To the east a passive margin developed, probably later than this uplift but the precise timing is poorly constrained. Sedimentation in this passive margin consisted of shallow-water clastic and chemical sediments (granular iron formation), which form the basal succession (Tooloo Subgroup) of the Earaheedy Basin. These events, deposition of the Mooloogool Group (uplift, rifting and volcanism) and the development of Earaheedy passive margin are difficult to explain within the framework of the Capricorn Orogeny. One possibility is that the Earaheedy passive margin formed as a result of continental breakup involving the Yilgarn

Craton, perhaps as part of an Archaean supercontinent. During the ca 1.74 Ga Yapungku Orogeny and the 1.65 Ga, Mangaroon Orogeny (Sheppard et al., 2005), the northern margin of the Earaheedy Basin and the western parts of the Yerrida Basin were deformed (Stanley Fold Belt; Fig. 3).

The basal units of the Yerrida and Earaheedy basins, although separated by ca. 300 million years, are characterised by extensive aprons of clastic sediments, mostly mature sandstone. These sediments were generated by erosion of peneplained surfaces. Peneplanation and the generation of large volumes of siliciclastic sediments have been related to domal uplift of continental crust (Pirajno et al. 2004). Basins were starved of clastic sediments after stripping of the craton, resulting in shallow-marine to coastal carbonate and evaporite deposition, possibly in late highstand and subsequent lowstand phase, which in the Earaheedy Basin coincided with increases in dissolved iron, initiating deposition of chert and iron formations. The magnitude of the eustatic change, as reflected by relative bathymetric change in the basins, was low, with prolonged highstand-type deposition. The group and subgroup lithostratigraphic divisions of the Yerrida and Earaheedy basins, respectively, indicate a change in the depositional settings, imposed by a high-energy tectonic regime, most likely due to orogenic uplifts, as previously mentioned. The Yerrida and Earaheedy basins are also characterised by an asymmetry in preserved cross-section, with undeformed southern platform margins and northern (Earaheedy), and northern-northwestern (Yerrida) margins of intensely deformed rocks, typical of foreland basin architecture (Stanley Fold Belt). This reflects the impingement of continental plates from the north and northeast.

The lithotectonic units and terranes of the Capricorn Orogen exhibit the cumulative result of tectonic events and reworking involving crustal attenuation, rifting with formation of passive margins, accretion, convergence and collision. The Capricorn, Yapungku and Mangaroon orogenies resulted in accretion of juvenile crust (Narracoota Formation), fold-and-thrust belts, uplift of continental margins (e. g. Gascoyne Complex, Bryah), and of fragments of Yilgarn Craton (e. g. Marymia and Goodin Inliers), inception of foreland basins (Padbury), rifting and emplacement of granitic plutons (Gascoyne Complex) and continental mafic volcanic rocks (Killara Formation in the Yerrida Basin), and deformation of passive margins (Earaheedy). The metallogeny of the Bryah-Padbury, Yerrida and Earaheedy basins is characterised

by a range of mineral systems that were formed during and as a result of these tectonic and magmatic events (Pirajno, 2004).

The granular iron formation beds of the Frere Formation in the Earaheedy Basin constitute a significant Fe resource, extending along strike for at least 280 km. In the western parts of the Basin, zones of enrichment due to supergene and tectonic deformation processes, contain between 21 and 66% Fe. Locally, stratiform Fe-Mn oxides with anomalous abundances of Cu, Ba and Pb are hosted in clastic beds of the Wongawol Formation. The origin of the vast amounts of iron and manganese required to form the observed iron and manganese formations in Proterozoic sedimentary basins is controversial, but the popular view is that submarine hydrothermal effluents are the major source of these metals as well as others, such as Cu, Co, Zn, Pb, Au and Ag. Upwelling currents transport iron and manganese in reduced form (Fe^{+2} and Mn^{+2}) from the discharge vents, with precipitation occurring just above the oxic-anoxic interface , where Fe^{2+} and Mn^{2+} are oxidised to Fe^{3+} and Mn^{4+}, with separation being constrained by the Eh-pH conditions (Trendall, 2002). Uplift of fold belts provide the topographic relief that is necessary to cause basinal brines to migrate across the basin, with rates that are measured in several m/year, but that decline over a few million years as erosion progresses. Tectonically- and/or gravity-driven flow in foreland basins is considered as one of the main causes for the origin of the second group of mineral systems, which includes Mississippi Valley type (MVT) deposits, exemplified by the carbonate-hosted Zn-Pb deposits in the Yelma Formation (Earaheedy Basin) and the Magellan non-sulphide Pb deposit. Magellan is an unusual, world-class, deposit with the only ore minerals being cerussite, coronodite and pyromorphite. The Pb ore could have resulted from the intense and deep weathering of a precursor MVT deposit, in which the sulfides were completely weathered out with removal of the more mobile elements such as S, Fe, and Zn.

Appendix. Supplementary data

Supplementary data associated with this paper can be found in the online version. At DOI:xxxxxxxxxx Ar-Ar data; geochem analyses

Acknowledgements

This paper is published with the permission of the Director of the Geological Survey of Western Australia.

References

Abeysinghe, B., 2005. Mineral occurrences and exploration potential of the Earaheedy area, Western Australia. Geological Survey of Western Australia Report 96, 820.

Adamides, N., 2000., Geology of the Merrie 1:100000 sheet. Geological Survey of Western Australia, 1:100 000 Geological Series Explanatory Notes, 37.

Adamides, N.G., Pirajno, F., and Farrell, T.R., 1999. Geology of the Cunyu 1:100 000 sheet. Geological Survey of Western Australia, 1:100000 Geological Series Explanatory Notes, 21.

Adamides, N.G., Pirajno, F., and Hocking, R.M., 2000a. Geology of the Fairbairn 1:100 000 sheet. Geological Survey of Western Australia, 1:100 000 Geological Series Explanatory Notes, 26.

Adamides, N.G., Pirajno, F., Hocking, R.M., and Jones, J.A., 2000b. Earaheedy, W.A. Sheet 3246. Geological Survey of Western Australia, 1:100000 Geological Series.

Allchurch, D., and Bunting, J.A., 1975. The Kaluweerie Conglomerate: A Proterozoic fluviatile sediment from the northeast Yilgarn Block, Western Australia. Geological Survey of Western Australia Annual Report 1975, 83-87.

Apak, S.N., and Moors, T., 2000. Basin development and petroleum exploration potential of the Yowalga area, Officer Basin, Western Australia. Geological Survey of Western Australia, Report 76, 61.

Apak, S.N., and Moors, H.T., 2001. Basin development and petroleum exploration potential of the Lennis area, Officer Basin, Western Australia. Geological Survey of Western Australia, Report 76, 42.

Aravanis, T., and May, R., 1988. Annual report on exploration completed within Exploration Licences 69/94 (Stanley 5), 69/97 (Stanley 8), 69/173 (Mt. Moore 1), 69/200 (Stanley 64), 69/217 (Stanley 67) and 69/220–222 (Stanley 70–72) Stanley 1:250000 Western Australia, CRA Exploration Pty Ltd. Geological Survey of Western Australia, Statutory mineral exploration report, Item 8361, A24045.

Bagas, L., 1998a. The Archaean Marymia Inlier — a review of its tectonic history and relationships to the Yilgarn Craton. Geological Survey of Western Australia, Annual Review 1997–1998, 85–90.

Bagas, L., 1998b. Geology of the Marymia 1:100000 sheet. Geological Survey of Western Australia, 1:100 000 Geological Series Explanatory Notes, 23.

Bagas, L., 2004. Proterozoic evolution and tectonic setting of the northwest Paterson Orogen, Western Australia. Precambrian Research, 128, 475-496.

Bagas, L., Hocking, R.M., and Williams, I.R., 1999. Neoproterozoic successions of the northwest Officer Basin: a re-appraisal. Geological Survey of Western Australia, Annual Review 1998–1999, 39–44.

Bagas, L., Smithies, R. H., 1998. Geology of the Connaughton 1:100 000 sheet, Western Australia. Western Australia Geological Survey, 1:100 000 Geological Series, Explanatory Notes, 38.

Bagas, L., Williams, I. R., and Hickman, A. H., 2000. Rudall, Western Australia (2nd Edition): Western Australia Geological Survey, 1:250 000 Geological Series Explanatory Notes, 50.

Barley, ME, Bekker, A, and Krapež, 2005, Late Archean to Early Paleoproterozoic global tectonics, environmental change and the rise of atmospheric oxygen: Earth and Planetary Science Letters 238, 156-171.

Bartlett, J.K., 1993. Annual combined Els 69/420–424, 426–428, January 2, 1992–January 1, 1993, Stockdale Prospecting Limited. Geological Survey of Western Australia, Statutory mineral exploration report, Item 8489, A37882.

2218 Bau, M. and Moller, P., 1993. Rare earth element systematics of the chenmically
2219 precipitated component in Early Precambrian iron formations and the evolution
2220 of the terestial atmosphere-lithopshere system. Geochimica et Cosmochimica
2221 Acta 57, 2239-2249.

2222 Beard, J.S., 1981. The vegetation of Western Australia at the 1:3000000 scale
2223 explanatory notes. Forests Department of Western Australia 32.

2224 Bettenay, E., 1983. Chapter 13, Western Region (II), *in* Soils–an Australian
2225 Viewpoint. CSIRO Division of Soils, CSIRO, Melbourne/Academic Press,
2226 London, 179–187.

2227 Beukes, N.J., and Klein, C., 1990. Geochemistry and sedimentology of a facies
2228 transition — from microbanded to granular iron-formation — in the early
2229 Proterozoic Transvaal Supergroup, South Africa. Precambrian Research 47, 99–
2230 139.

2231 Beukes, N.J., and Klein, C., 1992. Models of iron-formation deposition, *in* The
2232 Proterozoic biosphere: a multidisciplinary study, *edited by* W. Schope and C.
2233 Klein. Cambridge University Press, New York, 147–151.

2234 Biørlikke, A., and Sangster, D.F., 1981. An overview of sandstone lead deposits and
2235 their relation to Red-bed copper and carbonate-hosted lead-zinc deposits.
2236 Economic Geology 75th Anniversary Volume, 179-213.

2237 Blackburn, G., 2003. Troy Creek Pt-Pd-Au prospect, Nabberu District, Western
2238 Australia. CRC LEME Report, 1-2.

2239 Blatt, H., Middleton, G., Murray, R., 1980. Origin of sedimentary rocks, 2nd edition,
2240 Prentice Hall Inc. Englewood Cliffs, NJ, 782 pp.

2241 Brakel, A.T., and Leech, R.E.J., 1980. Trainor, W. A.. Geological Survey of Western
2242 Australia, 1:250 000 Geological Series Explanatory Notes 13.

Braun, J., Beaumont, C., 1989. A physical explanation of the relation between flank uplifts and the breakup unconformity at rifted continental margins. Geology 17, 760–764.

Broken Hill Proprietary Limited, 1978. Temporary Reserves 6492H, 6493H, 6494H, 6495H, 6496H and 6497H, Western Australia, final report. Geological Survey of Western Australia, Statutory mineral exploration report, Item 590, A7739.

Brown, D.A., Gross, G.A., and Sawicki, J.A., 1995. A review of the microbial geochemistry of banded iron-formations. Canadian Mineralogist 33, 1321-1333.

Bunting, J.A., 1980a. Kingston, W.A.. Geological Survey of Western Australia, 1:250 000 Geological Series Explanatory Notes 18.

Bunting, J.A., 1980b. Kingston, Western Australia, Sheet SG 51-10. Australia Bureau of Mineral Resources and Geological Survey of Western Australia 1:250 000 Geological Series.

Bunting, J.A., 1986. Geology of the eastern part of the Nabberu Basin. Geological Survey of Western Australia, Bulletin 131, 130.

Bunting, J.A., Brakel, A.T., and Commander, DP, 1982, Nabberu, Western Australia. Geological Survey of Western Australia, 1:250 000 Geological Series Explanatory Notes 27.

Bunting, J.A., Commander, D.P., and Gee, R.D., 1977. Preliminary synthesis of Lower Proterozoic stratigraphy and structure adjacent to the northern margin of the Yilgarn Block. Geological Survey of Western Australia, Annual Report for 1976, 43–48.

Bunting, J.A., de Laeter, J.R., and Libby, W.G., 1980. Evidence for the age and cryptoexplosive origin of the Teague Ring Structure, Western Australia. Western Australian Geological Survey, Annual Report 1979, 81–85.

Bureau of Mineral Resources, 1988. Trainor. Total Magnetic Intensity Map, Preliminary Edition, 1:250 000 scale, Australia BMR.

Butler, H., 1974. The Lake Ring Structure, Western Australia: an astrobleme?. Search 5, 536–537.

Butt, C.R.M., Horwitz, R.C., Mann A.W., 1977. Uranium occrrences in calcrete and associated sedimenst in Western Australia. CSIRO, Div Mineralogy, Minerals Research Laboratories, Report FP16.

Butt, C.R.M., Mann A.W., Horwitz, R.C., 1984. Regional setting, distribution and genesis of surficial uranium deposits in calcretes and associated sediments in Western Australia. In Surficial Uranium Deposits, TECDOC-322, IAEA, Vienna, 131-154.

Butterworth, M., 1999a. Report No. WA99/32S, Annual Mineral Exploration Report for the period 1 February 1998 to 31 January 1999 by North Limited for Exploration Licence E38/589, Bermuda, due on 1 April 1999, North Ltd. Geological Survey of Western Australia, Statutory mineral exploration report, Item 10729, A57837.

Butterworth, M., 1999b. Report No. WA2000/04S, Annual Mineral Exploration Report for period 15 May 1998 to 14 May 1999 by North Limited for Exploration Licence 38/940, Havana due on 15 July 1999, North Ltd. Geological Survey of Western Australia, Statutory mineral exploration report, Item 11218, A58529.

Butterworth, M., 2000. Report No. WA99/32S, Final Mineral Exploration Report for the period 1 February 1999 to 31 January 2000 by North Limited on Exploration Licence E38/589 Bermuda due on 1 March 2000, North Ltd. Geological Survey of Western Australia, Statutory mineral exploration report, Item 10729, A60808.

Caia, J., 1976. Paleogeographical and sedimentological controls of copper, lead and zinc mineralizations in the Lower Cretaceous sandstones of Africa. Economic Geology 71, 409-422.

Campbell, A.N., 1993. Combined Annual Report Exploration Licences 69/507–515 for the year ending 5/3/93, Lake Nabberu area W.A, Stockdale Prospecting Ltd.

2297 Geological Survey of Western Australia, Statutory mineral exploration report,
2298 Item 7939, A38356.

2299 Cawood, P.A. and Nemchin, A.A., 2000. Provenance record of a rift basin: U/Pb ages
2300 of detrital zircons from the Perth Basin, Western Australia. Sedimentary Geology
2301 134, 209-234.

2302 Cawood, P.A., Tyler, I.M., 2004. Assembling and reactivating the Proterozoic
2303 Capricorn Orogen: lithotectonic elements, orogenies and significance.
2304 Precambrian Research 128, 201-218.

2305 Chevron Exploration Corporation, 1979. Annual report, Miss Fairbairn Hills Prospect,
2306 Temporary Reserves 6807H and 6808H, Nabberu Mining District, Western
2307 Australia, Year ending – September 1979. Geological Survey of Western
2308 Australia, Statutory mineral exploration report, Item 1103, A8723.

2309 Chevron Exploration Corporation, 1980. Annual report for 1980, Mt. Fisher –
2310 Temporary Reserve 6800H, East Murchison Goldfield, Western Australia.
2311 Geological Survey of Western Australia, Statutory mineral exploration report,
2312 Item 1453, A9451.

2313 Chevron Exploration Corporation, 1981. Annual report for 1981, Mt. Fisher –
2314 Temporary Reserve 6800H, East Murchison Goldfield, Western Australia.
2315 Geological Survey of Western Australia, Statutory mineral exploration report,
2316 Item 1453, A10390.

2317 Chevron Exploration Corporation, 1982. Final Annual report, 1982, Mt. Fisher –
2318 Temporary Reserve 6800H, East Murchison Goldfield, Western Australia:
2319 Geological Survey of Western Australia, Statutory mineral exploration report,
2320 Item 1453, A11278.

2321 Chivas, A.R., Andrew, A.S., Lyons, W.B., Bird, M.I., and Donnelly, T.H., 1991.
2322 Isotopic constraints on the origin of salts in Australian playas. Sulphur.
2323 Palaeogeography, Palaeoclimatology, Palaeoecology 84, 309–332.

Clifford, P.R., 1993. Annual report on exploration completed within Exploration Licence 69/200 (Stanley 64), for the period ending 17 July 1993, Stanley 1:250 000 map sheet, Western Australia, CRA Exploration Pty Ltd. Geological Survey of Western Australia, Statutory mineral exploration report, Item 8361, A39265.

Colville, R.G., 1990. Annual Report for Exploration Licence 53/166 Mt Eureka - for the period 21 March 1989 to 20 March 1990, ACM Gold Ltd. Geological Survey of Western Australia, Statutory mineral exploration report, Item 6873, A30720.

Colville, R.G., 1991. Annual Report for Exploration Licence 53/166 Mt Eureka for the period 21 March 1990 to 20 March 1991, ACM Gold Ltd. Geological Survey of Western Australia, Statutory mineral exploration report, Item 6873, A33335.

Commander, D.P., Muhling, P.C., and Bunting, J.A., 1982. Stanley, W.A.. Geological Survey of Western Australia, 1:250 000 Geological Series Explanatory Notes 19.

Condie K.C., 2005. Earth as an evolving planetary system: Elsevier, Amsterdam, pp. 447.

Coveney, R.M., Murowchick, J.B., Grauch, R.I., Nansheng, C., and Glascock, M.D., 1992. Field relations, origins, and resource implications for platiniferous molybdenum–nickel ores in black shales of south China: Exploration and Mining Geology 1, 21–28.

Coveney, R.M., and Martin, S.P., 1983. Molybdenum and other heavy metals of the Mecca Quarry and Logan Quarry shales: Economic Geology 78, 132–149.

Cullen Resources Ltd, 2003a. ASX Announcement: Update on the Gunbarrel Gold Project, W.A.. Announcement to Australian Stock Exchange, 17 June 2003 (unpublished).

Cullen Resources Ltd, 2003b. ASX Announcement. Announcement to Australian Stock Exchange, 9 September 2003 (unpublished).

Daley, L., 1996. Project 450, Kingston JV, E53/369 and E53/370 Annual report, Period 23/7/95 – 22/7/96 and 10/8/95 – 9/8/96, Plutonic Operations Ltd.

Geological Survey of Western Australia, Statutory mineral exploration report, Item 9733, A48996.

Dashat Pty Ltd, 1995. Savory Basin gravity survey, operational and processing report. Geological Survey of Western Australia, S-series Report S10312 (unpublished).

Davie-Smythe, M.J., 1994. Exploration Licences 69/420–424, 426–428 "Nabberu Project" Annual Report for the period 2 January 1993 to 1 January 1994, Great Central Mines N.L.. Geological Survey of Western Australia, Statutory mineral exploration report, Item 8489, A40231.

Davy, R., Pirajno, F., Sanders, A., and Morris, P., 1999. Regolith geochemical mapping as an adjunct to geological mapping and exploration; examples from three contiguous Proterozoic basins in Western Australia. Journal of Geochemical Exploration 66, 37-53.

Deer W.A., Howie R.A., Zussman J., 1965. Rock forming minerals, vol 3, Sheet Silicates. Longmans, London, 270 pp.

Derry, L.A., and Jacobsen, S.B., 1990. The chemical evolution of Precambrian seawater: evidence from REEs in banded iron formations. Geochimica et Cosmochimica Acta 54, 2965-2977.

Donaldson, W.S., Plint, A.G., Longstaffe, F.J., 1999. Tectonic and eustatic control on deposition and preservation of Upper Cretaceous ooidal ironstone and associated facies: Peace River Arch area, NW Alberta, Canada. Sedimentology 46, 1159-1182.

Dorling, S.L., 1996a. Surrender Report, Teague Project E69/855, 1013, 1031, RGC Exploration Pty Ltd. Geological Survey of Western Australia, Statutory mineral exploration report, Item 9613, A49640.

Dorling, S.L., 1996b. Annual report, Teague Project E69/562, 855, 856, 857, 858, 975, 987, 988, 1012, 1013, 1014, 1031, 1036, 1059 and 1060, RGC Exploration Pty Ltd. Geological Survey of Western Australia, Statutory mineral exploration report, Item 10603, A49642.

Dorling, S.L., 1997a. Partial Surrender Report, Teague Project E69/975, RGC Exploration Pty Ltd. Geological Survey of Western Australia, Statutory mineral exploration report, Item 9455, A52175.

Dorling, S.L., 1997b. Surrender Report, Teague Project E69/987 and E69/988, RGC Exploration Pty Ltd. Geological Survey of Western Australia, Statutory mineral exploration report, Item 9481, A52177.

Dorling, S.L., 1997c. Partial Surrender Report 1997, Canning Gap Project, E69/597, RGC Exploration Pty Ltd. Geological Survey of Western Australia, Statutory mineral exploration report, Item 8071, A51110.

Dorling, S.L., 1997d. Partial Surrender Report, Teague Project E69/562, RGC Exploration Pty Ltd. Geological Survey of Western Australia, Statutory mineral exploration report, Item 10603, A52623.

Dorling, S.L., 1997e. Final Report, Teague Project E69/857 and E69/858, RGC Exploration Pty Ltd. Geological Survey of Western Australia, Statutory mineral exploration report, Item 10603, A53204.

Dorling, S.L., 1997f. Annual report, Canning Gap Project E69/597 for 3.2.96 to 2.2.97, RGC Exploration Pty Ltd. Geological Survey of Western Australia, Statutory mineral exploration report, Item 9569, A50728.

Dorling, S.L., 1998a. Partial Surrender Report, Teague Project E69/856, RGC Exploration Pty Ltd. Geological Survey of Western Australia, Statutory mineral exploration report, Item 10603, A53277.

Dorling, S.L., 1998b. Partial Surrender Report, Teague Project E69/1014, RGC Exploration Pty Ltd. Geological Survey of Western Australia, Statutory mineral exploration report, Item 10603, A53278.

Dorling, S.L., 1998c. Annual Report, Exploration activities during 13. 9. 96 to 12. 9. 97, Teague Project E69/562, 856, 857, 858, 975, 987, 988, 1012, 1014, 1036, 1059 and 1060, RGC Exploration Pty Ltd. Geological Survey of Western Australia, Statutory mineral exploration report, Item 10603, A53279.

Dorling, S.L., 1998d. Partial Surrender Report, Teague Project E69/1059 and E69/1060, RGC Exploration Pty Ltd. Geological Survey of Western Australia, Statutory mineral exploration report, Item 10603, A53567.

Doust, G., 1994. Glengarry Mining NL, Report on exploration, Yelma Project (E.L. 53/319, L. 53/629), Glengarry Mining NL. Geological Survey of Western Australia, Statutory mineral exploration report, Item 10178, A41264.

Edgar, W., 1993. RGC Exploration Pty Limited, Annual report, Period 18/07/92 to 17/07/93, Sweeney Creek E69/562, RGC Exploration Pty Ltd. Geological Survey of Western Australia, Statutory mineral exploration report, Item 10603, A38982.

Edgar, W., 1994. RGC Exploration Pty Limited, Annual report, Period 18/07/93 to 17/07/94, Teague E69/562, 855, 856, 857, 858, 975, RGC Exploration Pty Ltd. Geological Survey of Western Australia, Statutory mineral exploration report, Item 10603, A42560.

Eisenlohr, M., 1989. Final Report, E52/377, E52/378, Clover Tabletop, for the period 13 July 1989 to 27 October 1989, Newmont Australia Ltd. Geological Survey of Western Australia, Statutory mineral exploration report, Item 4138, A29115.

Elias, M., Bunting, J.A., 1982. Wiluna, W.A.: Geological Survey of Western Australia, 1:250 000 Geological Series Explanatory Notes 20.

Evans, W.J., 1994. Exploration Licence 53/510 – James Bore, RAB drilling programme, July 1994, Marymia Exploration NL. Geological Survey of Western Australia, Statutory mineral exploration report, Item 8223, A42946.

Einsele, G., 2000. Sedimentary basins: evolution, facies and sedimentary budget, 2nd Ed. Springer-Verlag, Heidelberg, 792 pp.

Erikson, P.G., Martins-Neto, M.A., Nelson, D.R., Aspoler, L.B., Chiarenzelli, J.R., Catuneau, O., Sarkar, S., Altermann, W., Rautenbach, C.J.D.E.W., 2001. An introduction to Precambrian basins: their characteristics and genesis. Sedimentray Geology 141-142, 1-35.

2434 Eyles, N., Mory, A.J., Backhouse, J., 2002. Carboniferous-Permian
2435 palynostratigraphy of west Australian marine rift basins: resolving tectonic and
2436 eustatic controls during Gondwana glaciations. Palaeogeography,
2437 Palaeoclimatology, Palaeoecology 184, 305-319.

2438 Fadda S., Fiori M., Pretti S., 1998. The sandstone-hosted Pb occurrence of Rio
2439 Pischinappiu (Sardinia, Italy): a Pb-carbonate end-member. Ore Geology
2440 Reviews 12, 355-377.

2441 Farrell, T.R., 1999. Wiluna, W.A. Sheet SG 51-2 (2nd Edition). Geological Survey of
2442 Western Australia, 1:250 000 Geological Series.

2443 Farrell, T.R., 2001, Wiluna, W.A. (Second Edition). Geological Survey of Western
2444 Australia, 1:250 000 Geological Series Explanatory Notes 28.

2445 Feldtmann, R., 1995. Annual report, Teague Project E69/562, 855, 856, 857, 858,
2446 975, 987, 988, 1012, 1013, 1014, 1031, 1059, 1060, 1036, RGC Exploration Pty
2447 Ltd. Geological Survey of Western Australia, Statutory mineral exploration
2448 report, Item 10603, A45916.

2449 Feldtmann, R., 1996. Canning Gap Project, E69/597, Annual report for 3.2.95 to
2450 2.2.96, RGC Exploration Pty Ltd. Geological Survey of Western Australia,
2451 Statutory mineral exploration report, Item 9569, A47278.

2452 Force, E.R. and Cannon, W.F., 1988. Depositional model for shallow-marine
2453 manganese deposits around black shale basins. Economic Geology 83, 93–117.

2454 Force, E.R. and Maynard, J.B., 1991. Manganese: Syngenetic deposits on the margins
2455 of anoxic basins: *in* Force E. R., Eidel, J. J. and Maynard, J. B., Sedimentary and
2456 diagenetic mineral deposits: a basin analysis approach. Reviews in Economic
2457 Geology 9, 147–157.

2458 Fowler, M., 1995. Annual Technical Report on exploration activity from July 1994 to
2459 December 1995, Kingston JV Project, Mt Eureka (E53/369) Red Bluff (E53/370),
2460 Dominion Mining Ltd. Geological Survey of Western Australia, Statutory
2461 mineral exploration report, Item 9733, A46927.

Fraser, A.R., and Pettifer, G.R., 1980. Reconnaissance gravity surveys in W. A. and S. A., 1969–1972. Australia Bureau of Mineral Resources, Geology and Geophysics Bulletin 196, pp. 60.

Garven, G., Raffensperger, J.P., 1997. Hydrogeology and geochemistry of ore genesis in sedimentary basins, in Barnes HL (ed), Geochemistry of ore deposits, 3rd edn, John Wiley & Sons, 125-189.

Geach, C., 1994. Annual Report to the Department of Minerals & Energy, Western Australia, Exploration Licence E69/859 (18/11/93 – 17/11/94), Warburton Mineral Field, Northling Pty Ltd, Geological Survey of Western Australia, Statutory mineral exploration report, Item 8439, A43041.

Gee, R.D., and Grey, K, 1993. Proterozoic rocks of the Glengarry 1:250 000 sheet: stratigraphy, structure, and stromatolite biostratigraphy. Geological Survey of Western Australia, Report 41, pp. 30.

Gifford, A.C., 1979. Exploration Report, Temporary Reserve 6800H Mount Fisher, year ending 12th September 1979, Chevron Exploration Corp. Geological Survey of Western Australia, Statutory mineral exploration report, Item 1453, A8732.

Giles, E., 1889. Australia twice traversed; the romance of exploration, being a narrative compiled from the journals of five exploring expeditions into and through central South Australia and Western Australia, from 1872 to 1876. London, Low, Marston, Searle and Rivington.

Glikson, A.Y., Stewart, A.J., Ballhaus, C.G., Clarke, G.L., Feeken, E.H.J., Leven, J.H., Sheraton, J.W., and Sun S-S., 1996. Geology of the western Musgrave Block, central Australia, with particular reference to the mafic–ultramafic Giles Complex. Australian Geological Survey Organisation, Bulletin 239, pp. 206.

Glover, D., 1996. Partial Surrender Report, Teague Project, E69/856, 857, 858, 562, RGC Exploration Pty Ltd. Geological Survey of Western Australia, Statutory mineral exploration report, Item 9279, A49643.

Goldfarb, R.J., Groves, D.I., Gardoll, S., 2001., Orogenic gold and geologic time: a global synthesis. Ore Geology Reviews 18, 1-75.

Goode, A.D.T., Hall, W.D.M., and Bunting, J.A., 1983. The Nabberu Basin of Western Australia, *in* Iron formation: Facts and problems edited by A. F. TRENDALL and R. C. MORRIS: Developments in Precambrian Geology. Elsevier Monograph 6, 295–323.

Great Central Mines Limited, 1993. Great Central Mines NL Quarterly Report. Statement released to the Australian Stock Exchange, 31 December 1993.

Great Central Mines Limited, 1999. Great Central Mines Limited Part B statement in response to the offer by Yandal Gold Pty Ltd. Statement released to the Australian Stock Exchange, 24 February 1999.

Grey, K., 1984. Biostratigraphic studies of stromatolites from the Proterozoic Earaheedy Group, Nabberu Basin, Western Australia. Geological Survey of Western Australia Bulletin 130, 123.

Grey, K., 1994. Stromatolites from the Palaeoproterozoic Earaheedy Group, Earaheedy Basin, Western Australia: Alcheringa 18, 187–218.

Grey, K., 1996a. Cunyu North, E69/531 Annual Report, 01/05/95 to 25/11/95, Cyprus Gold Australia Corporation. Geological Survey of Western Australia, Statutory mineral exploration report, Item 10744, A46716.

Grey, K., 1996b. Cunyu South, E69/529 Annual Report, 01/05/95 to 25/11/95, Cyprus Gold Australia Corporation. Geological Survey of Western Australia, Statutory mineral exploration report, Item 9705, A46715.

Grey, K., 1997a. Cunyu North, E69/531 Annual Report, 26/11/95 to 25/11/96, Cyprus Gold Australia Corporation. Geological Survey of Western Australia, Statutory mineral exploration report, Item 10744, A50194.

Grey, K., 1997b. Cunyu South, E69/529 Annual Report for the period 26/11/95 to 25/11/96, Cyprus Gold Australia Corporation. Geological Survey of Western Australia, Statutory mineral exploration report, Item 9705, A50196.

2517 Grey, K., Thorne, A.M., 1985. Biostratigraphic significance of stromatolites in
2518 upward shallowing sequences of the early Proterozoic Duck Creek Dolomite,
2519 Western Australia. Precambrian Research 29, 183-206.

2520 Griffin, T.J., 1990. Eastern Goldfields Province, *in* Geology and mineral resources of
2521 Western Australia. Geological Survey of Western Australia, Memoir 3, 77–119.

2522 Groenewald, P.B., Painter, M.G.M., and Mccabe, M., 2001. East Yilgarn geoscience
2523 database: north Eastern Goldfields, Cunyu to Cosmo Newbery 1:100 000 digital
2524 geological data package. Western Australia Geological Survey, Report 83, 39.

2525 Gromet, L.P., Dymek, R.F., Haskin, L.A., and Korotev, R.L., 1984. The "North
2526 American Shale Composite": its compilation, major and trace element
2527 characteristics. Geochimica et Cosmochinica Acta 48, 2469-2482.

2528 Gross, G.A., 1972. Primary features in cherty iron-formations: Sedimentary Geology
2529 7, 241–261.

2530 Haliovic, J., 1997. Cunyu North, E 69/531 Annual Report, 26/11/96 TO 25/11/97,
2531 Cyprus Gold Australia Corporation. Geological Survey of Western Australia,
2532 Statutory mineral exploration report, Item 10744, A53260.

2533 Hall, W.D.M., 1979. Annual report to the Mines Department, Temporary Reserve
2534 6639H Sweetwaters Well, Nabberu Mining District, Western Australia, Dampier
2535 Mining Co Ltd. Geological Survey of Western Australia, Statutory mineral
2536 exploration report, Item 2181, A8276.

2537 Hall, W.D.M., Goode, A.D.T., 1975. The Nabberu Basin; a newly discovered Lower
2538 Proterozoic basin in Western Australia. Geological Society of Australia, First
2539 Australian Geological Convention, Abs., 88–89.

2540 Hall, W.D.M., Goode, A.D.T., 1978. The early Proterozoic Nabberu Basin and
2541 associated iron formations of Western Australia. Precambrian Research 7, 129–
2542 184.

2543 Hall, W.D.M., Goode, A.D.T., Bunting, J.A., Commander, D.P., 1977. Stratigraphic
2544 terminology of the Earaheedy Group, Nabberu Basin. Geological Survey of
2545 Western Australia, Annual Report 1976, 40–43.

2546 Halilovic, J., Cawood, P.A., Jonaes, J.A., Pirajno, F., Nemchin, A.A., 2004.
2547 Provenance of the Earaheedy Basin, Western Australia: palaeogeographic and
2548 tectonic implications. Precambrian Research 128, 343-366.

2549 Hallberg, J.A., 1987. Postcratonization mafic and ultramafic dykes of the Yilgarn
2550 Block. Australian Journal of Earth Sciences 34, 135–149.

2551 Hamilton, R,. 1992. Geology and structural setting of ultramafic lamprophyres from
2552 Bulljah Pool, central Western Australia. Journal of the Royal Society of Western
2553 Australia 75, 51-56.

2554 Hamilton, R., and Rock, N.M.S., 1990. Geochemistry, mineralogy and petrology of a
2555 new find of ultramafic lamprophyres from Bulljah Pool, Nabberu Basin, Yilgarn
2556 Craton, Western Australia. Lithos 24, 275-290.

2557 Hays, J., 1967. Surfaces and laterites in the Northern Territory*, in* Landform studies
2558 from Australia and New Guinea *edited by* J. N. JENNINGS and J. A.
2559 MABBUTT. Canberra, Australia National University Press, 182 –210.

2560 Heikoop J.M., Tsujita C.J., Risk M.J., Tomascil T., Mah A.J., 1996. Modern iron
2561 ooids from a shallow-marine volcanic setting: Mahegetang, Indonesia. Geology
2562 24, 759-762.

2563 Hitzman, M.W., Reynolds, N.A., Sangster, D.F., Allen, C.R., Carman, C.E., 2003.
2564 Classification, genesis and exploration guides for nonsulfide zinc deposits.
2565 Economic Geology 98, 685-714.

2566 Hocking, R.M., 1994. Subdivisions of Western Australian Neoproterozoic and
2567 Phanerozoic sedimentary basins. Geological Survey of Western Australia, Record
2568 1994/4, 84.

Hocking, R.M., 2003. Nabberu, W.A. Sheet SG 51-5, Second Edition. Geological Survey of Western Australia, 1:250 000 Geological Series.

Hocking, R.M., Cockbain, A.E., 1990. Regolith, *in* Geology and Mineral Resources of Western Australia. Geological Survey of Western Australia, Memoir 3, 591–602.

Hocking, R.M., Mory, A.J., Williams, I.R., 1994. An Atlas of Neoproterozoic and Phanerozoic Basins of Western Australia, *in* The Sedimentary Basins of Western Australia *edited by* G. PURCELL and R. R. PURCELL, Proceedings West Australian Basins Symposium, Perth, Western Australia, 1994, 21–43.

Hocking, R.M., Preston, W.A., 1998. Western Australia; Phanerozoic geology and mineral resources. AGSO Journal of Australian Geology and Geophysics, 17 (3), 245–260.

Hocking, R.M., Jones, J.A., 1999. Methwin, W.A. Sheet 3047. Geological Survey of Western Australia, 1:100 000 Geological Series.

Hocking, R.M., Jones, J.A., Pirajno, F., Grey, K., 2000a. Revised lithostratigraphy for Proterozoic rocks in the Earaheedy Basin and nearby areas. Geological Survey of Western Australia, Record 2000/16, 22.

Hocking, R.M., Grey, K., Bagas, L., Stevens, M.K., 2000b. Mesoproterozoic stratigraphy in the Oldham Inlier, Little Sandy Desert, central Western Australia. Geological Survey of Western Australia, Annual Review 1999–2000, 49–56.

Hocking, R.M., Pirajno, F., Lizumi, S., Morris, P.A., 2000c. Barium-gold mineralization at Quadrio Lake, Oldham Inlier, Little Sandy Desert, Western Australia. Geological Survey of Western Australia, Annual Review 1999–2000, 72–79.

Hocking, R.M., Langford, R.L., Thorne, A.M., Sanders, A.J., Morris, P.A., Strong, C. A., Gozzard, J.R., 2001a. A classification system for regolith in Western Australia: Geological Survey of Western Australia, Record 2001/4, 22p.

Hocking, R.M., Adamides, N.G., Pirajno, F., Jones, J.A., 2001b. Geology of the Earaheedy 1:100 000 sheet. Geological Survey of Western Australia, 1:100 000 Geological Series Explanatory Notes 33.

Hocking, R.M., Jones, J.A., 2002. Geology of the Methwin 1:100 000 sheet. Geological Survey of Western Australia, 1:100 000 Geological Series Explanatory Notes 35.

Hocking, R.M., Pirajno, F., 2004. Lee Steere, W.A. Sheet 3346. Geological Survey of Western Australia, 1:100 000 Geological Series.

Horwitz, R.C., 1975a. The southern boundaries of the Hamersley and Bangemall Basins of sedimentation. Geological Society of Australia, First Australian Geological Convention, Abs., 88–89.

Horwitz, R.C., 1975b. Provisional geological map at 1:2 500 000 of the north-east margin of the Yilgarn Block, Western Australia. Australia Commonwealth Scientific Industrial Research Organization, Mineral Research Lab. Report F10.

Horwitz, R.C., 1976. Two unrecorded basal sections in older Proterozoic rocks of Western Australia. Australia CSIRO Mineral Research Lab. Report FP 10.

Horwitz, R.C., Mann, A.W., 1975. Malmac Well uranium prospect. Australia CSIRO Mineral Research Lab, Internal Report IR710R (unpublished).

Howland, J.P., 1999. Astro Exploration N.L., Exploration Licences E52/439–440, E69/420–424, 426, 428 “Nabberu” Surrender Report for the period ending 22–23 March 1999. Geological Survey of Western Australia, Statutory mineral exploration report, Item 10910, A58969.

Hutchison, N., 1996. Combined Exploration Report (M8075), E53/319, P53/629, Yelma Project, Wiluna Region, Western Australia, Annual Technical Report for period ending 31 March, 1996, Pegasus Gold Australia Pty Ltd. Geological Survey of Western Australia, Statutory mineral exploration report, Item 10178, A47993.

Hutchison, N., 1997. Combined Exploration Report, E53/319, P53/629, Yelma Project, Wiluna Region, Western Australia, Annual Technical Report for period 19 January 1996 to 18 January 1997, Pegasus Gold Australia Pty Ltd. Geological Survey of Western Australia, Statutory mineral exploration report, Item 10178, A51874.

Iasky, R.P., 1990. Officer Basin, *in* Geology and Mineral Resources of Western Australia. Geological Survey of Western Australia, Memoir 3, 362–380.

Isley, A.E., 1995. Hydrothermal plumes and the delivery of iron to banded iron formation. The Journal of Geology 103, 169-185.

Jacobsen, S.B., Pimentel-Klose, M.R., 1988. Nd isotopic variations in Precambrian banded ison formations. Geophysical Research Letters 15, 393-396.

Jackson, J.A., 1997, Glossary of geology (4^{th} edition). Virginia, U.S.A., American Geological Institute, 769.

Jackson, M.J., van de Graaff, W.J.E., 1981. Geology of the Officer Basin, Western Australia. Australia BMR, Bulletin 206, pp. 102.

Johnson, G.I., 1991. The petrology, geochemistry and geochronology of the felsic alkaline suite of the eastern Yilgarn block, Western Australia. South Australia, University of Adelaide, PhD thesis (unpublished).

Johnston, D.A., and Hall, W.D.M., 1980. Final report, Temporary Reserve 6639H, 7000H, 7001H, and 7002H and Mineral Claims 69/966 to 69/999 Sweetwaters Well, Nabberu Mining District, Western Australia. Geological Survey of Western Australia, Statutory mineral exploration report, Item 2181, A8876.

Jones, D.C., 1994. Gypsum Deposits in Western Australia. Geological Survey of Western Australia, Record 1993/5, 141.

Jones, J.A., 2002. Wongawol, W.A. Sheet 3245. Geological Survey of Western Australia, 1:100 000 Geological Series.

2649 Jones, J.A., Pirajno, F., 2000. Granite Peak, W.A. Sheet 3146. Geological Survey of
2650 Western Australia, 1:100 000 Geological Series.

2651 Jones, J.A., Pirajno, F., 2003. Crackle breccias in the Earaheedy Basin: implications
2652 for a newly recognised epithermal mineralization event, Geological Survey of
2653 Western Australia Record Record 2003/5, p. 20-24.

2654 Jones, J.A., Pirajno, F., Hocking, RM.., Grey, K., 2000. Revised stratigraphy for the
2655 Earaheedy Group: Implications for the tectonic evolution and mineral potential of
2656 the Earaheedy Basin. Geological Survey of Western Australia, Annual Review
2657 1999–2000, 57–63.

2658 Kappler, A., Pasquero, C., Konhauser, K.O., Newman, D.K., 2005. Deposition of
2659 banded iron formations by anoxygenic phototrophic Fe(II)-oxidizing bacteria.
2660 Geology 33, 865-868.

2661 Kellow, M.W., 1991. Troy Creek Mines Department report September 1991, Sons of
2662 Gwalia NL. Geological Survey of Western Australia, Statutory mineral
2663 exploration report, Item 8563, A34445.

2664 Kimberley, M.M., 1989. Nomenclature for iron formations: Ore Geology Reviews 5,
2665 1–12.

2666 Kinny, P.D., Nutman, A.P., Occhipinti, S.A., 2004. Recoinnasance dating of events
2667 recorded in the southern part of the Capricorn Orogen. Precambrian Research
2668 128, 279-294.

2669 Kitto, P.L., 1985. Progress Report on the Mount Eureka Project, EL's 53/62, 53/63
2670 and 53/64, Sundowner Minerals NL. Geological Survey of Western Australia,
2671 Statutory mineral exploration report, Item 6255, A17074.

2672 Klein, C., Beukes, N.J., 1992. Proterozoic iron-formations, *in* Proterozoic crustal
2673 evolution *edited by* K. C. CONDIE. Elsevier, Amsterdam, 383-418.

Klein, C., Ladeira, E.A., 2000. Geochemistry and petrology of some Proterzoic banded iron formations of the Quadriletero Ferrifero, Minas Gerais, Brazil. Economic Geology 95, 405-428.

Konhauser, K.O., Hamade, T., Morris, R.C., Ferris, F.G., Southam, G., Raiswell, R., Canfield, D., 2002. Could bacteria have formed the Precambrian banded iron formations? Geology 30, 1079-1082.

LaBerge G.L., 1966. Altered pyroclastic rocks in iron formations in the Hamersley Range, Western Australia. Economic Geology 61, 147-161.

Lambourn, S.S., 1972. Aeromagnetic survey of the Glengarry, Wiluna and Kingston 1:250 000 Sheet areas, W.A., 1970. Australia Bureau of Mineral Resources Rec. 1972/120.

Lancaster, R.D., 1970. Report on Regional Mapping Temporary Reserve 4583H, Wiluna, Western Australia, International Oils Exp NL. Geological Survey of Western Australia, Statutory mineral exploration report, Item 595, A73.

Langford, R.L., Wyche, S., Liu, S.F., 2000. Geology of the Wiluna 1: 100 000 sheet. Geological Survey of Western Australia, 1:100 000 Geological Series Explanatory Notes 26.

Le Blanc Smith G., Pirajno F., Nelson D.R., Grey K., 1995. Base-metal deposits in the Early Proterozoic Glengarry terrane, Western Australia. Annual Review Geological Survey of Western Australia 1993/94, 59-62.

Leech, R.E.J., and Brakel, A.T., 1980. Bullen, Western Australia. Geological Survey of Western Australia, 1:250 000 Geological Series Explanatory Notes 11.

Leishman, J., 1990. E53/225, Red Bluff, Western Australia, Final (surrender) Exploration Report, Hunter Resources Ltd. Geological Survey of Western Australia, Statutory mineral exploration report, Item 5148, A30989.

Li, Z.X., 2000. Palaeomagnetic evidence for unification of the North and West Australian cratons by ca 1.7 Ga: new results from the Kimberley Basin of northwestern Australia. Geophysical Journal International 142, 173–180.

Lindemann, W.L., 1972. Final; report on Mineral Claims 69/877 to 69/907, Esso Australia Ltd. Geological Survey of Western Australia, Statutory mineral exploration report, Item 134, A4417.

Lindsay, J., and Brasier, M., 2002. Did global tectonics drive early biosphere evolution? Carbon isotope record from 2.6 to 1.9 Ga carbonates of Western Australia. Precambrian Research 114, 1-34.

Linford, J.G., 1972. Report on Elfram Electromagnetic Surveys Eureka 'A', James Bore 'E' and Collin Well Leonora area, Western Australia on behalf of Tenneco Australia Inc.. Geological Survey of Western Australia, Statutory mineral exploration report, Item 595, A7037.

Livingstone Resources NL, 1998. Livingstone Resources NL Annual Report, 1998. Released to the Australian Stock Exchange.

Lowry, D.C., Jackson, M.J., van de Graaff, W.J.E, Kennewell, P.J., 1972. Preliminary results of geological mapping in the Officer Basin, Western Australia, 1972. Geological Survey of Western Australia, Annual Report 1971, 50–56.

Mabbutt, J.A., Litchfield, W.H., Speck, N.H., Sofoulis, J., Wilcox, D.G., Arnold, J.M., Brookfield, M., Wright, R.L., 1963. General report on lands of the Wiluna-Meekatharra area, Western Australia, 1958. Australia Commonwealth Scientific Industrial Research Organization Land Research Series No. 7, 215.

Magnet Metals, 1977a. TR 6379 Project Goat Blind River type uranium prospect. Geological Survey of Western Australia, Statutory mineral exploration report, Item 835, A7113.

Magnet Metals, 1977b. End year report on TR 6379. Geological Survey of Western Australia, Statutory mineral exploration report, Item 835, A7338.

Martin, D.McB., Thorne, A.M., 2001. New insights into the Bangemall Supergroup, in GSWA 2001 extended abstracts: New geological data for WA explorers. Geological Survey of Western Australia, Record 2001/5, 1–2.

Martin, D.McB., Thorne, A.M., 2004. Tectonic and basin evolution of the Bangemall Supergroup in the northwestern Capricorn Orogen. Precambrian Research, 128, 385-410.

Martin, D.McB., Thorne, A.M., Copp, I.A., 1999. A provisional revised stratigraphy for the Bangemall Group on the Edmund 1:250 000 sheet. Geological Survey of Western Australia, Annual Review 1998–1999, 51–55.

May, R., Aravanis, T., 1988b. Final report on Exploration Licences 69/90 (Stanley 1), 93 (Stanley 4), 174–178 (Mt Moore 2–6) and 190 (Stoney Point), Stanley 1:250 000 map sheet, Western Australia, CRA Exploration Pty Ltd. Geological Survey of Western Australia, Statutory mineral exploration report, Item 3603, A23102.

McMillan, N.M., McNaughton, N.J., 1995. The post-magmatic history of felsic rocks from the Archaean Marymia Dome — a SHRIMP study of the relationship between zircon morphology, Th/U and geological history. Third Australian Conference on Geochronology and Isotope Geoscience, Abstracts, 18.

McNaughton, N.J., Rasmussen, B., and Fletcher, I.R., 1999. SHRIMP uranium-lead dating of diagenetic xenotime in siliciclastic sedimentary rocks. Science 285, 78-80.

McQuitty, B.M., Pascoe D.J., 1998. Magellan lead deposit. Australasian Institute of Mining and Metallurgy, Monograph 22, 293-296.

Meakins, A.L., and Watsham, S., 1994. Annual Report for the period ended September 30/1993—E52/220, 222, 224, 226, 554, 555, 557, 587, 668, 670, 712, 732, and E51/321, 357, 367, 391, Ruby Bore–Good Pool Project, Peak Hill SG50-08, Western Australia (vol. 1 and 2). Western Australia, Geological Survey M-series Item 8477 (unpublished).

Merritt, B.D., 1991. Annual Combined Report, Exploration Licences 52/374, 52/375, 52/395, 69/329, 69/330, and 69/331, 30 August, 1990 – 29 August, 1991, Nabberu area, Western Australia, Stockdale Prospecting Ltd. Geological Survey of Western Australia, Statutory mineral exploration report, Item 9247, A34508.

Middleton, W., 1994. Galtrad Pty Ltd/Alkane Exploration NL Yadgymurrin/Simpson Well Prospect, Peak Hill Mineral Field - Western Australia, Annual Report 1994 Exploration Licence - 52/593 for the period 26/9/93 to 26/9/94. Geological Survey of Western Australia, Statutory mineral exploration report, Item 9016, A43255.

Middleton, W., 1995. Galtrad Pty Ltd, Simpson Well Prospect, Peak Hill Mineral Field - Western Australia, Annual Report 1995 Exploration Licence - 52/593 for the period 26/9/94 to 25/9/95. Geological Survey of Western Australia, Statutory mineral exploration report, Item 9016, A45944.

Middleton, W., 1996. Galtrad Pty Ltd, Simpson Well Prospect, Peak Hill Mineral Field - Western Australia, Final and Annual Report 1996 - E 52/593 for the period 26/9/95 to 25/9/96. Geological Survey of Western Australia, Statutory mineral exploration report, Item 9016, A48842.

Mitchell, M.S., 1995a. Final Report, Lake Nabberu Project, Exploration Licences E69/329 & E69/330B&C, and E69/331A&C, Stockdale Prospecting Ltd. Geological Survey of Western Australia, Statutory mineral exploration report, Item 7885, A43527.

Mitchell, M.S., 1995b. Final Report Exploration Licences 69/507–511 and E69/515 Lake Nabberu area WA, Stockdale Prospecting Ltd. Geological Survey of Western Australia, Statutory mineral exploration report, Item 7939, A43526.

Mitchell, M.S., 1994. Annual combined report E69/443, E69/498, E69/499 and E69/542 Earaheedy Aztec Joint Venture period ending 31 December 1993, Stockdale Prospecting Ltd. Geological Survey of Western Australia, Statutory mineral exploration report, Item 8563, A40343.

Mitchell, M.S., 1993, Annual Combined Report, Exploration Licences 52/374, 52/375, 52/395, 69/329, 69/330, and 69/331, 30 August 1991 – 29 August 1992, Nabberu areas, Western Australia, Stockdale Prospecting Ltd. Geological Survey of Western Australia, Statutory mineral exploration report, Item 9247, A37880.

Morey, G.B., 1983. Animikie Basin, Lake Superior region, USA, in Iron-formation: Facts and problems edited by A. F. TRENDALL and R. C. MORRIS. Developments in Precambrian Geology, Elsevier Monograph 6, 13–68.

Morris, P.A., McGuiness, S.A., Sanders, A.J., Coker, J., 2000. Geochemical mapping of the Stanley 1:250 000 sheet. Geological Survey of Western Australia, 1:250 000 Regolith Geochemistry Series Explanatory Notes 53.

Morris, P.A., Pirajno, F., 2005. Mesoproterozoic sill complexes in the Bangemall Supergroup, Western Australia. Geology, geochemistry and mineraliazation potential. Geological Survey of Western Australia Report 99, 75p.

Morris, P.A., Pirajno, F., and Shevchenko, S., 2003. Proterozoic mineralization identified by integrated regional regolith geochemistry, geophysics and bedrock mapping in Western Australia. Geochemistry, Exploration, Environment, Analysis 3, 2003, 13–28.

Morris, P.A., Sanders, A.J., and Faulkner, J.A., 1997. Geochemical mapping of the Nabberu 1:250 000 sheet. Geological Survey of Western Australia, 1:250 000 Regolith Geochemistry Series Explanatory Notes 63.

Morris, P.A., Sanders, A.J., Pirajno, F., Faulkner, J.A., and Coker, J., 1998. Regional-scale regolith geochemistry, identification of metalloid anomalies and the extent of bedrock in the Achaean and Proterozoic of Western Australia. Regolith'98, Proceedings of the 3rd Australian Regolith Conference, Kalgoorlie, 101–108.

Muhling, P.C., and Brakel, A.T., 1985. Geology of the Bangemall Group — The evolution of an intracratonic Proterozoic basin. Geological Survey of Western Australia, Bulletin 128, pp. 266.

Multi Metal Consultants Pty Ltd, 1992a. Galtrad Pty Ltd Cunyu prospect, Peak Hill Mineral Field, Western Australia, Annual Report 1992 Exploration Licences 69/529 & 531. Geological Survey of Western Australia, Statutory mineral exploration report, Item 10744, A37309.

Multi Metal Consultants Pty Ltd, 1992b. Galtrad Pty Ltd Alkane Exploration NL Yadgymurrin/Simpson Well Prospect, Peak Hill Mineral Field, Western Australia, Annual Report 1992 Exploration Licence 52/953. Geological Survey of Western Australia, Statutory mineral exploration report, Item 9016, A37164.

Multi Metal Consultants Pty Ltd, 1993. Galtrad Pty Ltd Alkane Exploration NL Yadgymurrin/Simpson Well Prospect, Peak Hill Mineral Field, Western Australia, Annual Report 1993 Exploration Licence 52/593. Geological Survey of Western Australia, Statutory mineral exploration report, Item 9016, A40142.

Myers, J.S., Swager, C.P., 1997. The Yilgarn Craton, *in* Greenstone belts *edited by* de Wit, M, and Ashwal, LD.. Oxford University Monographs on Geology and Geophysics, Monograph 35, 640–656.

Myers, J.S., Shaw, R., Tyler, I.M., 1996. Tectonic evolution of Proterozoic Australia. Tectonics 15-6, 1431-1446.

Nealson, K.H., 1982. Microbiological oxidation and reduction of iron, in Mineral Deposits and the Evolution of the Biosphere, H. D. Holland and M. Schidlowski (eds), Springer-Verlag, 51-66.

Nelson, D.R., 1995. Compilation of SHRIMP U–Pb zircon geochronology data, 1994. Geological Survey of Western Australia, Record 1995/3, 244.

Nelson, D.R., 1997. Compilation of SHRIMP U–Pb zircon geochronology data, 1996. Geological Survey of Western Australia, Record 1997/2, 189.

Nelson, D.R., 1999. Compilation of SHRIMP U–Pb zircon geochronology data, 1998. Geological Survey of Western Australia, Record 1999/2, 222.

Nelson, D.R., 2001a. An assessment of the determination of depositional ages for Precambrian clastic sedimentary rocks by U-Pb dating of detrital zircons. Sedimentary Geology 141-142, 37-60.

Nelson, D.R., 2001b. Compilation of geochronology data, 2000, Geological Survey of Western Australia Record, 2001/2, 205.

Nelson, D.R., 2002. Compilation of geochronology data, 2001, Geological Survey of Western Australia Record, 2002/2, 282.

Nemchin, A.A., Pidgeon, R.T., 1998. Precise conventional and SHRIMP baddelyite U-Pb age for the Binneringie Dyke, near Narrogin, Western Australia. Australian Journal of Earth Sciences 45, 673-675.

Newsom, H.E., Graup, G., Sewards, T., Keil, K., 1986. Fluidization and hydrothermal alteration of the suevite deposit at the Ries Crater, West Germany, and implications for Mars. Journal of Geophysical Research 91, E239-E251.

Nicolaysen, L., Ferguson, J., 1990. Cryptoexplosion structures, shock deformation and siderophile concentrations related to explosive venting of fluids associated with alkaline ultramafic magmas. Tectonophysics 171, 303–335.

Northcote, K.H., Wright, M.J., 1983. Chapter 12, Sandy Desert Region (I), *in* Soils–an Australian Viewpoint. CSIRO Division of Soils, CSIRO, Melbourne/Academic Press, London, 179–187.

Oocchipinti, S.A., Sheppard, S., 2001. Stuck between two cratons – latest Archaean crust in the Gascoyne Complex, Western Australia. In: The Fourth International Archaean Symposium, Extended Abstracts, 72-74.

Occhipinti, S.A., Sheppard, S., Nelson, D.R., Myers, J.S., Tyler, I.M., 1998. Syntectonic granite in the southern margin of the Palaeoproterozoic Capricorn Orogen, Western Australia. Australian Journal of Earth Sciences 45, 509–512.

Occhipinti, S.A., Sheppard, S., Myers, J.S., Tyler, I.M., Nelson, D.R., 2001. Archaean and Palaeoproterozoic geology of the Narryer terrane (Yilgarn Craton) and the

2861 southern Gascoyne Complex (Capricorn Orogen), Western Australia – A field
2862 guide. Geological Survey of Western Australia Record 2001/8, 70.

2863 Occhipinti, S.A., Sheppard, S., Passchier, C., Tyler, I.M., 2004. Paleoproterozoic
2864 crustal accretion and collision in the southern Capricorn Orogen: the Glenburgh
2865 Orogeny. Precambrian Research 198, 237-256.

2866 Oilmin N.L., Petromin N.L., Transoil N.L., 1983. Bullen copper-lead-zinc
2867 exploration: Geological Survey of Western Australia, Statutory mineral
2868 exploration report, Item 2435, A9862.

2869 Osinski, G.R., Spray, G., Lee, P., 2001. Impact-induced hydrothermal activity within
2870 the Haughton impact structure, arctic Canada: generation of a transient, warm,
2871 wet oasis. Meteoritic and Planetary Science 36, 731-745.

2872 Ostwald, J., Bolton, B.R., 1992. Glauconite formation as a factor in sedimentary
2873 manganese deposit genesis. Economic Geology 87, 1336–1344.

2874 Perring, R.J., 1994. Troy Creek Project E69/443, Partial Relinquishment Report, 26
2875 September 1990 to 25 September 1994, Nabberu SG51-5, Troy Creek Inlier,
2876 Stockdale Prospecting Ltd. Geological Survey of Western Australia, Statutory
2877 mineral exploration report, Item 7607, A41320.

2878 Pillans, B., 1998. Ancient weathering in an ancient landscape? Australian National
2879 University, Research School of Earth Sciences, Annual Report 1998, 107.

2880 Pillans, B., and Bateman, R., 2000. Palaoemagnetic dating of Phanerozoic weathering
2881 imprints, Mount Percy Mine, Kalgoorlie, Western Australia. Geological Society
2882 of Australia Abstracts no. 59, 15th Australian Geological Convention, Sydney,
2883 July 3–7, 390.

2884 Pirajno, F., 1999. Nabberu, W. A. Sheet 3046. Geological Survey of Western
2885 Australia, 1:100 000 Geological Series (1st Edition).

2886 Pirajno, F., 2002. Geology of the Shoemaker Impact Structure, Western Australia.
2887 Geological Survey of Western Australia, Report 82, 52.

Pirajno, F., 2004. Metallogeny in the Capricorn Orogen, Western Australia, the result of multiple ore-forming processes. Precambrian Research, 128, 411-440.

Pirajno, F., 2007. Metallogeny of Palaeoproterozoic depositional environments on the northern margin of the Yilgarn Craton. Proceedings of Kalgoorlie '07 Conference, Kalgoorlie, Bierlein F., Knoz-Robinson C. M. (editors), pp 77-79.

Pirajno, F., Bagas, L., Swager, C.P., Occhipinti, S.A., Adamides, N.G., 1996. A reappraisal of the stratigraphy of the Glengarry Basin, Western Australia. Geological Survey of Western Australia, Annual Review 1995–1996, 81–87.

Pirajno, F., Adamides, N.G., 1998. Geology of the Thaduna 1:100 000 sheet. Geological Survey of Western Australia, 1:100 000 Geological Series Explanatory Notes 24.

Pirajno, F., Glikson, A. 1998. Shoemaker impact structure, Western Australia. Celestial Mechanics and Dynamical Astronomy 69, 25–30.

Pirajno, F., Hocking, R.M., Jones, J.A., 1999. Geology, mineralization and geodynamic evolution of the Palaeoproterozoic Yerrida and Earaheedy Basins, W.A., *in* Two billion years of tectonics and mineralisation *edited by* Watt, GR, and Evans, DAD,: Curtin University of Technology, Tectonics Special Research Centre Conference, Perth, W.A., 1999, Proceedings. Geological Society of Australia, Abstracts Series, no. 56, 30–33.

Pirajno, F., Occhipinti, S.A., Swager, C.P., 1998. Geology and tectonic evolution of the Palaeoproterozoic Bryah, Padbury and Yerrida Basins (formerly Glengarry Basin), Western Australia: implications for the history of the south-central Capricorn Orogen. Precambrian Research 90, 119-140.

Pirajno, F., Adamides, N.G., 2000. Iron–manganese oxides and glauconite-bearing rocks of the Earaheedy Group: implications for the base metal potential of the Earaheedy Basin. Geological Survey of Western Australia, Annual Review 1999–2000, 65–71.

Pirajno, F., Hocking, R.M., Jones, J.A., 2000. Rhodes, W.A. Sheet 3147. Geological Survey of Western Australia, 1:100 000 Geological Series.

Pirajno, F., Hocking, R.M., 2001. Rhodes, W.A. Sheet 3147. Geological Survey of Western Australia, 1:100 000 Geological Series.

Pirajno, F., Hocking, R.M., 2001. Mudan, W.A. Sheet 3247. Geological Survey of Western Australia, 1:100 000 Geological Series.

Pirajno, F., Hocking, R.M., 2002. Glenayle, W.A. Sheet 3347. Geological Survey of Western Australia, 1:100 000 Geological Series.

Pirajno, F., Hawke, P., Glikson, A.Y., Haines, P.W., Uysal, T., 2003. Shoemaker impact structure, Western Australia: Australian Journal of Earth Sciences 34, No. 5, 775–796.

Pirajno, F., Morris, P.A., Wingate, M.T.D., 2002. A possible large igneous province (LIP) in central western Australia: implications for mineralisation models. Geological Society of Australia Abstracts volume 67: 140.

Pirajno, F., Jones, J.A., Hocking, R.M., Halilovic, J., 2004. Geology and tectonic evolution of Palaeoproterozoic basins of the eastern Capricorn Orogen, Western Australia. Precambrian Research 128, 315-342.

Playford, P.E., Cockbain, A.E., 1976. Modern algal stromatolites at Hamelin Pool, a hypersaline barred basin in Shark Bay, Western Australia. In Walter, M. R. (ed), Stromatolites. Elsevier, Amsterdam, 389-411.

Plescia, J.B., 1999. Gravity signature of the Teague Ring Impact Structure, Western Australia. Geological Society of America, Special Paper 339, 165–175.

Powell, G.R., 1986. Mount Eureka Project, Annual Report, 26 – 5 – 85 to 25 – 5 - 86, Exploration Licence 53/62–65, Sundowner Minerals NL. Geological Survey of Western Australia, Statutory mineral exploration report, Item 4031, A18653.

Powell, G.R., 1988a. Mount Eureka Project, Partial Surrender Report, 6 December 1986 to 5 December 1987, Exploration Licence 53/16, Sundowner Minerals NL.

Geological Survey of Western Australia, Statutory mineral exploration report, Item 3640, A26126.

Powell, G.R., 1988b. Mount Fisher Project, Surrender Report, 8 May 1987 to 7 May 1988, Exploration Licence 53/124, Sundowner Minerals NL. Geological Survey of Western Australia, Statutory mineral exploration report, Item 3640, A25258.

Powell, G.R., 1988c. Mount Eureka Project, Annual Report, 26 May 1987 to 25 May 1988, Sundowner Minerals NL. Exploration Licence 53/63 Geological Survey of Western Australia, Statutory mineral exploration report, Item 4031, A28190.

Powell, G.R., 1988d. Mount Eureka Project, Annual report, 25 July 1987 to 23 July 1988, Prospecting Licence 53/280, Sundowner Minerals NL. Geological Survey of Western Australia, Statutory mineral exploration report, Item 6255, A25257.

Powell, G.R., Leandri, P.S., O'Farrell, D.C., 1990. Mount Fisher gold deposit, *in* Geology of the mineral deposits of Australia and Papua New Guinea *edited by* Hughes, F.E., Australasian Institute of Mining and Metallurgy, Monograph 14, 507–509.

Pratt, B.R., 2002. Storms versus tsunamis: dynamic interplay of sedimentary, diageneitc and tectonic processes in the Cambrian of Montana. Geology 30, 423-426.

Preiss, W.V., Jackson, M.J., Page, R.W., Compston, W., 1975. Regional geology, stromatolite biostratigraphy and isotopic data bearing on the age of a Precambrian sequence near Lake Carnegie, Western Australia. Geological Society of Australia, 1st Australian Geological Convention, Abstracts, 92–93.

Price, J., 2003. Depositional setting of granular iron formation in the Palaeoproterozoic Frere Formation, Earaheedy Basin, Western Australia. BSc (Hon) thesis, unpublished, The University of Western Australia, 80p.

Pye, K.J., Morris, P.A., McGuinness, S.A., 2000. Geochemical mapping of the Kingston 1:250 000 sheet. Geological Survey of Western Australia, 1:250 000 Regolith Geochemistry Series Explanatory Notes 53.

2970 Rasmussen, B., Krapez, B., 2000. Evidence of hydrocarbon and metalliferous fluid
2971 migration in the Palaeoproterozoic Earaheedy Basin of Western Australia.
2972 Journal of the Geological Society, London 157, 355-366.

2973 Rasmussen, B., Fletcher, I.R., 2002. Indirect dating of mafic intrusions by SHRIMP
2974 U-Pb analysis of monazite in contact metamorphosed shale: an example from the
2975 Palaeoproterozoic Capricorn Orogen, Western Australia. Earth and Planetary
2976 Science Letters 197, 287-299.

2977 Read, J.F., Kerans, C., Webber, L.J., Sarg, J.F., Wright, F.M., (eds), 1995.
2978 Milankovich sea-level changes, cycles, and reservoirs on carbonate platforms
2979 in greenhouse and icehouse worlds. SEPM Short Course Notes 35, 212.

2980 Reddy, S.M., Collins, A.S., Buchan, A.C. & Mruma, A. 2004. Heterogeneous excess
2981 argon and Neoproterozoic heating in the Usagaran Orogen, Tanzania, revealed
2982 by single grain $^{40}Ar/^{39}Ar$ thermochronology. Journal of African Earth
2983 Sciences, 39, 165-176.

2984 Register of Australian Mining, 1994/95. Diamonds, Nabberu (Great Central), *in*
2985 Register of Australian Mining, published by Roger Bigum, Resource Information
2986 Unit Ltd, Subiaco, Western Australia, 232.

2987 Rex, D. C. & Guise, P. G. 1995. Evaluation of argon standards with special emphasis
2988 on time scale measurements. In: Odin, G. S. (ed) Phanerozoic Time Scale.
2989 IUGS Subcommision on Geochronology, 21–23.

2990 Richards, J.R., Gee, R.D., 1985. Galena lead isotopes from the eastern part of the
2991 Nabberu Basin, Western Australia. Australian Journal of Earth Sciences 32, 47–
2992 54.

2993 Rieth, O., 1998. Cunyu North, E 69/531 Annual Report for the year ended
2994 25/11/1998, Cyprus Amax Australia Corporation, Report No. 2409. Geological
2995 Survey of Western Australia, Statutory mineral exploration report, Item 10744,
2996 A57077.

Roberts, C., Jockel, F., 1994a. Project 543: Cunyu North, E69/531 Annual Report, period 23.6.93 to 31.12.93, Map Sheet No SG51-5 (Nabberu) 2946 IV (Merrie), Plutonic Operations Ltd. Geological Survey of Western Australia, Statutory mineral exploration report, Item 10744, A40523.

Roberts, C., Jockel, F., 1994b. Project 542: Cunyu South E69/529, ANNUAL REPORT, Period 23.6.93 to 31.12.93, Map Sheet No SG51-5 (Nabberu) 2946 III (Merrie), Plutonic Operations Ltd. Geological Survey of Western Australia, Statutory mineral exploration report, Item 9705, A40524.

Robertson, B., 1987. Progress Report for the Mt. Eureka Project, EL 53/63, P53/280 & P53/373, Sundowner Minerals NL. Geological Survey of Western Australia, Statutory mineral exploration report, Item 4031, A21075.

Robinson, K., Gellatly, D.C., 1978. Final report on iron ore exploration Nabberu Basin, Western Australia Iron Ore Temporary Reserves 6525H, 6526H, 6527H, 6528H, Amax Exploration Aust Inc. Geological Survey of Western Australia, Statutory mineral exploration report, Item 769, A7448.

Rock, N.M.S., 1990. Lamprophyres: the global occurrence, petrology, origin and economic significance of some rocks of deep origin. Blackie, Glasgow, 250 p.

Rodriguez-Pascua, M.A., Clavo, J.P., De Vicente, G., Gomez-Gras, D., 2000. Soft-sediment deformation structures interpreted as seismites in lacustrine sediments of the Prebetic Zone, SE Spain, and their potential use as indicators of earthquake magnitudes during the Late Miocene. Sedimentary Geology 135, 117–135.

Russell, J., Grey, K., Whitehouse, M., Moorbath, S., 1994. Direct Pb/Pb age determination of Proterozoic stromatolites from the Ashburton Nabberu basins, Western Australia, in 8th International Conference on Geochronology, Cosmochronology and Isotope Geology, Berkeley, California, U.S.A., Abstracts. U.S. Geological Survey Circular 1107, 275.

Sanders, A.J., 2002. Geochemical mapping of the Nicholls 1:100 000 sheet. Geological Survey of Western Australia, 1:100 000 Regolith Geochemistry Series Explanatory Notes 36.

Sanders, C.C., Harley, A.S., 1971. Hydrogeological reconnaissance of part of the Nabberu and East Murchison Mining Areas. Geological Survey of Western Australia Annual Report 1970, 23–27.

Schissel, D., Aro, P., 1992. The major early Proterozoic sedimentary iron and manganese deposits and their tectonic setting. Economic Geology 87, 1367–1374.

Schusterbauer, J., 1989a. Annual Report for Exploration Licence 53/166 Mt Eureka for the period 21 March 1988 to 20 March 1989, ACM Gold Ltd. Geological Survey of Western Australia, Statutory mineral exploration report, Item 6873, A27114.

Schusterbauer, J.R., 1989b. Annual/Final Report for Exploration Licence 53/167 Mt Eureka for the period 21 March 1988 to 20 March 1989, ACM Gold Ltd. Geological Survey of Western Australia, Statutory mineral exploration report, Item 3879, A27116.

Scrimgeour, I.R., Close, D.F., Edgoose, C.J., 1999. Petermann Ranges SG- 52-7. 1:250000 Geological map series, Explanatory Notes, Northern Territory Geological Survey.

Seccombe, P.K., Dellar, A., 1995. Fluid inclusion investigation of five samples: Teague Project, *in* Teague Project,E69/562, 855, 856, 857, 858, 975, 987, 988, 1012, 1013, 1014, 1031, 1059, 1060, 1036 *edited by* R. FELDTMANN. Western Australia Geological Survey, Statutory mineral exploration report, Item 10603 A45916 (unpublished).

Seccombe, P.K., Jiang Z., 1994. Fluid inclusion investigation of eight samples: Teague Project, *in* Teague Project, E69/562, 855,856, 857, 858, 975, 987, 988, 1012, 1013, 1014, 1031, 1059, 1060, 1036 *edited by* R. FELDTMANN. Western Australia Geological Survey, Statutory mineral exploration report, Item 10603 A45916 (unpublished). SEG Newsletter, 2006, Exploration Reviews, April 2006 issue, No. 65, 27.

Shaw, J., and Associates, 1985. Report on rotary drilling, Mount Eureka Project E53/62, E53/63, E53/64, East Murchison Mineral Field, Sundowner Minerals NL. Geological Survey of Western Australia, Statutory mineral exploration report, Item 6255, A17076.

Shaw, J., and Associates, 1988. P53/377 – James Bore, Progress report to 23 December 1987, Sundowner Minerals NL. Geological Survey of Western Australia, Statutory mineral exploration report, Item 3713, A23168.

Shee, S.R., Vercoe, S.C., Wyatt, B.A., Hwang, P.H., Campbell, A.N., Colgan, E.A., 1999. Discovery and geology of the Nabberu Kimberlite Province, Western Australia. In: Gurney J. J. (ed) Proceedings of the VIIth International kimberlite conference, Cape Town, 764-772.

Sheppard, S., Occhipinti, S., Nelson, D.R., Tyler, I.M., 1999. Granites of the southern Capricorn Orogen, Western Australia, two billion years of Tectonics and Mineralisation. In: Tectonics Special Research Centre Conference Proceedings, 44-46.

Sheppard, S., Occhpinti, S., Nelson, D.R., 2005. Intracontinental reworking in the Capricorn Orogen, Western Australia: the 1680-1620 Mangaroon Orogeny. Australian Journal of Earth Sciences 52, 443-460.

Sheppard, S., Occhipinti, S., Tyler, I.M., 2004. A 2005-1970 Ma Andean-type batholith in the southern Gascoyne Complex, Western Australia. Precambrian Research 128, 257-277.

Sheppard, S., Occhipinti, S., Tyler, I.M., 2001. The tectonic setting of granites in the southern Gascoyne Complex, in GSWA 2001 extended abstracts; New geological data for WA explorers. Geological Survey of Western Australia, Record 2001/5, 3–4.

Sheppard, S., Rasmussen, B., Muhling, J.R., Farrell, T.R., Fletcher, I.R., 2007. Grenvillian-aged orogenesis in the Palaeoproterozoic Gascoyne Complex,

Western Australia: 1030-950 Ma reworking of the Proterozoic Capricorn orogen: Journal of Metamorphic Geology 25, 477-494.

Shevchenko, S.I., 2000. Gravity data — KINGSTON and STANLEY, 1:250 000 sheets Western Australia. Geological Survey of Western Australia Record 2000/19, 29.

Shoemaker, E.M., Shoemaker, C.S., 1996. The Proterozoic impact record of Australia: Australian Geological Survey Organisation, Journal of Australian Geology and Geophysics 16, 379–398.

Simonson, B.M., Hassler, S.W., 1996. Was the deposition of large Precambrian iron formations linked to major marine transgressions? Journal of Geology 104, 665-676.

Smith, M.E., 1993. Summary report Troy Creek project E69/443, 498, 499, 542, 656–661, Aztec Mining Co Ltd. Geological Survey of Western Australia, statutory mineral exploration report, Item 8563, A37791.

Smith, M.E., 1994. Partial surrender report for E69/443, Troy Creek Nabberu, WA, 26 September 1990 to 25 September 1993, Aztec Mining Co Ltd. Geological Survey of Western Australia, Statutory mineral exploration report, Item 7428, A40255.

Smithies, R.H., Bagas, L., 1997. High pressure amphibolite-granulite facies metamorphism in the Palaeoproterozoic Rudall Complex, central Western Australia. Precambrian Research, 83, 243-265.

Smithies, R.H., Champion, D.C., 1999. Late Archaean felsic alkaline igneous rocks in the Eastern Goldfields, Yilgarn Craton, Western Australia: a result of lower crustal delamination?. London Geological Society, Journal 156, 561–576.

Steiger, R. H., Jager, E. 1977. Subcommision on Geochronology: Convention on the use of decay constants in geo- and cosmochronology. Earth and Planetary Science Letters**,** 36, 359-362.

Stevens, M.K., Adamides, N.G., 1998. GSWA Trainor 1 well completion report, Savory Sub-basin, Officer Basin, Western Australia, with notes on petroleum and mineral potential. Geological Survey of Western Australia, Record 1996/12, 69.

Stevens, M.K., Apak, S.N., 1999. GSWA Empress 1 and 1A well completion report, Yowalga Sub-basin, Officer Basin, Western Australia. Geological Survey of Western Australia, Record 1999/4, 110.

Stewart, A.J., Blake, D.H., Ollier, C.D., 1986. Cambrian river terraces and ridge tops in central Australia—oldest persisting landforms?. Science 233, 758 –761.

Swager, C.P., 1997. Tectono-stratigraphy of the late Archaean greenstone terranes in the southern Eastern Goldfields, Western Australia. Precambrian Research, 83, 11-42.

Talbot, H.W.B., 1910. Geological observations in the country between Wiluna, Hall's Creek, and Tanami. Geological Survey of Western Australia, Bulletin 39, 88.

Talbot, H.W.B., 1914. The country between lat. 23˚ and 26˚S, and long. 119˚and 121˚E. Geological Survey of Western Australia, Annual Report 1913, 24–25.

Talbot, H.W.B., 1919. Notes on the geology and mineral resources of parts of the North-West, Central and Eastern Divisions. Geological Survey of Western Australia, Annual Report 1918, 83–93.

Talbot, H.W.B., 1920. Geology and mineral resources of the North-west, Central, and Eastern Divisions. Between Long. 119˚ and 122˚ E., and Lat. 22˚ and 28˚ S.. Geological Survey of Western Australia, Bulletin 83, 226.

Talbot, H.W.B., 1926. A geological reconnaissance in the Central and Eastern Divisions between 122˚ 30'E and 123˚ 30'E Longitude, and Lat. 25˚ 30'S and 28˚ 15'S Latitude. Geological Survey of Western Australia, Bulletin 87, 30.

Taylor, K.S., 1980a. Final report on Temporary Reserve No. 7364H, Bridleface Outcamp – Nabberu, Western Australia, covering the period 7 December, 1979 –

15 January, 1980, Uranerz Australia Pty Ltd. Geological Survey of Western Australia, Statutory mineral exploration report, Item 1138, A8756.

Taylor, K.S., 1980b. Final report on Temporary Reserve No. 7365H, Bridleface Outcamp – Nabberu, Western Australia, covering the period 7 December, 1979 – 6 December, 1980, Uranerz Australia Pty Ltd. Geological Survey of Western Australia, Statutory mineral exploration report, Item 1138, A9470.

Teen, M.T., 1996. Silicification and base metal mineralization within the Earaheedy Basin, Western Australia. BSc (Hon) thesis (unpublished), Centre for Ore Deposit and Exploration Studies, University of Tasmania, 128 p.

Tobin, K.J., 1990. The paleoecology and significance of the Gunflint-type microbial assemblages from the Frere Formation (Early Proterozoic), Nabberu Basin, Western Australia. Precambrian Research, 47, 71–81.

Traves, D.M., Casey, J.N., Wells, A.T., 1956. The geology of the south-western Canning Basin, Western Australia. Australia Bureau of Mineral Resources, Report 29, pp. 76.

Trendall, A.F., 2002. The significance of iron-formation in the Precambrian stratigraphic record. In: Altermann, W. and Corcoran, L. (eds), Precambrian sedimentary environments: A modern approach to ancient depositional systems, 33-66, Blackwell Science, Oxford.

Twidale, C.R., Horwitz, R.C., Campbell, E.M., 1985. Hamersley landscapes of the northwest of Western Australia. Revue de geologie dynamique et de geographie physique 26, fasc. 3, 173–186.

Twidale, C.R., 2000. Early Mesozoic (?Triassic) landscapes in Australia:evidence, argument, and implications. Journal of Geology 108, 537–552.

Tyler, I.M., Thorne, A. M., 1990. The northern margin of the Capricorn Orogen, Western Australia — an example of an early Proterozoic collision zone. Journal of Structural Geology 12, 685–701.

Tyler, I.M., Hocking, R.M., 2002. A revision of tectonic units of Western Australia. Geological Survey of Western Australia, Annual Review 2000–2001, 33–44.

Tyler, I. M., Pirajno, F., Bagas, L., Myers, J.S., 1998. Geology and mineral deposits of the Proterozoic of Western Australia. AGSO Journal of Geology and Geophysics 17, 223–244.

Uranerz Australia Pty Ltd, 1978. Final report on exploration over Temporary Reserve Nos. 6555H and 6556H, Lake Nabberu area, Western Australia. Geological Survey of Western Australia, Statutory mineral exploration report, Item 730, A8413.

van de Graaff, W.J.E, Crowe, R.W.A., Bunting, J.A., Jackson, M.J., 1977. Relict Early Cainozoic drainages in arid Western Australia. Z. Geomorph. N. F. 21, 379–400.

Vielreicher, N.M., McNaughton, N.J., 2002. SHRIMP U-Pb geochronology of magmatism and thermal event in the Archaean Marymia Inlier, central Western Australia. International Journal of Earth Sciences (Geol Rundsch) 91, 406-432.

Walraven, F., Armstrong, R.A., Kruger, F.J., 1990. A chronostratigraphic framework for the north-central Kaapvaal Craton, the Bushveld Complex and the Vredefort structure. Tectonophysics 171 23-48.

Walter, M.R., Gorter, J.D., 1994. The Neoproterozoic Centralian Superbasin in Western Australia: the Savory and Officer Basins, *in* The Sedimentary Basins of Western Australia *edited by* G. PURCELL and R. R. PURCELL, Proceedings West Australian Basins Symposium, Perth, Western Australia, 1994, 851–864.

Walter, MR, Goode, ADT, and Hall, JA, 1976, Microfossils from the a newly discovered Precambrian stromatolitic iron formation in Western Australia: Nature, v261, 221-223.

Walter, M.R., Veevers, J.J., Calver, C.R., Grey, K., 1995. Late Proterozoic stratigraphy of the Centralian Superbasin, Australia. Precambrian Research, 73, 173–175.

Western Mining Corporation, 1979. Mt. Davis annual and terminal report 16th June 1978–15th June 1979. Geological Survey of Western Australia, Statutory mineral exploration report, Item 855, A8454.

Western Mining Corporation, 1988. Annual technical report Bulljah Project Exploration Licences 38/118–119, 69/65, 69/71–80 and 69/81–85. Geological Survey of Western Australia, Statutory mineral exploration report, Item 3598, A23061.

Wetherall, Q., 1995a. Project 543; Neds Creek joint venture, Cunyu North, E69/531 Annual Report, period 26/11/93 – 25/11/94, Plutonic Operations Ltd. Geological Survey of Western Australia, Statutory mineral exploration report, Item 10744, A43349.

Wetherall, Q., 1995b. Project 542: Neds Creek Joint Venture, E69/529, Annual Report, Period 26/11/93 – 25/11/94, WA Technical Report No 383, Map Sheet: SG51-5 (Nabberu) 2946 III (Merrie), Plutonic Operations Ltd. Geological Survey of Western Australia, Statutory mineral exploration report, Item 9705, A43350.

Wilkinson, J.J., 2001. Fluid inclusions in hydrothermal ore deposits. Lithos 55, 229-272.

Williams, I.R., 1990a. Savory Basin, *in* Geology and mineral resources of Western Australia. Geological Survey of Western Australia, Memoir 3, 329–335.

Williams, I.R., 1990b. Bangemall Basin, *in* Geology and mineral resources of Western Australia. Geological Survey of Western Australia, Memoir 3, 308–324.

Williams, I.R., 1992. Geology of the Savory Basin, Western Australia. Geological Survey of Western Australia, Bulletin 141, 115.

Williams, I.R., 1995a. Trainor, W.A (2nd Edition). Geological Survey of Western Australia, 1:250 000 Geological Series Explanatory Notes 31.

Williams, I.R., 1995b. Bullen, W.A (2nd Edition). Geological Survey of Western Australia, 1:250 000 Geological Series Explanatory Notes 23.

Williams, I.R., Leach, R.E.J., Bunting, J.A., Commander, D.P., Muhling, P.C., Brakel, A.T., 1981. Stanley, W.A. Sheet SG 51-6 (1st Edition). Geological Survey of Western Australia, 1:250 000 Geological Series.

Williams, I.R., Brakel, A.J, Leech, R.E.J., 1995a. Trainor, W.A. Sheet SG 51-2 (2nd Edition). Geological Survey of Western Australia, 1:250 000 Geological Series.

Williams, I.R., Leech, R.E.J., Brakel, A.J., 1995b. Bullen, W.A. Sheet SG 51-1 (2nd Edition). Geological Survey of Western Australia, 1:250 000 Geological Series.

Wingate, M.T.D., 2002. Age and palaeomagnetism of dolerite sills intruded into the Bangemall Supergroup on the Edmund 1:250 000 map sheet, Western Australia. Geological Survey of Western Australia, Record 2002/4, 48.

Wingate, M.T.D., 2003. Age and palaeomagnetism of dolerite intrusions of the southeastern Collier Basin and the Earaheedy and Yerrida Basins Western Australia. Geological Survey of Western Australia, Record 2003/3, 34.

Wingate, M.T.D., Pirajno, F., Morris, P.A., 2004. The Warakurna large igneous province: a new Mesoproterozoic large igneous province in west-central Australia. Geology 32, 105-108.

Woodhead, J.D., Hert, .J.M, 1997. Application of the 'double spike' technique to Pb-isotope geochronology. Chemical Geology 138, 311–321.

Wyche, S., Farrell, T.R., 2000. Regional geological setting of the Yandal greenstone belt, northeast Yilgarn Craton. Yandal Greenstone Belt, Australian Institute of Geoscientists, Bulletin 32, 41-50.

Young, D.J., 1987. Final report on exploration completed in Els 69/122–133, 138–149 Stanley, Stanley, Western Australia, report no. 14838, CRA Exploration Pty Ltd. Geological Survey of Western Australia, Statutory mineral exploration report, Item 3373, A22344.

Zhao G.C., Min, S., Wilde S.A., Li S.Z., 2005. Late Archean to Paleoproterozoic evolution of the North China Craton: key issues revisited. Precambrian Research 136, 177-202.